



The University of
Nottingham

UNITED KINGDOM • CHINA • MALAYSIA

**APOPTOTIC CELL DEATH *via* OXIDATIVE
STRESS MEDIATED CASPASE-DEPENDENT
MECHANISM IN JURKAT T CELLS BY
CARDAMONIN AND ITS TRANSITION METAL
Cu(II) AND Fe(II) COMPLEXES**

by
Khoo Yi Vonn

**Thesis submitted for the degree of Doctor of Philosophy at
the University of Nottingham
School of Pharmacy Faculty of Science**

October 2017

COPYRIGHT NOTICE

Under the Copyright Act of 1968, this thesis should not be reproduced in any form without the written permission of the author. I certify that reasonable efforts were made to acknowledge all third party contents used in this thesis.

TABLE OF CONTENTS

ABSTRACT.....	vii
DECLARATION	viii
ACKNOWLEDGEMENTS	ix
ABBREVIATIONS	x
LIST OF FIGURES	xii
LIST OF TABLES	xv
CHAPTER 1: INTRODUCTION.....	1
1.1 Cell death mechanism	2
1.1.1 Apoptosis	2
1.1.1.1 Morphological changes	3
1.1.1.2 Phosphatidylserine externalisation.....	5
1.1.1.3 Mitochondrial membrane potential	7
1.1.1.4 Caspases	8
1.1.1.5 Caspase inhibitors	11
1.1.2 Necrosis.....	12
1.2 Oxidative-stress-induced cell death	13
1.2.1 Reactive oxygen species	13
1.2.2 Glutathione.....	16
1.3 Semi-synthetic natural products and cancer	18
1.4 Cardamonin as potential lead compound.....	20
1.5 Adherent and suspension culture	29
1.5.1 THP-1 cell line and differentiation into mature macrophages.....	29
1.5.2 Mitogen-activated protein kinase.....	30
1.6 Aims.....	33
CHAPTER 2: MATERIALS AND METHODS	34
2.1 Materials	35
2.1.1 Reagents	35
2.1.2 Cell lines	37
2.1.3 Compounds	37
2.2 Methods	38
2.2.1 Cell Culture.....	38
2.2.1.1 Maintaining Adherent Cells.....	38
2.2.1.2 Maintaining Suspension Cells.....	39

2.2.1.2.1 Isolation of Mononuclear Cells	39
2.2.1.3 Cell Counting	40
2.2.1.4 Cryopreservation	40
2.2.1.5 THP-1 cells	41
2.2.1.5.1 Differentiation of THP-1 Monocytes to Macrophages	41
2.2.1.5.2 Expression of CD11b surface marker in THP-1-derived macrophages	42
2.2.2 MTS Cell Viability Assay	42
2.2.3 Nuclear Morphology for Detection of Apoptosis	44
2.2.4 Annexin V-FITC Analysis	45
2.2.5 Sodium dodecyl sulfate polyacrylamide gel electrophoresis and Western blot analysis	46
2.2.5.1 Buffers, resolving gel and stacking gel recipes	47
2.2.5.2 Preparation of Stacking and Resolving Gels	48
2.2.5.3 Preparation of Cell Lysates	49
2.2.5.4 Protein Estimation using Bradford Protein Assay	49
2.2.5.5 Sample Preparation for SDS-PAGE	50
2.2.5.6 Western Blotting	51
2.2.5.7 Immunodetection	52
2.2.5.8 Membrane stripping and re-probing	53
2.2.6 Measurement of MMP	54
2.2.7 Determination of intracellular GSH levels	55
2.2.8 Detection of ROS	56
2.2.9 Determination of anti-oxidant effects on cell viability	57
2.3 Statistical Analysis	57

**CHAPTER 3: CYTOTOXICITY AND STRUCTURE ACTIVITY
RELATIONSHIP OF CARDAMONIN DERIVATIVES AND COMPLEXES IN
NORMAL AND CANCER CELL LINES.....58**

3.1 Introduction.....	59
3.2 Results.....	60
3.2.1 Cytotoxicity and the structure activity relationship of cardamonin and its derivatives on human A549 and HK1 carcinoma cell lines.....	60
3.2.2 Cytotoxicity of cardamonin and its complexes assessed in normal human MRC5 and Hs68 cell lines	88

3.2.3 Cytotoxicity of cardamonin and its complexes assessed in human Jurkat T cells.....	94
3.3 Discussion.....	97

CHAPTER 4: THP-1-DERIVED MACROPHAGES INCREASED RESISTANCE TOWARDS CARDAMONIN, CARDAMONIN-Cu(II) AND CARDAMONIN-Fe(II) COMPLEXES WERE INDEPENDENT OF P38 α AND P38 β MAP KINASE PATHWAY.....100

4.1 Introduction.....	101
4.2 Results.....	102
4.2.1 Effects of cardamonin, cardamonin-Cu(II) and cardamonin-Fe(II) on THP-1 cell viability.....	102
4.2.2 Morphological changes in THP-1 monocytes differentiation to macrophages	104
4.2.3 Expression of CD11b surface marker	108
4.2.4 Effects of cardamonin, cardamonin-Cu(II) and cardamonin-Fe(II) on THP-1-derived macrophages cell viability	110
4.2.5 Effects of cardamonin, cardamonin-Cu(II) and cardamonin-Fe(II) on THP-1-derived macrophages cell viability in the presence of a MAP kinase inhibitor, p38 MAP kinase inhibitor IV	112
4.2.6 Effects of cardamonin, cardamonin-Cu(II) and cardamonin-Fe(II) on THP-1-derived macrophages cell viability in the presence of a MAP kinase inhibitor, SB202190 MAP kinase inhibitor	115
4.2.7 Comparative effects of cardamonin, cardamonin-Cu(II) and cardamonin-Fe(II) on cell viability of THP-1 monocytes, THP-1-derived macrophages, p38 _{in} THP-1-derived macrophages and SB202190 _{in} THP-1-derived macrophages	118
4.3 Discussion.....	122

CHAPTER 5: ELUCIDATING THE CYTOTOXIC MECHANISM OF ACTION INDUCED BY CARDAMONIN AND ITS COMPLEXES IN JURKAT T CELLS.....127

5.1 Introduction.....	128
5.2 Results.....	129

5.2.1 Effects of cardamonin, cardamonin-Cu(II) complex and cardamonin-Fe(II) complex on cell viability in the presence of a caspase inhibitor, Z-VAD-FMK, in Jurkat T cells	129
5.2.2 Morphological changes induced by cardamonin, cardamonin-Cu(II) complex and cardamonin-Fe(II) complex on Jurkat T cells	131
5.2.3 Analysis of phosphatidylserine externalisation during apoptosis using FITC-conjugated annexin in Jurkat T cells.....	134
5.2.4 Western blot analysis of caspase activation by cardamonin, cardamonin-Cu(II) complex and cardamonin-Fe(II) complex in Jurkat T cells	136
5.2.5 Effects of cardamonin, cardamonin-Cu(II) complex and cardamonin-Fe(II) complex on MMP in Jurkat T cells	138
5.3 Discussion	139

CHAPTER 6: OXIDATIVE MECHANISMS OF CARDAMONIN, CARDAMONIN-Cu(II) AND CARDAMONIN-Fe(II) COMPLEXES IN JURKAT T CELLS

6.1 Introduction.....	146
6.2 Results.....	148
6.2.1 Effects of cardamonin, cardamonin-Cu(II) and cardamonin-Fe(II) complexes on cell viability in the presence of NAC in Jurkat T cells	148
6.2.2 Effects of cardamonin, cardamonin-Cu(II) and cardamonin-Fe(II) complexes on intracellular ROS levels in Jurkat T cells	150
6.2.3 Effects of cardamonin, cardamonin-Cu(II) and cardamonin-Fe(II) complexes on intracellular GSH levels in Jurkat T cells	152
6.2.4 Effects of cardamonin, cardamonin-Cu(II) and cardamonin-Fe(II) complexes on cell viability in the presence of L-cysteine in Jurkat T cells ..	154
6.2.5 Effects of cardamonin, cardamonin-Cu(II) and cardamonin-Fe(II) complexes on cell viability in the presence of D-cysteine in Jurkat T cells ..	156
6.2.6 Effects of cardamonin, cardamonin-Cu(II) and cardamonin-Fe(II) complexes on cell viability in the presence of GSH in Jurkat T cells	158
6.2.7 Effects of cardamonin, cardamonin-Cu(II) and cardamonin-Fe(II) complexes on cell viability in the presence of Trolox in Jurkat T cells	160
6.2.8 Effects of cardamonin, cardamonin-Cu(II) and cardamonin-Fe(II) complexes on intracellular ROS levels in the presence of Z-VAD-FMK in Jurkat T cells	162

6.2.9 Effects of cardamonin, cardamonin-Cu(II) and cardamonin-Fe(II) complexes on intracellular GSH levels in the presence of Z-VAD-FMK in Jurkat T cells	164
6.3 Discussion	166
CHAPTER 7: CONCLUSION AND FUTURE WORK	173
7.1 General discussion and conclusion	174
7.2 Future work.....	180
REFERENCES.....	182

ABSTRACT

Cancer is a leading cause of death worldwide as cancer cells have the ability to develop resistance to chemotherapeutic agents due to their high expressions of resistance gene. More research on alternative strategies to eradicate this type of malignant cells is highly desired by using natural products with fewer side effects. This study initially investigates the cytotoxicity of 20 novel semi-synthetic cardamonin derivatives and complexes in A549 lung and HK1 nasopharyngeal cancer cell lines. Structure activity relationship analysis revealed the factors affecting cytotoxicity were modification of hydroxyl group, presence of alkene group, addition of chemical groups, with the greatest cytotoxicity advantage being complexing with metal ions. Cardamonin-Cu(II) and cardamonin-Fe(II) complexes were determined as the two most cytotoxic compounds and were selected for further cytotoxic analysis in normal MRC5 lung and normal Hs68 foreskin cell lines. Results showed toxicity in MRC5 lung cells but was less toxic in Hs68 foreskin cells, suggesting some level of selectivity from cardamonin, cardamonin-Cu(II) and cardamonin-Fe(II) depending on the type of cells exposed to. Subsequently, cardamonin and its two complexes were tested in Jurkat T leukaemic cells and results showed highest susceptibility in this leukaemic cell line prompting further investigation on differential susceptibility of adherent and suspension cells. THP-1 monocytic leukaemia cell line cultured in both suspension and adherent phase demonstrated increased resistance in THP-1-derived macrophages in adherent phase compared to THP-1 monocytes in suspension form. Herein, we investigated the effects of interference from inhibitors of p38 α and p38 β MAP kinase and found THP-1-derived macrophages' increased resistant towards cardamonin, cardamonin-Cu(II) and cardamonin-Fe(II) complexes were independent of p38 α and p38 β MAP kinase pathway. As Jurkat T cells exhibited lowest IC₅₀ values in cardamonin, cardamonin-Cu(II) and cardamonin-Fe(II)-treated cells, we next explored the underlying mechanism of action in this cell. All three compounds were found to induce apoptotic cell death *via* the intrinsic mitochondrial pathway in Jurkat T cells as evidenced by the morphological changes, phosphatidylserine externalisation, caspase-3, -9 and PARP-1 cleavage, and collapse of mitochondrial membrane potential. Caspase-8, an initiator caspase of the extrinsic pathway was not activated. The presence of a caspase inhibitor, Z-VAD-FMK, was able to inhibit caspase processing and block cell death, further confirming the induced apoptotic cell death was caspase-dependent. As previous studies have reported the ability of metals to induce apoptosis through oxidative stress, the effects of these three compounds on reactive oxygen species (ROS) generation and intracellular glutathione (GSH) levels were explored. Results revealed cardamonin and cardamonin-Fe(II)-induced depletion of intracellular GSH and production of ROS; whereas cardamonin-Cu(II) did not significantly affect intracellular GSH levels but generated ROS. The presence of low molecular weight thiols, N-acetylcysteine (NAC), L-cysteine and GSH as well as Trolox, a ROS scavenger, blocked cardamonin and cardamonin-Fe(II)-induced Jurkat T cell death, while D-cysteine, which cannot be metabolised to GSH had no effect. However, these low molecular weight thiols had no effect on cardamonin-Cu(II)-treated cells with the exception of Trolox, confirming the role of ROS in cardamonin-Cu(II)-induced Jurkat T cell death. Furthermore, intracellular ROS and GSH levels were recovered close to levels of untreated Jurkat T cells in the presence of Z-VAD-FMK. In conclusion, this study demonstrates cardamonin, cardamonin-Cu(II) and cardamonin-Fe(II) induced apoptotic cell death in Jurkat T cells *via* an oxidative stress mediated intrinsic mitochondrial pathway that was caspase-dependent.

DECLARATION

I hereby declare that this thesis is my original work and it has been written by me in its entirety. I have duly acknowledged all the sources of information, which have been used in this thesis. This thesis has not been submitted for any degree or examination at this or any other university previously.

.....
Khoo Yi Vonn
5th October 2017

Accepted by,

.....
Dr Khoo Teng Jin
5th October 2017

ACKNOWLEDGEMENTS

I would like to express my heartfelt gratitude to all those who have helped and inspired me during my PhD studies. This work would not have been possible without your continuous encouragement, support and motivation.

First and foremost, it gives me great pleasure to convey my sincere gratitude to my supervisor, Dr Khoo Teng Jin, for giving me this opportunity to take on this challenging yet rewarding project. Your invaluable guidance, patience and enthusiasm have always kept me motivated throughout these years. I am indebted to my co-supervisor, Professor Chow Sek Chuen, for generously providing me the necessary space and facilities in Monash University to carry out my research. Thank you for your advice, insightful suggestions and the constructive comments in my thesis write-up. Sincere gratitude to my internal examiner, Dr New Siu Yee, for providing me invaluable counsel during my 1st year of PhD research talk, manuscript write-up during my 2nd year and helpful suggestions for my final thesis write-up.

I would also like to express my appreciation to all academic and non-academic staff members from the Faculty of Science and School of Pharmacy at the University of Nottingham as well as the School of Science at Monash University, for making my experience in the department a most enjoyable one. Special thanks to all my friends and lab mates at the University of Nottingham and Monash University. Dr Yamina Boukari, Dr Ibrahim Babangida, Dr Lee Yee Mun, Dr Christine Leong, Khaled Break Mohammad, Ashwin Kaur, Aliana Mohamed, Athena, Eng Hwa, Jia Min, Koon Kee, Shu Qi, Peng Nian, Andrew, Li Fang, you have all created a very supportive, friendly and welcoming environment so wonderful that many sweet memories were made.

My deepest gratitude and appreciation goes to my family for their unflagging love and support throughout my PhD, as this journey is simply impossible without them. My beloved mom and dad, who shared my struggles and brimmed with pride at my accomplishments. My husband, Leow Fae Ben, thank you for your immense patience, understanding and love. You have worked hard to support us and spared no effort to provide the best for our future. You are my greatest motivator.

Finally, I am grateful to the MyBrain15 programme by the Ministry of Higher Education (MOHE) Malaysia and University of Nottingham for the financial assistance and making my research endeavours possible.

ABBREVIATIONS

•OH	Hydroxyl radical
Annexin V-FITC	Annexin V-fluorescence isothiocyanate
APAF1	Apoptotic protease-activating factor 1
APS	Ammonium persulfate
ATCC	American Type Culture Collection
BAK	BCL-2 antagonist
BAX	BCL-2 associated X proteins
BCL-2	B cell lymphoma 2
BH3	BCL-2 homology 3
BMK1	Big MAP kinase 1
BSA	Bovine serum albumin
DD	Death domain
DED	Death effector domain
DHC	4,4'-dihydroxylchalcone
DHE	Dihydroethidium
DHMC	4,4'-dihydroxy-2'-methoxychalcone
DMSO	Dimethyl sulfoxide
DTT	Dithiothreitol
ECL	Enhanced chemiluminescence
ECM	Extracellular matrix
EDTA	Ethylene-diaminetetraacetic acid
EMMPRIN	Extracellular matrix metalloproteinase inducer
ERKs	Extracellular signal-regulated kinases
FADD	FAS-associated death domain protein
FBS	Fetal bovine serum
GPx	Glutathione peroxidase
GSH	Glutathione
GSSG	Oxidised glutathione
H₂O₂	Hydrogen peroxide
HO-1	Heme oxygenase 1
HRP	Horseradish peroxidase
IC₅₀	Concentration of a compound with half-maximal cell viability
JNK	C-jun N-terminal
MAP	Mitogen-activated protein
MAPK	Mitogen-activated protein kinases
MCB	Monochlorobimane
MMP	Mitochondrial membrane potential
MTS	3-(4,5-dimethylthiazol-2-yl)-5-(3-carboxymethoxyphenyl)-2-(4-sulfophenyl)-2H- tetrazolium
NAC	N-acetyl cysteine
NaCl	Sodium chloride
NAD(P)H	Nicotine adenine dinucleotide phosphate
O₂^{•-}	Superoxide anion
p38ⁱⁿTHP-1-derived macrophages	P38 MAP kinase inhibited-THP-1-derived macrophages
pen/ strep	Penicillin/ streptomycin

PI	Propidium iodide
PKB/ PKC	Protein kinases –B/ -C
PKC	Protein kinase C
PMA	Phorbol-12-myristate-13-acetate
PMS	Phenazine methosulfate
PMSF	Phenylmethylsulfonyl fluoride
PS	Externalise phosphatidylserine
PSSG	Protein mixed disulfides
RIPA	Radio-immunoprecipitation assay
ROS	Reactive oxygen species
rpm	Revolutions per minute
SAPK	Stress-activated protein kinase
SAR	Structure activity relationship
SB202190_{in}THP-1-derived macrophages	SB202190 MAP kinase inhibited-THP-1-derived macrophages
SDS	Sodium Dodecyl Sulfate
SDS- PAGE	Sodium dodecyl sulfate polyacrylamide gel electrophoresis
SEM	Standard error of mean
SODs	Superoxide dismutase enzymes
STS	Staurosporine
TEMED	Tetramethylethylenediamine
TMRE	Tetramethyl rhodamine ethyl ester
TMRE	Tetramethylrhodamine, ethyl ester
TNF	Tumour necrosis factor
TRAIL	TNF-related apoptosis inducing ligand
VD3	1,25-dihydroxyvitamin D3
Z-FA-CMK	Benzyloxycarbonyl-phenylalanine-alanine-chloromethylketone
Z-VAD-FMK	Benzyloxycarbonyl-valine-alanine-aspartic acid-fluoromethylketone
$\Delta\psi_m$	Mitochondrial transmembrane potential

LIST OF FIGURES

Figure 1.1 Schematic representations of morphological changes during apoptotic cell death at various stages from left to right.	4
Figure 1.2 Phosphatidylserine exposure during apoptotic cell death.	6
Figure 1.3 Activation of caspase cascade and simplified model of intrinsic and extrinsic apoptotic pathways.....	10
Figure 1.4 Induction of apoptosis and GSH depletion.....	17
Figure 1.5 Chemical structures of cardamomin and chalcone.	20
Figure 1.6 THP-1 monocytes and THP-1-derived macrophages cell surface markers.	32
Figure 2.1 Assembly of transfer sandwich for western blotting.....	51
Figure 3.1 Effect of cardamomin in human cancer cell lines.....	64
Figure 3.2 Effect of cardamomin-Cu(II) in cancer human cell lines.....	65
Figure 3.3 Effect of cardamomin-Fe(II) in human cancer cell lines.	66
Figure 3.4 Effect of cardamomin-B in human cancer cell lines.....	67
Figure 3.5 Effect of hydrazinium-cardamomin in human cancer cell lines.	68
Figure 3.6 Effect of acetyl-cardamomin in human cancer cell lines.	69
Figure 3.7 Effect of allyl-cardamomin in human cancer cell lines.	70
Figure 3.8 Effect of methoxyamine-cardamomin in human cancer cell lines.	71
Figure 3.9 Effect of phenylamine-cardamomin in human cancer cell lines.	72
Figure 3.10 Effect of OBn-cardamomin in human cancer cell lines.	73
Figure 3.11 Effect of OMe-cardamomin in human cancer cell lines.....	74
Figure 3.12 Effect of 4-fluoro-cardamomin in human cancer cell lines.....	75
Figure 3.13 Effect of hydroxylamine-cardamomin in human cancer cell lines....	76
Figure 3.14 Effect of urea-cardamomin in human cancer cell lines.....	77
Figure 3.15 Effect of thiourea-cardamomin in human cancer cell lines.....	78
Figure 3.16 Effect of tetrahydro-cardamomin in human cancer cell lines.	79
Figure 3.17 Effect of flavanol-cardamomin in human cancer cell lines.....	80
Figure 3.18 Effect of flavanone-cardamomin in human cancer cell lines.....	81
Figure 3.19 Effect of cardamomin-I(II) in human cancer cell lines.	82
Figure 3.20 Effect of cardamomin-Br(II) in human cancer cell lines.	83
Figure 3.21 Effect of benzoyl-cardamomin in human cancer cell lines.	84
Figure 3.22 Effect of cardamomin in normal human cell lines.....	90

Figure 3.23 Effect of cardamonin-Cu(II) in normal human cell lines.	91
Figure 3.24 Effect of cardamonin-Fe(II) in normal human cell lines.	92
Figure 3.25 Effect of cardamonin, cardamonin-Cu(II) and cardamonin-Fe(II) in human Jurkat T cells.	96
Figure 4.1 Effect of cardamonin, cardamonin-Cu(II) complex and cardamonin-Fe(II) complex on THP-1 monocytes cell viability.	103
Figure 4.2 Cellular morphology of THP-1 monocytes and PMA-induced differentiation to THP-1-derived macrophages.	107
Figure 4.3 Expression of CD11b surface markers in THP-1 monocytes and THP-1-derived macrophages.	109
Figure 4.4 Effect of cardamonin, cardamonin-Cu(II) complex and cardamonin-Fe(II) complex on THP-1-derived macrophages cell viability.	111
Figure 4.5 p38 MAP kinase inhibitor IV. Synonym: 2,2'-Sulfonyl-bis-(3,4,6-trichlorophenol).	113
Figure 4.6 Effect of cardamonin, cardamonin-Cu(II) complex and cardamonin-Fe(II) complex on THP-1-derived macrophages cell viability in the presence of a MAP kinase inhibitor, p38 MAP kinase inhibitor IV.	114
Figure 4.7 SB202190 p38 MAP kinase inhibitor IV. Synonym: 4-(4-Fluorophenyl)-2-(4-hydroxyphenyl)-5-(4-pyridyl)-1H-imidazole.	116
Figure 4.8 Effect of cardamonin, cardamonin-Cu(II) complex and cardamonin-Fe(II) complex on THP-1-derived macrophages cell viability in the presence of a MAP kinase inhibitor, SB202190.	117
Figure 4.9 Comparative effects of cardamonin, cardamonin-Cu(II) complex and cardamonin-Fe(II) complex on cell viability of THP-1 monocytes, THP-1-derived macrophages and p38 MAPK-inhibited THP-1-derived macrophages.	121
Figure 5.1 Effects of cardamonin and its complexes (IC₅₀ values) on cell viability in Jurkat leukemia T cells in the absence or presence of caspase inhibitor, Z-VAD-FMK (50 or 100 μM).	130
Figure 5.2 Effects of cardamonin and its complexes (IC₅₀ values) on morphological and nuclear DNA changes in Jurkat leukemia T cells.	133
Figure 5.3 Flow cytometry examination of apoptosis, necrosis and cell viability – the Annexin V-FITC/PI assay.	135

Figure 5.4 Effect of cardamonin, cardamonin-Cu(II) and cardamonin-Fe(II) on the activation of caspase-3, -8 and -9 and the cleavage of PARP-1 in Jurkat T cells.	137
Figure 5.5 Effects of cardamonin and its complexes on the MMP in Jurkat T cells.	138
Figure 6.1 Effects of cardamonin, cardamonin-Cu(II) and cardamonin-Fe(II) complexes on cell viability in the presence or absence of NAC in Jurkat T cells.	149
Figure 6.2 Effects of cardamonin, cardamonin-Cu(II) and cardamonin-Fe(II) complexes on intracellular ROS levels in Jurkat T cells.	151
Figure 6.3 Effects of cardamonin, cardamonin-Cu(II) and cardamonin-Fe(II) complexes on intracellular GSH levels in Jurkat T cells.	153
Figure 6.4 Effects of cardamonin, cardamonin-Cu(II) and cardamonin-Fe(II) complexes on cell viability in the presence or absence of L-cysteine in Jurkat T cells.	155
Figure 6.5 Effects of cardamonin, cardamonin-Cu(II) and cardamonin-Fe(II) complexes on cell viability in the presence or absence of D-cysteine in Jurkat T cells.	157
Figure 6.6 Effects of cardamonin, cardamonin-Cu(II) and cardamonin-Fe(II) complexes on cell viability in the presence or absence of GSH in Jurkat T cells.	159
Figure 6.7 Effects of cardamonin, cardamonin-Cu(II) and cardamonin-Fe(II) complexes on cell viability in the presence or absence of Trolox in Jurkat T cells.	161
Figure 6.8 Effects of cardamonin, cardamonin-Cu(II) and cardamonin-Fe(II) complexes on intracellular ROS levels in the presence or absence of Z-VAD-FMK in Jurkat T cells.	163
Figure 6.9 Effects of cardamonin, cardamonin-Cu(II) and cardamonin-Fe(II) complexes on intracellular GSH levels in the presence or absence of Z-VAD-FMK in Jurkat T cells.	165
Figure 7.1 Proposed model of cardamonin-, cardamonin-Cu(II) and cardamonin-Fe(II)-induced apoptosis in Jurkat T cells.	179

LIST OF TABLES

Table 1.1 Inhibitory constant of Z-VAD-FMK caspase inhibitor for mammalian caspases and caspases function	12
Table 1.2 Inducers of oxidative stress and apoptosis.....	14
Table 1.3 Summary of cytotoxicity and oxidative/ anti-oxidative properties of cardamonin.....	22
Table 1.4 Chemical structure of cardamonin derivatives used in this study.....	25
Table 2.1 Number of cells seeded and volume of MTS / PMS solution added for the different cell lines.....	44
Table 2.2 Recipes for buffers and gels	47
Table 2.3 BSA standards preparation.....	50
Table 2.4 Dilutions of primary antibodies and secondary antibodies used for immunodetection.....	53
Table 3.1 IC₅₀ values of cardamonin and its derivatives in human lung A549 and human nasopharyngeal cancer HK1 cell lines following 24, 48 and 72 hrs treatment.....	85
Table 3.2 Summary of the IC₅₀ values in human lung cancer A549, human nasopharyngeal cancer HK1, human normal MRC5 lung, human normal Hs68 foreskin cell lines following 24 hrs treatment.....	93
Table 3.3 Selectivity of the cytotoxicity of cardamonin, cardamonin-Cu(II) and cardamonin-Fe(II) to A549 lung and HK1 nasopharyngeal cancer cell lines as compared with MRC5 lung and Hs68 foreskin normal cell lines.....	94
Table 3.4 Summary of the IC₅₀ values in human lung cancer A549, human nasopharyngeal cancer HK1, human normal MRC5 lung, human normal Hs68 foreskin and Jurkat T cell lines following 24 hrs treatment	96

CHAPTER 1: INTRODUCTION

1.1 Cell death mechanism

In response to cytotoxic stimuli, cell death can occur either through apoptotic or necrotic cell death. Identifying the cell death pathway provides important clues for designing and improving therapeutic approaches.

1.1.1 Apoptosis

One of the main targets for anti-cancer therapy is the induction of cell apoptosis, programmed cell death (Denicourt and Dowdy 2004). External signals generated in the mitochondria or propagated within cells by receptors in the plasma membrane trigger apoptosis. These pathways that trigger apoptosis involve the activation of caspases, which are previously dormant cysteine-proteases (Llado et al. 2008). Initiator caspases are the first caspases activated by cell death signals. Depending on the apoptotic pathway used, initiator caspase-8 is associated with the extrinsic pathway while caspase-9 is associated with the intrinsic mitochondrial pathway (Basu et al. 2006). These proteins that undergo proteolysis subsequently activate effector caspases, caspase-3, -6 and -7, which when activated results in the cleavage of multiple target proteins (Haupt 2003). Some morphological and functional changes identified during an apoptotic process have been characterised including the changes in cell membrane, mitochondrial dysfunction, and changes in cell nucleus (Geske and Gerschenson 2001). The cell membrane of apoptotic cells externalise phosphatidylserine (PS) to the outer cell membrane to trigger the removal of apoptotic cells by phagocytic cells *via* PS recognition (Krahling et al. 1999). During an apoptotic event, the opening of the permeable transition pore disrupts the

mitochondrial inner transmembrane potential (Green and Kroemer 1998) leading to the release of pro-apoptotic protein known as apoptosis-inducing factor. This protein induces DNA fragmentation and apoptosis by the activation of endonucleases (Susin et al. 1997). The morphology of dying cell undergoes rapid changes such as nucleus and chromatin condensation, cell shrinkage, nuclear fragmentation, as well as blebbing of the plasma membrane. Subsequently, cell breaks up into apoptotic bodies, which are membrane-enclosed fragments. These apoptotic bodies are recognised and engulfed by macrophages or neighbouring cells rapidly (Orrenius et al. 2011).

1.1.1.1 Morphological changes

Based on morphological grounds, Kerr et al. (1972) established the concept of cell death as a process of disposing unwanted cells during normal cell turnover in proliferating tissues, embryonic development and pathological situations. ‘Apoptosis’ was the term coined by these investigators to describe this form of cell death and has since found wide acceptance. Cells dying *via* apoptosis in general displays a very uniform pattern of morphological changes (Häcker 2000). Apoptosis can often be detected easily under the microscope. Various changes can be observed by light microscope and sometimes with the aid of specific dyes. However, certain changes such as the loss of microvilli, changes to organelles, mitochondria swelling or condensation as well as dilatation of the endoplasmic reticulum can only be detected by electron microscope. A dying cell, as observed by light microscopy, starts to show protrusions from the plasma membrane, known as “blebs” or cell “blebbling”. Blebs form when pressure is generated by actomyosin contraction. Proteins that are recruited to bleb membranes give rise to bleb contractions and retractions (Julian and

Olson 2015). Cells stained with DNA dyes allow direct observation of the cell nucleus condensation. Prominent morphological changes in apoptosis are most notable on the cell nucleus. Dying cells stained with DNA dye often display condensed ring/ sphere along the nuclear envelope in the beginning. The dye will continue to extend to encompass the entire nucleus of the dying cell. Subsequently, the condensed nucleus starts to sever attachments to disassemble into several fragments. Consequently, the entire cell condenses and reorganises into apoptotic bodies that are membrane-bound vesicles made up of cytosolic elements, parts of condensed nuclei or organelles in various combination containing the contents of the cell (Kerr et al. 1972, Häcker 2000, Ziegler and Groscurth 2004, Elmore 2007). These morphological changes during apoptosis are demonstrated in **Figure 1.1** as a schematic representation.

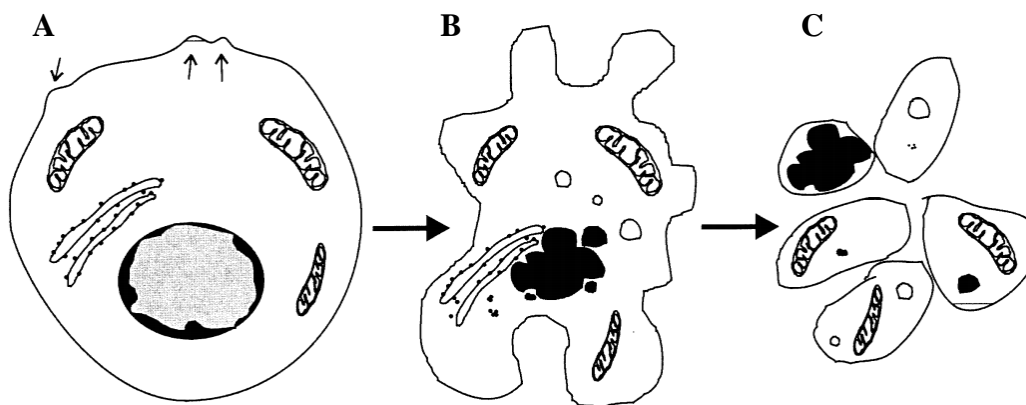


Figure 1.1 Schematic representations of morphological changes during apoptotic cell death at various stages from left to right.

Initial changes involved nuclear chromatin condensation along the perimeter of the cell nucleus and protrusion of the plasma membrane (A), as indicated by arrows. Blebbing of the cell starts to appear as the nucleus continues to condense completely and the cell shrinks (B). The nucleus segregates into several fragments while the organelles generally stays intact. During the late stages of apoptosis, cell disintegrates into apoptotic bodies that contain any parts of the cellular material (C). Finally, apoptotic bodies are taken up and digested by other cells *via* a lysosomal pathway. Figure adapted from Häcker (2000).

1.1.1.2 Phosphatidylserine externalisation

In normal cell membranes, the active maintenance of membrane phospholipid asymmetry is universal. Subsequent disruption with externalisation of PS is therefore a hallmark of apoptotic cells (Kagan et al. 2000). Studies have shown that the externalisation of PS serves as a vital signal for cell targeting and elimination of apoptotic cells by macrophages (Fadok et al. 1992, Savill et al. 1993, Savill 1997). The process of apoptosis includes important changes to the apoptotic cell membrane. The typical feature of eukaryotic cells' plasma membrane is asymmetric distribution of lipids between the outer and inner leaflet where phosphatidylcholine and sphingomyelin are predominantly presented on the outer leaflet. On the other hand, PS, phosphatidylethanolamine and phosphatidylinositol are confined to the inner leaflet of the membrane (Leventis and Grinstein 2010). During apoptosis, the plasma membrane loses its lipid asymmetry and extracellular exposure of PS increases (Bever and Williamson 2010). **Figure 1.2** displays the common feature of plasma membrane in normal eukaryotic cells, and the changes to PS exposure during apoptosis.

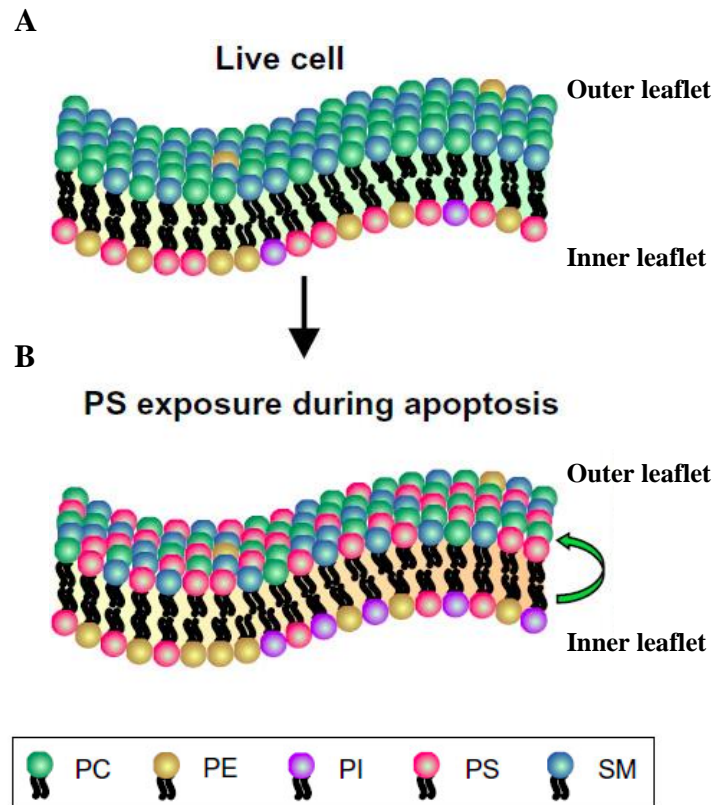


Figure 1.2 Phosphatidylserine exposure during apoptotic cell death.

Plasma membrane of normal eukaryotic cells (A) and plasma membrane of apoptotic eukaryotic cells (B). PC indicates phosphatidylcholine; PE indicates phosphatidylethanolamine; PI indicates phosphatidylinositol; PS indicates phosphatidylserine; and SM indicates sphingomyelin. Figure adapted from Julian and Olson (2015).

Translocation of PS to the external cell surface can be used as a sensitive probe to detect apoptosis. However, it is important to note that translocation of this phosphoprotein is not unique to apoptosis and occurs during cell necrosis. The major difference between apoptotic and necrotic cells is that immediately necrosis occurs, the cell membrane loses its integrity, while the cell membrane undergoing initial stages of apoptosis will remain intact. Therefore, the detection of externalised PS using a staining agent with an additional dye exclusion test of the cell membrane integrity allow discrimination between normal, early apoptotic, late apoptotic or necrotic cells (Vermes et al. 1995).

1.1.1.3 Mitochondrial membrane potential

Apart from being the source of energy in supporting life under aerobic conditions, the mitochondria is also the source of initiation in apoptotic cell death signaling pathway (Gottlieb 2000). Numerous studies have established that apoptotic cell death is related to mitochondrial membrane potential (MMP), typically for cancer cells (Scarlett et al. 2000, Hu and Kavanagh 2003). Mitochondrial regulation of apoptosis can be described at various levels including maintenance of ATP production (Leist and Nicotera 1997), regulation of MMP, as well as control of mitochondrial membrane permeability from the release of apoptogenic factors (Zoratti and Szabò 1996, Green and Kroemer 1998, Kroemer and Reed 2000). The inner membrane is highly resistant to proton leakage that leads to significant buildup of membrane potential. The decrease in MMP is known to cause activation of mitochondrial pro-apoptotic factors (Gottlieb 2000). Primarily, the mitochondrial inner membrane is rich of negatively charged glycoprotein giving the inner membrane a negatively charged potential. The presence of large proton accumulation outside the inner membrane result in the transmembrane potential between the mitochondrial membrane. Hence, the loss of MMP balance can be detected using permeable cationic dyes that have the ability to enter the mitochondria based on the highly negative mitochondrial potential. The depolarisation of MMP leads to loss of the cationic dye intensity indicating cells undergoing apoptotic cell death.

1.1.1.4 Caspases

Caspases are key effector molecules of apoptosis that exist mostly as inactive precursors. These effector molecules kill the cell once activated, playing a major role in the execution of apoptotic cell death. A total of 14 caspases, caspase-1 to caspase-14, have been identified in mammalian cells with all expressed in human except caspase -11, -12 and -13 (Yan and Shi 2005). These caspases are divided into three groups depending on the function and homology. These include initiator caspases (-2, -8, -9 and -10), effector caspases (-3, -6 and -7) and inflammatory mediator caspases (-1, -4, -5, -11, -12, -13 and -14) (Zimmermann et al. 2001). Initiator caspases in general works upstream of the effector caspases where activation of initiator caspases induce apoptotic signals by cleaving effector caspases. Activation of effector caspases leads to cleavage of essential proteins in the cells. The cleavage of cell chromatin (Margolin et al. 1997) and protein, that supports the cell nuclear membrane, leads to dismantling of cell nucleus (Nicholson and Thornberry 1997).

Two main pathways that activate caspases are the extrinsic and intrinsic pathways. Extrinsic pathway is activated due to receptor-mediated signalling such as binding of the Fas ligand leading to recruitment of FAS-associated death domain protein (FADD). The recruitment of FADD activates caspase-8, which cleaves executioner caspase-3 and -7 causing apoptosis as shown in **Figure 1.3A** (Hengartner 2000). Intrinsic pathway is activated by intracellular stress including cytotoxic drugs, radiation and nutrient starvation (Boatright and Salvesen 2003) and involves activation of B cell lymphoma 2 (BCL-2) family proteins (Hipfner and Cohen 2004, Julian and Olson 2015). Activated BCL-2 homology 3 (BH3)-only proteins leads to

BCL-2 antagonist (BAK) and BCL-2 associated X proteins (BAX) activation and mitochondrial outer membrane permeabilisation. The permeabilisation of the membrane leads to the release of proteins that promote caspase activation. The release of cytochrome c binds to apoptotic protease-activating factor 1 (APAF1) and forms apoptosome, which recruits and activates the initiator caspase-9 as shown in **Figure 1.3B**. The activation of caspase-9 further leads to the cleavage of executioner caspases, such as caspase-3 and -7, subsequently activating apoptosis (Tait and Green 2010).

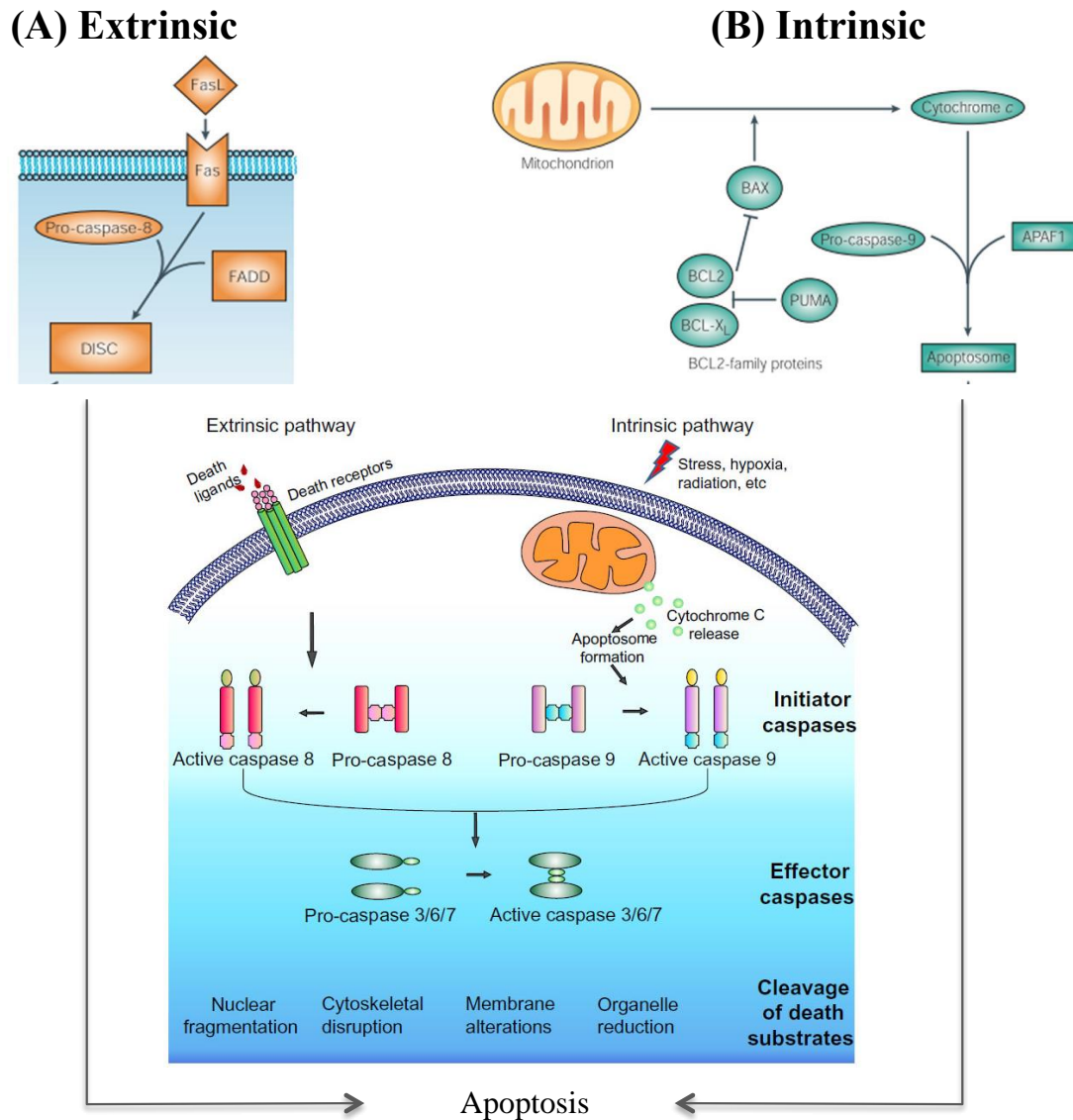


Figure 1.3 Activation of caspase cascade and simplified model of intrinsic and extrinsic apoptotic pathways.

Extrinsic pathway activated by receptor-mediated signalling such as binding of the Fas ligand and activation of initiator caspase-8 of the extrinsic pathway (A). Intrinsic pathway activated by intracellular stress stimulating BCL-2 family protein activation and mitochondrial outer membrane permeabilisation and release of cytochrome c that binds to APAF1 to form apoptosome and activation of caspase-9 (B). Figure adapted from Hipfner and Cohen (2004) and Julian and Olson (2015).

1.1.1.5 Caspase inhibitors

Activation of caspases is controlled by a variety of inhibitors which interact directly with the protease (Ekert et al. 1999). There are several types of caspase inhibitors available commercially including Z-VAD-FMK that works by inhibiting the activation of initiator or effector caspases. This peptide caspase inhibitor has been shown to block caspase activity *in vitro* with inhibitory constant at low nanomolar range. **Table 1.1** presents the research carried out by Garcia-Calvo et al. (1998) reporting the inhibitory constant of Z-VAD-FMK caspase inhibitor for mammalian caspases and the function of different caspases in mammals. Z-VAD-FMK was originally developed for therapeutic uses but unforeseen cytotoxicity of this compound limited its potential as a drug. However, to date, Z-VAD-FMK remains a key compound for studies on apoptosis (Van Noorden 2001).

Table 1.1 Inhibitory constant of Z-VAD-FMK caspase inhibitor for mammalian caspases and caspases function.

Caspases	Z-VAD-FMK inhibitory constant expressed as $t_{1/2}$ * at 1 μ M in seconds	Key Function
Caspase 1	2.5	Inflammation
Caspase 2	2400	Less easily categorised
Caspase 3	43	Apoptosis - executioner caspase
Caspase 4	130	Inflammation
Caspase 5	5.3	Inflammation
Caspase 6	98	Apoptosis – Executioner caspases
Caspase 7	39	Apoptosis – Executioner caspases
Caspase 8	2.5	Apoptosis – Initiator caspase (Extrinsic pathway)
Caspase 9	3.9	Apoptosis – Initiator caspase (Intrinsic pathway)

*Half-life ($t_{1/2}$) is the time required for the concentration to fall to 50% of its current value. Information gathered from (Garcia-Calvo et al. 1998, Ekert et al. 1999, Van Noorden 2001, McIlwain et al. 2013).

1.1.2 Necrosis

Necrosis is a very rapid form of cell death where every compartment of the cell disintegrates. Essentially, necrotic cell death is characterised by ion homeostasis dysregulation leading to dilation of endoplasmic reticulum and mitochondria, cell swelling and vacuoles formation in the cytoplasm. Contrary to apoptosis where caspases play a major role, lysosomal proteases mainly cathepsins B and D are mainly involved in necrosis. During necrosis, caspases may be activated due to cytochrome c release and mitochondrial damage but are not essential for cell death. During necrosis, chromatin forms clumps and the nuclear membrane disrupts. Cell lyses lead to the release of cell contents into the extracellular content where neighbouring cells may be

damaged and triggers an inflammatory response. In cells undergoing necrosis, ATP levels are depleted rapidly and the protein synthesis and genes transcription stops (Mattson and Bazan 2012).

1.2 Oxidative-stress-induced cell death

An appropriate balance in anti-oxidants and oxidants is required for the survival of mammalian cells (Buttke and Sandstrom 1994). Reactive oxidants encountered by organismal life are generated from internal metabolism and/ or exposure to environmental toxicants (Ma 2013). Buttke and Sandstrom (1994) suggested that mammalian cells actually benefit from this perilous existence mediating apoptosis by triggering oxidative stress. The authors reported that the depletion of cellular anti-oxidants or addition of reactive oxygen species (ROS) could result in apoptosis that is necessary for aerobic life and that oxidative stress mediated-apoptosis can be blocked by addition of compounds with anti-oxidant capabilities.

1.2.1 Reactive oxygen species

ROS can be divided into two groups: free radicals and non-radicals. Molecules of one or more unpaired electrons are free radicals, which give reactivity to the molecules. Non-radical forms are created when two free radicals share their unpaired electrons. The three main physiological significant ROS include superoxide anion ($O_2^{\bullet-}$), hydroxyl radical ($\bullet OH$), and hydrogen peroxide (H_2O_2) (Birben et al. 2012). Many studies have demonstrated that ROS and the resulting oxidative stress play a pivotal role in apoptosis (Forrest et al. 1994, Slater et al. 1995, Clutton 1997, Chandra et al.

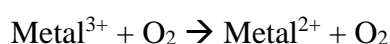
2000, Kannan and Jain 2000, Curtin et al. 2002, Ozben 2007, Franco et al. 2009, Matés et al. 2012). Reactive oxygen and nitrogen species are traditionally viewed as harmful. However, controlled production of ROS and antioxidants in normal cells is vital for regulating signalling pathways. Reactive oxidants act in concert with the antioxidant defence system to ensure the cells response to oxidants are adequate for the organism needs. Apoptosis can be triggered by numerous factors including drugs, pathophysiologic conditions, metals, ROS, pro-oxidants, ionising radiation and more (Kannan and Jain 2000). **Table 1.2** displays a partial list of some of these inducers.

Table 1.2 Inducers of oxidative stress and apoptosis.

Inducer of oxidative stress and apoptosis*	
Reactive oxygen species	Hydroxyl radical, superoxide radical, H ₂ O ₂
Diseases	Cancer, Alzheimer's, Parkinson's
Drugs	Staurosporine, taxol, cisplatin
Ionising radiation	Gamma, UV radiation
Metals	Iron, copper, chromium, cobalt, mercury, cadmium, nickel
Pro-oxidants	Diamide, etoposide, H ₂ O ₂ , semiquinones

*list is not inclusive. (Kannan and Jain 2000, Shi et al. 2004, Valko et al. 2005, Koppenol and Bounds 2012)

Addition of 1 electron to O₂ forms O₂^{•-}, a process mediated by xanthine oxidase, nicotine adenine dinucleotide phosphate [NAD(P)H], or mitochondrial electron transport system. Mitochondria are the main site for production of O₂^{•-} and usually oxygen reduction to water is through the mitochondrial electron transport chain. However, 1-3% of these electrons leak from the system and produce superoxides, which is converted into H₂O₂ by superoxide dismutase enzymes (SODs) and diffuse easily across the plasma membrane. In a series of reactions, Haber-Weiss and Fenton reactions, H₂O₂ and O₂^{•-} can interact with transition metals like copper and iron to form OH radicals *via* the metal catalysed reaction as shown in the equation below (Haber and Weiss 1934, Fenton 1984, Birben et al. 2012).



OH radicals are the most reactive form of ROS and can lead to DNA, proteins, lipids, and carbohydrates damage. Typically, the mechanisms by which ROS induce apoptosis involve caspase activation, receptor activation, mitochondrial dysfunction and BCL-2 family proteins. Depending on the cellular content, various protein kinase activities modulate the apoptotic program such as mitogen-activated protein kinases (MAPK), protein kinases -B/ -C (PKB/ PKC) as well as their corresponding phosphatases (Ryter et al. 2007).

1.2.2 Glutathione

Anti-oxidants function to counterbalance the effects of oxidants. There are enzymatic anti-oxidants (catalase, superoxide dismutase, glutathione peroxidase, etc.) and non-enzymatic anti-oxidants (vitamin A, vitamin C, vitamin E, β -carotene, low molecular weight compounds, GSH, etc.) (Birben et al. 2012). Glutathione (GSH) is a vital component in the cellular anti-oxidant defence mechanisms that protect cells from oxidative stress. The ratio between oxidised and reduced GSH in the body is one of the major determinants of oxidative stress. GSH exhibits anti-oxidant effects by detoxifying H_2O_2 and lipid peroxide *via* glutathione peroxidase (GPx). GSH donates its electron to H_2O_2 and reduce it to H_2O and O_2 . Oxidised glutathione (GSSG) is reduced into GSH by the enzyme GSH reductase using NADPH as the electron donor (Deponete 2013). GSH also protects cells from apoptosis by interacting with anti-apoptotic and pro-apoptotic signalling pathways (Masella et al. 2005). When cell undergoes oxidative stress, intracellular GSH is expected to deplete. Over formation of GSSG may exceed the ability of the cell to recycle it to GSH during oxidative stress resulting in a net loss of intracellular GSH (Nur et al. 2011). Consequently, depletion of intracellular GSH can cause or result in oxidative stress that leads to cell death through ROS or oxidative stress-mediated mechanisms. Cell death that is independent of ROS formation has also been reported in GSH depleted cells (Pias and Aw 2002, Franco et al. 2007). GSH depletion and the possible mechanisms involved in the induction of apoptosis are shown in **Figure 1.4**.

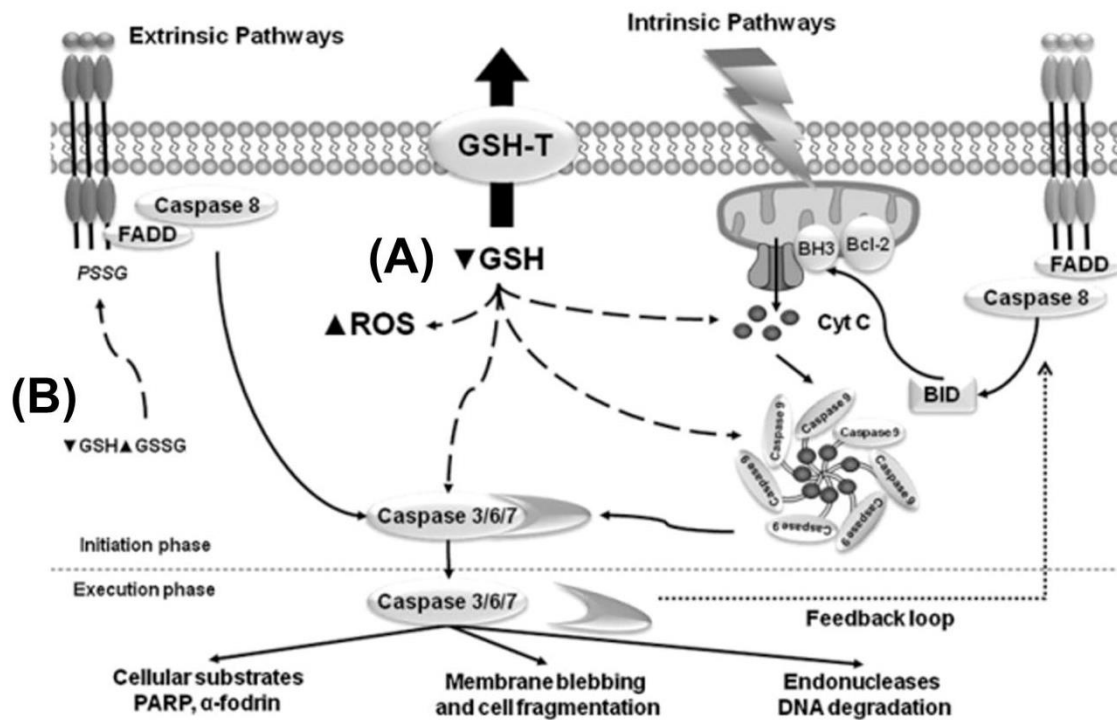


Figure 1.4 Induction of apoptosis and GSH depletion.

Apart from ROS formation, depletion of GSH is involved in the induction of apoptosis by activating executioner caspases and triggering transition of mitochondrial permeability. Depletion of GSH triggers pro-apoptotic functions like formation of apoptosome and release of cytochrome c (A). Increased GSSG induces formation of protein mixed disulfides (PSSG). Increased in PSSG accompanies apoptosis, induced by FasL (B). Hence depletion of GSH and increase in GSSG can promote formation of PSSG (Circu and Aw 2008, Franco and Cidlowski 2012). Figure taken from Franco and Cidlowski (2012).

1.3 Semi-synthetic natural products and cancer

It has been reported that in European pharmacies, 50% of the top fifty drugs sold are from natural products source and approximately 80% of the world's population rely on natural products as drugs or food/ herbal supplements (Zhu et al. 2004). Comparably, an analysis on source of novel drugs from 1981 to 2010 revealed that less than 40% of chemical entities were discovered without an inspiration from natural product structures (Newman and Cragg 2012). In pharmaceutical research, nature provides the main source of compounds. They present an organic chemical compound of interest or serves as a source of inspiration in novel drug designs.

Disease evolution and development of resistance from the human body desperately urge the development of new drugs in different areas of research including pharmacology, natural product chemistry, molecular biology, synthetic organic chemistry, biochemistry and more (Lourenço et al. 2012). The ability to complete- or semi-synthesise compounds is important in most cases where the availability of natural sources is scarce and there is a need to produce sufficient materials for biological screening and application. However, the biochemistry involved in the biosynthesis of active molecules is complex and continues to be challenging for scientists. The slow progress in treating fatal diseases such as cancer indicates a rising need for novel approaches to physiological targets through effective therapeutics delivery.

Development of natural product derivatives remains an important goal in enhancing the bioactivity of a compound. The different strategies for designing and semi-synthesising a natural product analogue include function-oriented synthesis, biology-oriented synthesis, hybrid molecules, and complexity to diversity (Maier 2015). Example of different ways to optimise a compound includes modification of the functional groups, inversion or addition of stereocentres (Cragg et al. 2009). The privileged structure of natural products is that there are endless ranges of new chemical structures yet to be discovered and these ready available structures are a large source of biologically active compounds. Introducing natural products derivatives to chemical structures, that are often considered extremely unstable, has the ability to develop a compound with increased stability. A major drawback of using natural products as drug leads is that they exist in very small quantities. For example, dolastatin, an inhibitor of the P388 lymphocytic leukaemia growth (Pettit et al. 1989), isolated from the Indian Ocean only yielded $4 \times 10^{-7}\%$ of 6.2 mg from 1,600 kg of wet sea hare. Hence, the great need to synthesise compounds in the laboratory becomes obvious considering the percentage of low yield and the damage made to the ecological system. These lead compounds can then be further developed into analogues and complexes, which in turn can be pharmacologically optimised *via* SAR studies (Cragg et al. 2009). A good example of the advantages of semi-synthesising is the semi-synthesis of Taxol, a naturally occurring compound isolated from Pacific yew tree (Wall and Wani 1996) that exhibits anti-cancer and anti-leukaemic properties (Wani et al. 1971). Total synthesis of Taxol involves 30 steps whereas the semi-synthesis of Taxol using 10-deacetylbaccatin as starting material, found abundantly in the needles of many of the *Taxus* species (Kingston 2008, Cragg et al. 2009), narrowed down the synthesis of Taxol to only 3 steps.

1.4 Cardamonin as potential lead compound

Cardamonin is a naturally occurring chalcone that was first isolated from the seeds section of *Amomum subulatum* from the Zingiberaceae family (Bheemasankara et al. 1976). Cardamonin was also reported in other species of the Zingiberaceae (Jantan et al. 2008, Chow et al. 2012, Zhang et al. 2014), Nepenthaceae (Ahmad et al. 2006) and Piperaceae (de Castro et al. 2015) family. **Figure 1.5** displays the chemical structure of cardamonin, a chalcone belonging to the flavonoid family.

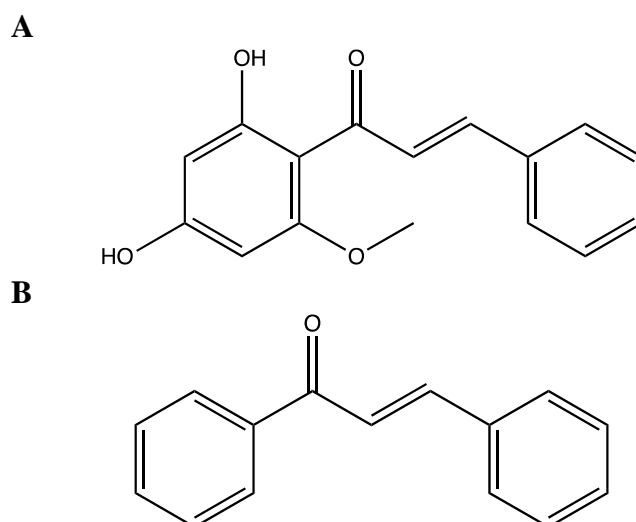


Figure 1.5 Chemical structures of cardamonin and chalcone.

1-(2,4-dihydroxy-6-methoxyphenyl)-3-phenyl-2-propen-1-one, cardamonin (**A**) and 1,3-diphenyl-2-propen-1-one, chalcone (**B**).

The aromatic enones core structure of chalcone, 1,3-diphenyl-2-propenone is often responsible for the yellow pigmentation of plants (Ni et al. 2004, Yadav et al. 2011, Sahu et al. 2012). In fact, the name chalcone originated from the Greek word *chalkos* meaning copper/ bronze. Flavonoids are subclasses of polyphenols, many of which have the ability to alter metabolic processes contributing to positive impact on health (Beecher 2003). Flavonoids are aromatic compounds with a phenylchromanone unit, which consists of two benzene rings linked by an oxygen atom and 3 carbons to

form a central pyrone ring. Previous studies have shown that flavonoids possess antimetabolic activity (Cárdenas et al. 2006), inhibition properties of cyclin-dependent kinases, aromatase, protein kinase C or topoisomerase (Hirvonen et al. 2001) making this group of family ideal as an anti-cancer treatment. A plethora of studies have shown the anti-cancer potential of both natural and synthetic flavonoids (Ren et al. 2003, Teillet et al. 2008, Khoo et al. 2010, Shukla and Gupta 2010, Batra and Sharma 2013). Natural flavonoids appear in diverse forms due to their substitution pattern *via* hydroxylation, methoxylation, glycosylation or prenylation (Menezes et al. 2016). Depending on the opening of the central pyran ring or the saturation level of flavonoids, they are further categorised into different subclasses including chalcones, flavanones, flavonols, flavones and isoflavones (Harborne and Williams 2000). In the last decades, several types of chalcones have attracted much attention in medicinal chemistry including cardamonin (Win et al. 2007, Ohtsuki et al. 2009, Lin et al. 2012, Qin et al. 2012, Yadav et al. 2012), licochalcone A (Xiao et al. 2011), xanthoangelol (Tabata et al. 2005), xanthohumol (Gerhauser et al. 2002, Magalhães et al. 2009), and hesperidin methyl-chalcone that has reached clinical trials testing stage (Boyle et al. 2003). Numerous studies have reported the cytotoxicity (Murakami et al. 1993, Li et al. 2008, Simirgiotis et al. 2008, Dzoyem et al. 2012, Kuete et al. 2014) and oxidative state (Mohamad et al. 2004, Ahmad et al. 2006, Li et al. 2008, Simirgiotis et al. 2008, Aderogba et al. 2012, Yadav et al. 2012) of cardamonin. **Table 1.3** summarises various studies carried out to determine the cytotoxicity and oxidative/ anti-oxidative properties of cardamonin. Overall, a large number of studies reported notable cytotoxicity properties in cardamonin however; there are conflicting findings on the oxidative state of this compound where cardamonin has shown the ability to act as a pro-oxidant as well as an anti-oxidant.

Table 1.2 Summary of cytotoxicity and oxidative/ anti-oxidative properties of cardamonin.

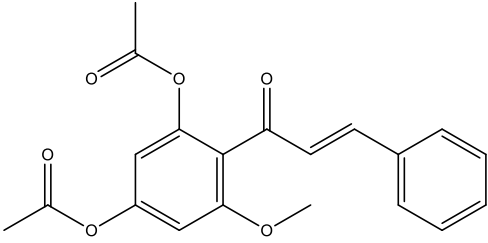
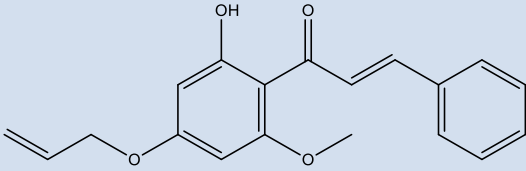
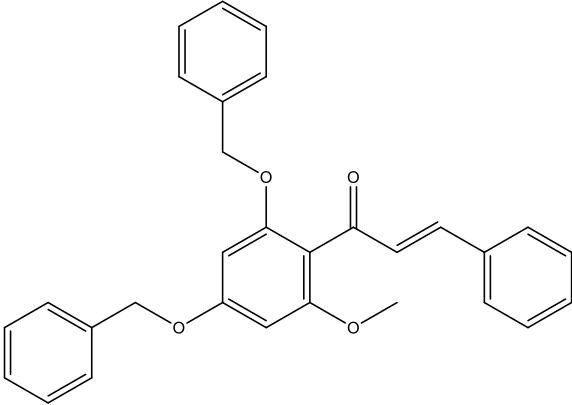
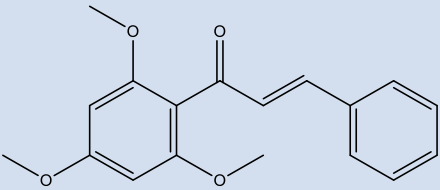
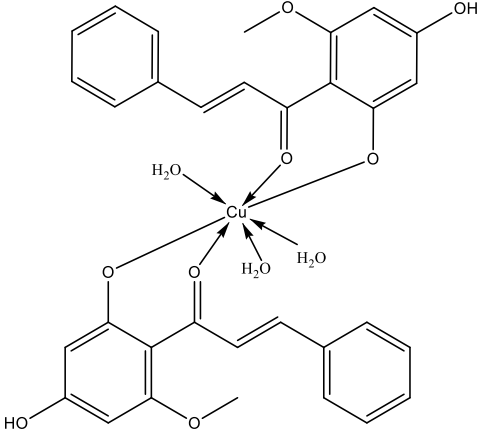
Cytotoxicity Studies		
Findings	Mode of study	Reference
Cardamonin inhibited the growth and proliferation of multiple myeloma cells in a dose dependent manner against RPMI 8226, U-266, and ARH-77 cell lines following 24 hrs and 48 hrs treatment. In RPMI 8226 cells, Cardamonin activated caspase-3 and PARP; down-regulated the expression of anti-apoptotic proteins Bcl-2, Bcl-xL, survivin, XIAP, cIAP-1 and cIAP-2; down-regulated expression of IKK α , IKK- β , I κ B α ; inhibited phosphorylation of NF- κ B which led to significant decrease of intracellular p65 in cell nucleus.	Human multiple myeloma cells (RPMI 8226, U-266, ARH-77)	Qin et al. (2012)
Cardamonin displayed cytotoxicity against K-562 and SMMC-7721 cell lines with IC ₅₀ values of 3.2 mg/L (11.84 μ M) and 3.5 mg/L (12.95 μ M) respectively.	Human chronic myelogenous leukemia (K-562) and human hepatoma (SMMC-7721) cells	Tang et al. (2010)
Cardamonin exhibited cytotoxicity against DLD1 cells with IC ₅₀ values of 41.8 μ M following 24 hrs treatment; lowered the expression of Bcl-xL protein, enhanced death receptor 5 (DR5) and death receptor 4 (DR4) following the activation of caspase-3, -8 and -9 in DLD-1/TR cells, sensitising TRAIL-resistant cells.	Human gastric adenocarcinoma (AGS) and TRAIL-resistant human colon cancer (DLD-1/TR) cells	Ohtsuki et al. (2009)
Cardamonin displayed cytotoxicity against A549, L-02, SGC-7901, MDA-MB-231, SMMC-7721, H7402, HepG2, 4T1 ^{luc} with IC ₅₀ values of 109.79 μ g/mL (406.21 μ M), 33.16 μ g/mL (122.69 μ M), 16.58 μ g/mL (61.34 μ M), 12.32 μ g/mL (45.58 μ M), 16.74 μ g/mL (61.94 μ M), 4.91 μ g/mL (18.17 μ M), and 14.34 μ g/mL (53.06 μ M), respectively following 48 hrs treatment; Cardamonin decreased Bcl-2 expression, increased Bax protein expression, cleaved caspase-3 and -9, and induced G2/M-phase arrest in MDA-MB-231 cells.	Human lung carcinoma (A549), normal human hepatocyte (L-02), human gastric carcinoma (SGC-7901), human breast cancer (MDA-MB-231), human hepatocarcinoma (SMMC-7721), human liver cancer (H7402), and human liver carcinoma (HepG2)	Mi et al. (2016)
Cell viability of HCT116, KBM-5, U-266, MIA PaCa-2, DU145 and PC-3 cell lines pre-treated with 20 μ M Cardamonin for 24 hrs were \approx 45, 91, 93, 90, 88 and 89% respectively. Cardamonin enhanced TRAIL-induced apoptosis from 7 to 81% and activates caspase-3, -8, -9 and cleaved PARP in HCT116 cells. Cardamonin up-regulated DR5 and DR4 expression in a dose- and time-dependent manner; down-regulated expression of decoy receptor 1 (DcR1) but did not affect decoy receptor 2 (DcR2), effects were not cell-type specific. Cardamonin down-regulated expression of survival proteins (cIAP-1, cFLIP, XIAP, Bcl-2 and survivin) and up-regulated expression of pro-apoptotic protein (Bax) in HCT116 cells.	Human colon adenocarcinoma (HCT116), human chronic leukemic cells (KBM-5), human multiple myeloma (U-266), human pancreatic carcinoma (MIA PaCa-2), human prostate cancer cells (PC-3 and DU145)	Yadav et al. (2012)
Cardamonin displayed cytotoxicity against PC-3 cells with 50% of growth inhibition (GI ₅₀) of 11.35 μ g/mL (42 μ M) following 48 hrs treatment; decreased expression of NF- κ B1 and induced apoptotic cell death as proven by DNA degradation Cardamonin-treated PC3 cells.	Human prostate cancer cells (PC-3)	Pascoal et al. (2014)

Cardamonin (30 μ M) exhibited 63.2% inhibitory effect against A549 cells following 48 hrs treatment. Cardamonin decreased number of synthesis (S) phase cells, inhibited DNA synthesis and increased A549 apoptotic cells.	Human lung carcinoma (A549)	Tang et al. (2014)
Cardamonin displayed no effect on cell viability at all concentrations tested (\leq 50 μ M) following 17-20 hrs treatment.	RAW 264.7 cells	Israf et al. (2007)
Cardamonin displayed cytotoxicity against SW480 cells with IC_{50} value of 35 μ M following 72 hrs treatment.	Human colon cancer cells (SW480)	Simirgiotis et al. (2008)
Cardamonin inhibited proliferation of β -catenin response transcription (CRT)-positive SW480, DLD-1, HCT116 and LS174T cells in a dose-dependent manner following 48 hrs treatment; increased cells in G2/M phases from 18.55% to 35.42% compared to untreated control following 24 hrs treatment with 80 μ M cardamonin.	Human colon cancer cells (SW480, DLD-1, HCT116, LS174T)	Park et al. (2013)
Cardamonin did not affect cell viability at all concentrations tested (50-0.78 μ M) and viability was always more than 95% following 17-20 hrs treatment.	Recombinant mouse interferon gamma and <i>E. coli</i> LPS (strain 055:B5)-induced RAW 264.7 cells	Ahmad et al. (2006)
Cardamonin displayed cytotoxicity against L-02 and HepG2 cells with IC_{50} value of 30.90 μ M and 22.63 μ M respectively following 48 hrs treatment.	Human normal liver cells (L-02) and human hepatoma cells (HepG2)	Li et al. (2008)
Cardamonin displayed cytotoxicity against THP-1, PC-3 and MCF-7 cells with IC_{50} value of 32.5 μ M, 49 μ M and 44 μ M respectively, both A549 and HeLa cells displayed IC_{50} values $>$ 50 μ g/ mL (184.99 μ M).	Human lung carcinoma (A549), human breast carcinoma (MCF-7), human prostate cancer cells (PC-3), human cervical carcinoma (HeLa), and human acute monocytic leukemic cell (THP-1) cell lines	Dzoyem et al. (2012)
Cardamonin inhibited cell viability against SKOV3 cells in a dose-dependent manner from the concentrations tested (1, 3, 10 and 30 μ M) following 48 hrs treatment.	Human epithelial ovarian cancer (SKOV3) cell line	Xue et al. (2016)
Cardamonin inhibited cell viability CD133 ⁺ GSC in a dose-dependent manner from the concentrations tested (20, 30 and 40 μ M) following 72 hrs treatment.	Human glioblastoma stem cells (CD133 ⁺ GSC)	Wu et al. (2015)
Oxidative/ Anti-oxidative Studies		
Cardamonin inhibited the generation of intracellular ROS.	Intracellular ROS level of recombinant mouse interferon gamma and <i>E. coli</i> LPS (strain 055:B5)-induced RAW 264.7 cells	Ahmad et al. (2006)
Cardamonin generated ROS in a dose-dependent manner; pre-treatment with NAC reduced DR5 and DR4 expression; NAC reversed effect of TRAIL-induced cardamonin cleavage of caspase-3, -8 and PARP in HCT116 cells.	Intracellular ROS level of HCT116 cells	Yadav et al. (2012)
DPPH: Cardamonin displayed anti-radical DPPH activity with IC_{50} value of 124 μ M; FRAP: Cardamonin displayed ferric reducing anti-oxidant power of 173 μ M (expressed as Trolox equivalents/ 500 μ mol).	Anti-radical DPPH activity, FRAP	Simirgiotis et al. (2008)
DPPH and superoxide anion assay: effects of Cardamonin were negligible at tested concentrations (\leq 200 μ M).	DPPH, superoxide anion	Li et al. (2008)
Cardamonin and pinocembrin did not inhibit 50% of DPPH free radical at 200 μ M, the highest concentration tested.	DPPH activity	Aderogba et al. (2012)

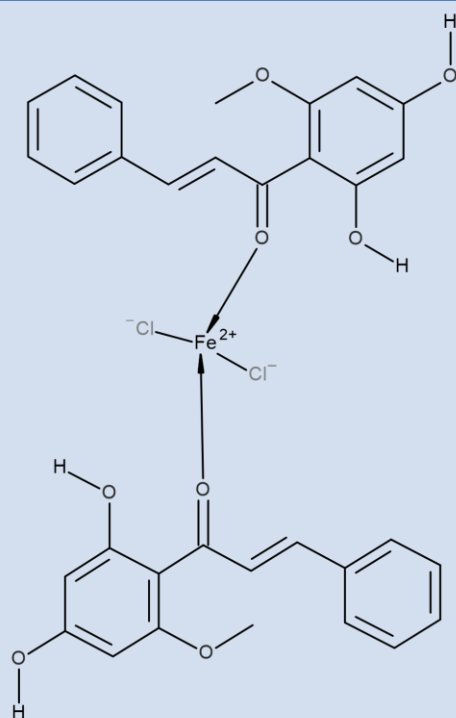
Recently, cardamonin has also attracted researchers to produce semi-synthetic derivatives/ analogues using cardamonin as the lead compound. A recent study investigated the cytotoxicity properties of two cardamonin analogues, 4,4'-dihydroxylchalcone (DHC) and 4,4'-dihydroxy-2'-methoxychalcone (DHMC), on lung cancer cells and results revealed that these analogues inhibited the survival of both primary lung cancer cells and lung cancer cell lines by suppressing the activation of NF-kappaB pathway (He et al. 2014). Furthermore, these two analogues were reported to show low cytotoxicity against normal lung cell lines, highlighting the cytotoxic selectivity of these analogues. Other studies carried out on compounds structurally related to cardamonin have demonstrated inhibitory effects on prostate cancer cells (Sun et al. 2010) as well as lung cancer cells (Nam et al. 2003, Srinivasan et al. 2009).

In this study, cardamonin derivatives semi-synthesised *via* metal complexation, cyclisation and condensation reactions (Break et al. 2018) were used to identify the bioactivity of novel bioactive analogues. **Table 1.4** displays the chemical structures of the cardamonin analogues used in this study.

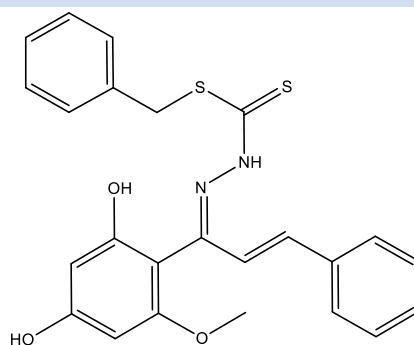
Table 1.4 Chemical structures of the cardamonin analogues used in this study.

Compounds	Chemical Structures
Acetyl-cardamonin	
Allyl-cardamonin	
OBn-cardamonin	
OMe-cardamonin	
Cardamonin-Cu(II)	

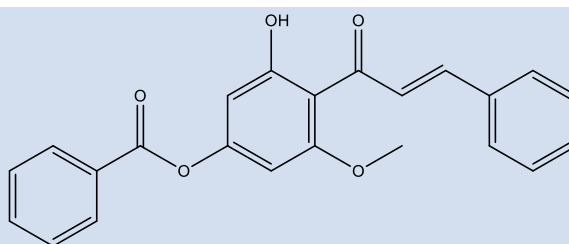
Cardamonin-Fe(II)



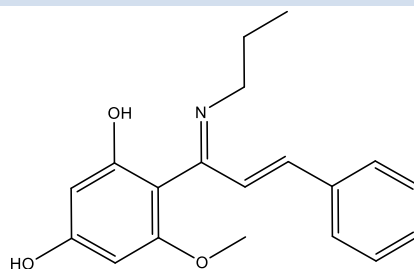
Cardamonin-B



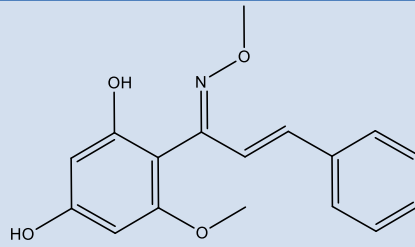
Benzoyl-cardamonin



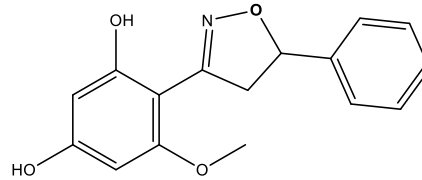
Phenylamine-cardamonin



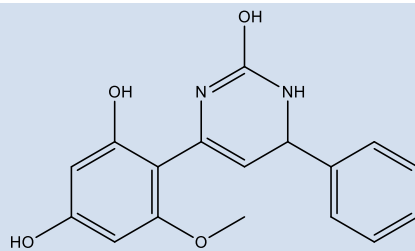
Methoxyamine-
Cardamonin



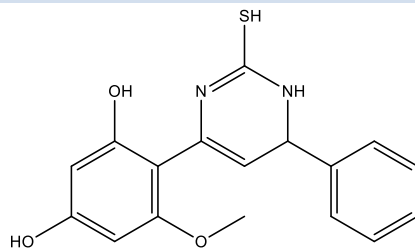
Hydroxylamine-
Cardamonin



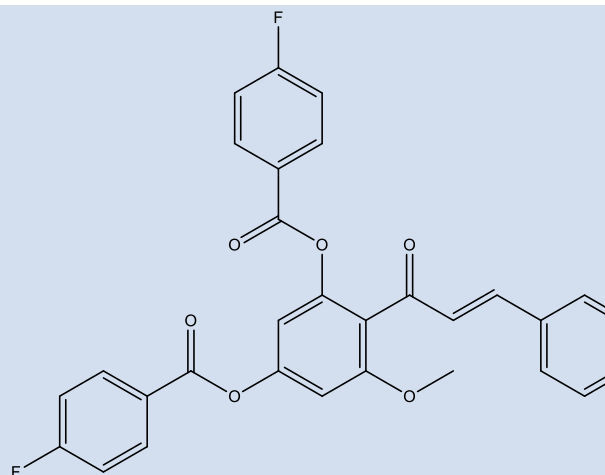
Urea-cardamonin



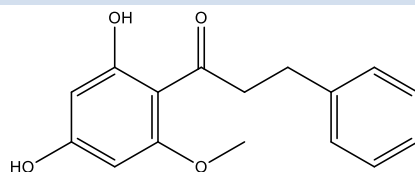
Thiourea-cardamonin



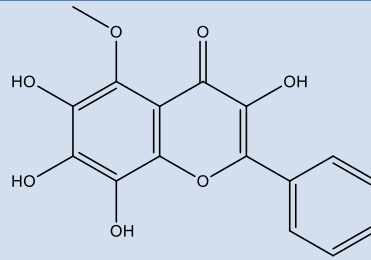
4-fluoro-cardamonin



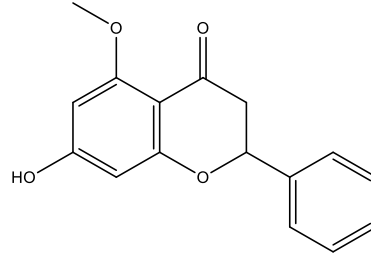
Tetrahydro-
cardamonin



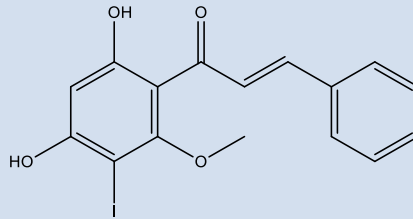
Flavanol-cardamonin



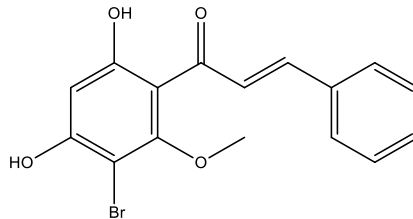
Flavanone-Cardamonin



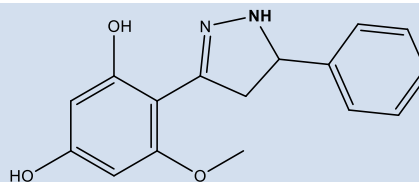
Cardamonin-I(II)



Cardamonin-Br(II)



Hydrazinium-cardamonin



1.5 Adherent and suspension culture

To date, the most common and simplest way to measure susceptibility of cells to any treatment is the cytotoxicity test (Kepp et al. 2011, Riss et al. 2013). Understanding the susceptibility difference between adherent and suspension cell culture is crucial for drug discovery and development. In general, suspension type cells lack the expression of adhesion molecules. Thus, suspension cells are non-adhesive and are suspended in the growth medium. Examples of suspension cells are monocytes and T-lymphocytes derived from myeloid and lymphoid hematopoietic stem cells, which can be isolated from leukaemic patients (Sloma et al. 2010, Buss and Ho 2011, Jan et al. 2011). In contrast, adherent cells derive from solid tissues with surface integrin expressions and focal adhesion molecules (Gumbiner 1996, Giancotti and Ruoslahti 1999, Hood and Cheresch 2002, Meyer et al. 2004). Examples of adherent cells are mature macrophages, breast cancer, lung cancer, liver cancer and other solid tumours.

1.5.1 THP-1 cell line and differentiation into mature macrophages

THP-1 cell line is a human monocytic cell first established from an individual with acute monocytic leukaemia. These cells have the ability to produce esterase and lysosomes and were characterised as phagocytes. The Fc receptor and complement receptor 1 on THP-1 recognises antibodies and complement component 3 on pathogens or infected cells, triggering phagocytosis (Tsuchiya et al. 1980). Subsequently, researchers found that introduction of THP-1 to phorbol-12-myristate-13-acetate (PMA) changed the cells from suspension to adherent phase (Tsuchiya et al. 1982) and PMA was determined as the most effective differentiation agent for

obtaining mature THP-1-derived macrophages (Chanput et al. 2014). These differentiated THP-1 cells exhibit striking similarities to macrophages morphologically. Since then, many studies have been carried out using THP-1-derived macrophages as a representative macrophage cell line and an investigative model in *in vitro* studies (Auwerx 1991, Schroecksnadel et al. 2011). Another type of stimuli often used to induce macrophage differentiation in monocytes is 1,25-dihydroxyvitamin D3 (VD3) (Daigneault et al. 2010). Further studies have shown that before PMA initiates cell differentiation, treatment with these stimuli must first induce an inhibition of cell growth (Traore et al. 2005). PMA has been shown to initiate cellular generation of ROS, modulate expression of some cell cycle regulators and inhibit the cell cycle of THP-1 cells at G₁-phase. PMA-induced differentiation in THP-1 cells also up-regulates p21 at protein and mRNA level through a protein kinase C (PKC)-mediated signaling mechanism that involves mitogen-activated protein (MAP) kinase activation (Traore et al. 2005).

1.5.2 Mitogen-activated protein kinase

There are four subgroups of the MAP kinase including extracellular signal-regulated kinases (ERKs), stress-activated protein kinase or c-jun N-terminal kinase (SAPK/JNK), big MAP kinase 1 (BMK1) and p38 group (Zarubin and Han 2005). p38 MAP kinase plays a pivotal role in several biological processes and signal transduction. To date, there are four identified p38 family variants: p38 α , p38 β (Jiang et al. 1996), p38 γ (Li et al. 1996) and p38 δ (Jiang et al. 1997). Of these four p38 groups, p38 γ are expressed differentially depending on type of cells whereas p38 α and p38 β are expressed ubiquitously. Other study reports the activation of MAP kinase signaling

cascade is downstream of PKC activation, an early event in the differentiation process inducing cell cycle arrest (Sugibayashi et al. 2001). The team reported that PKC inhibitor and MAP kinase inhibitor could inhibit the differentiation and growth arrest of human prostate cancer cell line, TSU-Pr1. Furthermore, MAP kinase species such as p38 have been shown to be strongly activated by ROS or intracellular redox state oxidative shift (Soh et al. 2003). PMA-stimulated THP-1 monocytes that promote myeloid cells maturation to mature macrophages also leads to surface expression of differential cell markers. **Figure 1.6** depicts the differential antibody markers of THP-1 monocytes and THP-1-derived macrophages after 72 hrs 100 nmol/L PMA treatment followed by 24 hrs PMA-free medium using flow cytometry (Mittar et al. 2011).

Among these markers, CD11b integrins are significantly expressed on the cell surface of THP-1-derived macrophages and commonly used as a macrophage marker (Gonzalez-Juarrero et al. 2003, Murray and Wynn 2011). It is well established that cell matrix adhesion *via* integrins allow cell survival and protects cells from undergoing apoptosis (Frisch and Ruoslahti 1997).

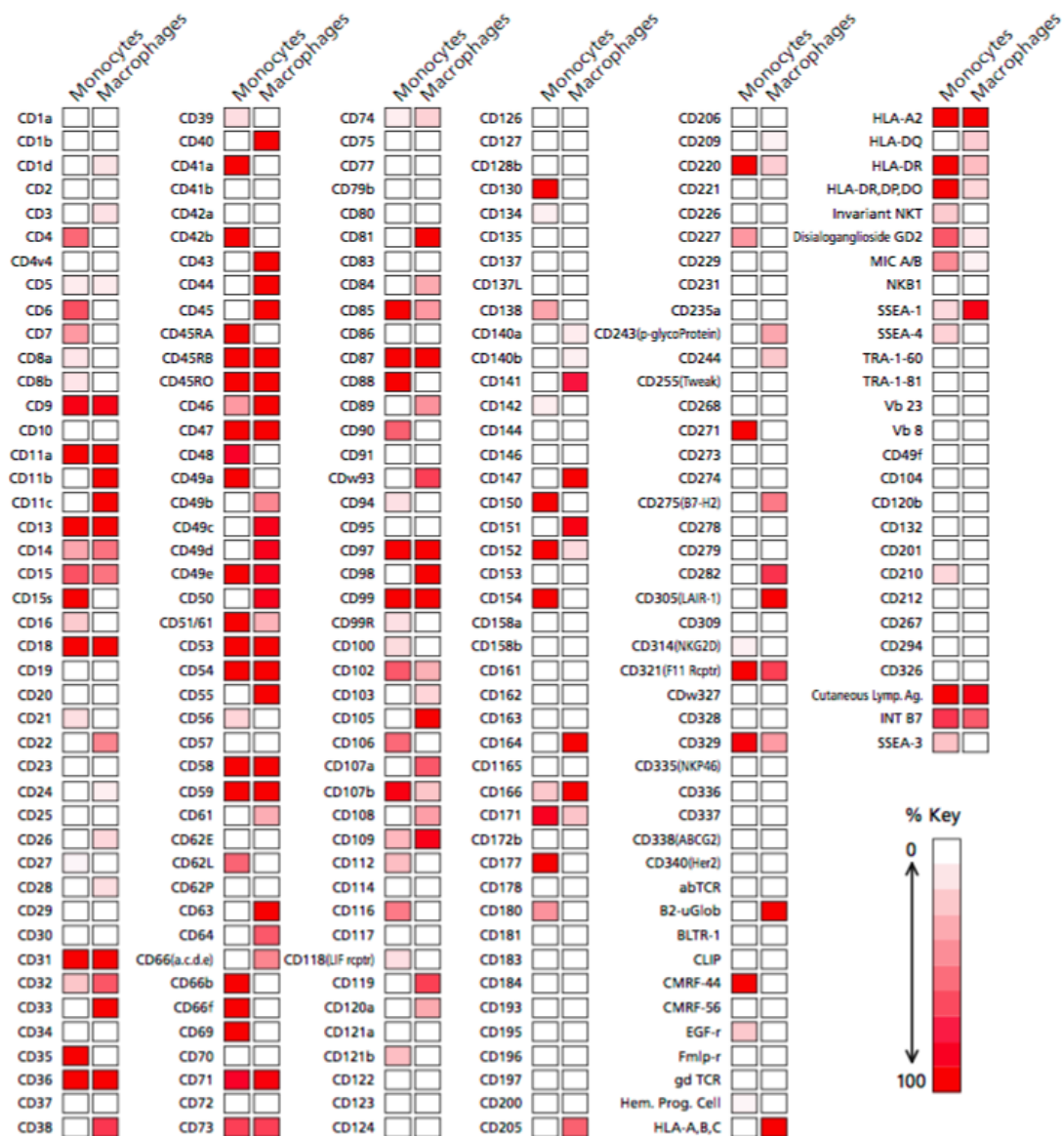


Figure 1.6 THP-1 monocytes and THP-1-derived macrophages cell surface markers.

Comparison of antibody markers in THP-1 monocytes and THP-1-derived macrophages using flow cytometry and expressed as percentage of positive cells in a heat map. Figure taken from Mittar et al. (2011).

1.6 Aims

Previous studies have shown that cardamomin exhibit cytotoxic and oxidative/ anti-oxidative properties in different cell lines. Efforts were made to enhance the bioactivity of cardamomin by producing semi-synthetic derivatives using cardamomin as the lead compound. The objectives of this study are to screen these novel cardamomin derivatives and to determine compounds that are more cytotoxic than cardamomin and to further investigate the structure activity relationship of these compounds. Furthermore, the identified active compounds will be tested for cytotoxicity against a range of normal and carcinoma cell lines to establish the toxicity of the compounds. As previous studies have reported that suspension cells are more susceptible to inhibition of cell growth compared to adherent cells, this study intends to examine the differential susceptibility between both cell state by looking at their response towards cardamomin and its active derivatives/ complexes. Overall, the cell line that is most susceptible to these compounds will be further used to investigate the mode of cell death looking into the effects on morphological changes, PS externalisation, caspase activation and MMP alteration. Finally, as cardamomin has been reported to possess both oxidative and anti-oxidative properties, this study aims to elucidate the oxidative effects in the cells in the presence of cardamomin and its derivatives/ complexes. The change in oxidative state will be determined by quantifying the intracellular levels of ROS and GSH. The effects on cell viability will also be determined in the presence or absence of various anti-oxidants. Generally, this study will provide a better understanding of cardamomin as a lead compound and its active derivatives/ complexes may offer a number of targets for therapeutic intervention particularly in cancer research.

CHAPTER 2: MATERIALS AND METHODS

2.1 Materials

2.1.1 Reagents

Materials	Source
2x Laemmli Sample Buffer (1610737)	Bio-Rad, USA
3-(4,5-dimethylthiazol-2-yl)-5-(3-carboxymethoxyphenyl)-2-(4-sulfophenyl)-2H-tetrazolium (G1111)	Promega, USA
40% acrylamide solution	Sigma, USA
Absolute ethanol (E0105/3000)	J Kollin Chemical, UK
Ammonium persulfate (A9164)	Sigma, USA
Annexin V-FITC binding buffer (556454)	BD Pharmingen, USA
Annexin V-fluorescence isothiocyanate (556420)	BD Pharmingen, USA
Anti- human FITC-CD11b	Biologend, USA
Anti-caspase-3 (SC-7148)	Santa Cruz Biotechnology, USA
Anti-caspase-8 (D35G2)	Cell signalling Techonology, USA
Anti-caspase-9 (9508)	Cell signalling Techonology, USA
Anti-PARP (ALX-804-210-R050)	Alexis Biochemicals, Switzerland
Anti- β -actin (A5441)	Sigma, USA
Benzyloxycarbonyl-phenylalanine-alanine-chloromethylketone, Z-FA-CMK (03CK009)	MP Biomedicals, USA
Benzyloxycarbonyl-valine-alanine-aspartic acid-fluoromethylketone, Z-VAD-FMK (N-1560)	Bachem, Switzerland
Bovine serum albumin (A2058)	Sigma, USA
D-cysteine	Sigma, USA
Dihydroethidine (D-23107)	Molecular Probes, USA
Dimethyl sulfoxide (D2650)	Sigma, USA
Dithiothreitol (D9779)	Sigma, USA
Enhanced chemiluminescence reagent (RPN2106)	GE Healthcare, UK
Ethylene-diamineteraacetic acid (E5134)	Sigma, USA
Fetal bovine serum	Gibco, USA
Glutathione	Sigma, USA
Glycerol (G5516)	Sigma, USA
Glycine (G7126)	Sigma, USA
Goat anti-mouse IgG horseradish peroxidase (P0447)	Dako, Denmark
Goat anti-rabbit IgG HRP(P0448)	Dako, Denmark
Hoechst 33358 (H1398)	Molecular Probes, USA

Hybond C membrane (RPN2020D)	GE Healthcare, UK
L-cysteine	Sigma, USA
Lymphoprep	Axis Shield, Norway
Methanol (106009)	Merck, USA
Monochlorobimane (69899)	Sigma, USA
Mouse FITC-IgG1 negative control	Dako, Germany
N-acetyl cysteine (A9165)	Sigma, USA
p38 MAP Kinase Inhibitor IV (SML0543)	Sigma, USA
Paraformaldehyde (P6148)	Sigma, USA
Penicillin-streptomycin antibiotic	Sigma, USA
Phenazine methosulfate (P9625)	Sigma, USA
Phenylmethylsulfonyl fluoride (P7626)	Sigma, USA
Phorbol 12-myristate 13-acetate (P8139)	Sigma, USA
Phosphate buffered saline	Sigma, USA
Ponceau S (P3504)	Sigma, USA
Propidium iodide (P4170)	Sigma, USA
Quick Start Bradford (500-0205)	Bio-Rad, USA
Rabbit anti-goat IgG HRP (P0160)	Dako, Denmark
RPMI-1640 with L-glutamine (11875-093)	Gibco, USA
SB202190 (S7067)	Sigma, USA
Skim milk	Sunlac, Malaysia
Sodium chloride (6533-00)	R&M, UK
Sodium Dodecyl Sulfate (161-0418)	Bio-Rad, USA
Staurosporine (S4400)	Sigma, USA
SuperSignal molecular weight protein ladder	Thermo Scientific
Tetramethyl rhodamine ethyl ester (T-669)	Molecular Probes, USA
Tetramethylethylenediamine (T9281)	Sigma, USA
Tris base (T1503)	Sigma, USA
Triton X-100 (T8787)	Sigma, USA
Trolox	Sigma, USA
Tryphan blue (T8154)	Sigma, USA
Trypsin EDTA	Gibco, USA
Tween-20 (P5927)	Sigma, USA

2.1.2 Cell lines

THP-1 human acute monocytic leukaemic, A549 human lung adenocarcinoma, MRC5 human lung normal, Hs68 human normal foreskin and Jurkat T human acute lymphoblastic leukaemia cell lines used in this study were obtained from American Type Culture Collection (ATCC). HK1 human nasopharyngeal carcinoma cell line was generously provided by the University of Hong Kong through local collaboration with the Institute of Medical Research Malaysia.

2.1.3 Compounds

The following compounds were semi-synthesised and provided by Mohammed Khaled Break from the Centre for Natural and Medicinal Product Research at the University of Nottingham Malaysia Campus: cardamonin, acetyl-cardamonin, allyl-cardamonin, OBn-cardamonin, OMe-cardamonin, cardamonin-Cu(II), cardamonin-Fe(II), cardamonin-B, benzoyl-cardamonin, phenylamine-cardamonin, methoxyamine-cardamonin, hydroxylamine-cardamonin, urea-cardamonin, thiourea-cardamonin, 4-fluoro-cardamonin, tetrahydro-cardamonin, flavanol-cardamonin, flavanone-cardamonin, cardamonin-I(II), cardamonin-Br(II), and hydrazinium-cardamonin. The structures of these novel compounds were established using infrared spectroscopy, ¹H NMR, ¹³C NMR and mass spectrometry techniques (Break et al. 2018).

2.2 Methods

2.2.1 Cell Culture

2.2.1.1 Maintaining Adherent Cells

Adherent cells including human lung cancer A549, human nasopharyngeal cancer HK1, human normal lung MRC5, human normal foreskin Hs68, THP-1-derived macrophages were maintained as monolayer in T25 or T75 flasks of 10 mL or 20 mL RPMI-1640 growth medium with L-glutamine supplemented with 10% heat-inactivated fetal bovine serum (FBS) and 5% penicillin/ streptomycin (pen/ strep) (RPMI₁₀) respectively at 37°C in a humidified atmosphere and 5% CO₂. All cells except THP-1-derived macrophages were split and passaged by trypsinisation to a fresh culture vessel when growth reached 70-80% confluency. Old medium in the flask was discarded and cells were washed twice with phosphate buffered saline (PBS) then added with 1X trypsin and incubated for 5 mins at 37 °C. To dislodge cells, cells were passaged mechanically by tapping the flask gently. Equal parts of RPMI-1640 complete medium were added to trypsinised cells in order to neutralise trypsin. Cells were collected and centrifuged at 1,800 revolutions per minute (rpm) for 5 mins and the pellet was re-suspended in 1 mL RPMI₁₀ where cell number was determined.

2.2.1.2 Maintaining Suspension Cells

The human acute lymphoblastic leukemic cell line, Jurkat T cells, used in this study was clone E6-1 established from a 14 year old male's peripheral blood suffering from acute lymphoblastic leukaemia (Schneider et al. 1977). The human acute monocytic leukemic cell, THP-1, was derived from a one year old male's peripheral blood. Both Jurkat T cells and THP-1 monocytes were cultured in RPMI₁₀ and kept in a 37 °C incubator with humidified atmosphere and 5% CO₂. Cells were seeded at a density between 3 x 10⁶ cells/mL to 5 x 10⁶ cells/mL and subcultured every 2-3 days. For experimental studies, suspension cells were collected and centrifuged at 1,000 rpm for 5 minutes and the pellet was re-suspended in 1 mL RPMI₁₀ where cell number was determined.

2.2.1.2.1 Isolation of Mononuclear Cells

Lymphoprep™ is a density gradient medium used to isolate live from dead mononuclear cells. 20 mL of Jurkat T cells growing in RPMI₁₀ were collected from T75 flask and carefully layered onto 20 mL of Lymphoprep™ in a tilted 50 mL tube and centrifuged at 1,800 rpm for 20 mins at 25 °C (without break). The Jurkat mononuclear cells that retained at the medium/ Lymphoprep™ interface were gently removed. Collected Jurkat T cells were washed with PBS twice at 1,000 rpm for 10 mins at 25 °C and re-suspended in RPMI₁₀, kept at 37 °C incubator with humidified atmosphere and 5% CO₂ until needed. Layered Jurkat T cells' viability was routinely found to be higher than 90%.

2.2.1.3 Cell Counting

Cell pellet re-suspended in 1 mL RPMI₁₀ medium was carefully and gently pipetted to break the cell pellet. 20 μ L of cell suspension and 180 μ L of Tryphan blue solution were transferred to a centrifuge tube giving a 10x dilution of the cell suspension. The suspension was gently mixed and 10 μ L of the solution was carefully placed into each side of the haemocytometer with coverslip. A handheld counter was used to count cells in each of the four corners and centre squared of the haemocytometer. Total number of viable cells, unstained by Tryphan blue, was counted. The calculation for number of cells per mL is described below:

-
- $\text{Cells/mL} = \text{average count per square} \times \text{dilution factor} \times 10^4$ (volume correction factor for the haemocytometer where each square is 1 x 1 mm and the depth is 0.1 mm)
 - $\text{Total cells} = \text{cells/mL} \times \text{total original volume of cell suspension from which the sample was taken}$
-

2.2.1.4 Cryopreservation

Cryopreservation technique is used to conserve cells in earlier passage in order to maintain the consistency of cell characteristic throughout the experiment. Retrieval of cryopreserved cells is needed when cells reached a higher passage number or in the case of contamination of cultures. Confluent cells were brought into suspension form and centrifuged to obtain the cell pellet. The supernatant was discarded and pellet was gently pipetted in 0.9 mL chilled FBS and the suspension was transferred into a cryovial where 0.1 mL of dimethyl sulfoxide (DMSO) was slowly added to the FBS

giving a 9:1 ratio of FBS to DMSO. The cryovial was then placed into a pre-chilled passive freezer “Mr Frosty” and stored in -20 °C freezer for 1 hr prior to storing in -80 °C freezer overnight. For long-term storage, cryovial was removed from “Mr Frosty” and transferred to the vapour phase of liquid nitrogen storage vessel the next day. To retrieve cells from frozen storage, RPMI₁₀ medium was firstly pre-warmed to 37 °C and cryovial containing cell culture was retrieved from the frozen storage and warmed in 37 °C water bath until semi-thawed. 1 mL of the pre-warmed RPMI₁₀ medium was added to the cell suspension and gently pipetted then transferred to a T75 flask and topped with 20 mL of the pre-warmed RPMI₁₀ medium. Cells were incubated overnight in humidified atmosphere at 37 °C with 5% CO₂. The next day, RPMI₁₀ medium containing traces of DMSO was discarded and replaced with fresh DMSO-free RPMI₁₀ medium. Cell cultures were maintained for at least one week before being used for experimental studies.

2.2.1.5 THP-1 cells

2.2.1.5.1 Differentiation of THP-1 Monocytes to Macrophages

THP-1 cells growing in suspension were pellet down at 1,000 rpm for 10 mins. THP-1 monocytes of 5×10^6 cells in 20 mL RPMI₁₀ were used for differentiation in T75 flask. THP-1 monocytes were induced to differentiate into macrophages with phorbol-12 myristate 12-acetate (PMA) at a final concentration of 20 ng/mL in RPMI₁₀. Cells were incubated for 72 hrs. Differentiated cells were then replaced with fresh PMA-free RPMI₁₀ medium for 48 hrs (resting phase) before being used for experimental studies. THP-1-derived macrophages were displaced as described in Section 2.2.1.1 followed by cell number determination in Section 2.2.1.3.

2.2.1.5.2 Expression of CD11b surface marker in THP-1-derived macrophages

CD11b surface receptors, an α -subunit of β 2 integrin, is known to increase significantly on surface of mature THP-1-derived macrophages (**Figure 1.6**). Following 72 hrs PMA-induced differentiation and 48 hrs in resting phase, mature THP-1-derived macrophages were analysed for the expression of CD11b surface antigen. Cells were washed and trypsinised as described in Section 2.2.1.1 and brought into suspension form. Once the cell number was determined, 5×10^5 cells were aliquot into centrifuge tubes and centrifuged at 1,000 rpm for 10 mins followed by washing twice in cold 1X PBS at 1,000 rpm, 4°C for 10 mins. For unstained samples, cells were re-suspended in 300 μ L staining buffer (1% BSA in PBS); for stained samples, cells were re-suspended in 50 μ L staining buffer and 2 μ L FITC anti-human CD11b; whereas for isotype sample, cells were re-suspended in 50 μ L staining buffer and 2 μ L FITC mouse IgG1 negative control. All samples were kept on ice for 1 hr protected from light. Following incubation, samples were washed twice with 1X PBS before being re-suspended in 500 μ L staining buffer and analysed with BD FACS Calibur flow cytometer.

2.2.2 MTS Cell Viability Assay

The cell viability was evaluated using the Cell Titer 96TM Aqueous Cell Proliferation Assay (MTS) containing the reactive compound, 3-(4,5-dimethylthiazol-2-yl)-5-(3-carboxymethoxyphenyl)-2-(4-sulfophenyl)-2H-tetrazolium, and an electron-coupling reagent, phenazine methosulfate, (PMS). This assay is based on the reduction of MTS tetrazolium into water-soluble purple formazan dye by the mitochondrial succinate

dehydrogenase enzymes available in metabolically active cells. The amount of purple formazan dye directly correlates to the number of metabolically active cells and can be measured at 490 nm wavelength (Cory et al. 1991).

For adherent cells, cells were firstly plated out in RPMI₁₀ in 96-well flat-bottomed plates and incubated for 24 hrs to allow for cell attachment and recovery. RPMI₁₀ was then carefully removed and replaced with the appropriate treatments in RPMI₁ and incubated for 24, 48 and 72 hrs. For suspension cells, cells were plated with the appropriate treatments in RPMI₁ and incubated for 24 hrs. Following treatment and incubation, freshly prepared MTS/PMS solution (5 parts of 2 mg/mL MTS and 1 part of 0.92 mg/mL PMS) was added to each well and incubated at 37 °C in the dark for an hour. The number of cells seeded and volume of MTS/PMS solution added in the 96-well plates for the different cell lines are as described in **Table 2.1**. Prior to measuring the absorbance at 490 nm, plates were agitated gently to fully dissolve the formazan product. The absorbance was read using a Tecan Infinite 200 microplate reader. Absorbance of each sample was subtracted from the blank absorbance value, containing media alone and cell viability was expressed as percentage activity corresponding to the control. All samples were performed in triplicates for three independent experiments.

Table 2.1 Number of cells seeded and volume of MTS/ PMS solution added for the different cell lines.

Cell lines	Number of cells/ well in 96-Well Plates	MTS/PMS solution (μL)
A549	10,000	10
HK1	10,000	10
MRC5	10,000	10
Hs68	10,000	10
THP-1 monocytes	50,000	20
THP-1-derived macrophages	50,000	20
Jurkat T cells	50,000	20

2.2.3 Nuclear Morphology for Detection of Apoptosis

The morphological changes in Jurkat T cells were determined using a nuclear stain Hoechst 33358 and examined using UV microscopy. This DNA-binding dye emits blue fluorescence following UV excitation (Latt and Stetten 1976). In brief, cells (5×10^5 cells/ well) were treated with the IC_{50} concentrations and incubated for 24 hrs. After treatment, cells were collected and washed with chilled PBS (centrifuge at 3,000 rpm for 15 mins) prior to fixing with 4% paraformaldehyde for 30 mins at room temperature. Fixed cells were then counter-stained with $8 \mu\text{g/mL}$ Hoechst 33358 for 30 mins at room temperature protected from light. The stained cells were centrifuged at 3,000 rpm for 10 mins and pellet was re-suspended in $10 \mu\text{L}$ glycerol/ PBS (50:50, v/v). $5 \mu\text{L}$ was aliquot from the cell suspension and mounted onto glass slide and viewed for morphological changes using an Olympus fluorescence microscope (Model BX51). For storage and later viewing, slides were sealed with nail varnish around the edge of the cover slips and kept in the dark at 4°C . Cells were deemed to be apoptotic based upon the characteristic of highly condensed chromatin and/ or

presence of fragmented DNA into apoptotic bodies. In contrast to normal cells, condensed chromatin may cause the cell nuclei to appear smaller, crescent-shaped or spherical beads around the nucleus of the cell.

2.2.4 Annexin V-FITC Analysis

The externalisation of PS from the inner part to the outer side of the cell bilayer membrane is one of the hallmarks of apoptotic cell death. Annexin-V is a calcium dependent protein that binds to PS with higher affinity. Hence, Annexin-V conjugated with FITC was used to probe externalised PS on the outer cell membrane enabling identification and quantification of apoptotic cells by flow cytometry (Van Engeland et al. 1998). A second dye, propidium iodide (PI) was used as a counter stain to discriminate between viable cells, early apoptotic and late apoptotic or necrotic cells. Cells without Annexin V-FITC and PI stained (AV⁻PI⁻) are considered viable cells with non-exposed PS and intact cell membrane that excludes both Annexin-V and PI stains respectively. AV⁺PI⁻ stained cells are deemed early apoptotic cells with externalised PS but with an intact cell membrane, hence taking up the Annexin-V but not PI stain. Cells stained positively with both Annexin-V and PI stains (AV⁺PI⁺) are regarded as late apoptotic or necrotic cells as PS is translocated to the outer leaflet of the plasma membrane and there is loss of cell membrane integrity. In this study, the binding of Annexin-V to externalised PS and PI to DNA of membrane-ruptured cells on apoptotic cells was measured by flow cytometry (BD FACSVerseTM). Following 24 hrs treatment with the IC₅₀ concentrations, Jurkat T cells (1×10^6) were washed twice with chilled PBS and suspended in 1 mL 1 mM CaCl₂ (1X Binding Buffer). 100 μ L of the solution was transferred to a 5 mL culture tube and incubated with 2 μ L

each of Annexin V-FITC and PI in the dark for 30 mins. After incubation, 400 μ L of 1X Binding Buffer was added to the cells and analysed using flow cytometry within 1 hr. Excitation wavelengths of 488 nm (Annexin V-FITV) and 595 nm (PI) were used. Fluorescence data was acquired for 10,000 cells. Staurosporine (STS) was used as positive control in this study following 4 hrs treatment of Jurkat T cells with 1 μ M STS.

2.2.5 Sodium dodecyl sulfate polyacrylamide gel electrophoresis and Western blot analysis

Western blotting technique was used to separate and identify the presence of specific proteins from a complex mixture of proteins of the cell lysates. The protein fractions were separated based on molecular weight through sodium dodecyl sulfate polyacrylamide gel electrophoresis (SDS- PAGE). Prior to separation, the proteins were denatured and conferred to negative charge in the presence of reducing agent dithiothreitol (DTT), SDS and heat. Proteins separated after SDS-PAGE were transferred to a membrane and then incubated with proper primary and secondary antibodies specific to the protein of interest for visualisation.

2.2.5.1 Buffers, resolving gel and stacking gel recipes

Table 2.2 Recipes for buffers and gels.

Buffers	Recipe
10X TBS (pH 7.6)	24.2g trizma base, 80g NaCl, top up to 700 mL with deH ₂ O (adjust pH to 7.6)
1X TBS	100 mL 10X TBS + 900 mL deH ₂ O
1X TBS-T (0.1% Tween-20)	100 mL 10X TBS + 900 mL deH ₂ O, remove 1 mL and add 1 mL Tween-20
RIPA lysis buffer	1mL 1M NaCl, 20 μ L 0.5M EDTA, 100 μ L 1M Tris-HCl at pH 7.6, 100 μ L triton-X, 8.73 mL deH ₂ O and 50 μ L 0.2M PMSF (add fresh)
2X Laemmli loading buffer	20 μ L 1M DTT, 500 μ L 2X Laemmli loading buffer sample buffer (to mix with sample 1:1 ratio)
5X electrode buffer (1L)	15.5g trizma base, 72g glycine, 25 mL 20% SDS, top up with 1000 mL deH ₂ O
1X electrode buffer	200 mL 5X electrode buffer + 800 mL deH ₂ O
Transfer buffer	14.4g glycine, 3.03g trizma base, 800 mL deH ₂ O and 200 mL methanol
12% Resolving gel buffer (16 mL)	6.9 mL deH ₂ O, 4.8 mL 40% acrylamide, 4 mL 1.5M Tris-HCl pH 8.8, 80 μ L 20% SDS, 160 μ L 10% APS, 16 μ L TEMED
4% Stacking gel buffer (5 mL)	3.1 mL deH ₂ O, 0.5 mL 40% acrylamide, 1.25 mL 0.5M Tris-HCl pH 8.8, 25 μ L 20% SDS, 50 μ L 10% APS, 5 μ L TEMED
Membrane stripping solution (10 mL)	1.25 mL 0.5M Tris-HCl, 1 mL 20% SDS, 1 mL 1M DTT, 6.75 mL deH ₂ O (adjust pH to 2.2)

2.2.5.2 Preparation of Stacking and Resolving Gels

The gels were cast using Bio-Rad Mini-PROTEAN apparatus. All large (tall plate with 1.5 mm spacer) and small glass plates were washed with deH₂O and dried thoroughly then arranged and locked together securely by a casting frame. A sponge was placed between the casting frame containing the glass plates and the casting stand to prevent leakage. The casting chamber was checked for leakage by adding 2 mL of deH₂O. Once no leakage is detected, the deH₂O was poured off and any traces of deH₂O were removed with filter paper. Resolving gel prepared according to **Table 2.2**, was carefully pipetted into the space between the large and small glass plates up to a level of 2 cm from the top of the short plate. Immediately after pipetting the resolving gel, approximately 2 mL of deH₂O was gently added onto the resolving gel to obtain an even top layer. The resolving gel was then left to polymerise for 1 hr before pouring off and removing all traces of deH₂O with filter paper. Polymerisation is initiated by ammonium persulfate (APS) and catalysed by TEMED (Shi and Jackowski 1998). Subsequently, the stacking gel prepared according to **Table 2.2** was carefully cast on top of the resolving gel and a 10-well comb with 1.5 mm thickness was inserted into the space between the plates and left to polymerise for an hour. After the stacking gel had polymerised, the plates containing the polymerised gels were removed from the casting stand and casting frame and placed in the electrode assembly and inside the tank with the short plate facing inwards. The tank was then filled up with electrode buffer above the level covering the short plates. The comb was then gently removed and the wells were carefully rinsed with electrode buffer. The wells were then loaded with the protein fractions.

2.2.5.3 Preparation of Cell Lysates

Following 24 hrs treatment with cardamonin, cardamonin-Cu(II) and cardamonin-Fe(II) using the IC₅₀ values and 4 hrs treatment with 1 μM STS (positive control), Jurkat T cells (2 x 10⁶ cells/ mL) were collected and centrifuged at 1,500 rpm for 15 mins at 4 °C. Cell pellets were washed with chilled PBS twice before being re-suspended in 50 μL radio-immunoprecipitation assay (RIPA) cell lysis buffer. Freeze-thaw cycle was carried out three times using liquid nitrogen and 37 °C water bath to obtain the cell lysates. The cell lysates were kept at -20 °C freezer until use.

2.2.5.4 Protein Estimation using Bradford Protein Assay

The extracted protein fractions of cell lysates were corrected for amount of protein present using the Bradford protein assay. Bovine serum albumin (BSA) was prepared as a standard to construct the standard curve at different concentrations of 0, 62.5, 125, 250, 500, 750, 1000 and 1500 μg/mL as described in **Table 2.3**. The cell lysate samples including the BSA standards were diluted 1:20 with deH₂O and 5 μL were transferred to 96-well plate containing 250 μL of Bradford reagent. The plate was incubated at room temperature protected from light for 30 mins. The absorbance was read at 595 nm using a Tecan Infinite 200 microplate reader. A standard curve was constructed from the BSA protein standards and the protein concentration of the cell lysates were calculated. All samples were performed in triplicates for three independent experiments.

Table 2.3 BSA standards preparation.

Tubes	Volume of Diluent (μL)	Volume of Protein Standard (μL)	Final BSA Concentration (μg/mL)
A	10	30 from 2 mg/mL BSA Stock	1500
B	20	20 from 2 mg/mL BSA Stock	1000
C	20	20 from Tube A	750
D	20	20 from Tube B	500
E	20	20 from Tube D	250
F	20	20 from Tube E	125
G	20	20 from Tube F	62.5
H	20	deH ₂ O only	0

2.2.5.5 Sample Preparation for SDS-PAGE

Cell lysates containing 30 μg of protein were transferred to micro-centrifuge tubes and added with equal volume of lysis buffer. Samples were vortexed before and after 10 mins of boiling at 96 °C. Protein samples were placed on ice until further use once cooled down. Protein samples and 1 μL of protein ladder (Thermo Fisher) were carefully loaded into the SDS-PAGE gel wells and the gel was left to run at 120 V until the dye reaches the bottom of the resolving gel, approximately 90 mins. Following protein separation, the gels were removed from the glass plates and the stacking gel was cut away. The resolving gel was left to soak in pre-chilled transfer buffer for at least 15 mins prior to western blotting.

2.2.5.6 Western Blotting

The separated protein on the SDS-PAGE gel was transferred onto Hybond C membrane (Amersham, UK) using the Mini Trans-Blot[®] Electrophoretic Transfer Cell (Bio-Rad). Initially, a piece of Hybond C membrane was cut to size 7 x 10 cm along with two pieces of filter paper. The membrane was saturated with deH₂O and then soaked in pre-chilled transfer buffer with the filter papers and fiber pads for 30 mins at 4 °C. The transfer sandwich was assembled on the transfer cassette as shown in **Figure 2.1**. The transfer cassette was then placed inside an electrode module and transferred into a mini tank filled with transfer buffer and the proteins were transferred at 100 V for 1 hr. Once the transfer is completed, the membrane was carefully removed and stained with Ponceau-S solution for approximately 1 min to confirm the transfer of protein onto the membrane has been successful. The Ponceau-S solution was then removed by washing with deH₂O and TBS-T followed by blocking the membrane with freshly prepared TBS-T + 5% skimmed dried milk for 1 hr at room temperature with gentle agitation.

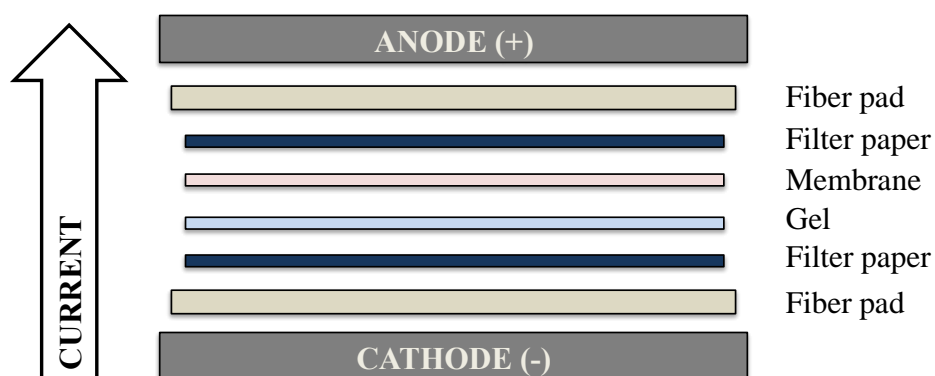


Figure 2.1 Assembly of transfer sandwich for western blotting.

2.2.5.7 Immunodetection

Following membrane blocking, the membrane was washed twice with TBS-T for 5 mins and probed with 20 mL antibodies against caspase-3, -8, -9, PARP-1 and β -actin (**Table 2.4**) at 4 °C overnight. After the overnight primary antibody incubation, the antibody was removed and kept at -20 °C for future use. The membrane was taken through one complete cycle of washing steps with agitation: 1) TBS-T + 5% skimmed dried milk (15 mins); 2) TBS-T + 5% skimmed dried milk (2 x 5 mins); 3) TBS-T (15 mins); 4) TBS-T (2 x 5 mins); and lastly 5) TBS (10 mins). The membrane was then incubated for 1 hr at room temperature with the 20 mL of the appropriate horseradish peroxidase (HRP)-conjugated secondary antibody (**Table 2.4**) under gentle agitation. Subsequently, the membrane was taken through another complete cycle of washing steps prior to being overlaid with 2 mL of the enhanced chemiluminescence (ECL) detection reagent for 1 min sealed with cling film at room temperature. The ECL detection reagent was drained off with a piece of filter paper. The membrane was then transferred on to a Li-Cor membrane reader faced-down, and trapped air bubbles were removed with a roller and analysed immediately.

Table 2.4 Dilutions of primary antibodies and secondary antibodies used for immunodetection.

Primary Antibodies (Host Species)	Dilution
Caspase-3 (Rabbit)	1:1,000
Caspase-8 (Rabbit)	1:1,000
Caspase-9 (Mouse)	1:1,000
PARP-1 (Mouse)	1:1,000
β -actin (Mouse)	1:5,000
Secondary Antibodies (Host Species)	Dilution
Anti-rabbit-HRP	1:2,000
Anti-mouse-HRP	1:2,000

2.2.5.8 Membrane stripping and re-probing

Membranes can be stripped and re-probed with another protein by gently stripping off the antibodies from the membrane. Following blot analysis, membrane was washed with TBS-T twice for 5 mins each. Membrane was incubated with membrane stripping buffer for 30 mins at 60 °C with slight agitation every 10 mins interval. The membrane was washed with TBS-T four times for 5 mins each. Membrane was blocked with freshly prepared TBS-T + 5% skimmed dried milk for 1 hr at room temperature with gentle agitation. The blocked membrane was then taken through one complete cycle of washing step before re-probing with another primary antibody.

2.2.6 Measurement of MMP

Another distinct feature of apoptosis is the disruption of active mitochondria that leads to changes in the mitochondria membrane potential and altered oxidation-reduction mitochondria potential. An intact mitochondrion actively transfers protons from the inner matrix to the intermembrane mitochondrial space creating a mitochondrial transmembrane potential ($\Delta\psi_m$). Negative in the inner matrix and positive in the intermembrane space creating a $\Delta\psi_m$ of approximately 180 mV (Chen 1988). The opening of the mitochondrial permeable transition pore in cells undergoing apoptosis allows passage of small molecules and ions, and results in depolarisation of the transmembrane potential, which is detectable using $\Delta\psi_m$ -sensitive dyes. Tetramethylrhodamine, ethyl ester (TMRE), a positively charged, cell permeant, red-orange dye is able to accumulate within the mitochondria of healthy cells due to their relative negative charge. A decrease in the MMP and failure to sequester TMRE dye indicates inactive or depolarised mitochondria. Jurkat T cells (1×10^5 cells) were treated with the IC_{50} concentrations and incubated at 37°C for 24 hrs. Following treatment, TMRE at a final concentration of 0.2 μ M was added to cells and incubated at 37 °C protected from light for 30 mins. After incubation, the plate was centrifuged down at 3,500 rpm for 10 mins and washed with chilled PBS. Fluorescence readings were obtained on a fluorescence microplate reader (Tecan Infinite 200) with excitation and emission wavelengths of 549 nm and 575 nm respectively. TMRE accumulated in the mitochondria of normal cells with intact MMP exhibits high fluorescence intensity while a decrease in fluorescence intensity indicate cells with loss of MMP and are not able to accumulate TMRE in the mitochondria.

2.2.7 Determination of intracellular GSH levels

The diminished cellular GSH levels in cells serve as an indicator of cellular oxidative stress. A common method used to determine the change in GSH levels in cells is *via* a cell permeable thiol probe, monochlorobimane (MCB) (Rice et al. 1986). MCB strongly fluoresce in blue when bound to reduced GSH. Jurkat T cells (5×10^4 cells/well) were treated with the IC_{50} concentrations of cardamonin, cardamonin-Cu(II) and cardamonin-Fe(II) and incubated in humidified atmosphere at 37°C with 5% CO₂ for 24 hrs. After treatment, cells in the 96-well plate (5×10^4 cells/well) were centrifuged and washed twice with 100 μ L PBS at 3500 rpm for 10 mins. After the final wash, the supernatant was carefully removed and replaced with 100 μ M of MCB in 100 μ L PBS and incubated at 37 °C for 30 mins in the dark. The GSH levels in the samples correlate with fluorescent intensity and was determined using a Tecan Infinite M200 fluoro-plate reader with excitation and emission wavelengths of 390 nm and 460 nm, respectively. The appropriate blank, MCB in PBS alone, was subtracted from all the sample absorbance to obtain the corrected values. Percentage of intracellular GSH level was calculated using the formula as below:

$$\text{Intracellular GSH (\%)} = \frac{\text{Fluorescence of treated cells} - \text{blank} \times 100\%}{\text{Fluorescence of untreated cells} - \text{blank}}$$

2.2.8 Detection of ROS

The production of ROS indicates the presence of oxidative damage in cells. Intracellular ROS was measured using an oxidant-sensitive fluorescent dye, dihydroethidium (DHE). This cell-permeable dye reacts with ROS to form a red fluorescent product, 2-hydroxyethidium, which intercalates with DNA. The fluorescence intensity is proportional to the amount of ROS generated (Cai et al. 2007). Jurkat T cells (5×10^4 cells) were treated with the IC_{50} concentrations of cardamonin, cardamonin-Cu(II) and cardamonin-Fe(II) and incubated at 37°C for 24 hrs. Following treatment, cells in the 96-well plate (5×10^4 cells/ well) were centrifuged and washed twice with 100 μ L PBS at 3,500 rpm for 10 mins. After the final wash, the supernatant was carefully removed and replaced with DHE at a final concentration of 10 μ M in pre-warmed RPMI₀ and incubated at 37 °C for 30 mins in the dark. Cells were subsequently washed with cold PBS twice and re-suspended in 100 μ L PBS prior to measuring the fluorescence intensity using the Tecan Infinite M200 fluoro-plate reader with excitation and emission wavelengths of 535 nm and 635 nm, respectively. The appropriate blank, DHE in RPMI₀, was subtracted from all the sample absorbance to obtain the corrected values.

2.2.9 Determination of anti-oxidant effects on cell viability

Anti-oxidants were used to determine the possible role of pro-oxidative cell death induced by cardamonin, cardamonin-Cu(II) and cardamonin-Fe(II) on Jurkat T cells. Jurkat T cells (5×10^4 cells) were treated with the IC_{50} concentrations of cardamonin, cardamonin-Cu(II) and cardamonin-Fe(II) in the presence or absence of anti-oxidants (1 mM NAC, 1 mM GSH, 1 mM Trolox, 1 mM L-cysteine or 1 mM D-cysteine) and incubated in humidified atmosphere at 37°C with 5% CO₂ for 24 hrs. Following treatment, the cell viability of Jurkat T cells was determined using the MTS cell viability assay as described in Section 2.2.2.

2.3 Statistical Analysis

The experimental data were analysed using a two-tailed distribution, paired, Student's *t*-test where error bars indicate mean \pm SEM ($n = 3$ replicates) and representative of three independent experiments. Difference between the mean values where $p < 0.05$ was considered significantly different.

**CHAPTER 3: CYTOTOXICITY AND STRUCTURE
ACTIVITY RELATIONSHIP OF CARDAMONIN
DERIVATIVES AND COMPLEXES IN NORMAL AND
CANCER CELL LINES**

3.1 Introduction

The chalcone, cardamonin, has attracted much attention for its ability to kill cancer cells (Murakami et al. 1993, Li et al. 2008, Simirgiotis et al. 2008, Dzoyem et al. 2012, Kuete et al. 2014) among other biological properties. In an attempt to improve the anti-tumour activity of cardamonin, numerous derivatives and metal complexes were screened for their cytotoxic activity. The generation of natural product derivatives/ complexes remains an important goal to enhance bioactivity of a compound. To date, there are no methods for accurate prediction of biological activity of a designed compound and the processes largely rely on trial and error where knowledge and experience are advantageous. A quick and effective way to determine the bioactivity is through preliminary screening carried out using cell lines *in vitro*. In this chapter, the cytotoxicity of cardamonin and its derivatives were initially tested against the A549 epithelial cell line derived from human lung adenocarcinoma and HK1 squamous carcinoma from nasopharyngeal cancer cell lines. The influences of cardamonin structural modifications were discussed in relation to the cytotoxic activity as part of the SAR studies. Subsequently, the two most cytotoxic compounds were selected for further cytotoxicity studies against human normal MRC5 lung fibroblast cell line, human normal Hs68 foreskin fibroblast cell line and a leukaemic cell line, Jurkat T cell.

3.2 Results

3.2.1 Cytotoxicity and the structure activity relationship of cardamonin and its derivatives on human A549 and HK1 carcinoma cell lines

Initial studies were carried out to determine the cytotoxicity of cardamonin and its derivatives in human A549 lung and human HK1 nasopharyngeal carcinoma cell lines where the IC_{50} values were obtained at 24, 48 and 72 hrs treatment as summarised in **Table 3.1**. **Figures 3.1 - 3.21** present the dose response curves for each compound. An overall comparison on the cytotoxicity of cardamonin and its derivatives in A549 and HK1 cancer cell lines revealed a hint of selectivity towards HK1 cells making this cell line more susceptible to treatment compared to A549 cells. Between cardamonin and its 20 derivatives, only six of the compounds were more cytotoxic to A549 cells, having lower IC_{50} values compared to HK1 cells. These six compounds include urea-cardamonin (**Figure 3.14**), cardamonin-B (**Figure 3.4**), cardamonin-I(II) (**Figure 3.19**), cardamonin-Br(II) (**Figure 3.20**), and benzoyl-cardamonin (**Figure 3.21**). However, there are no apparent structural correlations that can be observed among these six compounds that could account for the difference seen in A549 cells being more susceptible. This selectivity towards HK1 cells suggests that A549 cells are more resistant. Compounds cardamonin-Cu(II) (**Figure 3.2**) and cardamonin-Fe(II) (**Figure 3.3**) exhibited the two highest cytotoxic activity in the two cancer cell lines. IC_{50} values over 24, 48 and 72 hrs treatment ranged from 17.3 to 58.3 μ M in A549 cells and 0.76 to 9 μ M in HK1 cells for cardamonin-Cu(II); and 22.7 to 38.0 μ M in A549 cells and 16.6 to 23.2 μ M in HK1 cells for cardamonin-Fe(II) as summarised in **Table 3.1**. These results indicated that complexing cardamonin to metal complexes such as copper and iron can increase the cytotoxic activity significantly. Cardamonin-

Cu(II) in particular decreased the cell viability of HK1 by more than ten-fold compared to the parent compound, cardamonin, at all the time points. The less effective compounds with $IC_{50} > 200 \mu\text{M}$ in both cell lines were OMe-cardamonin (**Figure 3.11**), hydroxylamine-cardamonin (**Figure 3.13**), thiourea-cardamonin (**Figure 3.15**), tetrahydro-cardamonin (**Figure 3.16**) and flavanone-cardamonin (**Figure 3.18**). Interestingly, replacing both the hydroxyl groups of cardamonin with hydrophobic groups, OBn and OMe, in OBn-cardamonin (**Figure 3.10**) and OMe-cardamonin (**Figure 3.11**) respectively resulted in a loss of cytotoxicity in both cell lines. However, the cytotoxicity was enhanced upon the addition of the less hydrophobic allyl group to allyl-cardamonin (**Figure 3.7**). Loss of the carbonyl group in both phenylamine-cardamonin (**Figure 3.9**) and methoxyamine-cardamonin (**Figure 3.8**) resulted in significantly less cytotoxicity in both cell lines. Conversely, the loss of carbonyl group in cardamonin-B (**Figure 3.4**) resulted in an increased cytotoxicity compared to the parent compound in both cell lines, highlighting that modifications to the carbonyl group significantly alter the cytotoxicity effect. Compounds hydroxylamine-cardamonin and hydrazinium-cardamonin possessed very similar structures. Instead of an alkene group linking the two benzene rings in cardamonin, hydroxylamine functional group and hydrazinium connect the two benzene rings in hydroxylamine-cardamonin and hydrazinium-cardamonin respectively. Interestingly, these two compounds exhibited very different cytotoxic activities. Hydroxylamine-cardamonin (**Figure 3.13**) is one of the weakest compound with $IC_{50} > 200 \mu\text{M}$ tested in both cells lines whereas the IC_{50} of hydrazinium-cardamonin (**Figure 3.5**) was $\geq 80 \mu\text{M}$ in both cell lines. This data demonstrated that the position of the alkene group also has an important influence on the cytotoxicity of these compounds. Evidently, replacement of the alkene group with methylene bridge

in tetrahydro-cardamonin (**Figure 3.16**) resulted in a total loss of cytotoxicity in both cell lines with $IC_{50} > 200 \mu M$ at all the time points examined. Additionally, both urea-cardamonin (**Figure 3.14**) and thiourea-cardamonin (**Figure 3.15**) have very similar structures except that the oxygen atom of urea in urea-cardamonin is replaced by a sulphur atom in thiourea-cardamonin linking the two benzene rings. The replacement of oxygen with sulphur atom results in a loss of cytotoxicity in both cell lines as seen in thiourea-cardamonin. On the other hand, introduction of urea group to the cardamonin structure showed better activity towards both cell lines compared to the parent compound. With regards to the effect of hydroxyl groups at position 2 and 4 on cytotoxic activity of cardamonin, results illustrate that loss of both hydroxyl groups altered the cytotoxicity of cardamonin. The two additional methyl group and carbonyl group replacing the hydroxyl groups in acetyl-cardamonin (**Figure 3.6**) greatly increased the cytotoxicity in both cell lines. Whereas the fluoro-benzene derivative of cardamonin, 4-fluoro-cardamonin (**Figure 3.12**) resulted in a loss of cytotoxicity in both cell lines compared to acetyl-cardamonin. This data suggest that the improved cytotoxicity observed in acetyl-cardamonin is due to the substitution of fluoro-benzene rings with methyl groups at position 2. Comparing flavanol-cardamonin (**Figure 3.17**) and flavanone-cardamonin (**Figure 3.18**), the removal of three hydroxyl groups in flavanone-cardamonin resulted in a drop of cytotoxicity in both cell lines compared to flavanol-cardamonin. This is in contrast to the conclusion drawn from above where a decrease in cardamonin hydroxyl groups increases the cytotoxicity. It is however important to note that the introduction of the three additional hydroxyl groups in flavanol-cardamonin was at different positions. Therefore, the position of the hydroxyl groups was proven to be a greater factor in affecting the cytotoxic activities of the tested compounds compared to the number of

hydroxyl groups present in the compounds. Two halogen elements, iodine and bromine, were bonded to cardamonin at position 5 resulting in compounds cardamonin-I(II) and cardamonin-Br(II) respectively. Cardamonin-I(II) (**Figure 3.19**) showed much higher cytotoxic activity than that of cardamonin-Br(II) (**Figure 3.20**) in both cancer cell lines. This finding further suggest that the C5 position on the benzene ring of cardamonin also has an important influence on the cytotoxicity of these compounds.

In the present study, cardamonin and its 20 derivatives were initially tested in human lung cancer A549 and nasopharyngeal cancer HK1 cell lines. The SAR analyses suggested that the cytotoxic activities of diverse cardamonin derivatives was affected by a range of factors including the modification of hydroxyl group, presence of alkene group, addition of chemical groups, with the greatest cytotoxicity advantage being complexing with metal ions.

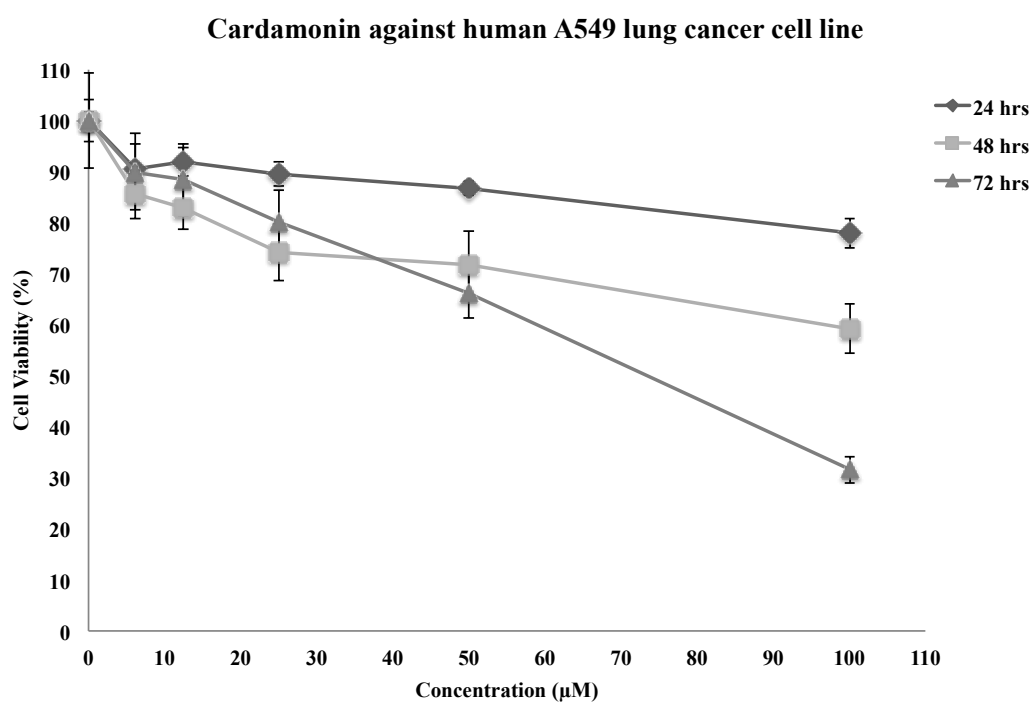
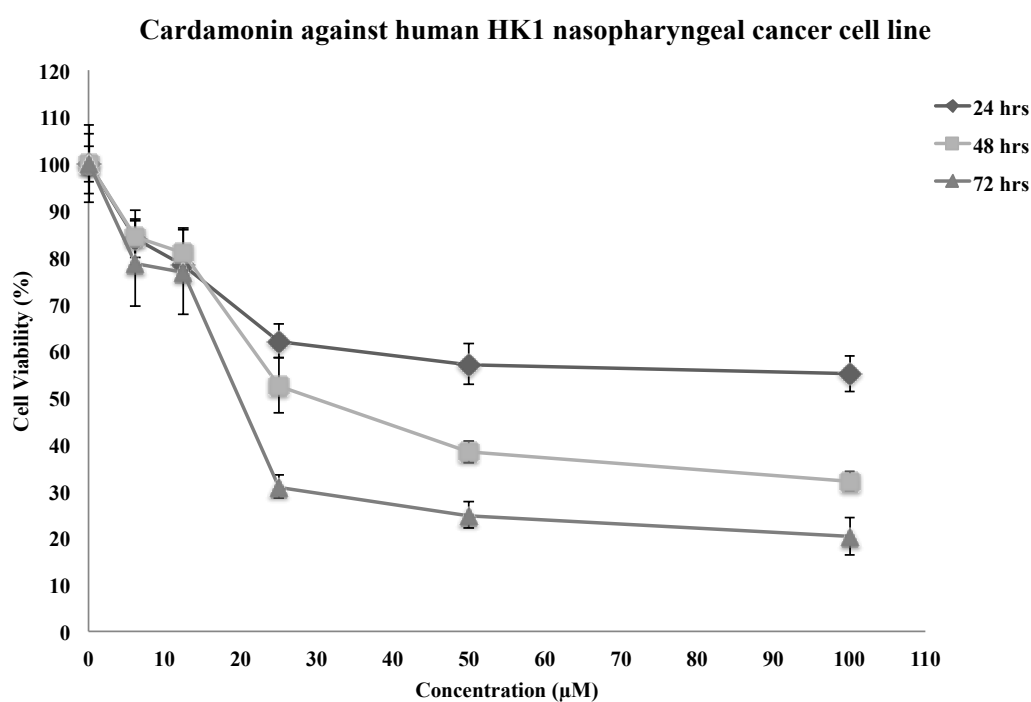
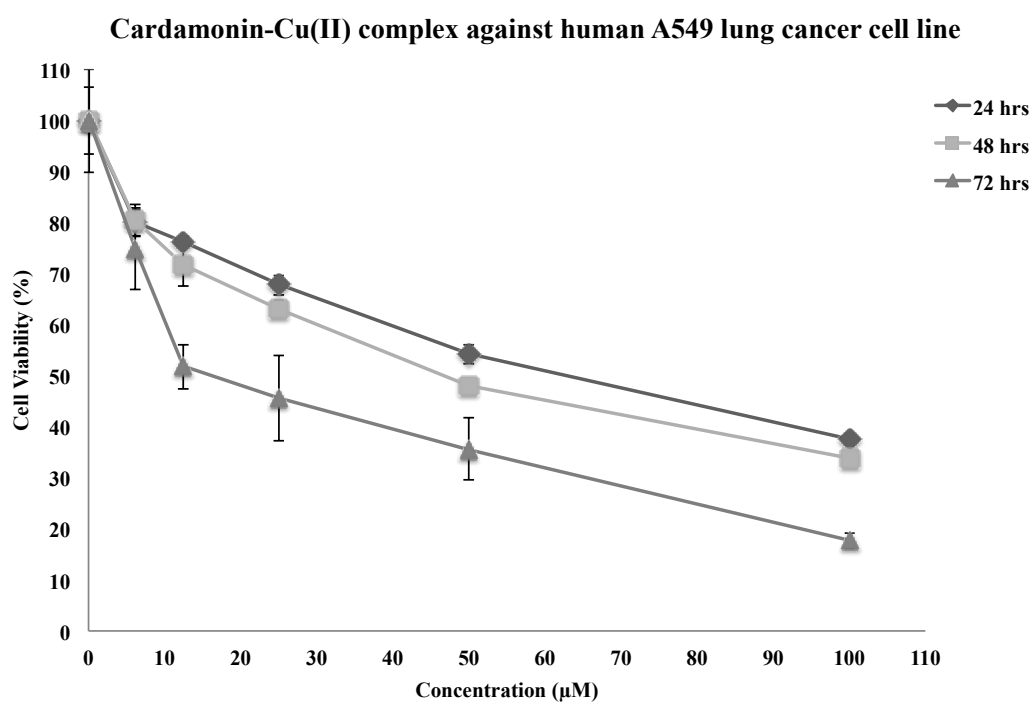
A**B**

Figure 3.1 Effect of cardamonin in human cancer cell lines.

Human A549 lung cancer cells (**A**) and human HK1 nasopharyngeal cancer cells (**B**). Cells were treated with cardamonin for 24, 48 and 72 hrs and cell viability was assessed *via* the MTS assay as outlined in the Materials and Methods section. Results are means \pm SEM of three independent experiments.

A



B

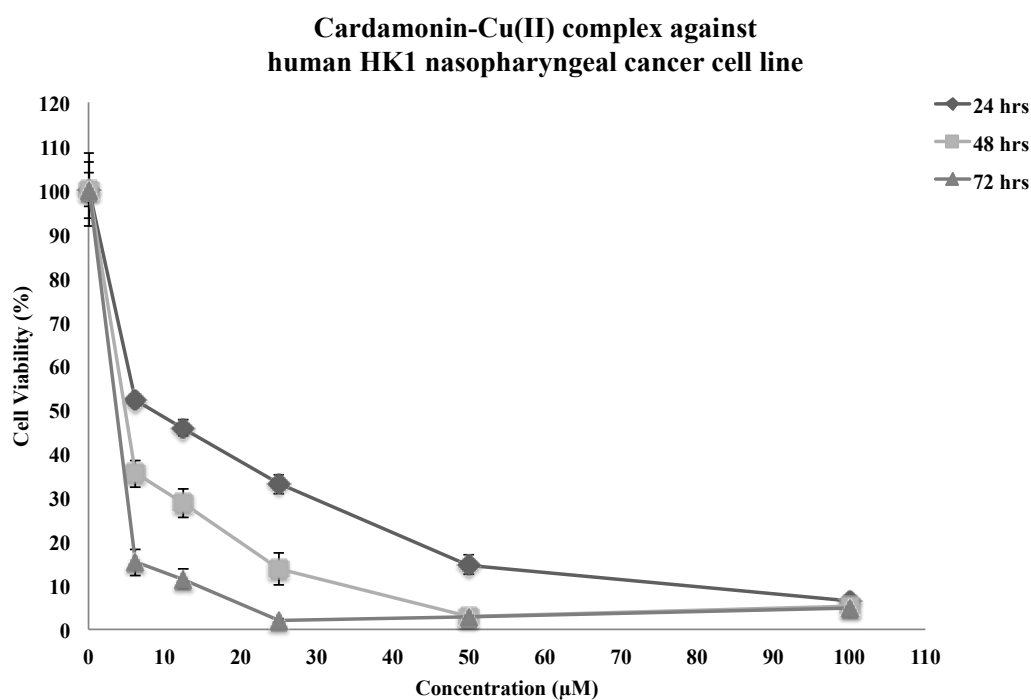
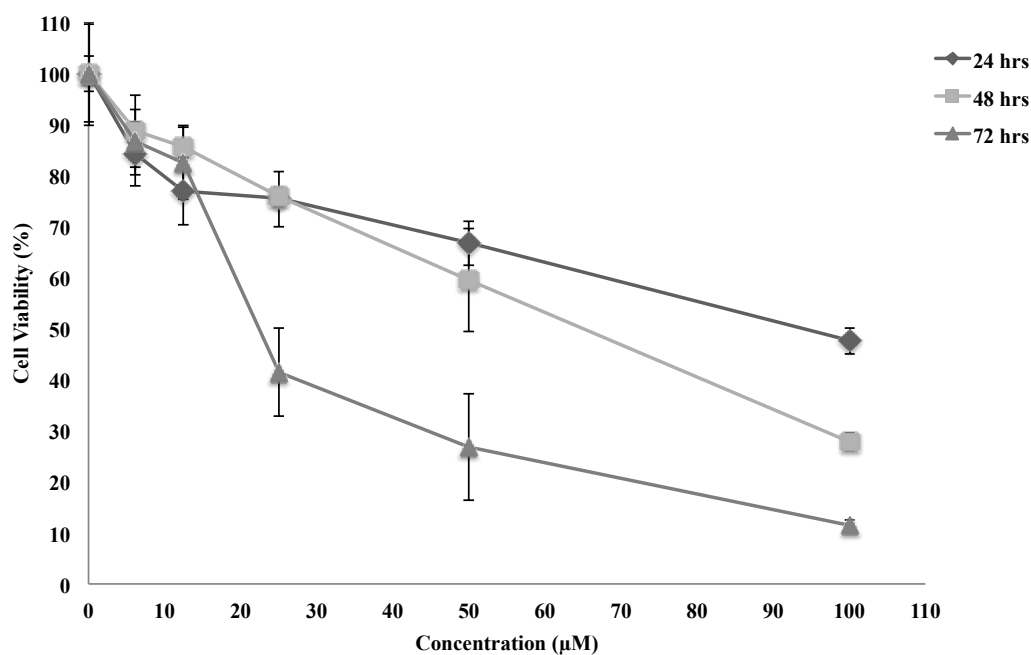


Figure 3.2 Effect of cardamonin-Cu(II) in cancer human cell lines.

Human A549 lung cancer cells (A) and human HK1 nasopharyngeal cancer cells (B). Cells were treated with cardamonin-Cu(II) for 24, 48 and 72 hrs and cell viability was assessed *via* the MTS assay as outlined in the Materials and Methods section. Results are means \pm SEM of three independent experiments.

A

Cardamonin-Fe(II) complex against human A549 lung cancer cell line



B

Cardamonin-Fe(II) complex against human HK1 nasopharyngeal cancer cell line

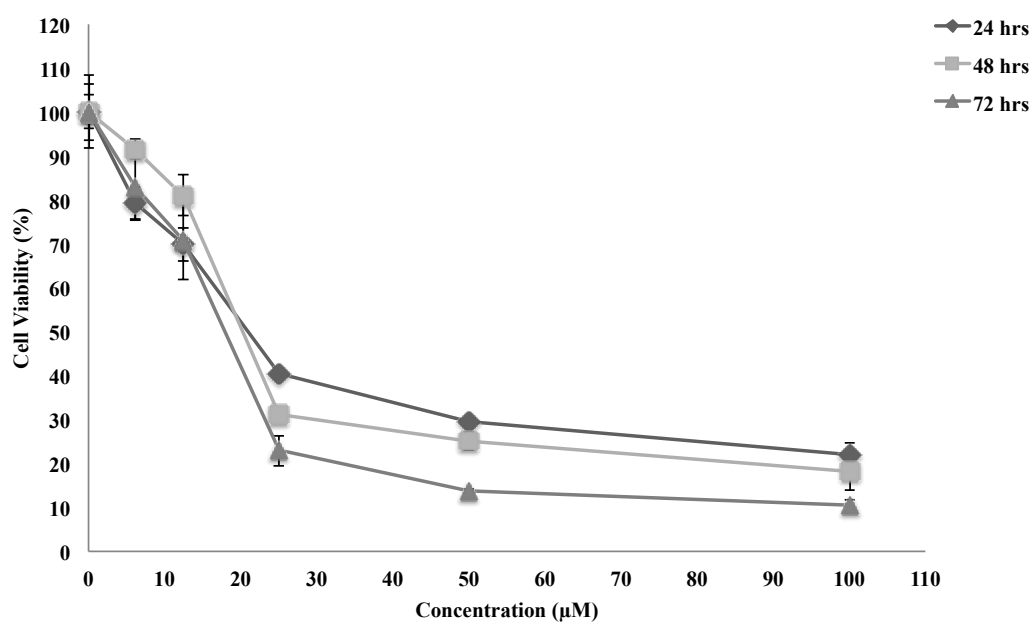


Figure 3.3 Effect of cardamonin-Fe(II) in human cancer cell lines.

Human A549 lung cancer cells (**A**) and human HK1 nasopharyngeal cancer cells (**B**). Cells were treated with cardamonin-Fe(II) for 24, 48 and 72 hrs and cell viability was assessed *via* the MTS assay as outlined in the Materials and Methods section. Results are means \pm SEM of three independent experiments.

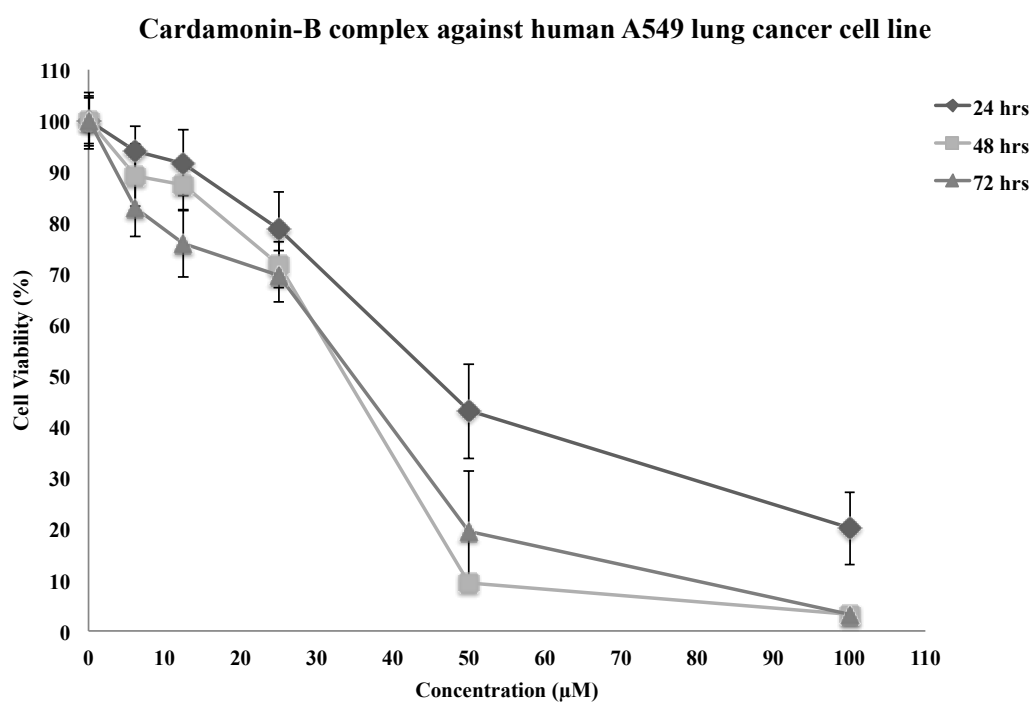
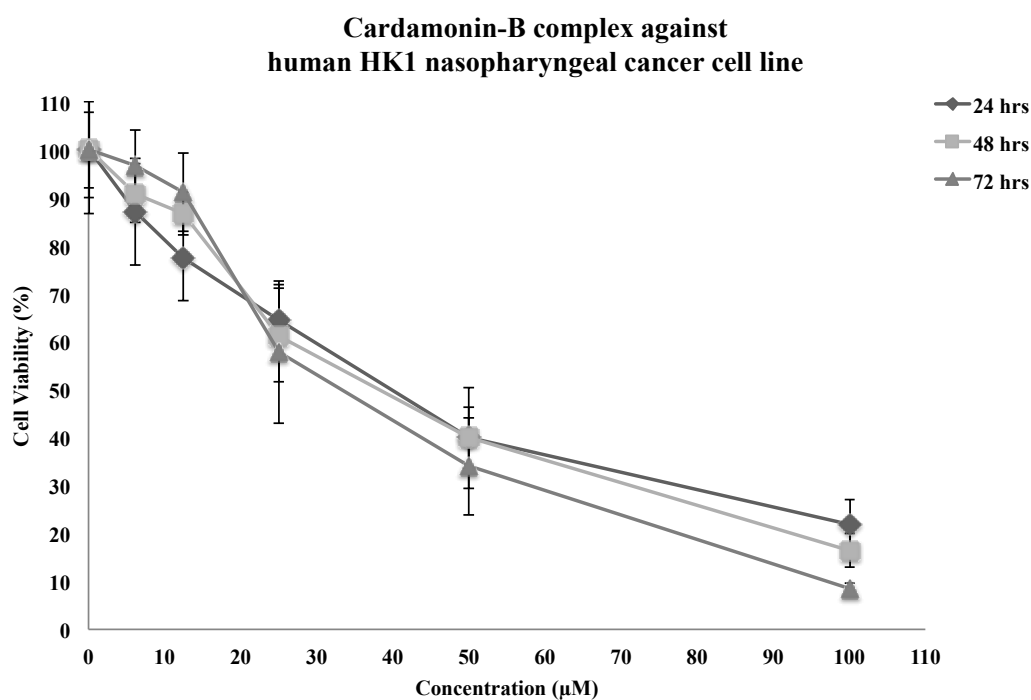
A**B**

Figure 3.4 Effect of cardamonin-B in human cancer cell lines.

Human A549 lung cancer cells (**A**) and human HK1 nasopharyngeal cancer cells (**B**). Cells were treated with cardamonin-B for 24, 48 and 72 hrs and cell viability was assessed *via* the MTS assay as outlined in the Materials and Methods section. Results are means \pm SEM of three independent experiments.

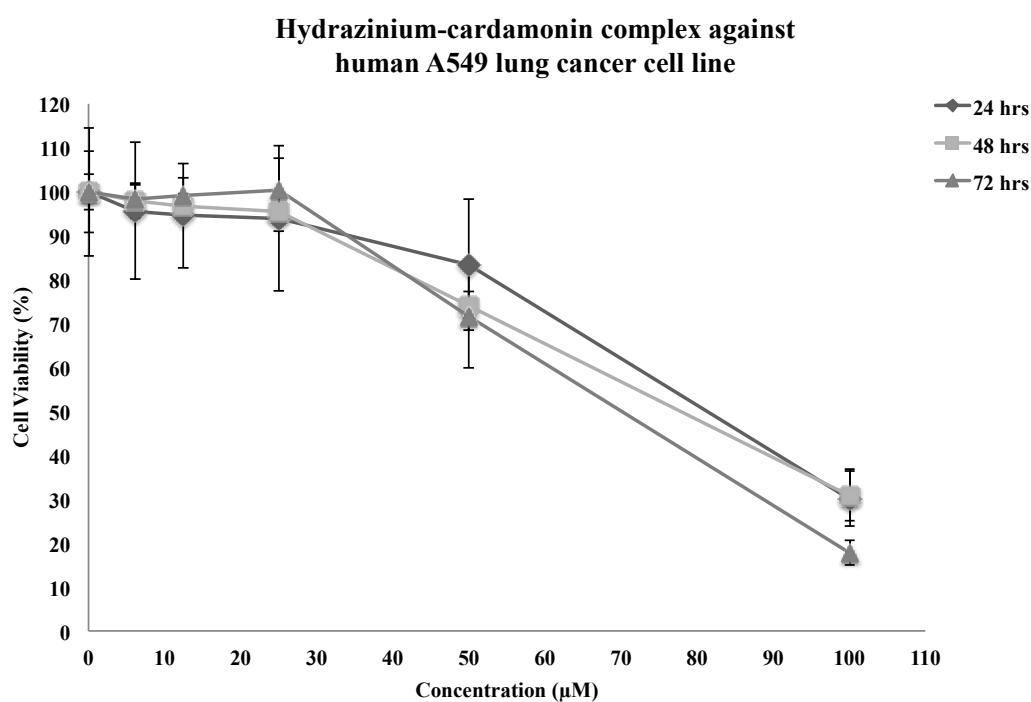
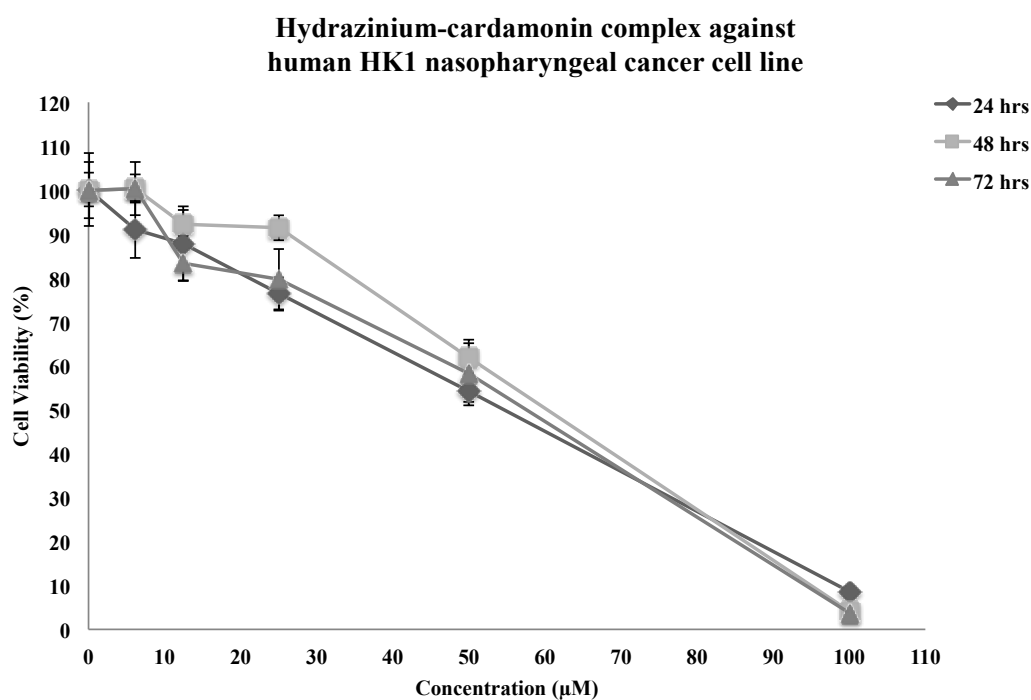
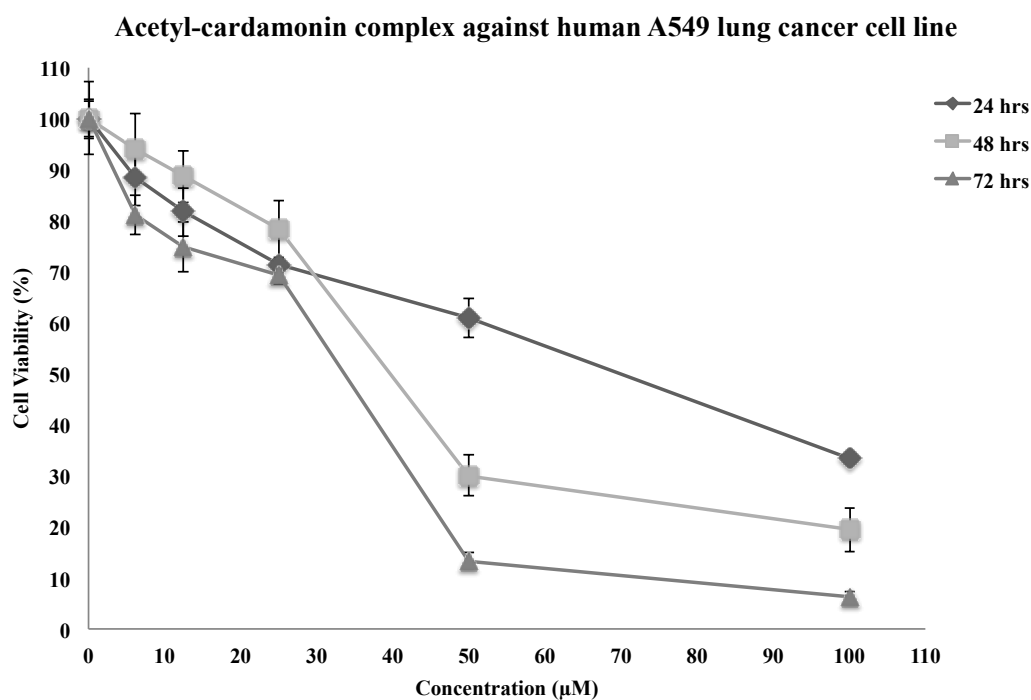
A**B**

Figure 3.5 Effect of hydrazinium-cardamonin in human cancer cell lines.

Human A549 lung cancer cells (**A**) and human HK1 nasopharyngeal cancer cells (**B**). Cells were treated with hydrazinium-cardamonin for 24, 48 and 72 hrs and cell viability was assessed *via* the MTS assay as outlined in the Materials and Methods section. Results are means \pm SEM of three independent experiments.

A



B

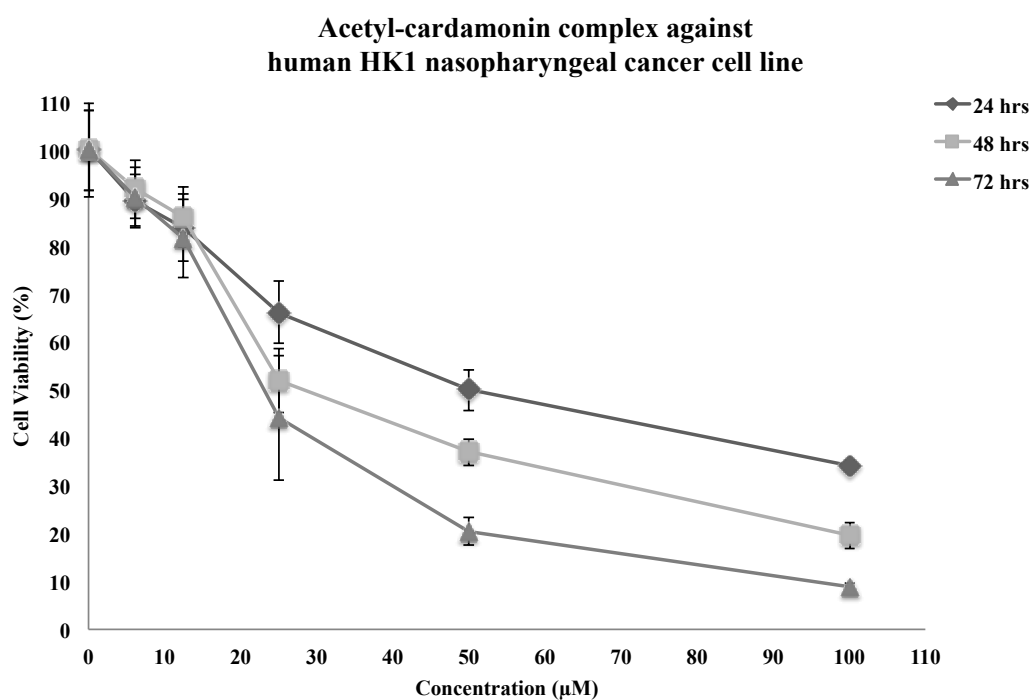


Figure 3.6 Effect of acetyl-cardamonin in human cancer cell lines.

Human A549 lung cancer cells (A) and human HK1 nasopharyngeal cancer cells (B). Cells were treated with acetyl-cardamonin for 24, 48 and 72 hrs and cell viability was assessed *via* the MTS assay as outlined in the Materials and Methods section. Results are means \pm SEM of three independent experiments.

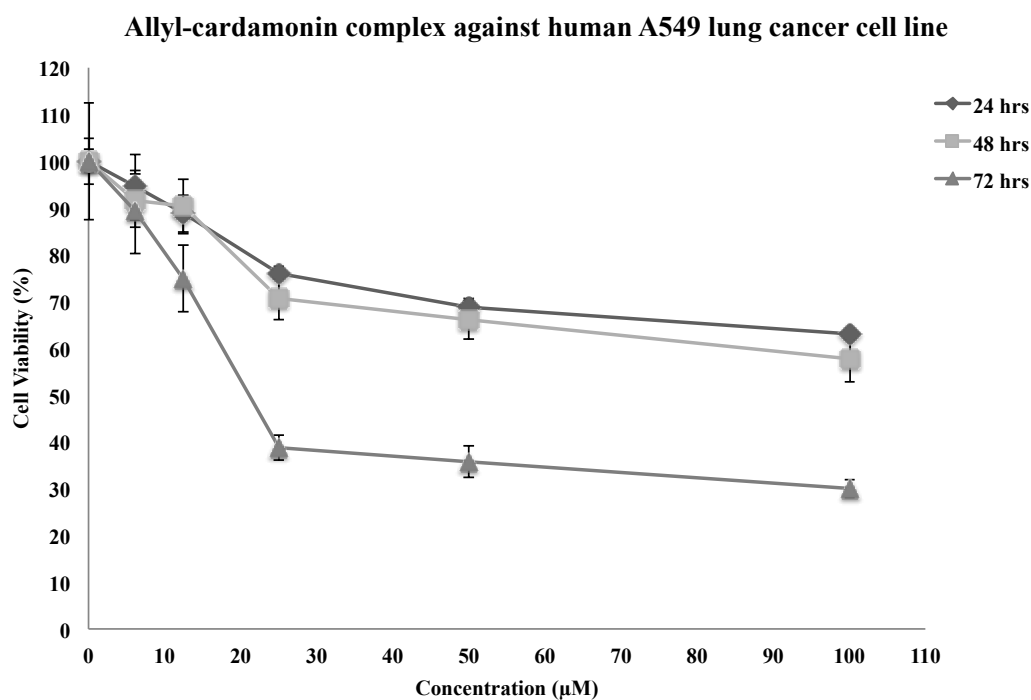
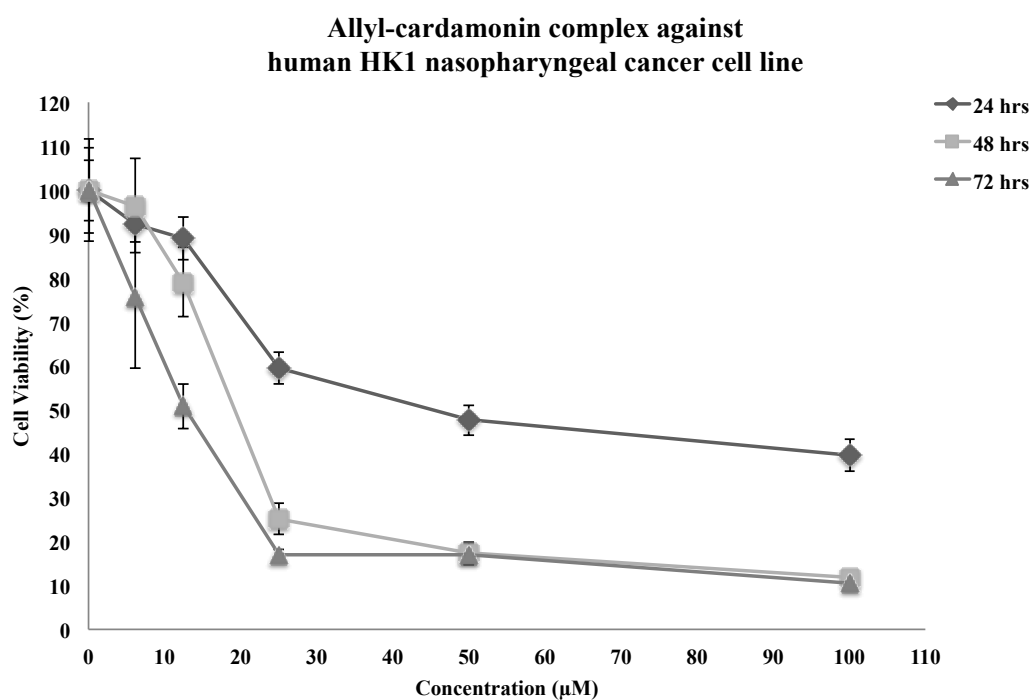
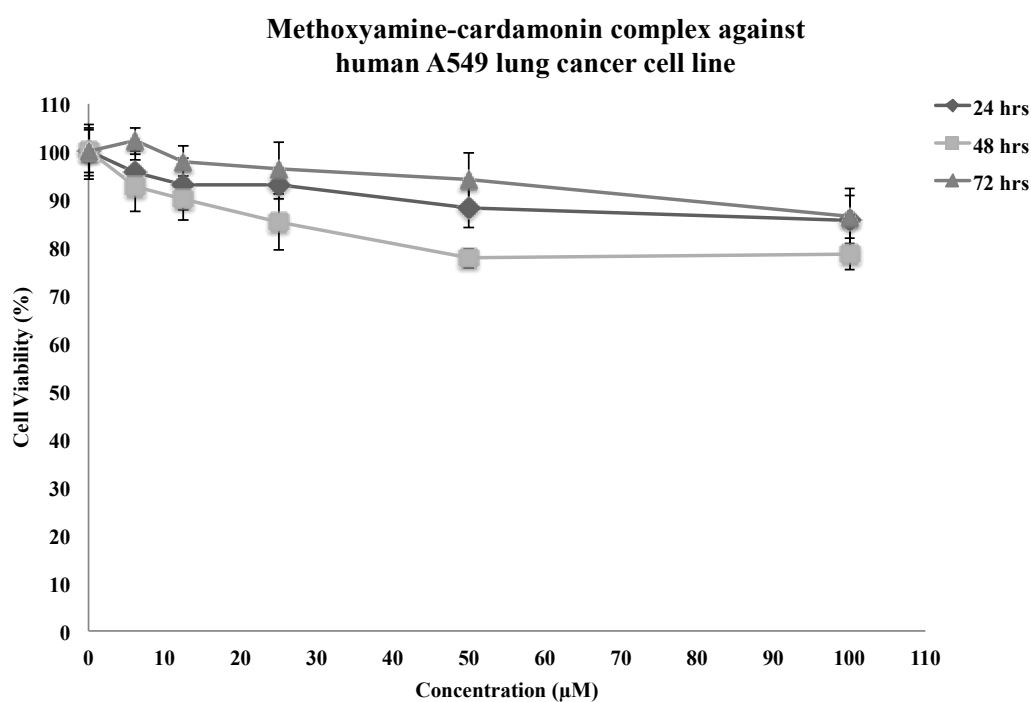
A**B**

Figure 3.7 Effect of allyl-cardamonin in human cancer cell lines.

Human A549 lung cancer cells (**A**) and human HK1 nasopharyngeal cancer cells (**B**). Cells were treated with allyl-cardamonin for 24, 48 and 72 hrs and cell viability was assessed *via* the MTS assay as outlined in the Materials and Methods section. Results are means \pm SEM of three independent experiments.

A



B

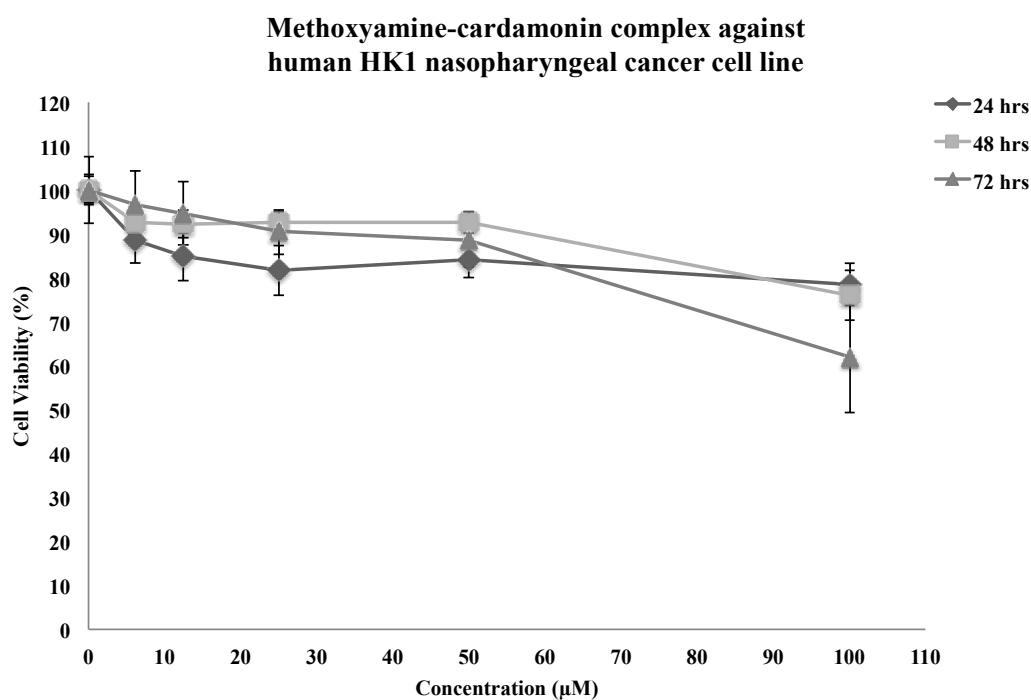
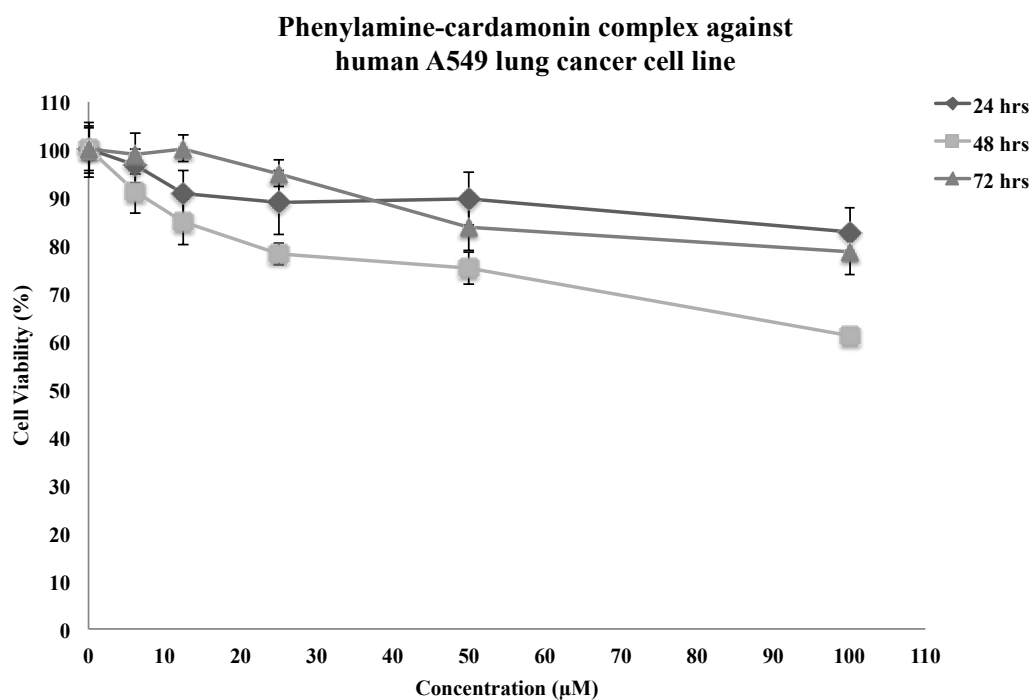


Figure 3.8 Effect of methoxyamine-cardamomin in human cancer cell lines.

Human A549 lung cancer cells (A) and human HK1 nasopharyngeal cancer cells (B). Cells were treated with methoxyamine-cardamomin for 24, 48 and 72 hrs and cell viability was assessed *via* the MTS assay as outlined in the Materials and Methods section. Results are means \pm SEM of three independent experiments.

A



B

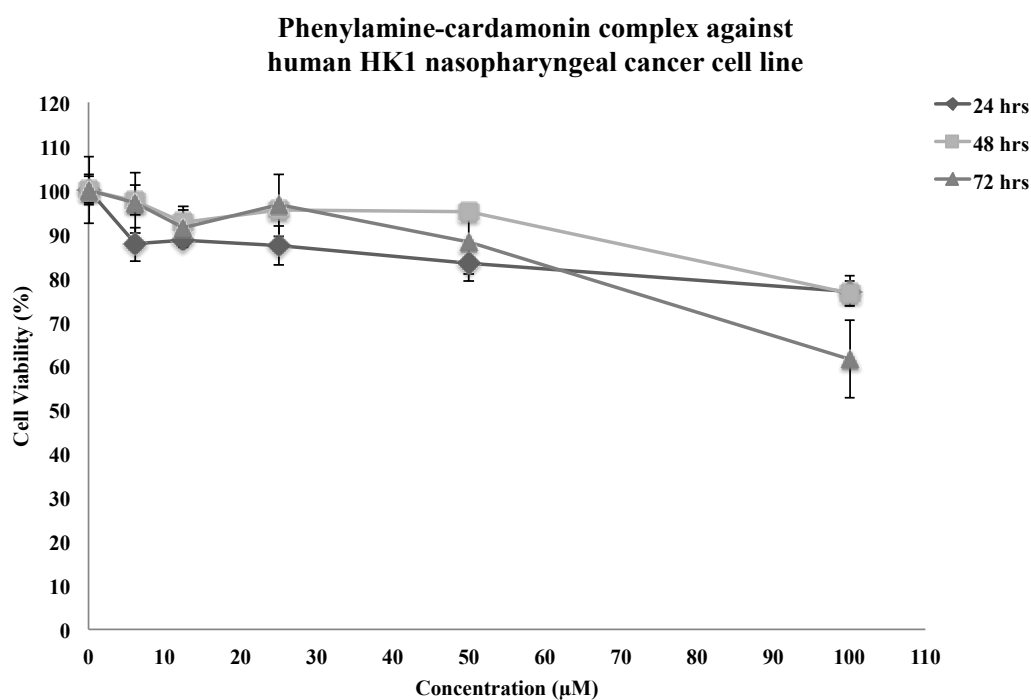
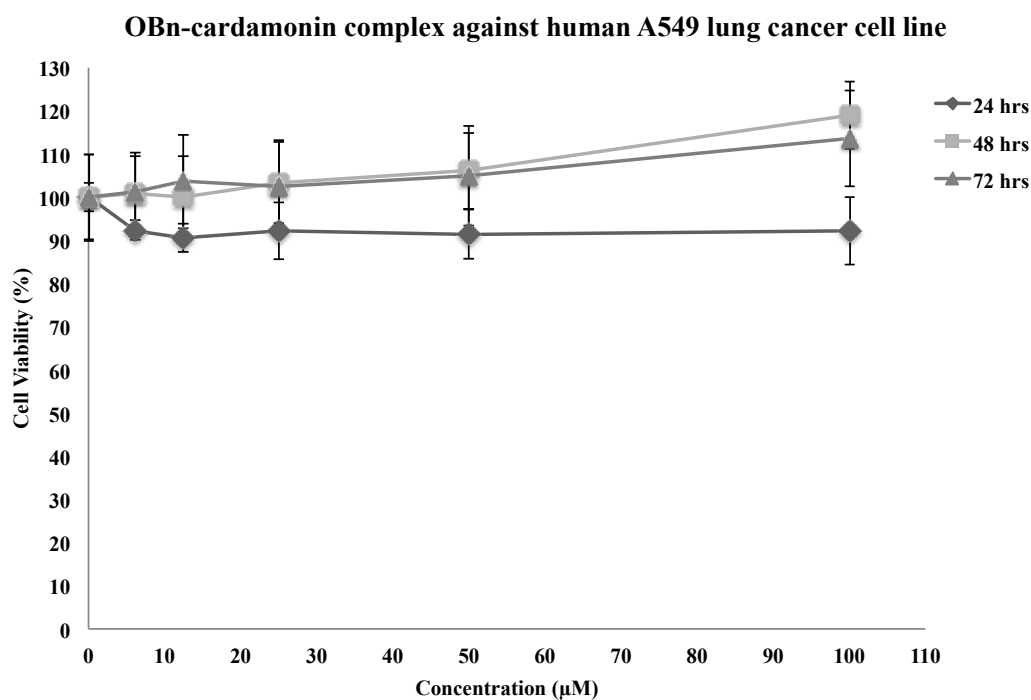


Figure 3.9 Effect of phenylamine-cardamonin in human cancer cell lines.

Human A549 lung cancer cells (A) and human HK1 nasopharyngeal cancer cells (B). Cells were treated with phenylamine-cardamonin for 24, 48 and 72 hrs and cell viability was assessed *via* the MTS assay as outlined in the Materials and Methods section. Results are means \pm SEM of three independent experiments.

A



B

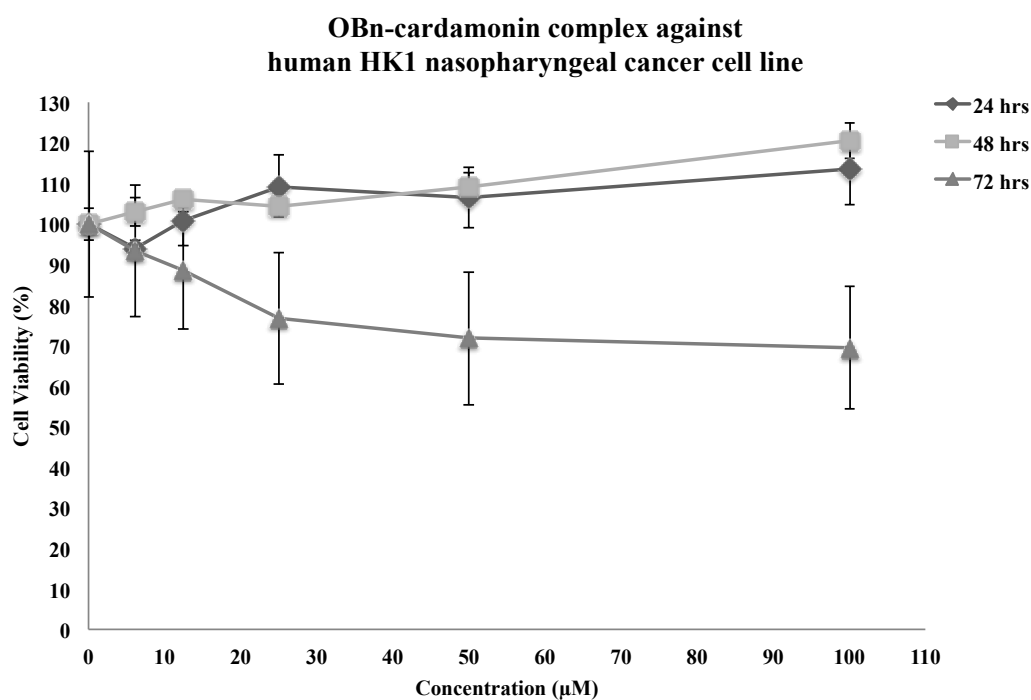


Figure 3.10 Effect of OBn-cardamonin in human cancer cell lines.

Human A549 lung cancer cells (**A**) and human HK1 nasopharyngeal cancer cells (**B**). Cells were treated with OBn-cardamonin for 24, 48 and 72 hrs and cell viability was assessed *via* the MTS assay as outlined in the Materials and Methods section. Results are means \pm SEM of three independent experiments.

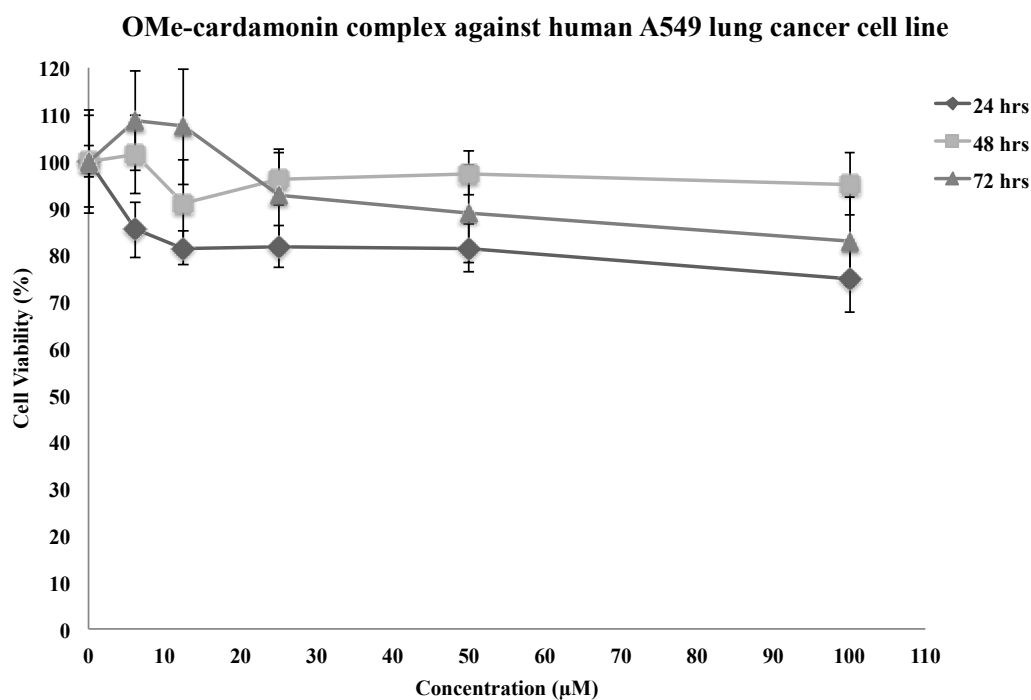
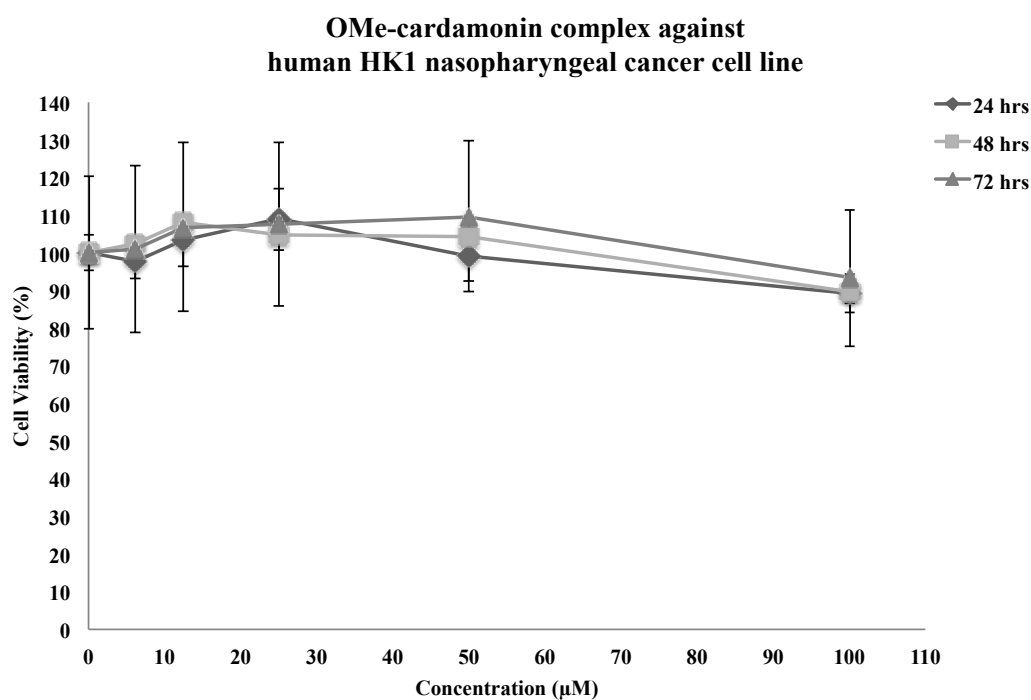
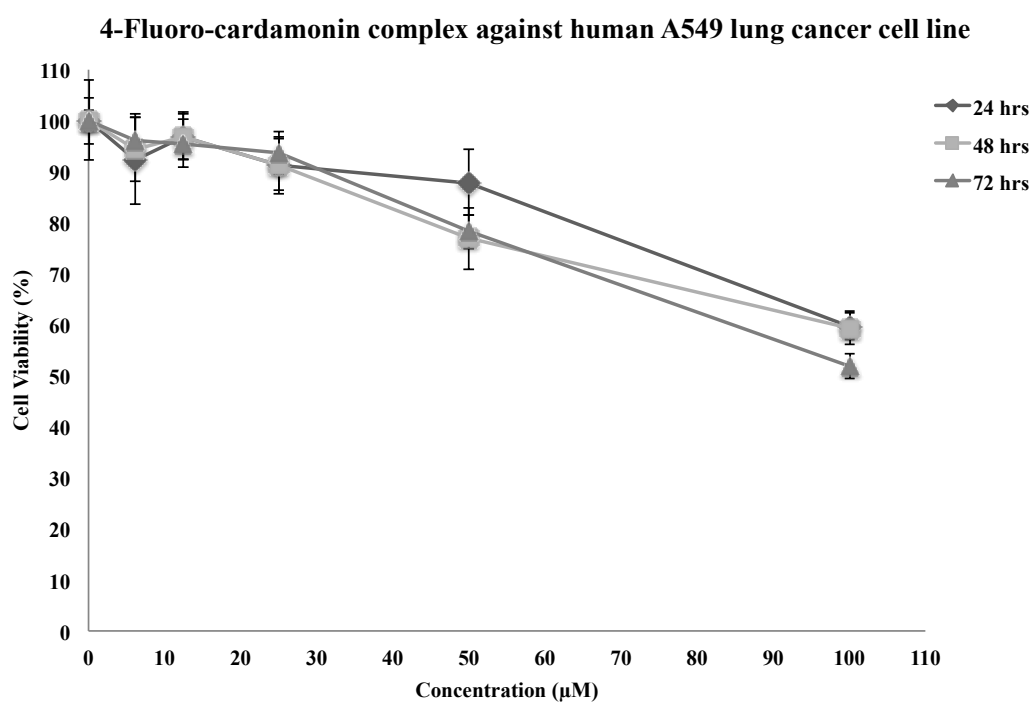
A**B**

Figure 3.11 Effect of OMe-cardamonin in human cancer cell lines.

Human A549 lung cancer cells (**A**) and human HK1 nasopharyngeal cancer cells (**B**). Cells were treated with OMe-cardamonin for 24, 48 and 72 hrs and cell viability was assessed *via* the MTS assay as outlined in the Materials and Methods section. Results are means \pm SEM of three independent experiments.

A



B

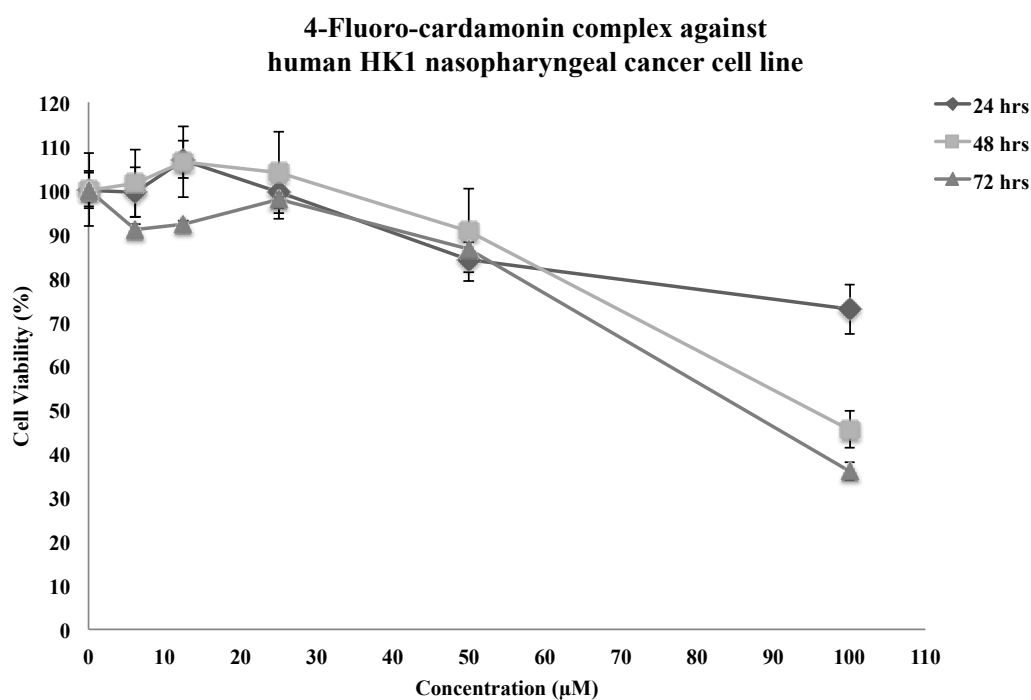
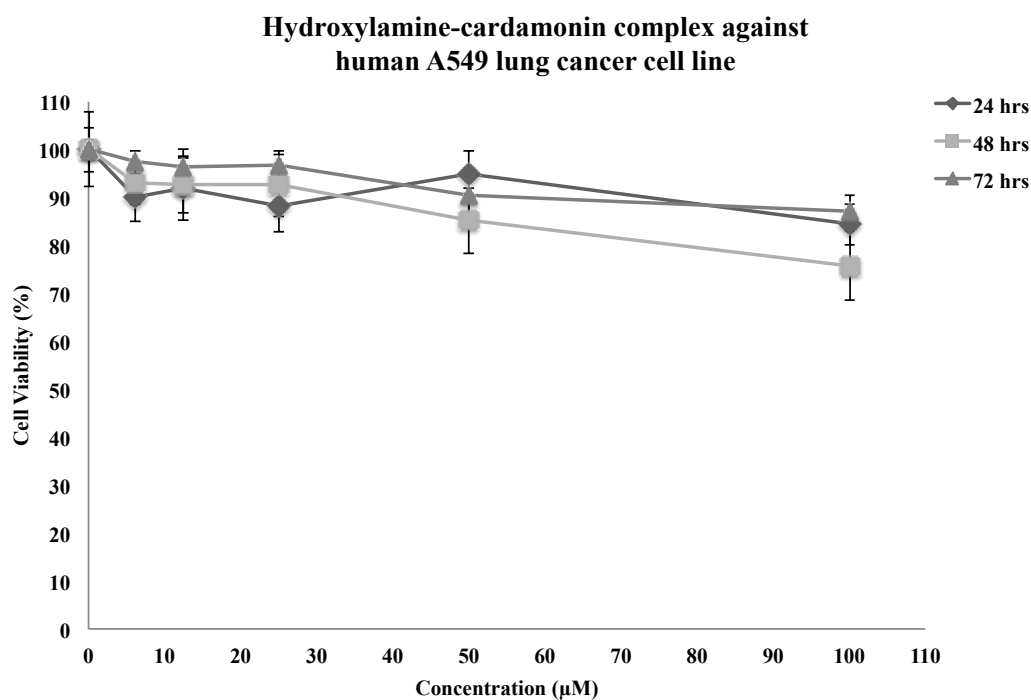


Figure 3.12 Effect of 4-fluoro-cardamonin in human cancer cell lines.

Human A549 lung cancer cells (**A**) and human HK1 nasopharyngeal cancer cells (**B**). Cells were treated with 4-fluoro-cardamonin for 24, 48 and 72 hrs and cell viability was assessed *via* the MTS assay as outlined in the Materials and Methods section. Results are means \pm SEM of three independent experiments.

A



B

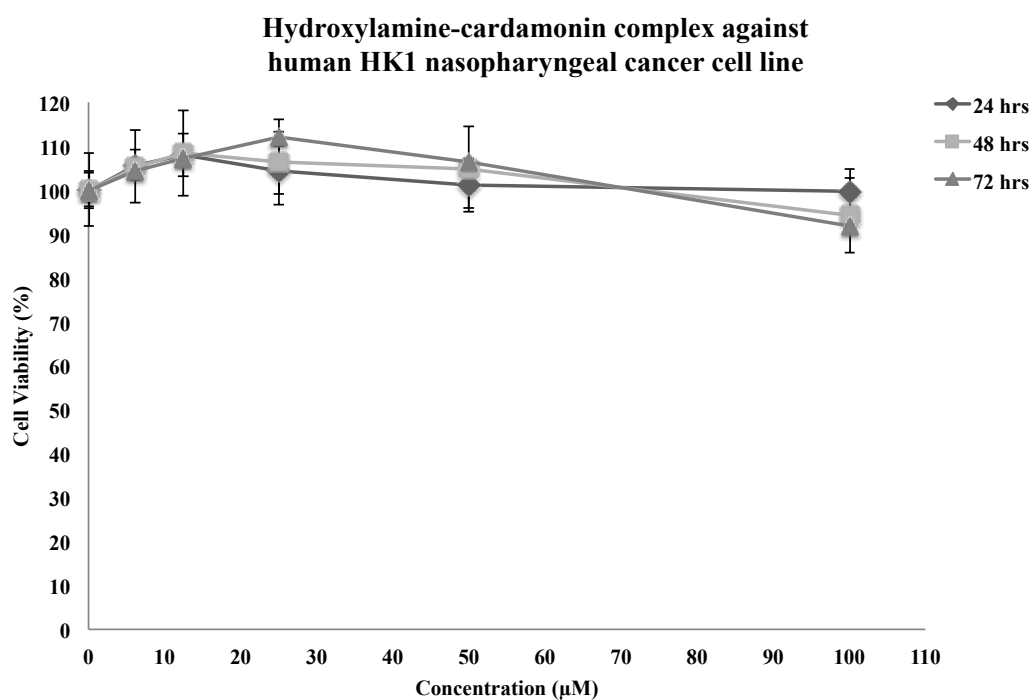


Figure 3.13 Effect of hydroxylamine-cardamomin in human cancer cell lines.

Human A549 lung cancer cells (A) and human HK1 nasopharyngeal cancer cells (B). Cells were treated with hydroxylamine-cardamomin for 24, 48 and 72 hrs and cell viability was assessed *via* the MTS assay as outlined in the Materials and Methods section. Results are means \pm SEM of three independent experiments.

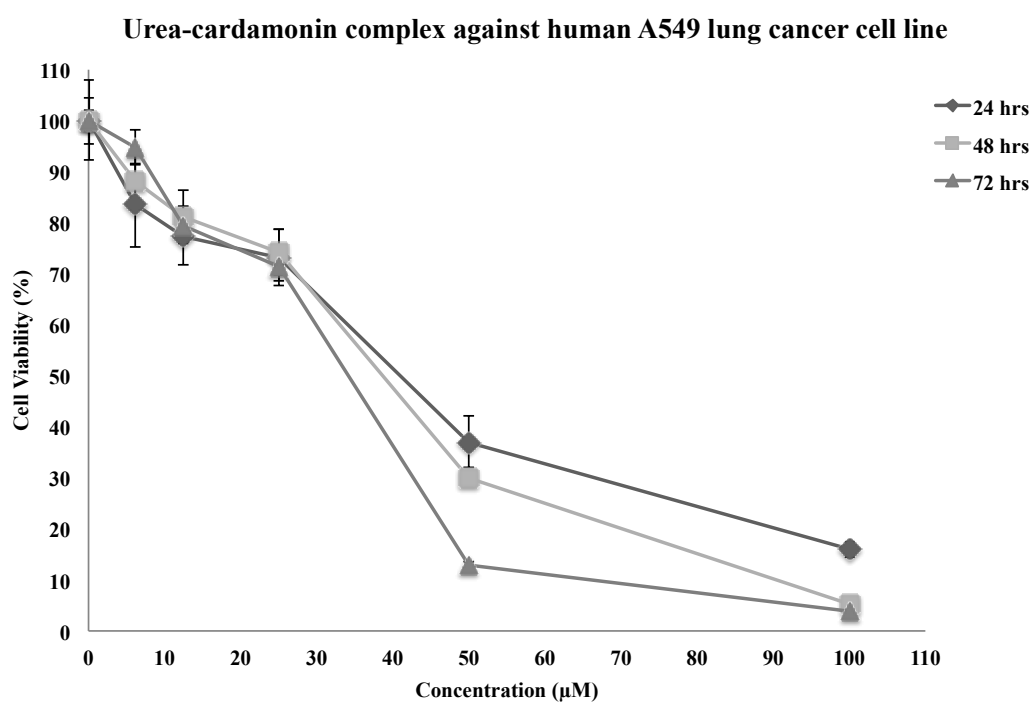
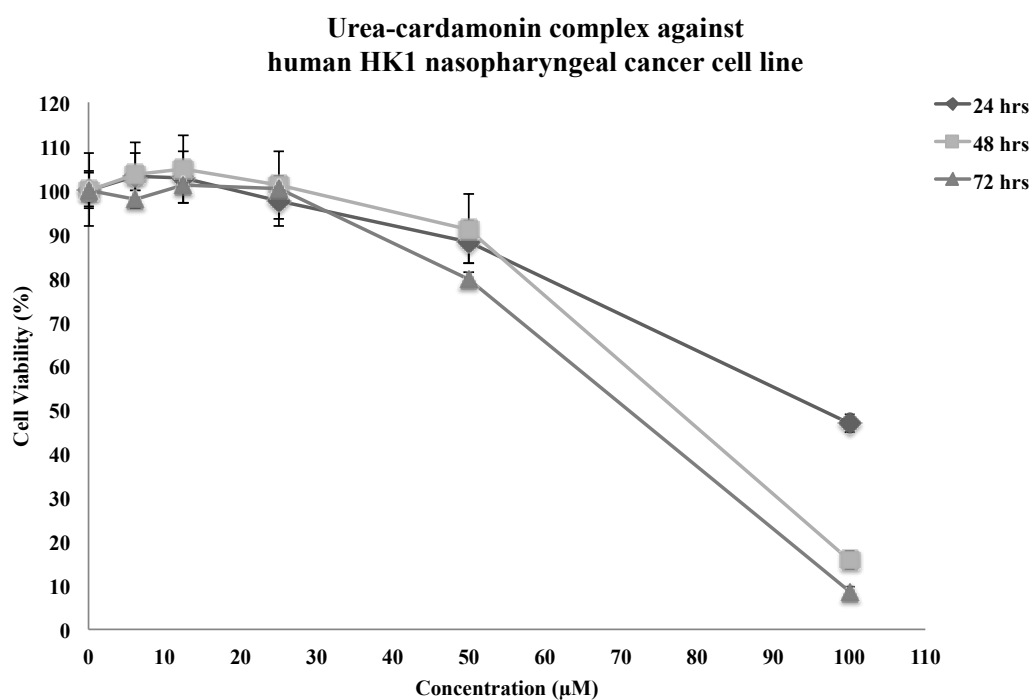
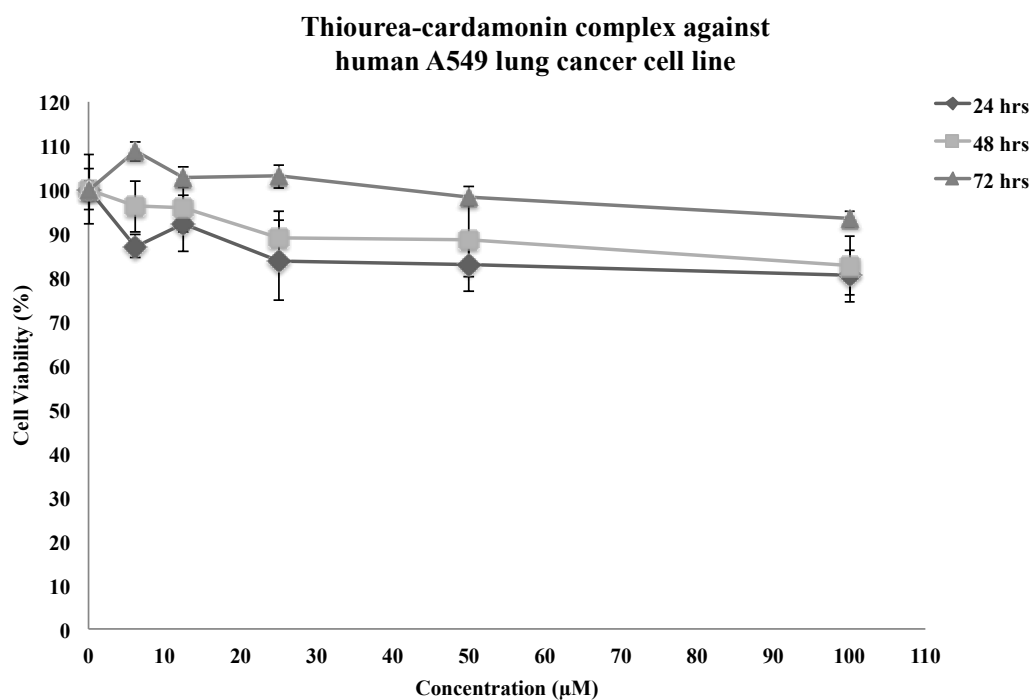
A**B**

Figure 3.14 Effect of urea-cardamonin in human cancer cell lines.

Human A549 lung cancer cells (**A**) and human HK1 nasopharyngeal cancer cells (**B**). Cells were treated with urea-cardamonin for 24, 48 and 72 hrs and cell viability was assessed *via* the MTS assay as outlined in the Materials and Methods section. Results are means \pm SEM of three independent experiments.

A



B

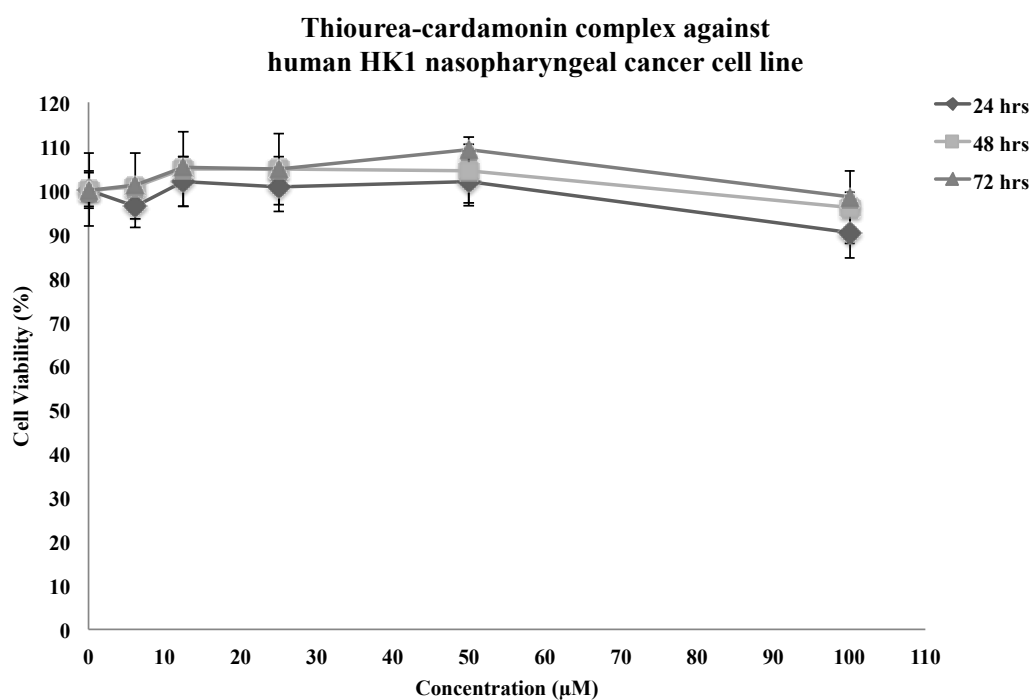
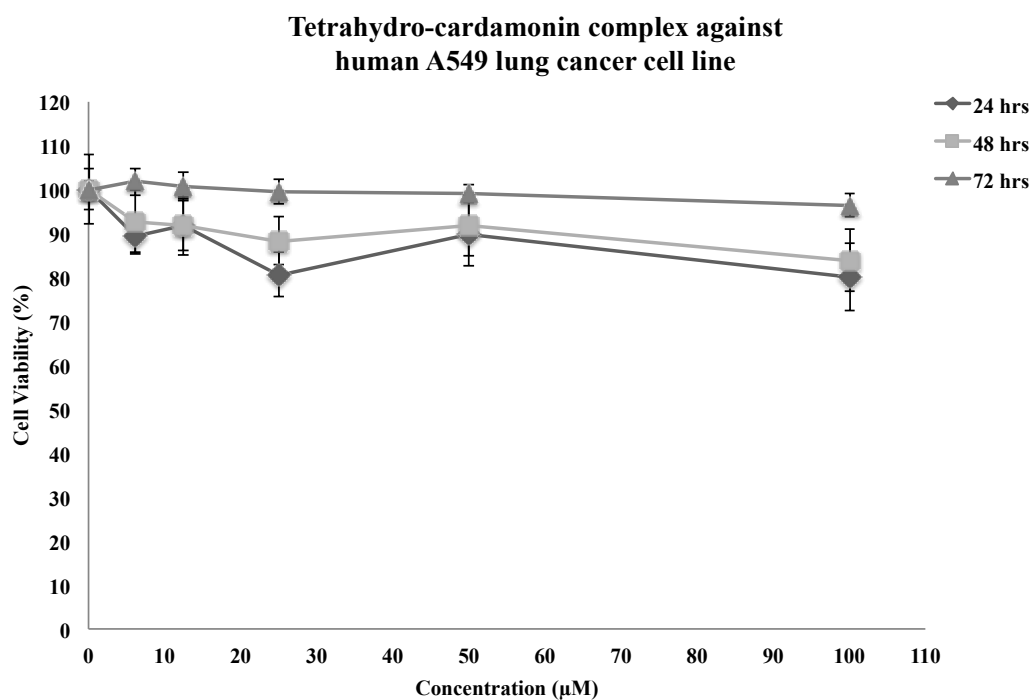


Figure 3.15 Effect of thiourea-cardamonin in human cancer cell lines.

Human A549 lung cancer cells (**A**) and human HK1 nasopharyngeal cancer cells (**B**). Cells were treated with thiourea-cardamonin for 24, 48 and 72 hrs and cell viability was assessed *via* the MTS assay as outlined in the Materials and Methods section. Results are means \pm SEM of three independent experiments.

A



B

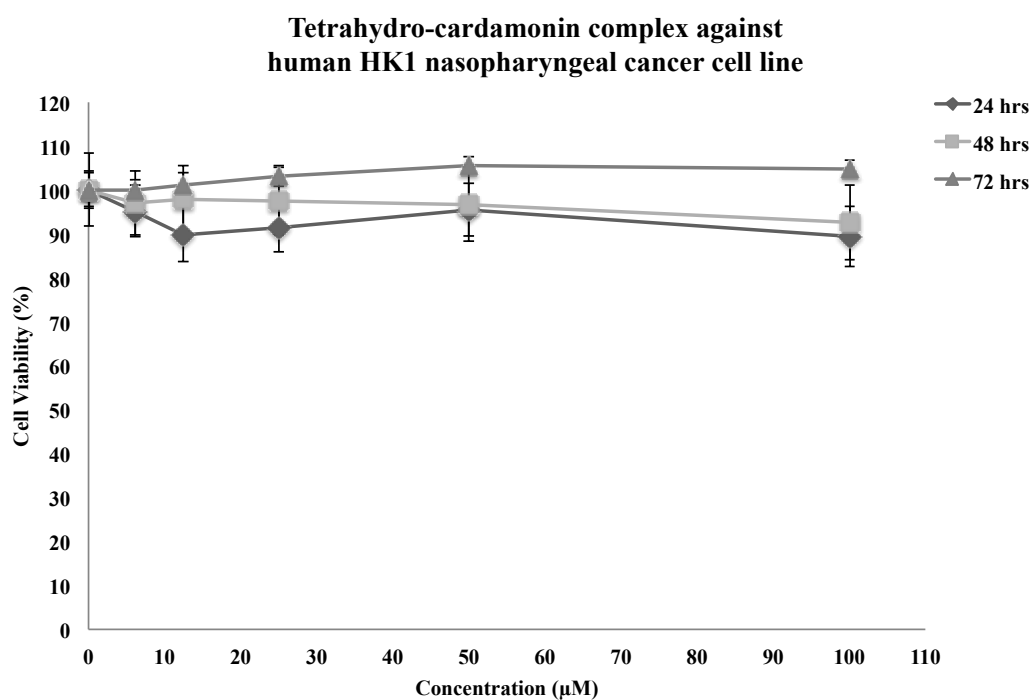
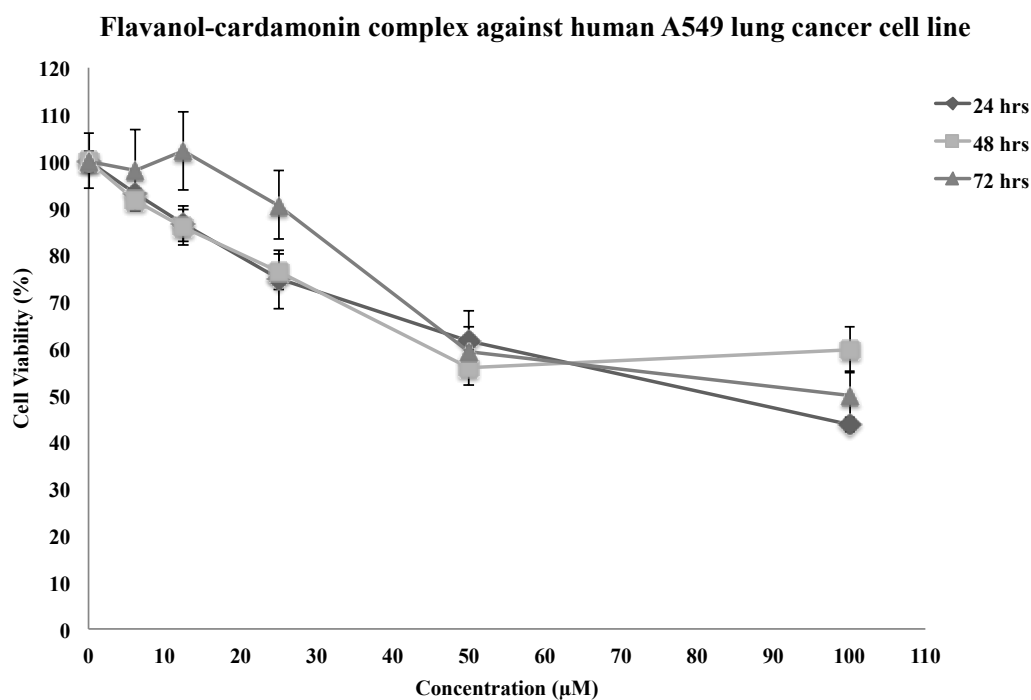


Figure 3.16 Effect of tetrahydro-cardamonin in human cancer cell lines.

Human A549 lung cancer cells (A) and human HK1 nasopharyngeal cancer cells (B). Cells were treated with tetrahydro-cardamonin for 24, 48 and 72 hrs and cell viability was assessed *via* the MTS assay as outlined in the Materials and Methods section. Results are means \pm SEM of three independent experiments.

A



B

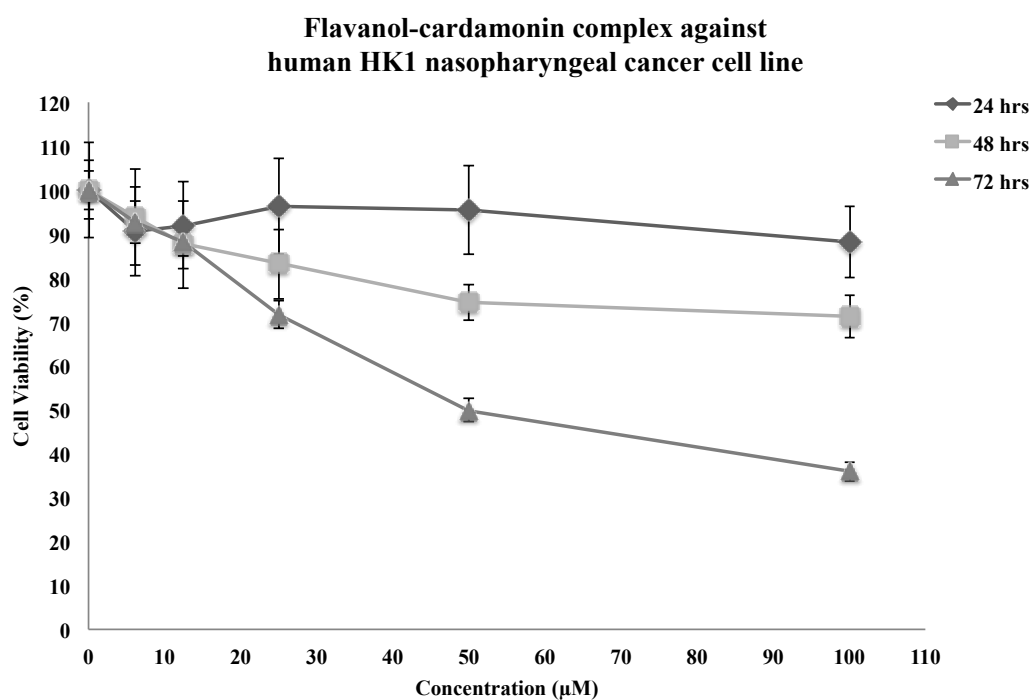
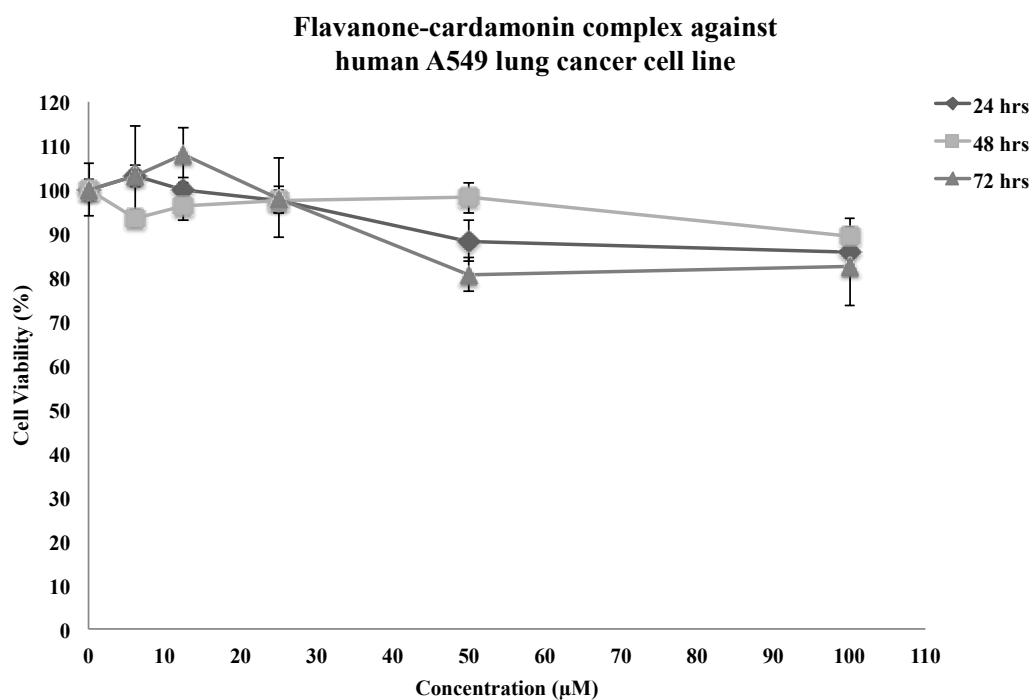


Figure 3.17 Effect of flavanol-cardamomin in human cancer cell lines.

Human A549 lung cancer cells (**A**) and human HK1 nasopharyngeal cancer cells (**B**). Cells were treated with flavanol-cardamomin for 24, 48 and 72 hrs and cell viability was assessed *via* the MTS assay as outlined in the Materials and Methods section. Results are means \pm SEM of three independent experiments.

A



B

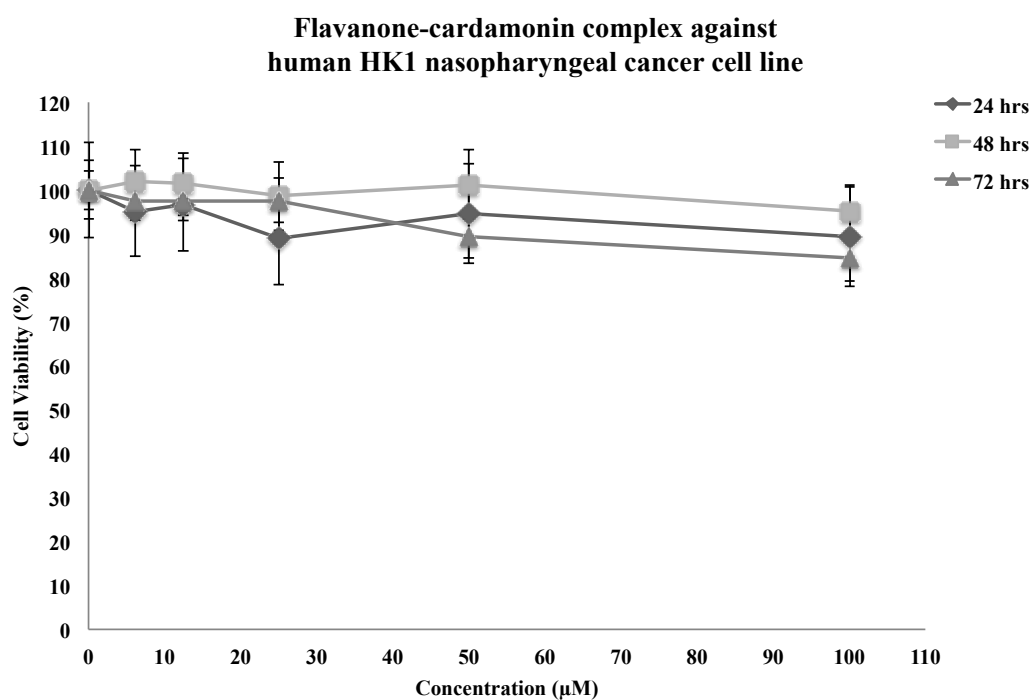
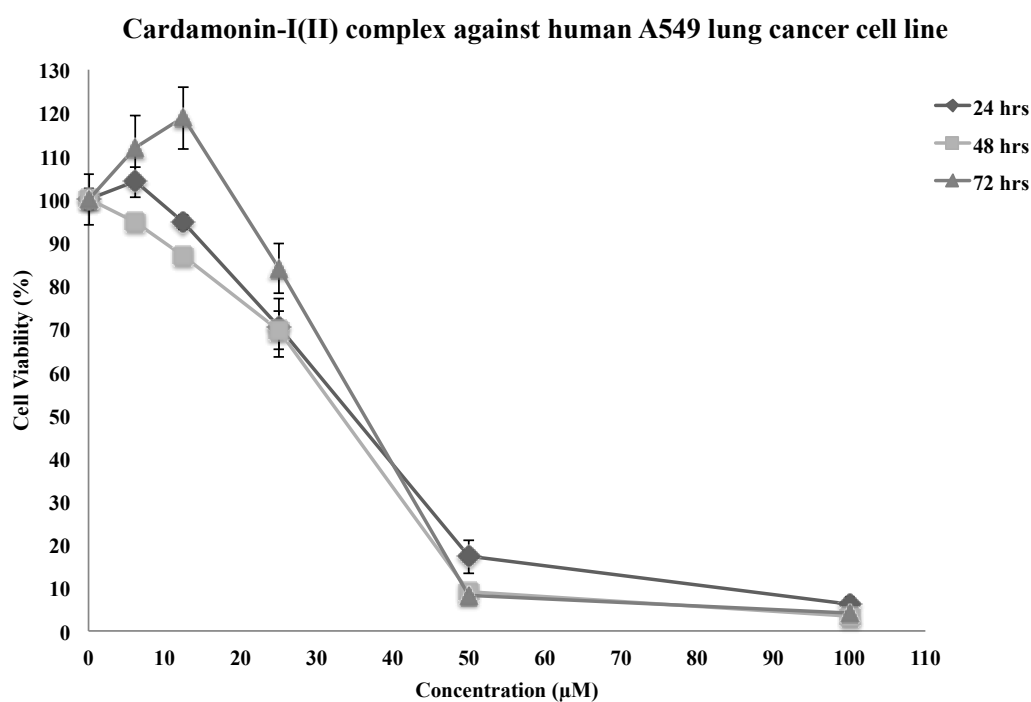


Figure 3.18 Effect of flavanone-cardamomin in human cancer cell lines.

Human A549 lung cancer cells (A) and human HK1 nasopharyngeal cancer cells (B). Cells were treated with flavanone-cardamomin for 24, 48 and 72 hrs and cell viability was assessed *via* the MTS assay as outlined in the Materials and Methods section. Results are means \pm SEM of three independent experiments.

A



B

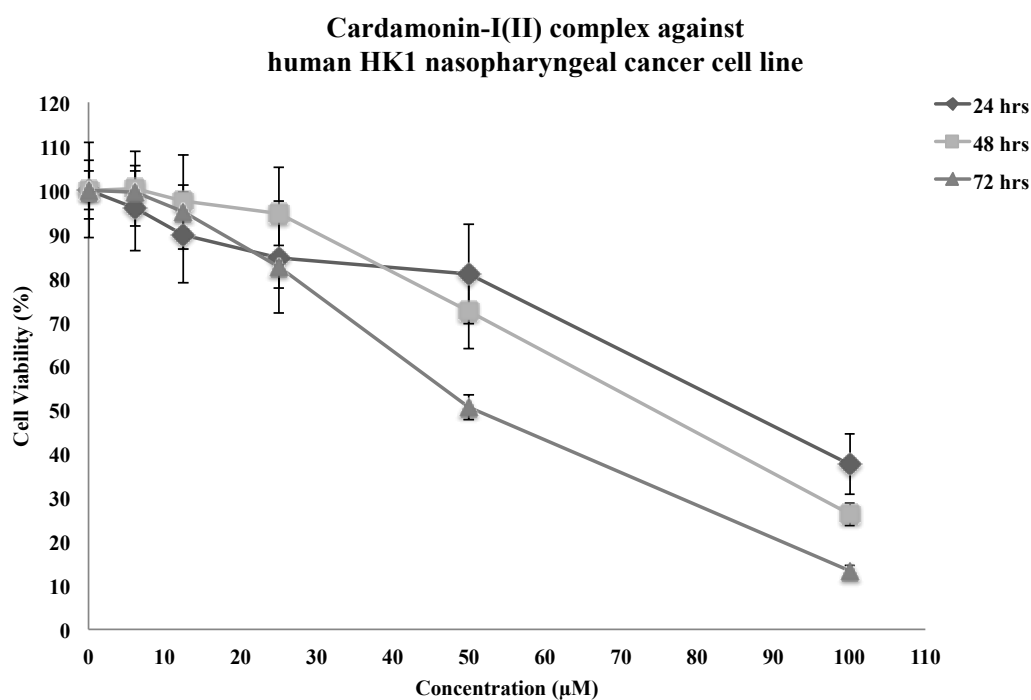
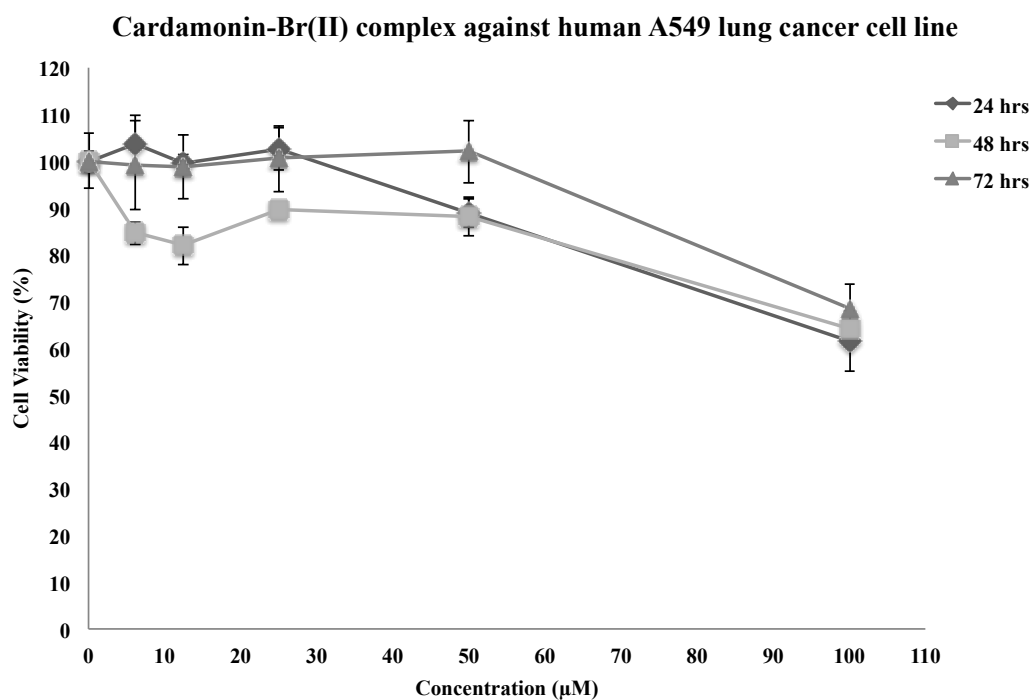


Figure 3.19 Effect of cardamonin-I(II) in human cancer cell lines.

Human A549 lung cancer cells (**A**) and human HK1 nasopharyngeal cancer cells (**B**). Cells were treated with cardamonin-I(II) for 24, 48 and 72 hrs and cell viability was assessed *via* the MTS assay as outlined in the Materials and Methods section. Results are means \pm SEM of three independent experiments.

A



B

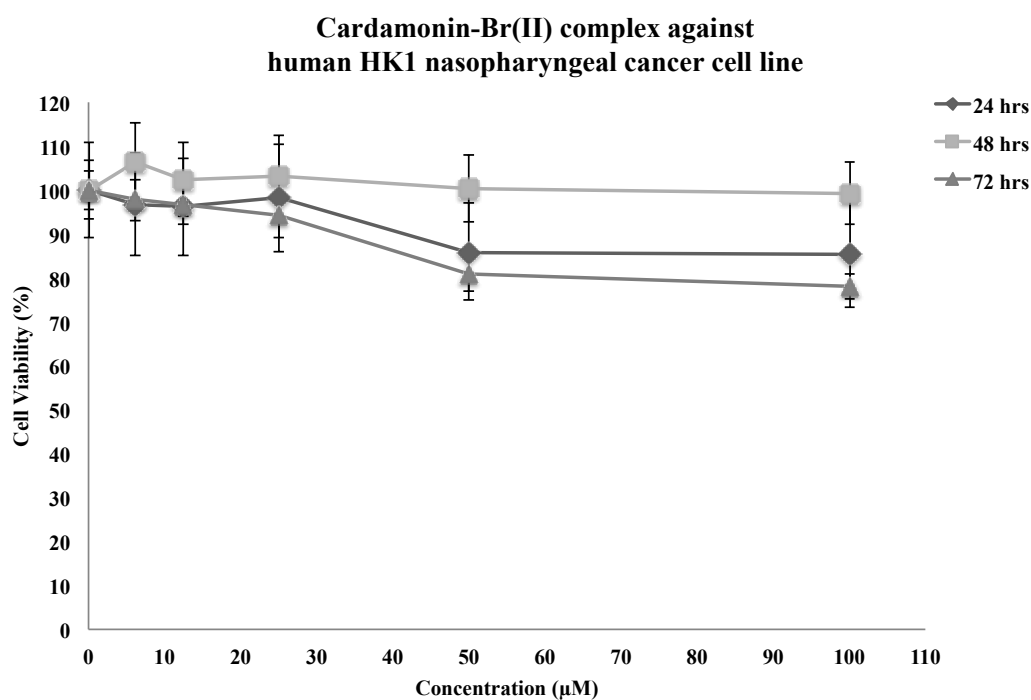


Figure 3.20 Effect of cardamonin-Br(II) in human cancer cell lines.

Human A549 lung cancer cells (A) and human HK1 nasopharyngeal cancer cells (B). Cells were treated with cardamonin-Br(II) for 24, 48 and 72 hrs and cell viability was assessed *via* the MTS assay as outlined in the Materials and Methods section. Results are means \pm SEM of three independent experiments.

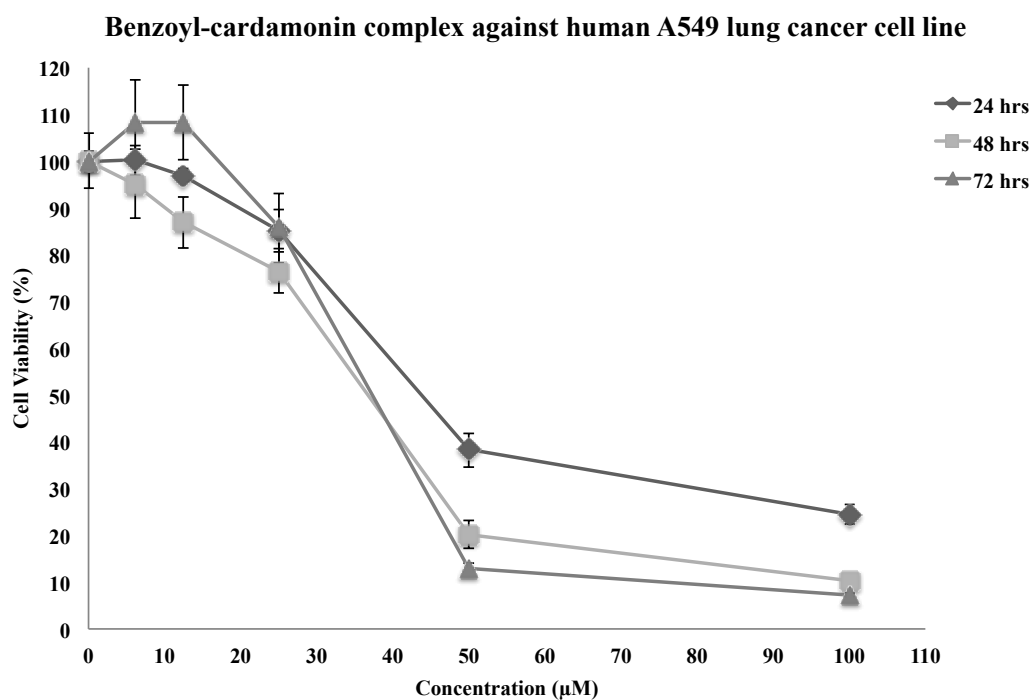
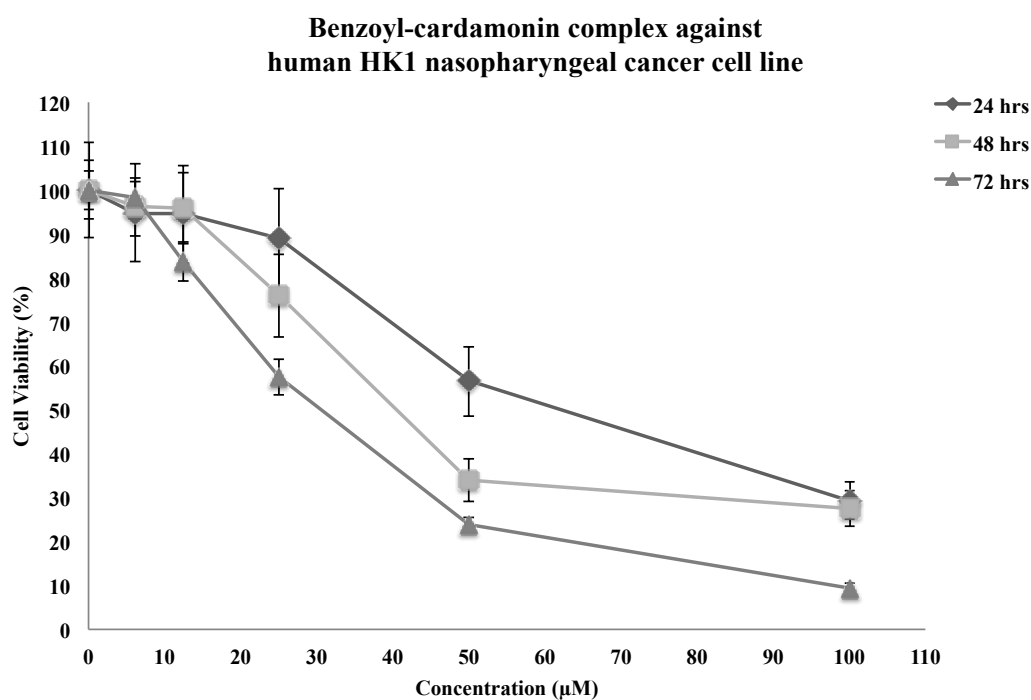
A**B**

Figure 3.21 Effect of benzoyl-cardamonin in human cancer cell lines.

Human A549 lung cancer cells (**A**) and human HK1 nasopharyngeal cancer cells (**B**). Cells were treated with benzoyl-cardamonin for 24, 48 and 72 hrs and cell viability was assessed *via* the MTS assay as outlined in the Materials and Methods section. Results are means \pm SEM of three independent experiments.

Table 3.1 IC₅₀ values of cardamonin and its derivatives in human lung A549 and human nasopharyngeal cancer HK1 cell lines following 24, 48 and 72 hrs treatment.

Compounds	A549, IC ₅₀ (μM)			HK1, IC ₅₀ (μM)		
	24 hrs	48 hrs	72 hrs	24 hrs	48 hrs	72 hrs
Cardamonin	>200	110.4	67.0	92.7	54.8	22.6
Acetyl-cardamonin	69.7	41.2	33.6	55.2	40.1	33.4
Allyl-cardamonin	152.5	101.5	35.1	59.3	21.6	4.95
OBn-cardamonin	>200	>200	>200	>200	>200	150.3
OMe-cardamonin	>200	>200	>200	>200	>200	>200
Cardamonin-Cu(II)	58.3	47.1	17.3	9.0	3.7	0.76
Cardamonin-Fe(II)	38.0	26.0	22.7	23.2	22.5	16.6
Cardamonin-B	40.9	30.2	23.9	52	53	36.6

Benzoyl-cardamonin	61.7	48.8	37.6	68.4	58.0	29.4
Phenylamine-cardamonin	>200	>200	>200	>200	>200	139
Methoxyamine-Cardamonin	>200	>200	>200	>200	>200	140
Hydroxylamine-Cardamonin	>200	>200	>200	>200	>200	>200
Urea-cardamonin	50.2	45.9	29.9	102.5	75.4	66.5
Thiourea-cardamonin	>200	>200	>200	>200	>200	>200
4-fluoro-cardamonin	134.8	121.41	106.4	170.5	104.2	89.5
Tetrahydro-cardamonin	>200	>200	>200	>200	>200	>200
Flavanol-cardamonin	85.8	101.2	106.0	>200	166.0	57.2
Flavanone-cardamonin	>200	>200	>200	>200	>200	>200

5-Iodo- cardamonin	46.4	42.2	36.1	85.1	73.0	49.7
5-Bromo- cardamonin	135.86	164	186	>200	>200	>200
Hydrazinium- cardamonin	80.4	77.3	63.8	54.1	58.6	46.8

3.2.2 Cytotoxicity of cardamonin and its complexes assessed in normal human MRC5 and Hs68 cell lines

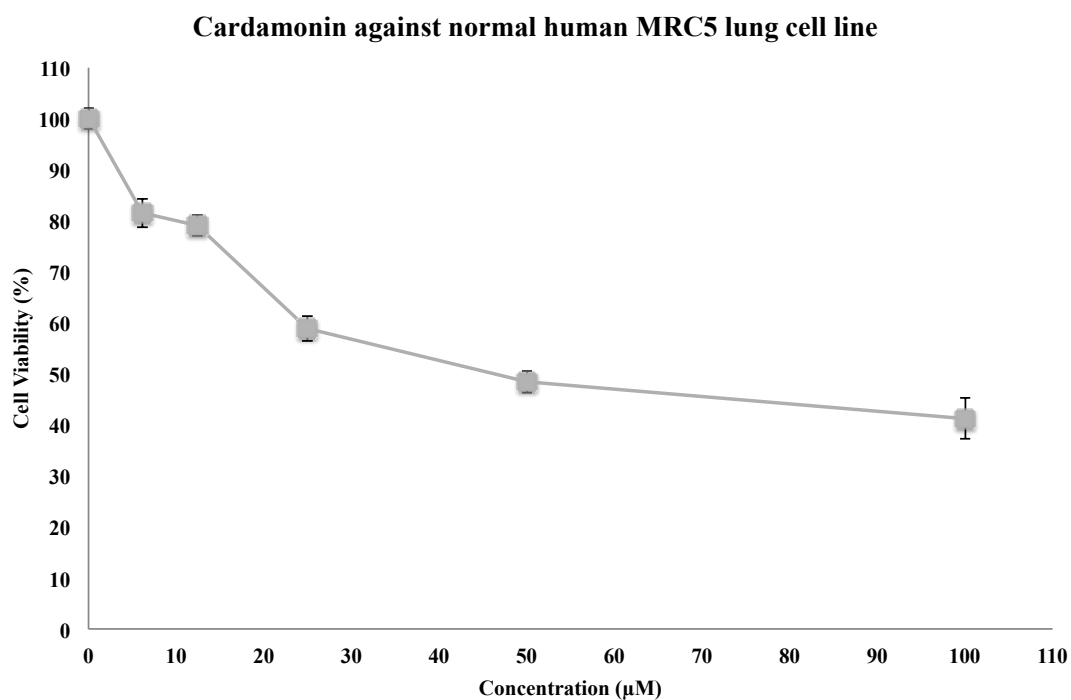
As previously shown in **Table 3.1**, compounds cardamonin-Cu(II) and cardamonin-Fe(II) overall exhibited the two highest cytotoxic activity in A549 and HK1 cell lines. IC₅₀ values ranged from 17 to 58 µM in A549 cells and 0.76 to 9 µM in HK1 cells for cardamonin-Cu(II); 22 to 38 µM in A549 cells and 16 to 23 µM in HK1 cells for cardamonin-Fe(II).

Based on these results, the two complexes and the parent compound, cardamonin, were further assessed for their cytotoxicity in normal human lung MRC5 and normal human foreskin Hs68 cell lines for 24 hrs to determine whether the cytotoxicity of these compounds were selective towards carcinoma cell lines.

Figures 3.22 - 3.24 display the dose response curves for each compound. **Table 3.2** summarise the IC₅₀ values of cardamonin, cardamonin-Cu(II) and cardamonin-Fe(II) in MRC5 and Hs68 lines following 24 hrs treatment. The cytotoxic effectiveness in order of decreasing IC₅₀ values for both MRC5 and Hs68 lines were as follow: cardamonin (**Figure 3.22**) < cardamonin-Fe(II) (**Figure 3.24**) < cardamonin-Cu(II) (**Figure 3.23**). This order of effectiveness was observed in all cell lines tested with the exception of A549 cell line where cardamonin-Fe(II) appeared more cytotoxic compared to cardamonin-Cu(II) and cardamonin was again least cytotoxic.

A direct comparison of IC₅₀ values between A549 lung carcinoma cell line and MRC5 lung normal cell line revealed the normal cells were more susceptible to cardamonin, cardamonin-Cu(II) and cardamonin-Fe(II) suggesting these compounds are not only cytotoxic towards carcinoma cells (**Table 3.2**). However, Hs68 cells were less sensitive towards these compounds implying some level of selectivity from cardamonin, cardamonin-Cu(II) and cardamonin-Fe(II) depending on the type of cells exposed to.

A



B

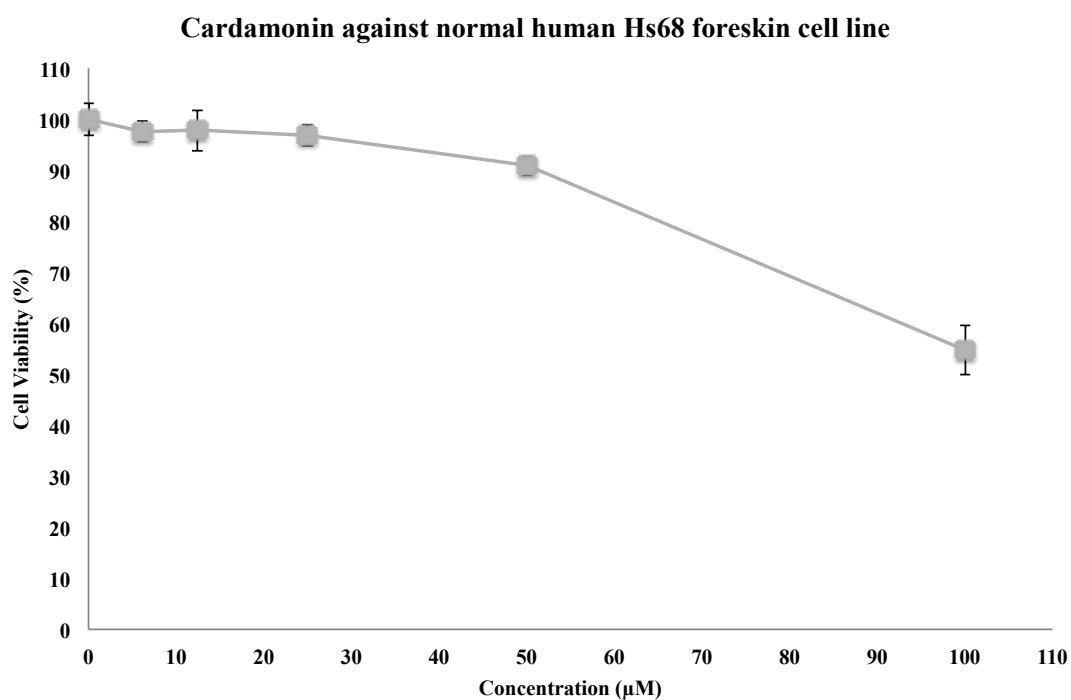
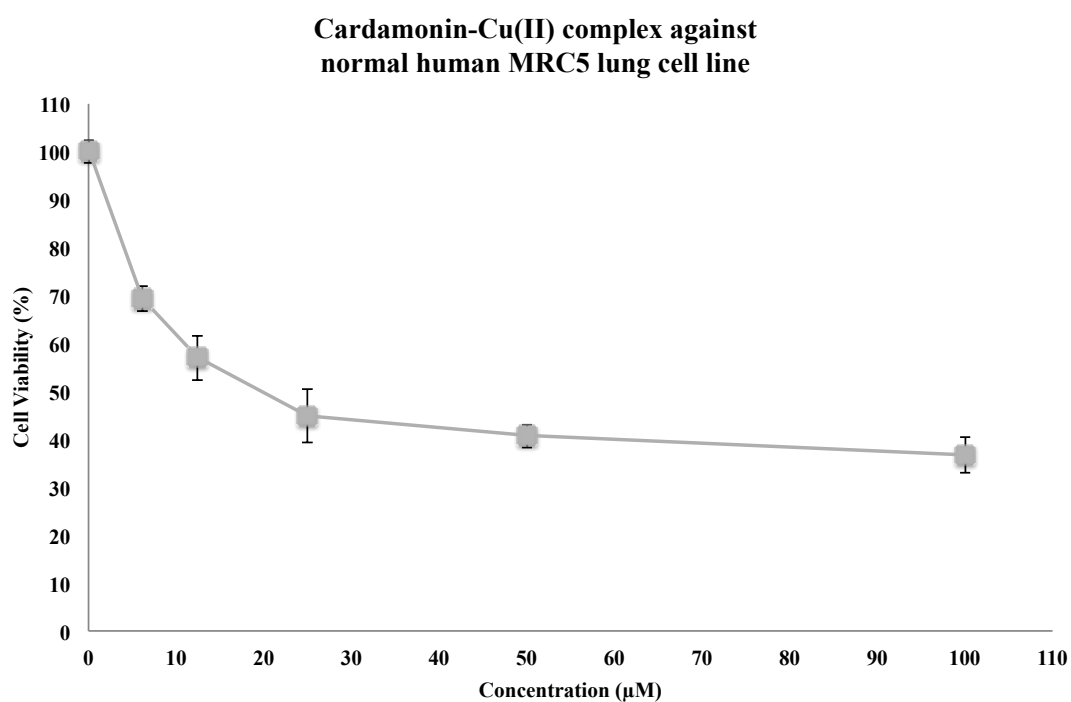


Figure 3.22 Effect of cardamonin in normal human cell lines.

Human MRC5 lung cells (**A**) and human Hs68 foreskin cells (**B**). Cells were treated with cardamonin for 24 hrs and cell viability was assessed *via* the MTS assay as outlined in the Materials and Methods section. Results are means \pm SEM of three independent experiments.

A



B

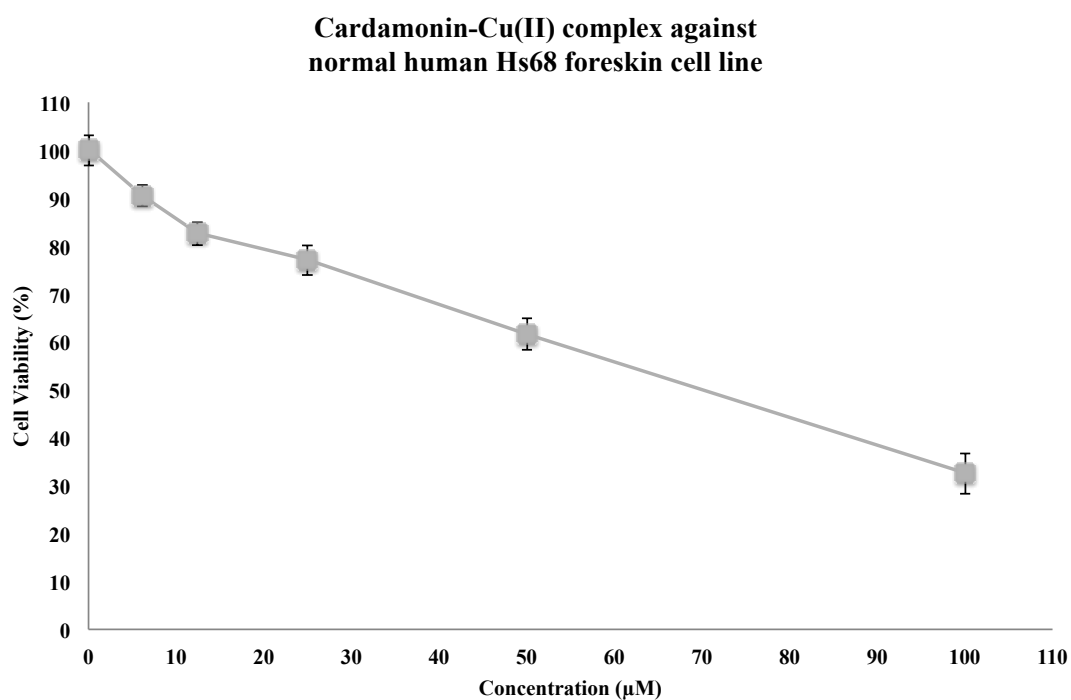
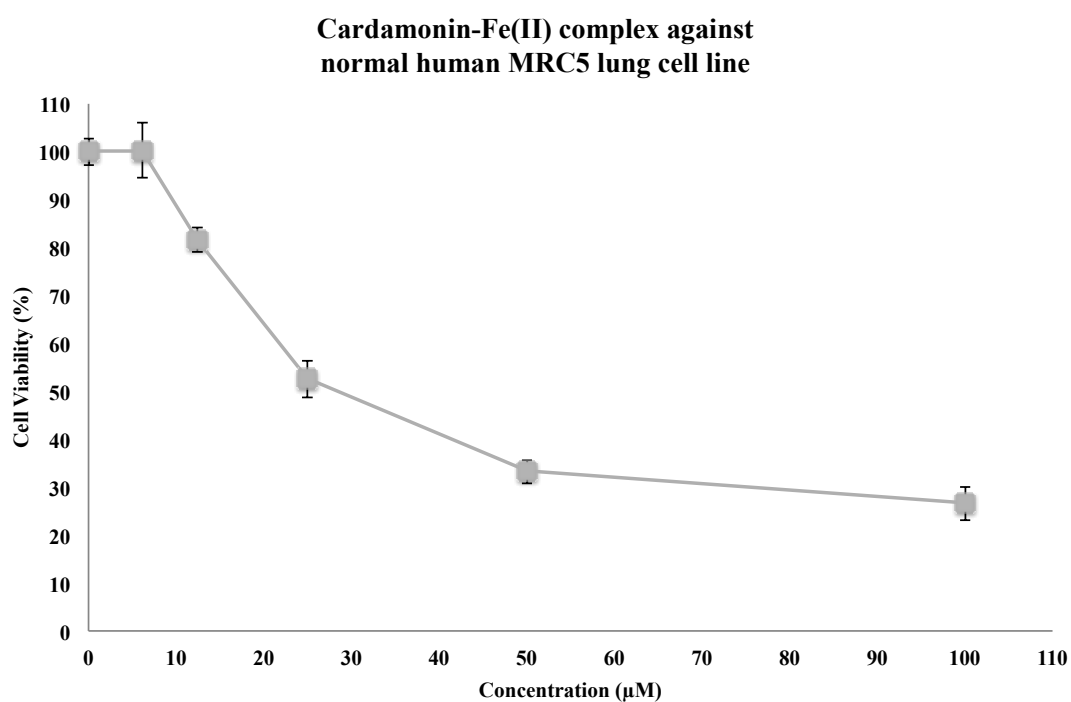


Figure 3.23 Effect of cardamonin-Cu(II) in normal human cell lines.

Human MRC5 lung cells (**A**) and human Hs68 foreskin cells (**B**). Cells were treated with cardamonin-Cu(II) for 24 hrs and cell viability was assessed *via* the MTS assay as outlined in the Materials and Methods section. Results are means \pm SEM of three independent experiments.

A



B

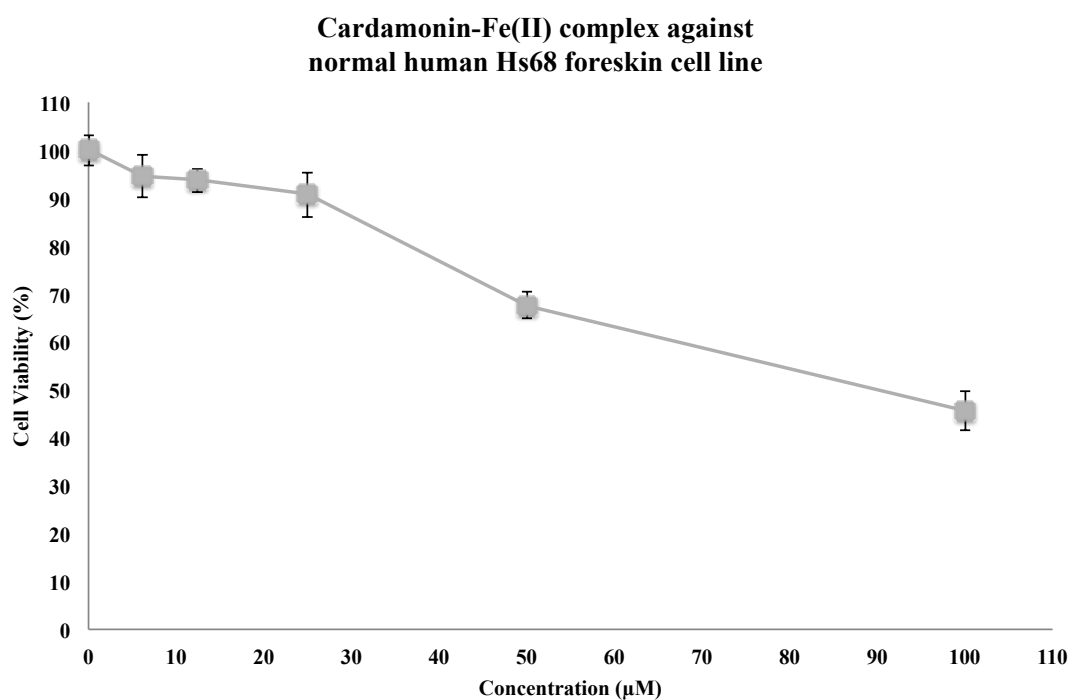


Figure 3.24 Effect of cardamonin-Fe(II) in normal human cell lines.

Human MRC5 lung cells (**A**) and human Hs68 foreskin cells (**B**). Cells were treated with cardamonin-Fe(II) for 24 hrs and cell viability was assessed *via* the MTS assay as outlined in the Materials and Methods section. Results are means \pm SEM of three independent experiments.

Table 3.2 Summary of the IC₅₀ values in human lung cancer A549, human nasopharyngeal cancer HK1, human normal MRC5 lung, human normal Hs68 foreskin cell lines following 24 hrs treatment.

Compounds	A549, IC ₅₀ (μM)	HK1, IC ₅₀ (μM)	MRC5, IC ₅₀ (μM)	Hs68, IC ₅₀ (μM)
Cardamonin	>100	94.7	47.0	>100
Cardamonin-Cu(II)	58.3	9.0	19.79	70.5
Cardamonin-Fe(II)	38.0	23.2	30.1	89.9

Selectivity index was further calculated to determine the level of selectivity of active derivatives towards cancer cell lines compared to normal cell lines. **Table 3.3** showed cardamonin-Cu(II) selectivity index was greatest in HK1 nasopharyngeal cancer cell lines with highest value of 7.83, indicating this compound is more than seven times more cytotoxic to the HK1 cancer cell line compared to Hs68 normal cell line. Data also revealed the complexes were less cytotoxic to Hs68 normal foreskin cell line compared to MRC5 normal lung cell line. Furthermore, it was not possible to obtain the selectivity index of cardamonin, since this compound was more cytotoxic to the normal lung cell lines compared to the cancer cell lines tested. Similarly, cardamonin-Cu(II) and cardamonin-Fe(II) treatments were more cytotoxic to normal lung cell line compared to the cancer lung cell line. Hence, the selectivity index value was unattainable.

Table 3.3 Selectivity of the cytotoxicity of cardamonin, cardamonin-Cu(II) and cardamonin-Fe(II) to A549 lung and HK1 nasopharyngeal cancer cell lines as compared with MRC5 lung and HS68 foreskin normal cell lines.

Compounds	MRC5 selectivity index		Hs68 selectivity index	
	A549	HK1	A549	HK1
Cardamonin	NA	NA	NA	NA
Cardamonin-Cu(II)	NA	2.2	1.21	7.83
Cardamonin-Fe(II)	NA	1.30	2.37	3.88

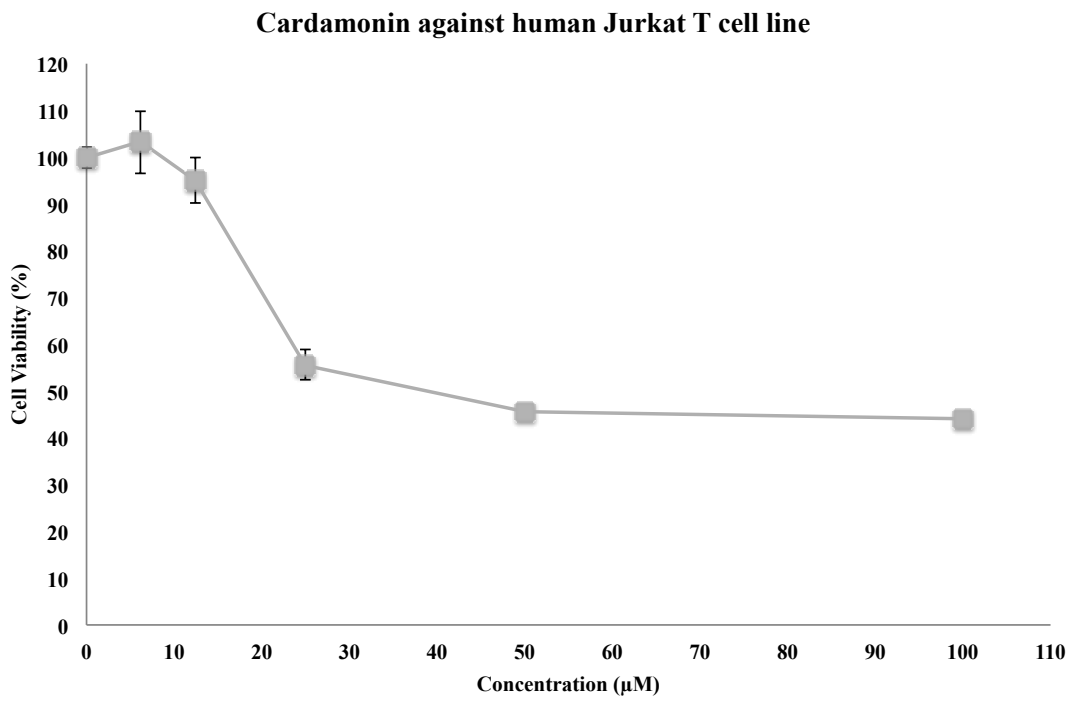
Selectivity index = (IC₅₀ of normal cells) / (IC₅₀ of A549 or HK1 cancer cells)

3.2.3 Cytotoxicity of cardamonin and its complexes assessed in human Jurkat T cells

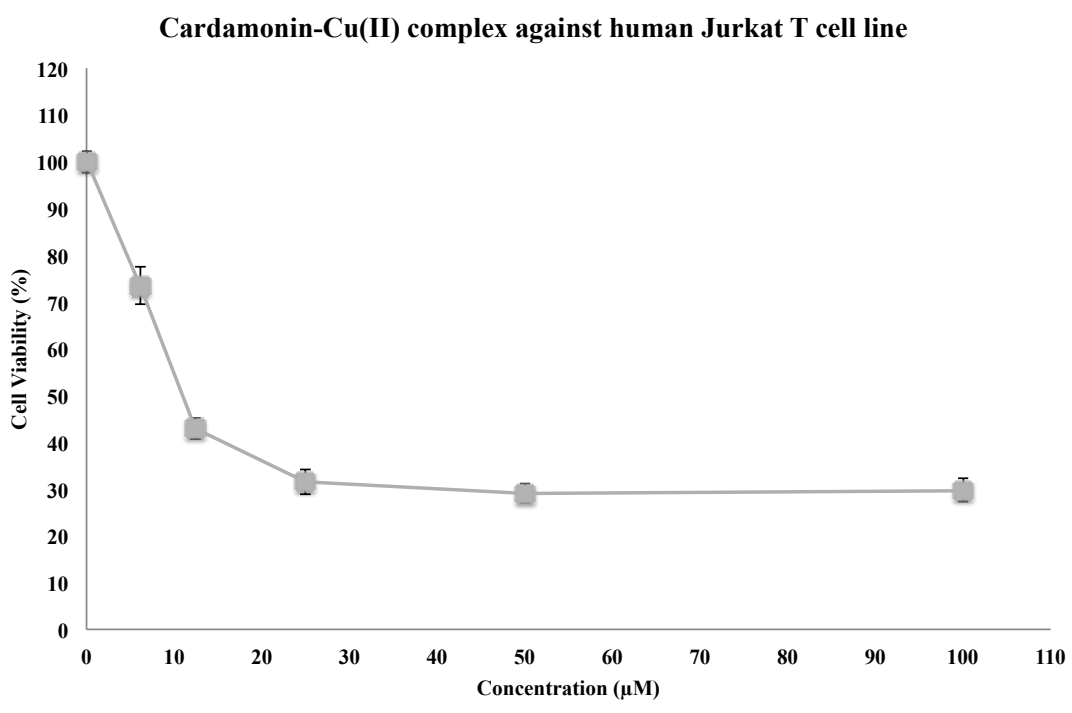
Since cardamonin, cardamonin-Cu(II) and cardamonin-Fe(II) were found to be toxic in normal cells, specifically the MRC5 lung cell line, we next investigate the cytotoxicity of these compounds in Jurkat T leukaemic cells, a commonly used cell line in determining the mechanism of differential susceptibility to drugs (Howe 2016).

Figure 3.25 display the dose response curves for each compound. As summarised in **Table 3.4**, Jurkat T cells were most susceptible following 24 hrs treatment compared to all other cell lines tested. IC₅₀ values were lowest in Jurkat T cells across all three compounds tested at 37.6, 7.9 and 17.4 μ M for cardamonin, cardamonin-Cu(II) and cardamonin-Fe(II), respectively. As shown in **Figure 3.25**, all three compounds induced a dose-dependent decrease in Jurkat T cell viability.

A



B



C

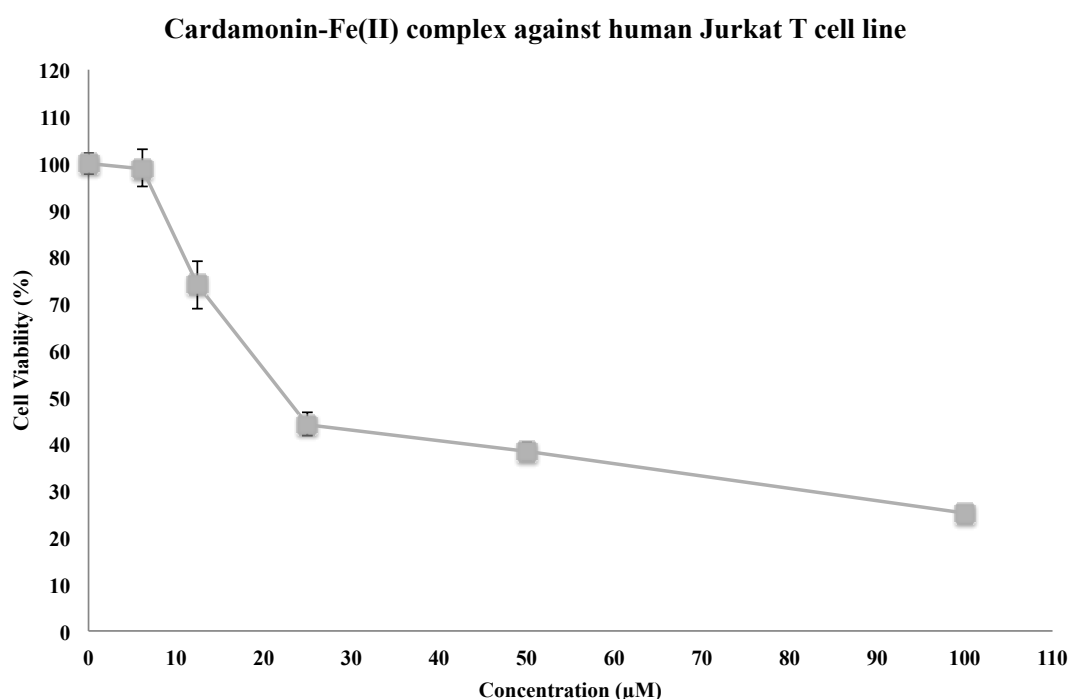


Figure 3.25 Effect of cardamonin, cardamonin-Cu(II) and cardamonin-Fe(II) in human Jurkat T cells.

Cells were treated with cardamonin (A), cardamonin-Cu(II) (B) and cardamonin-Fe(II) (C) for 24 hrs and cell viability was assessed *via* the MTS assay as outlined in the Materials and Methods section. Results are means \pm SEM of three independent experiments.

Table 3.4 Summary of the IC₅₀ values in human lung cancer A549, human nasopharyngeal cancer HK1, human normal MRC5 lung, human normal Hs68 foreskin and Jurkat T cell lines following 24 hrs treatment.

Compounds	A549, IC ₅₀ (µM)	HK1, IC ₅₀ (µM)	MRC5, IC ₅₀ (µM)	Hs68, IC ₅₀ (µM)	Jurkat T, IC ₅₀ (µM)
Cardamonin	>100	94.7	47.0	>100	37.6
Cardamonin-Cu(II)	58.3	9.0	19.79	70.5	7.9
Cardamonin-Fe(II)	38.0	23.2	30.1	89.9	17.4

3.3 Discussion

The cytotoxicity was initially assessed for all 20 cardamonin derivatives including cardamonin using human A549 lung and human HK1 nasopharyngeal cell lines. All cardamonin derivatives were tested at the same concentration and incubated under constant conditions. The colorimetric MTS assay was used to assess compounds' cytotoxicity and results were expressed as IC₅₀ values representing the concentration of a compound with half-maximal cell viability compared to the untreated control.

Cardamonin-Cu(II) and cardamonin-Fe(II) complexes were the two most cytotoxic derivatives of cardamonin. According to Graf and Lippard (2012), various synthetic and natural drugs require the activation by metal ions acting as pro-drugs in the body. A review on metal-mediated drugs has suggested that metal ions are able to coordinate with natural or organic compounds providing advantages over the original drugs themselves (Tang and Liang 2013). As seen in this study, both cardamonin-Cu(II) and cardamonin-Fe(II) complexes improved cytotoxicity which could be due to copper and iron both having variable oxidation states and therefore are involved in the redox reactions. They donate or accept electrons and initiate the reduction-oxidation reactions. The metal ions can function to generate reactive species in redox reaction and facilitate binding in catalysis (Petrucci et al. 2002).

Recently, copper metal ions were used as a potential delivery agent for the anti-cancer drug taxol (Manning et al. 2014). The efficacy of copper-taxol and copper-taxol-hydroxychloroquin complexes was compared to pure taxol (Manning et al. 2013). The researchers reported the complexation of the copper ions to taxol

improved the efficacy of taxol in a range of cell lines studied. Manning et al. (2014) also suggested that copper ions might have promising applications as a cancer drug as they have the ability to improve water solubility of drugs and stabilise a drug structure. As for iron metal ions, they have been reported in some studies to cause DNA cleavage by forming a complex with a drug that is further activated by the reaction with oxygen (Hecht 1986, Stubbe and Kozarich 1987, Chen and Stubbe 2005).

Overall, the cytotoxicity of cardamonin-Cu(II) and cardamonin-Fe(II) complexes was related to inhibition of certain specific processes in the cells. Further studies are required to understand better the mechanisms of bioactivity for these compounds. The following study examined the cytotoxicity of cardamonin-Cu(II) and cardamonin-Fe(II) complexes in normal human cell lines to determine whether these novel compounds were only selective towards cancer cells. A direct comparison of IC_{50} values between A549 lung carcinoma cell line and MRC5 lung normal cell line revealed the normal cells were more susceptible to cardamonin, cardamonin-Cu(II) and cardamonin-Fe(II) suggesting these compounds are not only cytotoxic towards carcinoma cells. However, Hs68 cells were less sensitive towards these compounds implying some level of selectivity from cardamonin, cardamonin-Cu(II) and cardamonin-Fe(II) depending on the type of cells exposed to.

Subsequently, Jurkat T cells were found to be most susceptible to cardamonin, cardamonin-Cu(II) and cardamonin-Fe(II) treatment compared to all other cell lines tested. The high susceptibility of Jurkat T cells to these compounds may be due to the state of the cells being in suspension form, while all other cell lines tested were

adherent cells. Furthermore, chalcones have been reported to be particularly cytotoxic towards leukaemic cell lines (Dimmock et al. 1998, Maioral et al. 2013). Generally, the data in this chapter demonstrated that the generation of cardamonin derivatives and complexes resulted in enhanced cytotoxicity in several of these compounds, particularly cardamonin-Cu(II) and cardamonin-Fe(II) complexes. These results indicated that complexing cardamonin to metal complexes such as copper and iron increased the cytotoxic activity significantly.

Overall, cardamonin, cardamonin-Cu(II) and cardamonin-Fe(II) complexes were found to be cytotoxic in normal lung A549 cell line but less cytotoxic in normal foreskin Hs68 cell line. Following 24 hrs treatment, the increased resistance in order of increasing IC₅₀ values for cardamonin were as follow: Jurkat T < MRC5 < HK1 < A549 = Hs68; for cardamonin-Cu(II) complex: Jurkat T < HK1 < MRC5 < A549 < Hs68; and for cardamonin-Fe(II) complex: Jurkat T < HK1 < MRC5 < A549 < Hs68. On the whole, Jurkat T cells were most sensitive to all three treatments. As previous studies have shown that chalcones are particularly cytotoxic towards leukaemic cell lines, the following chapter explores the differential susceptibility of adherent and suspension cells towards cardamonin, cardamonin-Cu(II) and cardamonin-Fe(II).

**CHAPTER 4: THP-1-DERIVED MACROPHAGES
INCREASED RESISTANCE TOWARDS CARDAMONIN,
CARDAMONIN-Cu(II) AND CARDAMONIN-Fe(II)
COMPLEXES WERE INDEPENDENT OF P38 α AND
P38 β MAP KINASE PATHWAY**

4.1 Introduction

As illustrated in Chapter 3, cardamonin and its derivatives/ complexes induced cell death at different sensitivity depending on the different cell origin. Compared to both cancer and normal adherent cell lines tested, the suspension Jurkat T cells were most sensitive to cardamonin, cardamonin-Cu(II) and cardamonin-Fe(II) complexes. This difference in cell susceptibility between adherent and suspension cell lines is particularly interesting and should be further investigated as a number of studies have also reported that suspension cells are more susceptible to inhibition of cell growth compared to adherent cells (Dimmock et al. 1998, Kimura et al. 2004, Daigneault et al. 2010, Maioral et al. 2013). Moreover, studies have shown an increase in survival signals in adherent cells compared to suspension cells (Kohro et al. 2004). The present study was initiated to examine the differential susceptibility between suspension and adherent cells as well as the changes in cell susceptibility following inhibition of a key survival signal in adherent cells. Since the susceptibility of the suspension and adherent cells previously tested in this study are from a range of different tissue origin, a true comparison cannot be established due to the different characteristics and diverse receptor expressions of the different cell lines. Hence, in this study, THP-1 cells were used as our experimental model since this particular cell line can be cultured in both suspension and adherent phase. Considering these cells were derived from the same tissue origin, the susceptibility studies will be more comparable. Also, matured macrophages are known to mediate signaling mechanism that involves mitogen-activated protein (MAP) kinase activation (Traore et al. 2005). This chapter will explore the effects of interference from inhibitors of p38 α and p38 β MAP kinase on differentiated mature THP-1 macrophages compared to monocytes.

4.2 Results

4.2.1 Effects of cardamonin, cardamonin-Cu(II) and cardamonin-Fe(II) on THP-1 cell viability

Initial studies were carried out to examine the cytotoxic effect of cardamonin, cardamonin-Cu(II) complex and cardamonin-Fe(II) complex on THP-1 monocytes. A dose response curve was obtained following 24 hrs treatment with cardamonin, cardamonin-Cu(II) and cardamonin-Fe(II) at concentrations ranging from 6.25 μ M to 100 μ M. Control cells were not treated with any compounds. Results reveal, THP-1 cell viability decreased in a dose-dependent manner following treatment with all three compounds tested. Cardamonin-Cu(II) complex was more cytotoxic to THP-1 cells compared to cardamonin and cardamonin-Fe(II) treatment. Results in **Figure 4.1** demonstrate Cardamonin-Cu(II) caused a drastic decrease in cell viability from 92% to 13% when exposed to treatment concentrations from 6.25 μ M to 100 μ M for 24 hrs. THP-1 cell viability decreased dose-dependently from 99% to 51% when exposed to cardamonin-Fe(II) concentrations ranging from 6.25 μ M to 100 μ M for 24 hrs. THP-1 cells were least sensitive towards cardamonin treatment, where cells maintained >70% in cell viability after 24 hrs treatment. Taken together, a similar cytotoxicity trend was observed with Jurkat T cells where cardamonin-Cu(II) and cardamonin-Fe(II) were more active than the parent compound with cardamonin being least cytotoxic and cardamonin-Cu(II) being most cytotoxic.

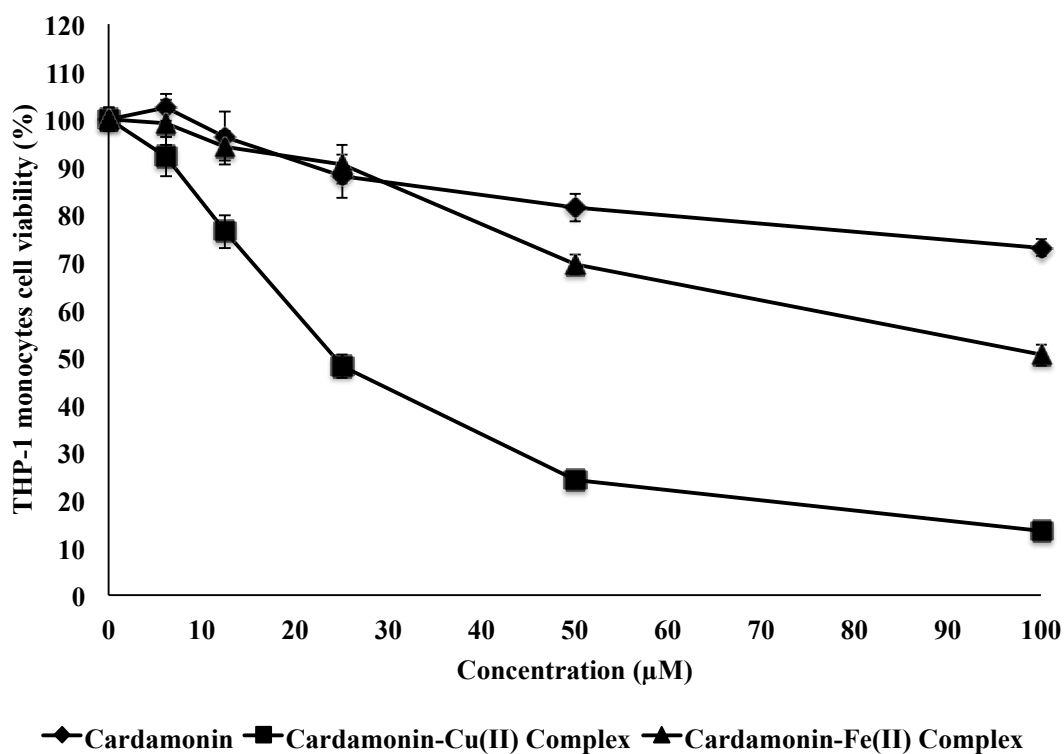


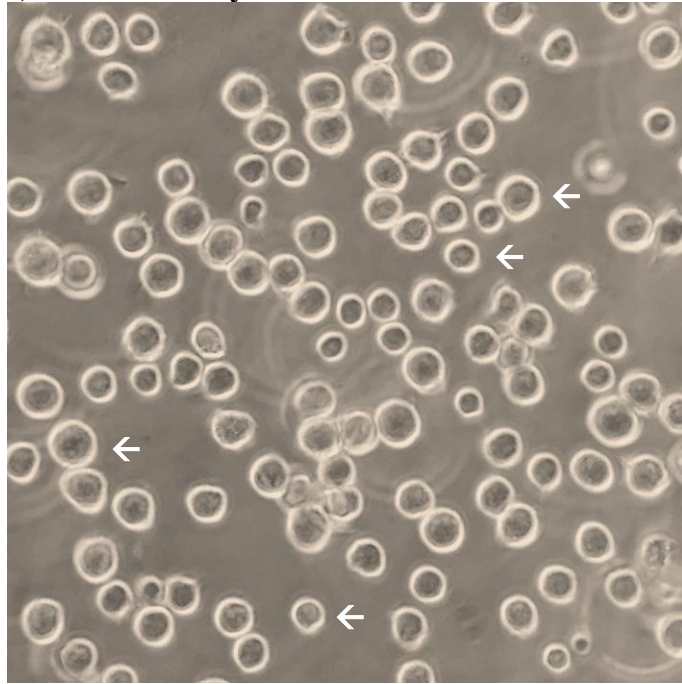
Figure 4.1 Effect of cardamonin, cardamonin-Cu(II) complex and cardamonin-Fe(II) complex on THP-1 monocytes cell viability.

THP-1 cells were exposed to various concentrations (6.25, 12.5, 25, 50 and 100 µM) of cardamonin, cardamonin-Cu(II) complex and cardamonin-Fe(II) complex for 24 hrs. The MTS assay was used to assess cell viability as described in the Materials and Methods section. Results were expressed as mean \pm SEM from three independent experiments.

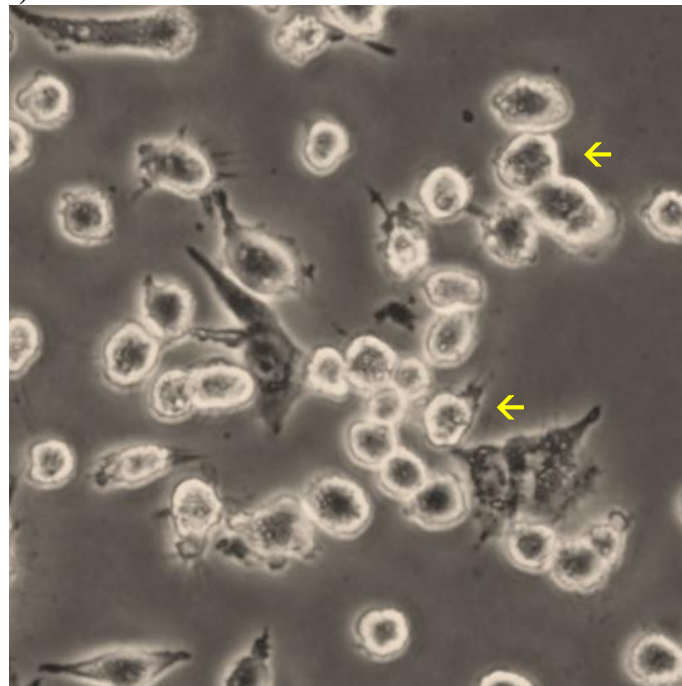
4.2.2 Morphological changes in THP-1 monocytes differentiation to macrophages

In an effort to investigate the differential susceptibility between suspension and adherent cells, THP-1 monocytes were differentiated into macrophages by stimulating the cells with PMA. THP-1 cells were treated with PMA up to five days and the morphological changes were observed every 24 hrs using a phase contrast microscopy (**Figure 4.2**). As seen in **Figure 4.2A**, non-stimulated THP-1 monocytes appear rounded and floated in the medium. These spherical cells were more regular morphologically and appear homogenous. Following 24 hrs PMA-stimulation (**Figure 4.2B**), more than 80% of the cells started to adhere but was loosely attached to the culture flask. Only 10-20% of the cells appear to spread out with spindle-like shapes and was morphologically irregular. After 48 hrs of exposure to PMA (**Figure 4.2C**), almost all of the cells have adhered firmly to the culture flask excluding any dead cells and cell debris. Approximately 50% of the cells have now developed into fibroblast-like cells with spindles spreading from the cells with a lesser mix population of rounded cells. By 72 hrs (**Figure 4.2D**), more than 90% of the cells exhibited significant morphology change exhibiting long and thin body similar to fibroblast-like cells. The cells were more defined and appeared flattened, well spread, attaching very firmly to the culture flask. Following 96 hrs (**Figure 4.2E**) and 120 hrs (**Figure 4.2F**) treatment, cells appear to shrink and start to detach from the culture flasks respectively. Prolonged PMA stimulation of more than 72 hrs could be toxic to THP-1 cells leading to progression to unhealthy macrophages. Hence, 72 hrs treatments were used for subsequent experiments involving THP-1-derived macrophages.

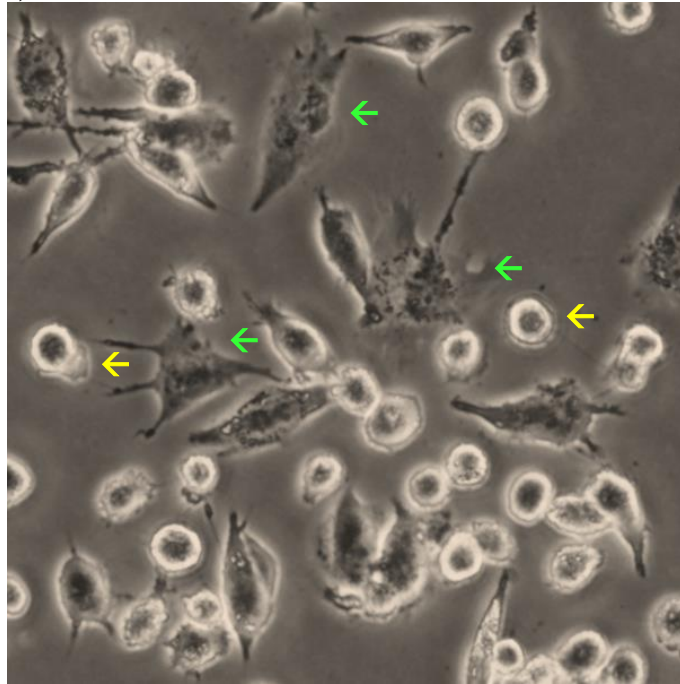
(A) THP-1 monocytes



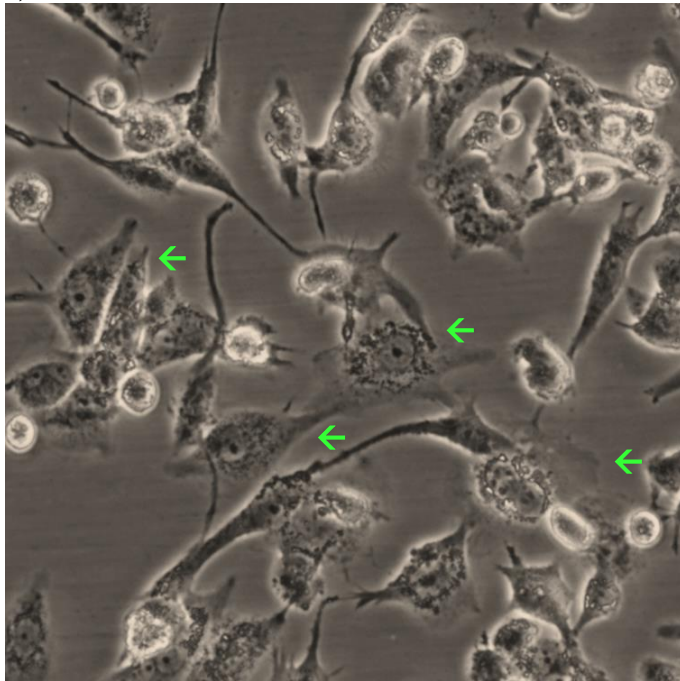
(B) PMA 24 hrs



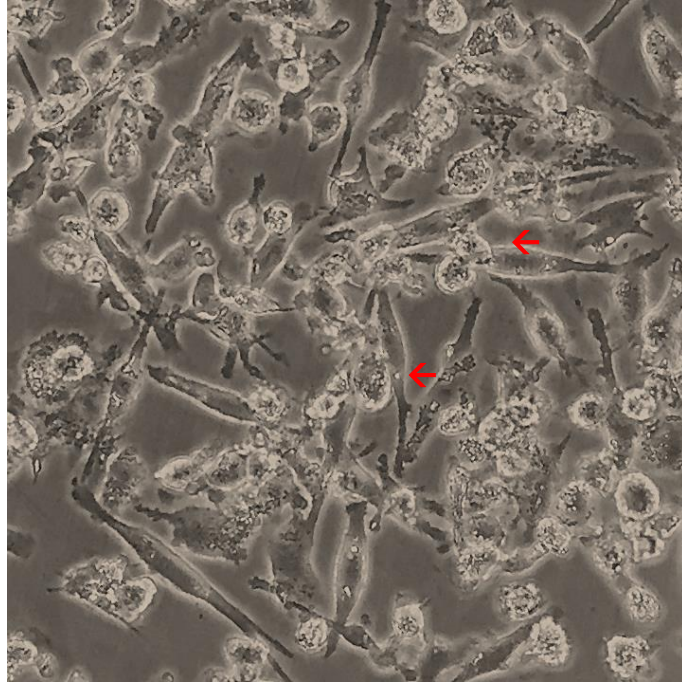
(C) PMA 48 hrs



(D) PMA 72 hrs



(E) PMA 96 hrs



(F) PMA 120 hrs

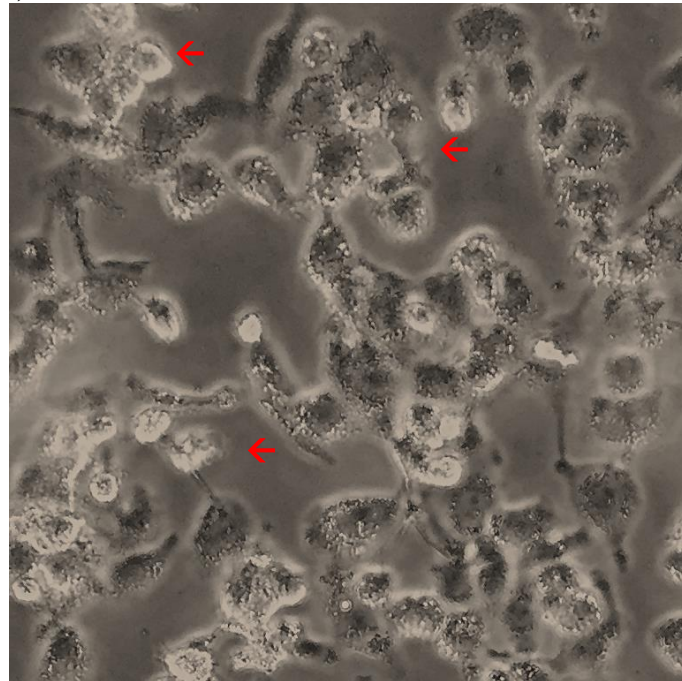


Figure 4.2 Cellular morphology of THP-1 monocytes and PMA-induced differentiation to THP-1-derived macrophages.

Non-stimulated THP-1 monocytes (A) and 50 ng/mL PMA-stimulated for 24 hrs (B), 48 hrs (C), 72 hrs (D), 96 hrs (E) and 120 hrs (F) were observed using a phase contrast microscopy. Indication of arrows: white indicates non-stimulated THP-1 monocytes; yellow indicates loosely attached pre-mature THP-1 cells; green indicates well-defined, flatten, fibroblast-like cells; and red indicates shrinkage, clumping and loss of cell membrane integrity cells. Results shown are one representation from three independent experiments. Original magnification x200.

4.2.3 Expression of CD11b surface marker

Apart from morphological changes, maturation of THP-1 cells to mature macrophages can be further assessed. Following 72 hrs stimulation of THP-1 cells to 50 ng/mL PMA, cells were subjected for further analysis using specific cell surface markers, CD11b. CD11b, an α -subunit of β 2 integrin is up-regulated in differentiated THP-1-derived macrophages (Mittar et al. 2011). Results in **Figure 4.3** revealed unstained and isotype control of both THP-1 and THP-1 macrophages have low fluorescence intensity. By contrast, following 72 hrs of 50 ng/mL PMA treatment, there was a positive shift in mature THP-1 macrophages expressing CD11b. These data further confirms that the THP-1 cells have successfully differentiated to mature macrophages.

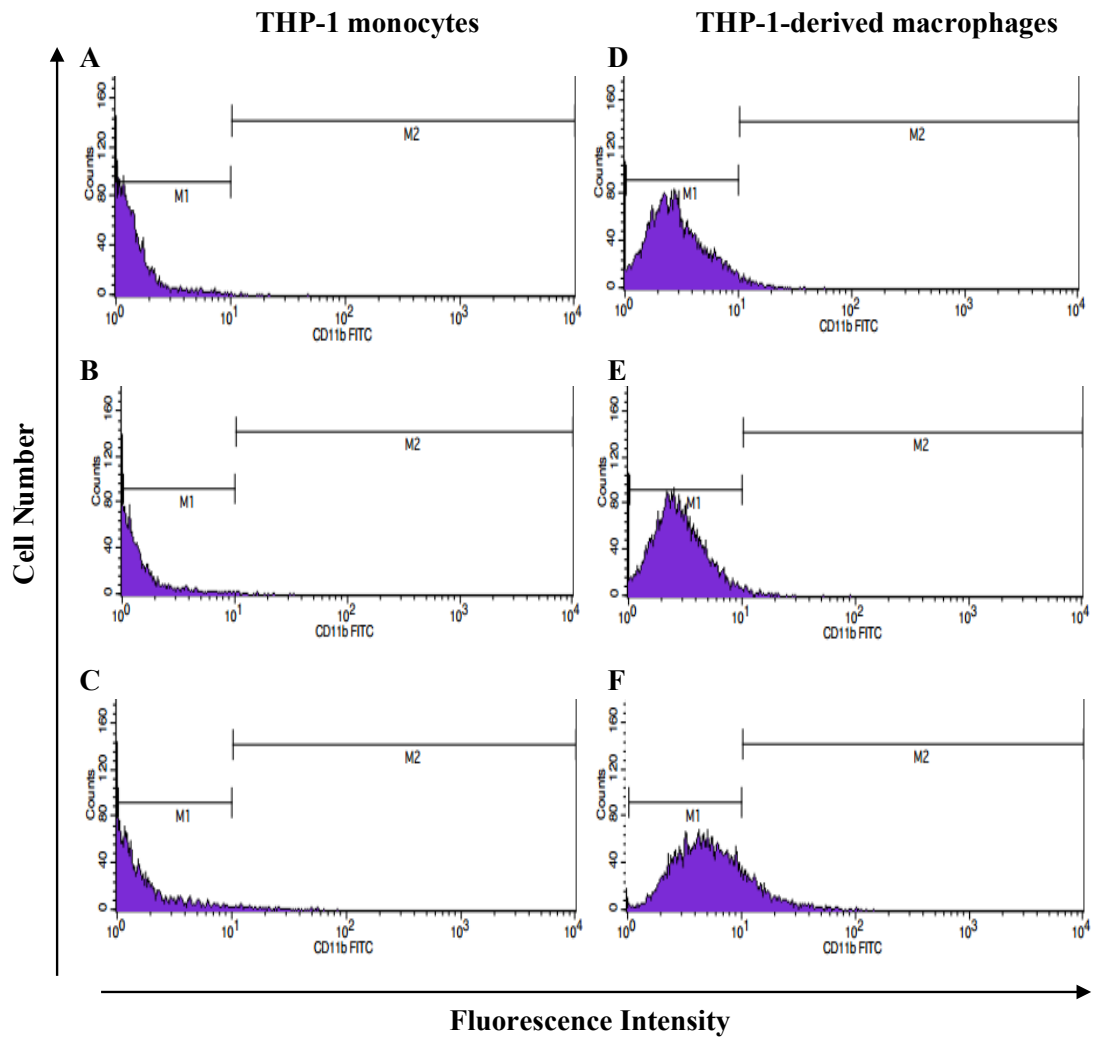


Figure 4.3 Expression of CD11b surface markers in THP-1 monocytes and THP-1-derived macrophages.

THP-1-derived macrophages were differentiated with 50 ng/mL PMA for 72 hrs. Fluorescence intensity histogram of unstained (A), mouse IgG1 isotype control stained (B) and FITC-anti CD11b stained samples (C) of THP-1 monocytes; and unstained (D), mouse IgG1 isotype control stained (E) and FITC-anti CD11b stained samples of (F) of THP-1-derived macrophages.

4.2.4 Effects of cardamonin, cardamonin-Cu(II) and cardamonin-Fe(II) on THP-1-derived macrophages cell viability

Once THP-1 monocytes have been differentiated to mature macrophages, the cytotoxicity of cardamonin, cardamonin-Cu(II) and cardamonin-Fe(II) complexes on THP-1-derived macrophages cell viability was examined. Results reveal, the cell viability of THP-1-derived macrophages decreased in a dose-dependent manner following treatment with cardamonin-Cu(II) complex. However, cardamonin and cardamonin-Fe(II) complex had minimal effect on the viability of THP-1-derived macrophages. Cardamonin-Cu(II) complex was most cytotoxic to THP-1-derived macrophages compared to cardamonin and cardamonin-Fe(II) treatment. Results in **Figure 4.4** demonstrate Cardamonin-Cu(II) caused a decrease in cell viability from 90% to 33% when exposed to treatment concentration from 6.25 μM to 100 μM for 24 hrs. The macrophages maintained >90% and >80% in cell viability in the presence of cardamonin and cardamonin-Fe(II) respectively, even at the highest concentration tested, 100 μM . An interesting trend was observed across all THP-1-derived macrophages compared to THP-1 monocytes where the macrophages were comparatively more resistant to all three treatments suggesting that monocytes were indeed more susceptible to treatment. A similar trend to the THP-1 monocytes and Jurkat T cells was observed where the order of cytotoxicity was cardamonin < cardamonin-Fe(II) < cardamonin-Cu(II) with IC_{50} values of >100, >100 and 40 μM respectively. Collectively, these results confirm that differentiation of THP-1 monocytes to macrophages indeed reduced the susceptibility and increase some resistance towards cardamonin, cardamonin-Cu(II) and cardamonin-Fe(II) complexes-induced cell death.

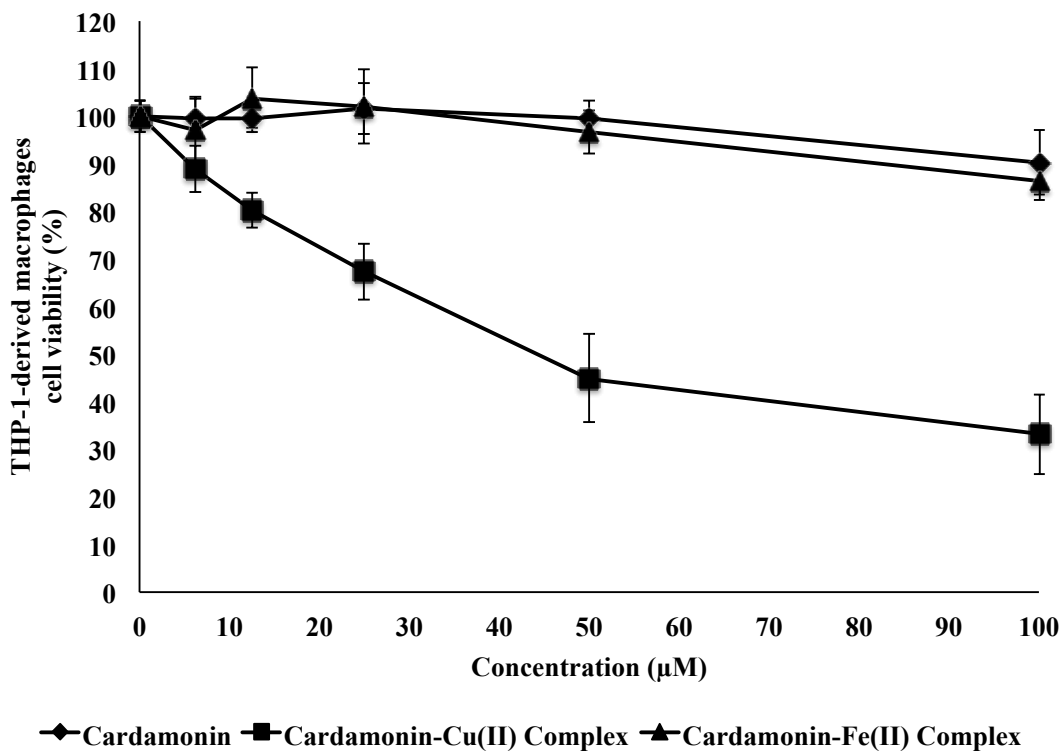


Figure 4.4 Effect of cardamonin, cardamonin-Cu(II) complex and cardamonin-Fe(II) complex on THP-1-derived macrophages cell viability.

THP-1-derived macrophages were exposed to various concentrations (6.25, 12.5, 25, 50 and 100 µM) of cardamonin, cardamonin-Cu(II) complex and cardamonin-Fe(II) complex for 24 hrs. The MTS assay was used to assess cell viability as described in the Materials and Methods section. Results were expressed as mean \pm SEM from three independent experiments.

4.2.5 Effects of cardamonin, cardamonin-Cu(II) and cardamonin-Fe(II) on THP-1-derived macrophages cell viability in the presence of a MAP kinase inhibitor, p38 MAP kinase inhibitor IV

Subsequent to observing an increased resistance towards treatment following the differentiation of THP-1 monocytes to macrophages, efforts were made to determine the possible correlation of the differential susceptibility. In order to dissect the possible signaling network causing a change in cell viability from THP-1 monocytes to macrophages, a chemical inhibitor was used. A MAP kinase inhibitor specific in blocking p38 α and p38 β (**Figure 4.5**) was added to THP-1-derived macrophages prior to treatment with cardamonin, cardamonin-Cu(II) complex and cardamonin-Fe(II) complex. This inhibitor was introduced to THP-1-derived macrophages in order to evaluate whether the perceived differential susceptibility was associated with activation of p38 MAP kinase. The cytotoxic effect on cell viability of p38 MAP kinase inhibited-THP-1-derived macrophages (p38_{in}THP-1-derived macrophages) of cardamonin, cardamonin-Cu(II) complex and cardamonin-Fe(II) complex was assessed. **Figure 4.6A** shows the effect of cardamonin, cardamonin-Cu(II) complex and cardamonin-Fe(II) complex on p38_{in}THP-1-derived macrophages following 24 hrs treatment. Results revealed, similar to THP-1-derived macrophages, cells maintained their viability >90% after cardamonin treatment on p38_{in}THP-1-derived macrophages. Like both THP-1 monocytes and THP-1-derived macrophages, p38_{in}THP-1-derived macrophages was most susceptible to cardamonin-Cu(II) complex. p38_{in}THP-1-derived macrophages treatment with cardamonin-Fe(II) complex appeared to show similar effects on cell viability as THP-1-derived macrophages. Cell viability maintained above 80% at the highest concentration of

cardamonin-Fe(II) complex tested. Overall, these findings appear to suggest that p38 α and p38 β MAP kinase signaling pathway was not mainly responsible for the THP-1-derived macrophages differential susceptibility observed when treated with cardamonin, cardamonin-Cu(II) complex and cardamonin-Fe(II) complex.

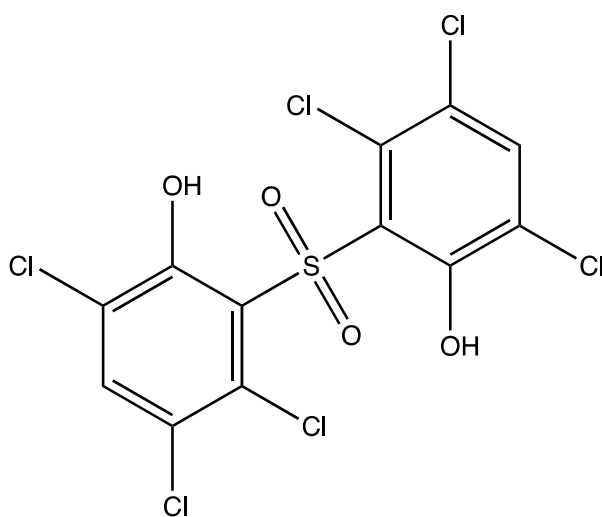


Figure 4.5 p38 MAP kinase inhibitor IV. Synonym: 2,2'-Sulfonyl-bis-(3,4,6-trichlorophenol).

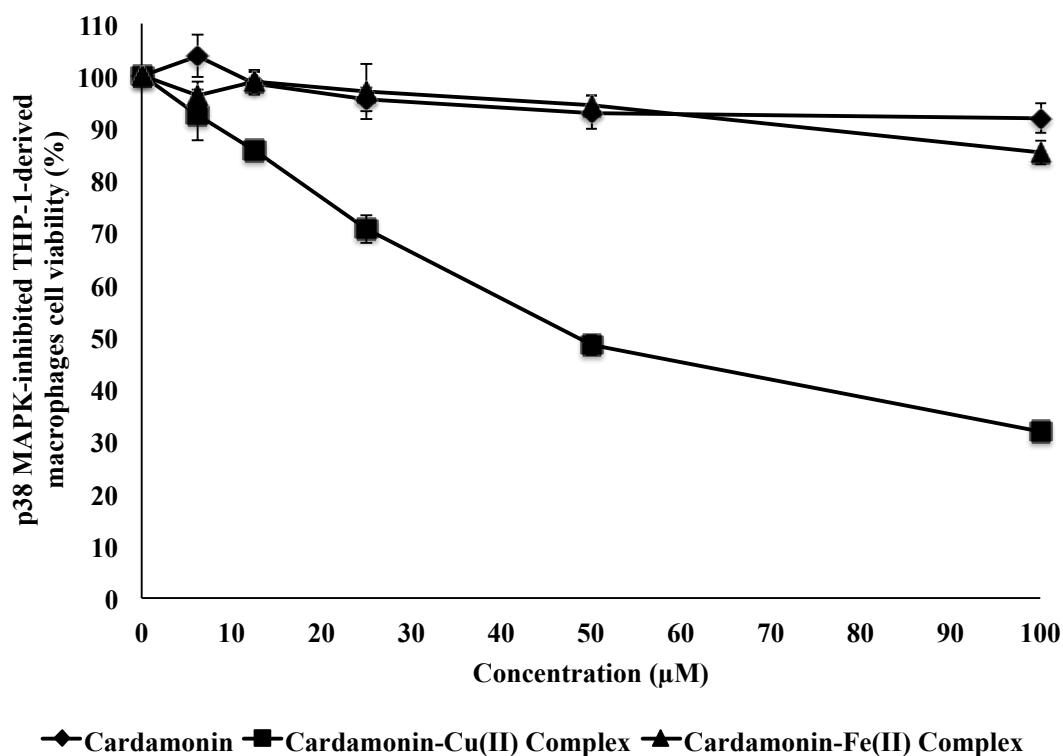


Figure 4.6 Effect of cardamomin, cardamomin-Cu(II) complex and cardamomin-Fe(II) complex on THP-1-derived macrophages cell viability in the presence of a MAP kinase inhibitor, p38 MAP kinase inhibitor IV.

THP-1-derived macrophages were exposed to various concentrations (6.25, 12.5, 25, 50 and 100 µM) of cardamomin, cardamomin-Cu(II) complex and cardamomin-Fe(II) complex in the presence of 1 µM p38 MAP kinase inhibitor for 24 hrs. The MTS assay was used to assess cell viability as described in the Materials and Methods section. Results were expressed as mean \pm SEM from three independent experiments.

4.2.6 Effects of cardamonin, cardamonin-Cu(II) and cardamonin-Fe(II) on THP-1-derived macrophages cell viability in the presence of a MAP kinase inhibitor, SB202190 MAP kinase inhibitor

To validate the above findings, a second inhibitor of the p38 MAP kinase was used, SB202190 (**Figure 4.7**) as Davies et al. (2000) highlighted the importance of using at least two structurally unrelated inhibitors for cell-based assays. Previous study has shown that SB202190 by itself was able to induce cell death (Nemoto et al. 1998). The recommended concentration of 10 μ M (Arana-Argáez et al. 2010) was further confirmed to not affect cell viability and was used in this study to pre-treat THP-1-derived macrophages. The cytotoxic effect on cell viability of SB202190 MAP kinase inhibited-THP-1-derived macrophages (SB202190_{in}THP-1-derived macrophages) of cardamonin, cardamonin-Cu(II) complex and cardamonin-Fe(II) complex was assessed. **Figure 4.8** showed the effect of cardamonin, cardamonin-Cu(II) complex and cardamonin-Fe(II) complex on SB202190_{in}THP-1-derived macrophages following 24 hrs treatment. Results revealed a similar trend to p38_{in}THP-1-derived macrophages and THP-1-derived macrophages where cells maintained their viability above 90% following cardamonin treatment on SB202190_{in}THP-1-derived macrophages. Similarly, cardamonin-Cu(II) complex was most cytotoxic towards SB202190_{in}THP-1-derived macrophages and cardamonin-Fe(II) was equally non-cytotoxic towards SB202190_{in}THP-1-derived macrophages as p38_{in}THP-1-derived macrophages.

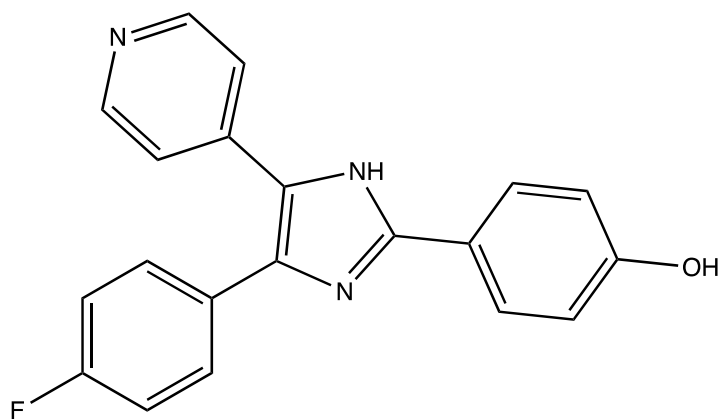


Figure 4.7 SB202190 p38 MAP kinase inhibitor IV. Synonym: 4-(4-Fluorophenyl)-2-(4-hydroxyphenyl)-5-(4-pyridyl)-1H-imidazole.

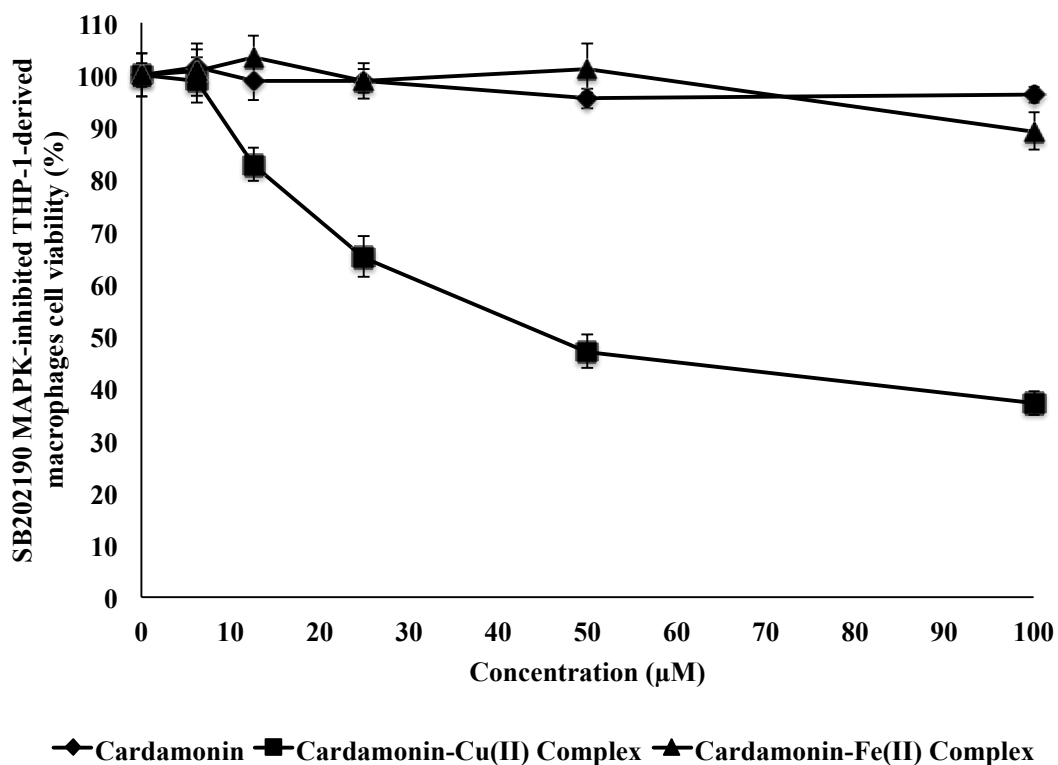


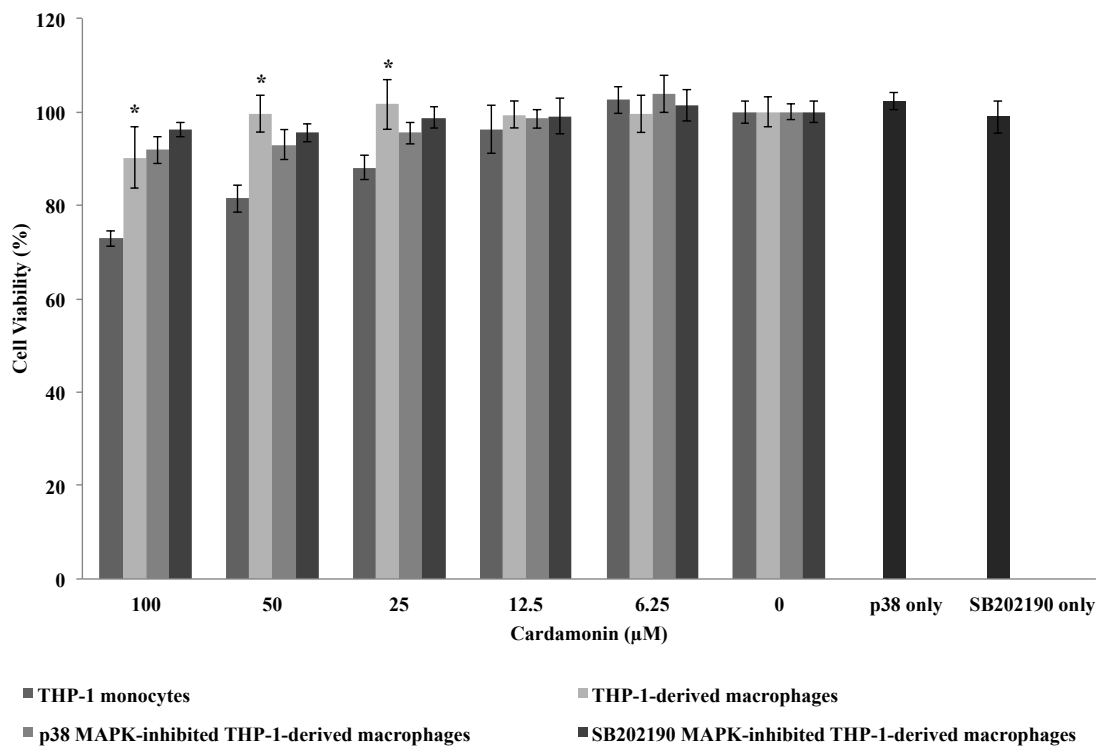
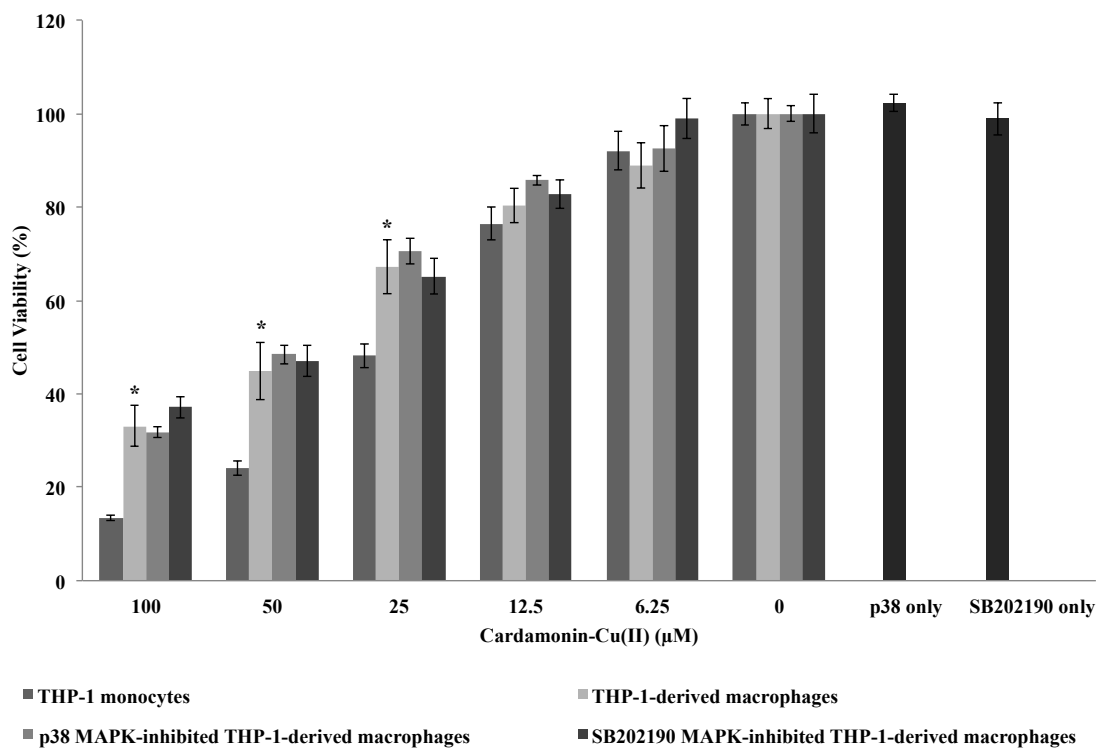
Figure 4.8 Effect of cardamomin, cardamomin-Cu(II) complex and cardamomin-Fe(II) complex on THP-1-derived macrophages cell viability in the presence of a MAP kinase inhibitor, SB202190.

THP-1-derived macrophages were exposed to various concentrations (6.25, 12.5, 25, 50 and 100 µM) of cardamomin, cardamomin-Cu(II) complex and cardamomin-Fe(II) complex in the presence of 10 µM SB202190 MAP kinase inhibitor for 24 hrs. The MTS assay was used to assess cell viability as described in the Materials and Methods section. Results were expressed as mean ± SEM from three independent experiments.

4.2.7 Comparative effects of cardamonin, cardamonin-Cu(II) and cardamonin-Fe(II) on cell viability of THP-1 monocytes, THP-1-derived macrophages, p38_{in}THP-1-derived macrophages and SB202190_{in}THP-1-derived macrophages

Building from the results obtained from Section 4.2.1, 4.2.4, 4.2.5 and 4.2.6, the effect on cell viability following THP-1 cell differentiation and inhibition of p38 MAP kinase was evaluated for each compound. **Figure 4.9A** shows the effect of cardamonin (6.25, 12.5, 25, 50 and 100 μ M) after 24 hrs against THP-1 monocytes, THP-1-derived macrophages, p38_{in}THP-1-derived macrophages and SB202190_{in}THP-1-derived macrophages. Results revealed a significant increase in cell viability at the three highest concentrations of cardamonin tested for THP-1-derived macrophages when compared to non stimulated-THP-1 monocytes. At 25, 50 and 100 μ M cardamonin, the THP-1-derived macrophages viability increased 14%, 19% and 17% respectively compared to THP-1 monocytes. Even though there was an increase in cell viability for THP-1-derived macrophages at 12.5 μ M compared to THP-1 monocytes, this increase was insignificant. Following the inhibition of p38 MAP kinase activity, there were no significant changes in cell viability of p38_{in}THP-1-derived macrophages and SB202190_{in}THP-1-derived macrophages compared to THP-1-derived macrophages. Overall, THP-1 monocytes were more susceptible to cardamonin treatment compared to the macrophages. 1 μ M p38 MAP kinase inhibitor and 10 μ M SB202190 MAP kinase inhibitor were confirmed to have no affect on the cell viability of THP-1-macrophages. **Figure 4.9B** compares the effect of cardamonin-Cu(II) complex on THP-1 monocytes, THP-1-derived macrophages, p38_{in}THP-1-derived macrophages and SB202190_{in}THP-1-derived macrophages where results revealed a significant increase in cell viability at 25, 50 and 100 μ M

cardamonin-Cu(II) for THP-1-derived macrophages compared to non stimulated-THP-1 monocytes. The increase in THP-1-derived macrophages cell viability at 12.5 μ M was insignificant from the monocytes. The observed trend was very similar to cardamonin and the inhibition of p38 MAP kinase activity did not significantly affect cell viability of p38_{in}THP-1-derived macrophages and SB202190_{in}THP-1-derived macrophages compared to THP-1-derived macrophages when treated with cardamonin-Cu(II). Overall, THP-1 monocytes were more susceptible to cardamonin-Cu(II) complex treatment compared to the macrophages. In **Figure 4.9C**, cardamonin-Fe(II) complex significantly improved cell viability by >25% and >35% in THP-1-derived macrophages at 50 and 100 μ M respectively compared to THP-1 monocytes. Following the inhibition of p38 MAP kinase activity, there were no significant changes in cell viability of the p38_{in}THP-1-derived macrophages and SB202190_{in}THP-1-derived macrophages compared to THP-1-derived macrophages. In general, THP-1 monocytes were most susceptible to all treatments compared to THP-1-derived macrophages, p38_{in}THP-1-derived macrophages and SB202190_{in}THP-1-derived macrophages. Taken together, interference from inhibitors of p38 α and p38 β on THP-1-derived macrophages did not alter cell susceptibility towards cardamonin, cardamonin-Cu(II) and cardamonin-Fe(II) treatments suggesting p38 MAP kinase was not mainly involved in THP-1-derived macrophages increased cell viability and resistance.

A**B**

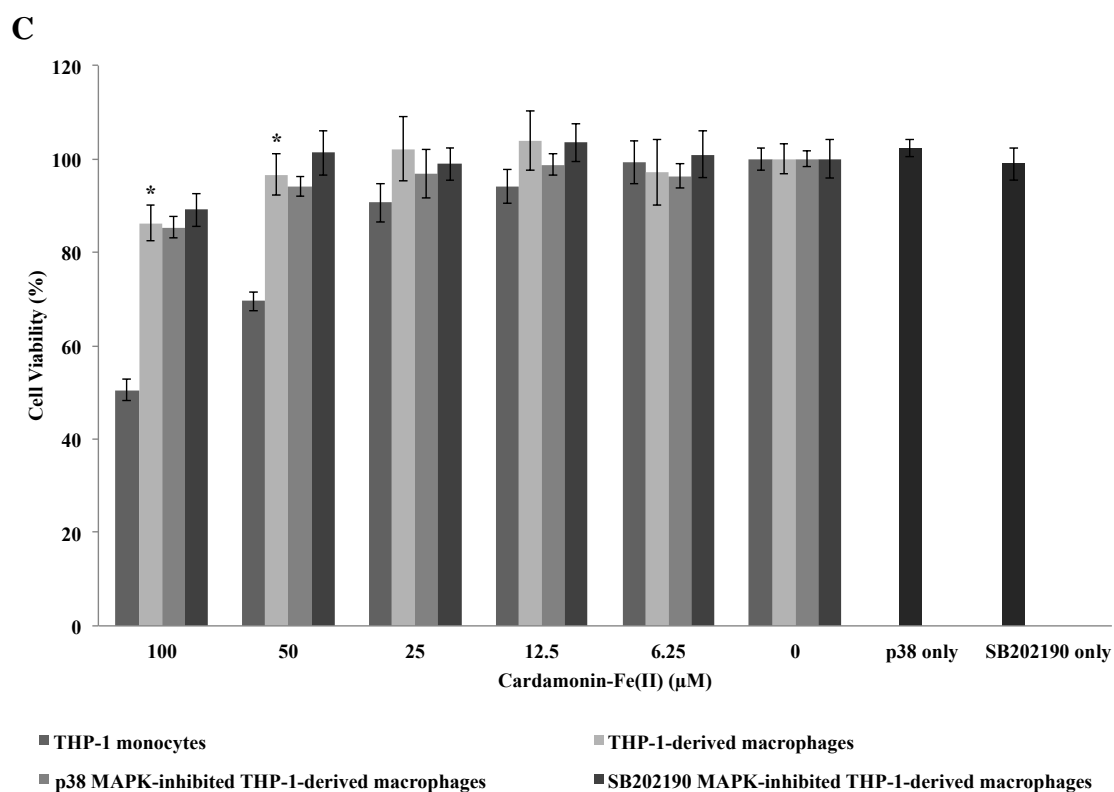


Figure 4.9 Comparative effects of cardamonin, cardamonin-Cu(II) complex and cardamonin-Fe(II) complex on cell viability of THP-1 monocytes, THP-1-derived macrophages and p38 MAPK-inhibited THP-1-derived macrophages.

Cells were exposed to various concentrations (6.25, 12.5, 25, 50 and 100 μM) of cardamonin (A), cardamonin-Cu(II) complex (B) and cardamonin-Fe(II) complex (C) for 24 hrs and MTS assay was used to assess cell viability as described in the Materials and Methods section. Results were expressed as mean ± SEM from three independent experiments. *indicates significant increase ($p < 0.05$) from THP-1 monocytes cell viability.

4.3 Discussion

Even though the role of cell adhesion as a growth regulatory mechanism has not been studied extensively, earlier investigations confirmed a direct relationship between cell spreading and DNA synthesis (Ben-Ze'ev et al. 1980, O'Neill et al. 1986, Ingber et al. 1987). In this study, a single cell line capable of dual adherent-suspension culture environments was used to study the role of cell adhesion in regulating cell death. Results clearly demonstrated that cardamonin, cardamonin-Cu(II) and cardamonin-Fe(II) complexes were relatively more cytotoxic in THP-1 monocytes compared to THP-1-derived macrophages, suggesting that suspension cells are indeed more susceptible compared to adherent cells that were more resistant. This occurrence is most likely due to the fact that adherent cells exhibit cell to cell and cell to matrix interactions, a distinct feature from suspension cells (Meredith et al. 1993, Salge et al. 2001). Previous studies have shown that extracellular matrix (ECM) interaction prevented cells from undergoing apoptosis and served as a survival factor for mesangial cells (Sugiyama et al. 1998). Gut epithelial and ureteral epithelial cells have also been reported to undergo cell death when detached (Meredith et al. 1993), demonstrating that ECM cell adhesion is critical for cell survival and growth (Lock and Debnath 2008, Marastoni et al. 2008). Additionally, integrins are main receptor proteins cells used to bind and respond to the extracellular matrix. They are made up of transmembrane $\alpha\beta$ heterodimers and responsible for mediating cell-cell attachment (Franceschi et al. 2015, Pan et al. 2016). It is well established that integrin-mediated adhesions to the extracellular matrix is vital for survival of numerous cell types and the activation of various integrins is needed to facilitate cells differentiating from suspension to adherence (Faull and Ginsberg 1995). The integrin-dependent survival

in epithelial and vascular endothelial cells was first described by Meredith et al. (1993). Cells undergo apoptosis in the absence of proper extracellular matrix contact and activation of specific integrins is able to prevent entry into this programmed cell death pathway (Meredith and Schwartz 1997, Gilmore et al. 2000). Interestingly, a study has found that the inhibition of fibroblast adherence to extracellular matrix did not actually alter certain integrin cell surface expression (Margarona et al. 1997). A previous study carried out to elucidate the structure and function of $\beta 5$ integrins reported that the $\beta 5$ integrins subunit involved both fibronectin and vitronectin adhesion, with fibronectin being the preferred ligand for K562 myeloid leukaemia cells (Pasqualini et al. 1993). $\beta 5$ expression was also found to be absent from all lymphoid cell lines examined, weakly expressed on myeloid cells but expressed at moderate to high levels in all the adherent cells examined. Furthermore, Pasqualini et al. (1993) confirmed integrin $\beta 5$ was highly expressed on carcinoma cell and on all adherent cell lines tested. Most notably, integrin $\beta 5$ was absent from the B and T lymphoid cell lines tested and expressed weakly in some myeloid cell lines.

Additionally, a similar trend has been reported by another study carried out on methotrexate, a treatment of rheumatoid arthritis, comparing the uptake of methotrexate in suspension cells versus adherent cells (Kimura et al. 2004). The researchers compared the IC_{50} of methotrexate against 3 types of suspension cells (FM3A, 2B4 and THP-1) and adherent cells (NIH3T3 and V79). They found that the IC_{50} values of all three cell lines in suspension were lower compared to the two adherent cell lines tested. They suggested that this preferential effect of inhibition by methotrexate in suspension cells was mainly due to a more rapid uptake of the compound. The rapid uptake of compounds by suspension cells could also be due to

the larger surface area of suspension cells compared to adherent cells hence the compound is easily accumulated in suspension cells. These findings further support our results and provided some understanding as to why THP-1-macrophages were more resistant to cardamonin, cardamonin-Cu(II) and cardamonin-Fe(II) compared to the THP-1 monocytes.

Also, the highly motile macrophages respond to a wide range of motility and adhesion signals *via* complex signalling pathways such as the G protein-coupled receptors, tyrosine kinase receptors and integrin mediated signalling pathways (Neumeister et al. 2003). Studies found that the extracellular matrix metalloproteinase inducer (EMMPRIN) is up regulated in THP-1 matured macrophages (Huang et al. 2008, Mittar et al. 2011). The up-regulation of EMMPRIN, also known as CD147, increased the secretion of matrix metalloproteinase-2 and matrix metalloproteinase-9 leading to THP-1 cells enhanced invasive ability (Zhou et al. 2005). This finding is in accordance with Kohro et al. (2004) who previously reported a significant increase in MMP-9 gene following THP-1 differentiation into matured macrophages. Huang et al. (2008) also highlighted that during the up-regulation of EMMPRIN expression in THP-1 matured macrophages, the MAP kinases p38 pathway and ERK 1/2 are activated, but not the JNK pathway.

Overall, the MAP kinase signalling pathways play a vital role in regulating life and death in cancer cells and sensitivity to drug therapy as emphasised by Dhillon et al. (2007) and Yang et al. (2012). To investigate the role of MAP kinase signaling pathway on THP-1-derived macrophages in this study, the p38 MAP kinase inhibitor was selected as it inhibits key intermediates at various upstream/ downstream levels

of the MAP kinase pathway. The ATP-competitive inhibitors used in this study actively target the p38 α and p38 β receptors as well as less active targets p38 γ , p38 δ , ERK1/2, and JNK1/2/3 receptors (Sigma-Aldrich 2017). Results revealed that the THP-1 cells adapted to grow in adherent macrophage-like conditions in the presence of p38 MAP kinase inhibitor and SB202190 MAP kinase inhibitor were equally resistant to treatment as THP-1-derived macrophages, suggesting the p38 α and p38 β MAP kinase pathway was not mainly responsible for the increase in cell resistance.

Interestingly, a recent study carried out by Yang et al. (2012) reported that curcumin, a chalcone similar to cardamomin, induced apoptotic cell death in THP-1 cells through activation of JNK/ERK/AP1 pathways. Curcumin was found to elevate JNK/ERK much greater than p38 in THP-1 cells and subsequently augment downstream transcription factors of JNK and ERK, c-Jun and JunB. In line with the findings in this study, the differentiated cells dramatically reversed curcumin-induced cell death of THP-1 cells from 25% to 96% cell viability. This study underlines the significance of other MAP kinase pathways beside p38. In a separate study, a polyphenol, resveratrol, has been reported to inhibit EMMPRIN expression through the MAP kinase pathway, namely the p38 and ERK1/2 pathways in differentiated THP-1 cells (Huang et al. 2008). Interestingly, when we compared the chemical structure of cardamomin to resveratrol, there were undeniable resemblance between the two compounds with both compounds have a total of two benzene rings, an alkene group connecting the two benzene rings as well as the presence of phenolic groups that are almost at the same sites of the rings. These data suggest p38 MAP kinase, specifically p38 α and p38 β , may not be directly involved in THP-1-macrophages increased resistance towards cardamomin, cardamomin-Cu(II) and cardamomin-Fe(II)

treatment but further studies should be carried out to determine the involvement of other MAP kinase pathways involving JNK and ERK protein kinases.

Taken together, differentiation of leukaemic cells has been thought as an anti-leukaemia approach for the aberrant immature blood cells. Indeed this study has shown that cardamonin and its two complexes became less cytotoxic following THP-1 differentiation into THP-1-derived macrophages stimulation compared to the monocytes counterpart. Even though the inhibition of p38 MAP kinase did not alter the cell susceptibility towards cardamonin and its complexes in THP-1-derived macrophages, the involvement of the MAP kinase pathway particularly in human acute myeloid leukaemia is certain and should be further investigated. Subsequent work should be carried out to confirm the MAP kinase activity in THP-1 monocytes and THP-1-derived macrophages. Besides, various studies have highlighted the activation of ERK and JNK and/ or p38 protein kinases by anti-cancer compounds in human leukaemia cells (Chen et al. 2008, Torres et al. 2008, Chang et al. 2010, Jin et al. 2010). Hence, future studies should further focus on ERK and JNK activation in determining the molecular mechanism of cardamonin and its complexes as well as elucidating the different death mechanism of THP-1 cells compared to matured THP-1 macrophages. Lastly, our data implies the novel use of cardamonin and its complexes as potential anti-leukemia agent that was more effective against immature leukaemic cells than mature cells.

**CHAPTER 5: ELUCIDATING THE CYTOTOXIC
MECHANISM OF ACTION INDUCED BY
CARDAMONIN AND ITS COMPLEXES IN JURKAT T
CELLS**

5.1 Introduction

As previously reported in Chapter 3, cardamonin-Cu(II) complex and cardamonin-Fe(II) complex were the two most cytotoxic cardamonin derivatives against A549 lung and HK1 nasopharyngeal human carcinoma cell line. Subsequent cytotoxicity studies carried out using these compounds on the human leukemia T cells, Jurkat T cells, revealed that these two complexes were again most cytotoxic with lowest IC₅₀ values reported. Hence, in this study, Jurkat T cells were chosen as the cell culture model to explore the cytotoxicity of cardamonin and its metal complexes and the underlying mechanism of action leading to Jurkat T cell death. As previous studies showed that cardamonin activates cell death mainly through apoptosis (**Table 1.3**), we determine the involvement in apoptotic cell death by introducing a caspase inhibitor since one of the characteristic features of apoptosis is caspase activation. This study further concentrates on elucidating whether mitochondria dysfunction, PS externalisation and caspase cascades are involved in Jurkat T cell death that potentially leads to apoptosis. To our best knowledge, this study is the first to demonstrate the induction of apoptosis by cardamonin and its two novel metal complexes in Jurkat T cells.

5.2 Results

5.2.1 Effects of cardamonin, cardamonin-Cu(II) complex and cardamonin-Fe(II) complex on cell viability in the presence of a caspase inhibitor, Z-VAD-FMK, in Jurkat T cells

To examine whether cardamonin-, cardamonin-Cu(II)- and cardamonin-Fe(II)-induced cell death in Jurkat T cells is *via* apoptosis, the effects of Z-VAD-FMK, a cell-permeable caspase inhibitor was investigated. As shown in **Figure 5.1**, Z-VAD-FMK was able to block cell death induced by cardamonin and its complexes. The cell viability of Jurkat T cells treated with 50 and 100 μ M of Z-VAD-FMK were significantly higher compared to cells treated with cardamonin and its complexes alone. The increased Z-VAD-FMK concentration from 50 to 100 μ M also revealed an increased in cell viability further suggesting that caspases are involved in all three compounds-induced apoptotic cell death.

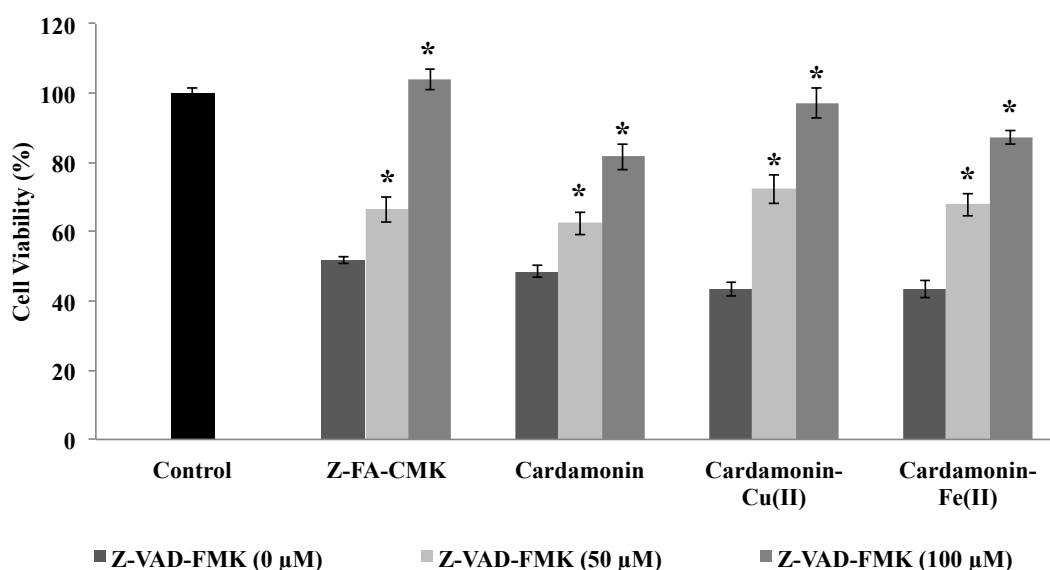
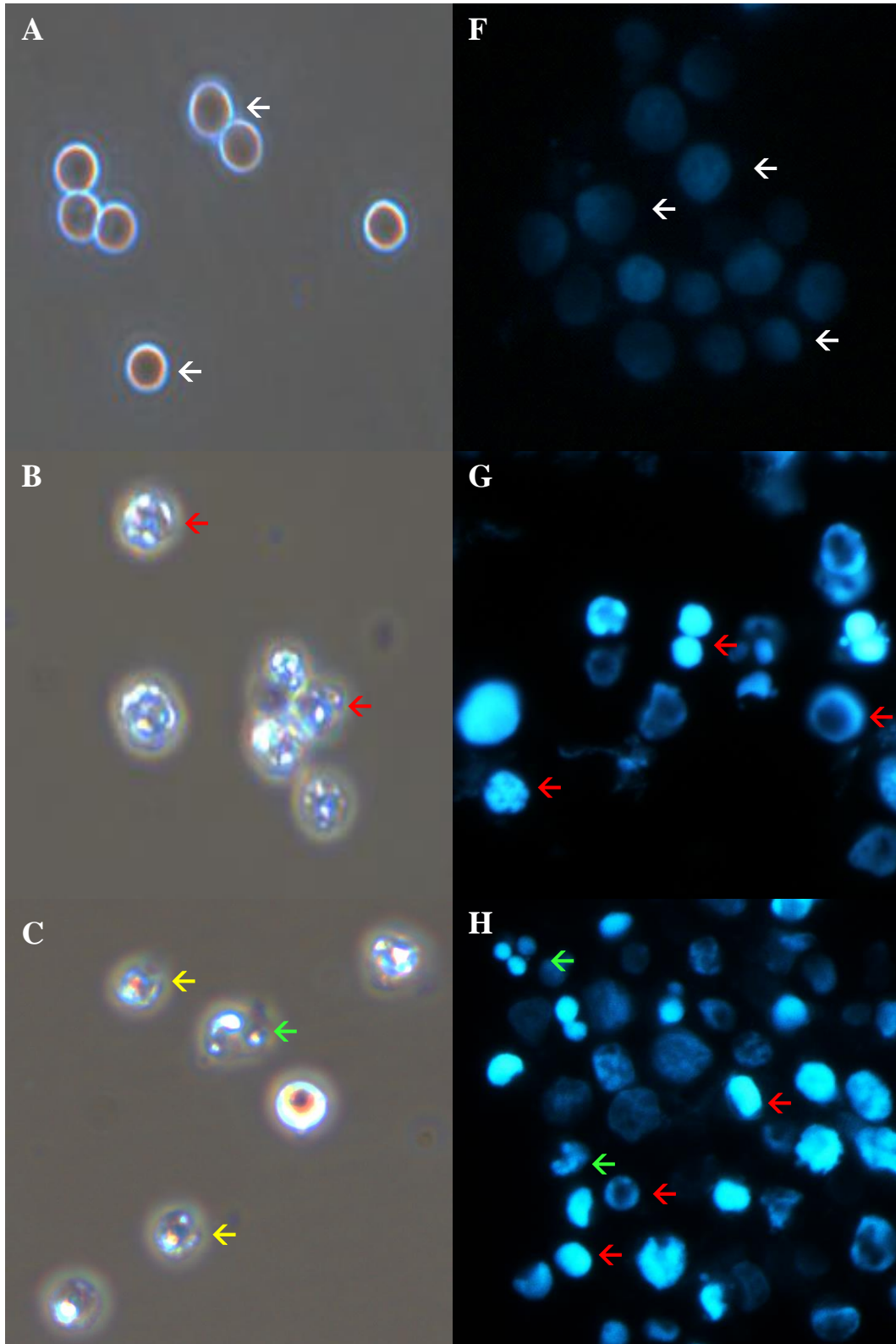


Figure 5.1 Effects of cardamonin and its complexes (IC_{50} values) on cell viability in Jurkat leukemia T cells in the absence or presence of caspase inhibitor, Z-VAD-FMK (50 or 100 μ M).

A cathepsin B inhibitor, Z-FA-CMK, which is known to induce apoptosis at low concentrations in Jurkat leukemia T cells, was used as the positive control (8 μ M). Control cells represent untreated cells. Cells were treated and incubated for 24 hrs then assessed for cell viability using the MTS assay. Data represents the mean \pm SEM (n = 3 replicates) and representative of three independent experiments. *indicates significantly different (p < 0.05) from treated cells in the absence of Z-VAD-FMK.

5.2.2 Morphological changes induced by cardamonin, cardamonin-Cu(II) complex and cardamonin-Fe(II) complex on Jurkat T cells

Hallmarks of apoptotic cell death can be detected in the changes of nuclear morphology such as nuclear DNA condensation, cell shrinkage, plasma membrane blebbing and nuclear fragmentation into apoptotic bodies. Jurkat T cells were exposed for 24 hrs to cardamonin, cardamonin-Cu(II) and cardamonin-Fe(II) using the IC₅₀ values. **Figure 5.2A-E** illustrated the cell morphology using contrast phase microscopy. Cells were fixed and stained with the DNA Hoechst dye after treatment and viewed using fluorescence microscopy as shown in **Figure 5.2F-J**. As demonstrated in **Figure 5.2F**, normal control Jurkat T cells were lightly stained with the DNA dye and exhibited normal nuclear morphology. However, apoptotic characteristics were presented in cells treated with cardamonin and both its complexes such as shrinkage of cells, chromatic condensation, and cell membrane blebbing (**Figure 5.2G-J**).



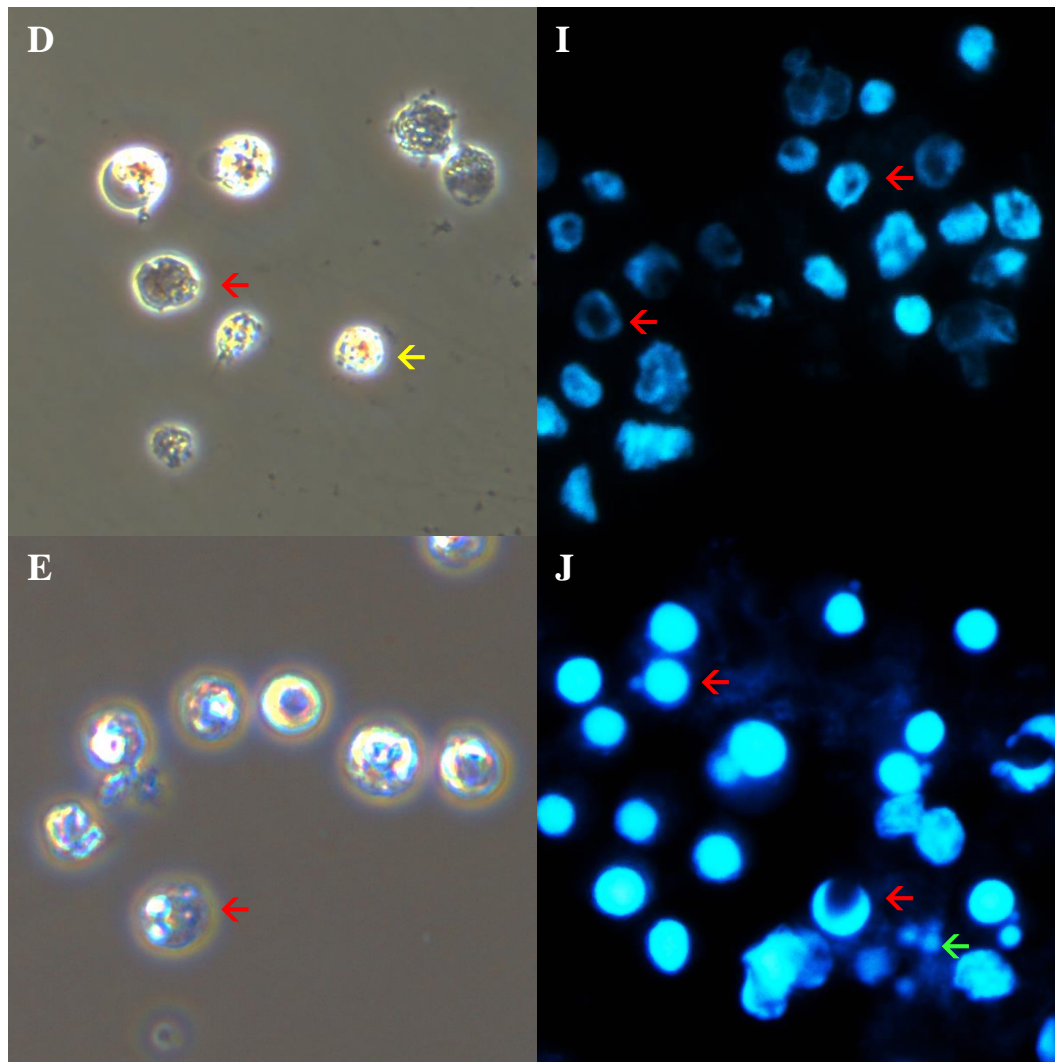


Figure 5.2 Effects of cardamonin and its complexes (IC_{50} values) on morphological and nuclear DNA changes in Jurkat leukemia T cells.

Cells were treated and incubated for 24 hrs then fixed with 4% paraformaldehyde and stained with Hoechst 33358 dye. Cell morphological changes typical of apoptosis were observed using the Olympus fluorescence microscope. The optical microscopic images of control cells (**A**), cardamonin-treated cells (**B**), cardamonin-Cu(II)-treated cells (**C**), cardamonin-Fe(II)-treated cells (**D**), and STS-treated cells (**E**). Nuclear DNA morphology of control cells (**F**), cardamonin-treated cells (**G**), cardamonin-Cu(II)-treated cells (**H**), cardamonin-Fe(II)-treated cells (**I**), and STS-treated cells (**J**) by Hoechst 33358 staining. Original magnification X400. White arrows indicate normal cell morphology, yellow arrows indicate cell shrinkage, red arrows indicate DNA/ chromatin condensation, nuclear fragmentation, plasma membrane blebbing and green arrows indicate formation of apoptotic bodies.

5.2.3 Analysis of phosphatidylserine externalisation during apoptosis using FITC-conjugated annexin in Jurkat T cells

For further assessment of apoptosis, the exposure of PS on the cell surface was examined using Annexin-V/PI double staining and determined by flow cytometer. Cells were treated with IC_{50} values of cardamonin, cardamonin-Cu(II) and cardamonin-Fe(II) for 24 hrs prior to Annexin-V/PI assessment. STS, a non-selective protein kinase inhibitor that is known to induce apoptosis, was used as the positive control where cells were treated with 1 μ M STS for 4 hrs. **Figure 5.3A** represents the dot plots of control cells, STS, cardamonin-treated cells, cardamonin-Cu(II)-treated cells, and cardamonin-Fe(II)-treated cells. As illustrated in **Figure 5.3B**, the viable cells of all treated cells were significantly lower when compared to control cells, which has the most viable cells. Conversely, all treated cells were significantly higher in the number of early apoptotic cells when compared to number of control cells. In parallel with this, there was an increase in late apoptotic cells where cardamonin- and cardamonin-Fe(II)-treated cells were significantly higher than the control cells. On the contrary, the necrotic cells population seemed rather constant in these conditions.

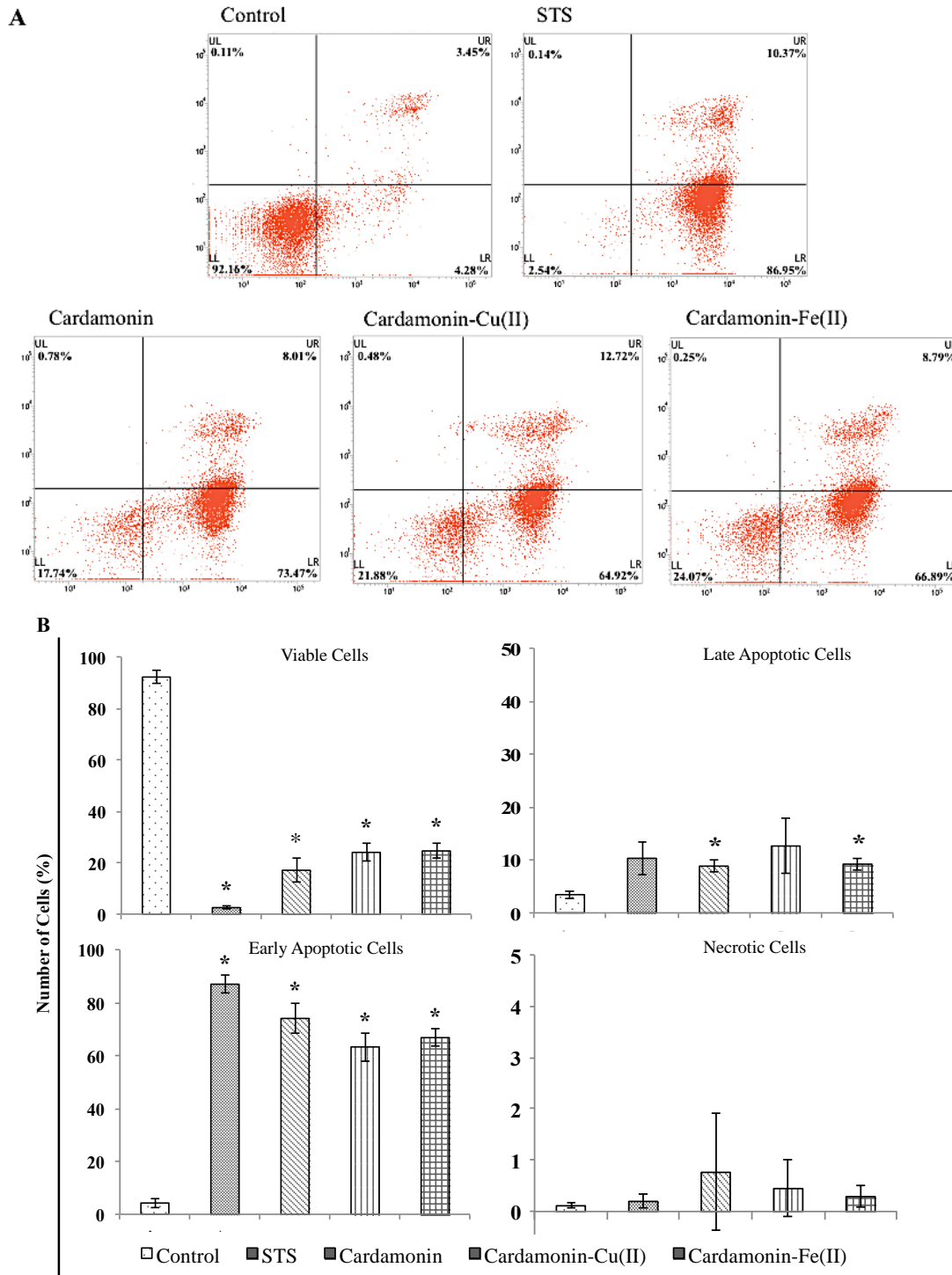


Figure 5.3 Flow cytometry examination of apoptosis, necrosis and cell viability – the Annexin V-FITC/PI assay.

Representative dot plots of control cells, STS, cardamomin-treated cells, cardamomin-Cu(II)-treated cells, and cardamomin-Fe(II)-treated cells (A). LL: viable cells, LR: early apoptotic cells, UR: late apoptotic cells, and UL: necrotic cells. The percentage of viable, early apoptotic, late apoptotic, and necrotic cells (B). Data represents the mean \pm SEM (n = 3 replicates) and representative of three independent experiments. *indicates significantly different (p < 0.05) from control with media alone.

5.2.4 Western blot analysis of caspase activation by cardamonin, cardamonin-Cu(II) complex and cardamonin-Fe(II) complex in Jurkat T cells

Since Z-VAD-FMK alleviates cell death induced by cardamonin and its complexes, we examined the activation of caspases in Jurkat T cells exposed to cardamonin, cardamonin-Cu(II) and cardamonin-Fe(II) as well as STS (positive control). Results in **Figure 5.4** reveal all the caspases, caspase-3, -8 and -9 remained intact in the control untreated cells. On the contrary, treatment with cardamonin, cardamonin-Cu(II) and cardamonin-Fe(II) resulted in the processing of caspase-3 and -9 but not -8 in Jurkat T cells. Pro-forms of caspase-3 and -9 were cleaved into their p17/19/20 and p35/37 fragments, respectively. PARP-1, a caspase-3 substrate, was also cleaved from p116 to the signature p85 fragment. These results further confirmed that cell death induced by cardamonin and its complexes is *via* the apoptotic pathway. In the presence of the caspase inhibitor, Z-VAD-FMK, the processing of all the caspases were inhibited and the cleavage of PARP-1 was completely suppressed.

Z-VAD-FMK	-	+	+	+	+	-	-	-	-
staurosporine	-	-	-	-	-	-	-	-	+
cardamonin	-	-	+	-	-	+	-	-	-
cardamonin-Cu(II)	-	-	-	+	-	-	+	-	-
cardamonin-Fe(II)	-	-	-	-	+	-	-	+	-

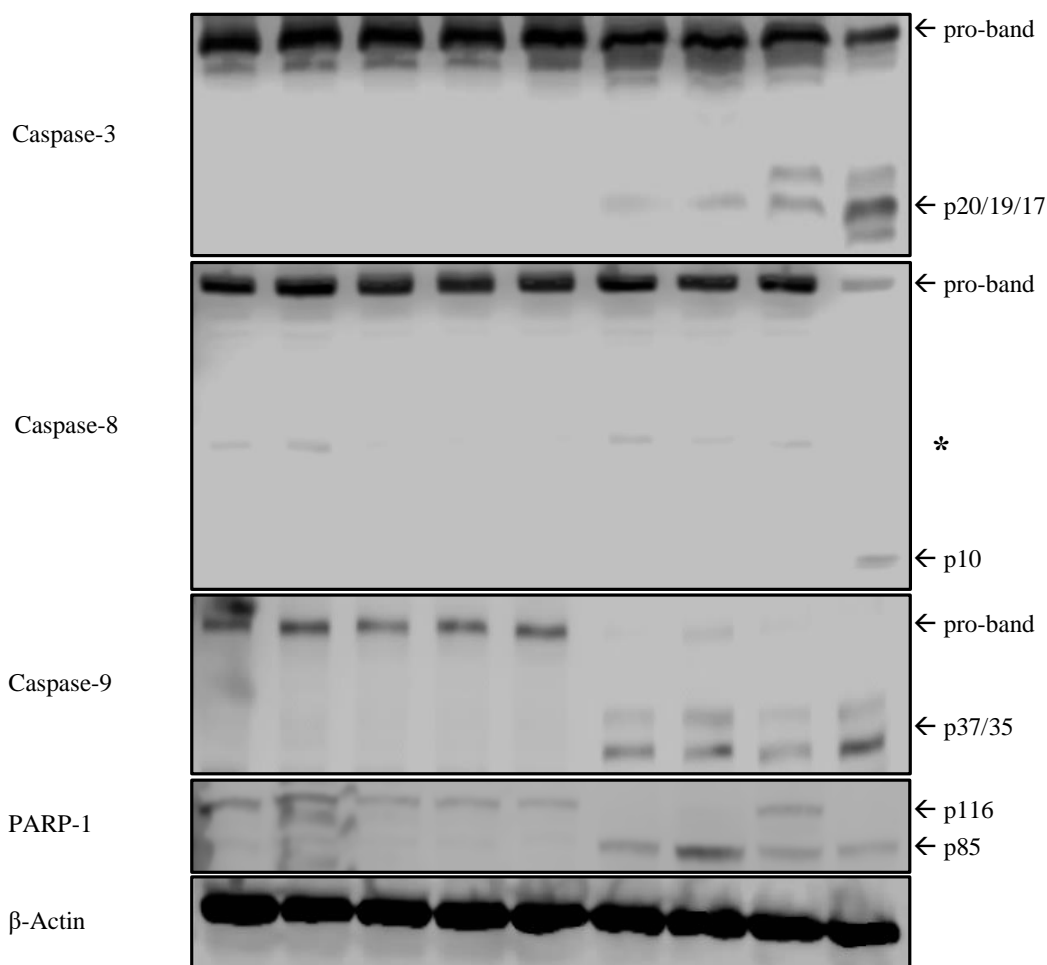


Figure 5.4 Effect of cardamonin, cardamonin-Cu(II) and cardamonin-Fe(II) on the activation of caspase-3, -8 and -9 and the cleavage of PARP-1 in Jurkat T cells.

Cells were treated in the presence or absence of caspase inhibitor, Z-VAD-FMK (100 μ M). Cells were treated with 1 μ M STS for 4 hrs as a positive control. SDS-PAGE and western blotting techniques were used to analyse the activation of caspases and the cleavage of PARP-1 as described in Materials and Methods section. Results are representative of at least three separate experiments. *indicates non-specific bands on blots.

5.2.5 Effects of cardamonin, cardamonin-Cu(II) complex and cardamonin-Fe(II) complex on MMP in Jurkat T cells

Collapse of the MMP on the cell surface membrane of cells undergoing apoptosis is one of the earliest changes that precedes the externalisation of PS. As witnessed in **Figure 5.5**, exposure to cardamonin and both its complexes for 24 hrs significantly decreased the percentage of positively stained TMRE cells, contrary to the untreated control cells where the MMP remained intact. Overall, this study shows cardamonin induces apoptosis in a similar way to the known apoptotic inducer, STS.

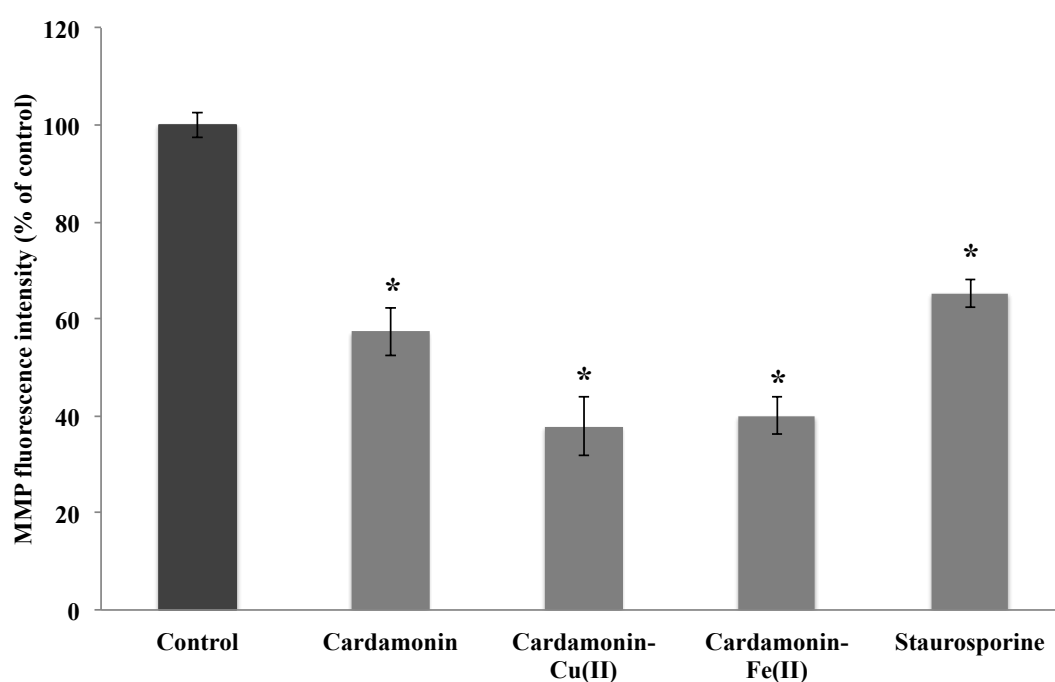


Figure 5.5 Effects of cardamonin and its complexes on the MMP in Jurkat T cells.

After 24 hrs treatment with IC_{50} values of cardamonin, cardamonin-Cu(II) and cardamonin-Fe(II), the MMP was measured by the percentage of fluorescence intensity compared to the control using the TMRE assay. Cells were treated with 1 μ M STS for 4 hrs as a positive control. Data represents the mean \pm SEM (n = 3 replicates) and representative of three independent experiments. *indicates significantly different ($p < 0.05$) from control with media alone.

5.3 Discussion

To date, many natural products have been screened for their anti-cancer potential *via* different experimental models. In the present study, cardamonin was complexed with copper and iron metal ions and assessed for the cytotoxicity profile. Transition-metal complexes are increasingly being considered as promising anti-cancer drugs (Deegan et al. 2006) as metal ions are vital for many biological processes and are constantly available in the human body (Tang and Liang 2013). Results in Chapter 3 revealed both cardamonin-Cu(II) and cardamonin-Fe(II) complexes showed an increased cytotoxicity as the concentration increased. Compared to the original parent compound, cardamonin, addition of copper and iron to cardamonin increased the cytotoxic efficacy of the compounds by more than fourfold and twofold, respectively.

To examine the mode of action of cardamonin and its complexes, we first used Z-VAD-FMK to block the activation of caspases and their activity in Jurkat T cells. The synthetic broad-spectrum caspase inhibitor, Z-VAD-FMK, is used extensively in elucidating the role of caspases during apoptosis. The presence of Z-VAD-FMK markedly inhibited cell death induced by cardamonin and its complexes. When concentration of Z-VAD-FMK was increased from 50 to 100 μ M, the cell viability was almost completely restored. These results suggest that cell death induced by cardamonin and its complexes is caspase-dependent. As activation of caspase is known to promote apoptosis, we next observed the cell nuclear morphology changes after treatment using the fluorescent DNA-binding agent, Hoechst stain. The morphological changes revealed distinct hallmarks of apoptosis and caspases have been implicated to play a major role in this process. To examine this in greater detail,

cells were observed under both contrast phase and fluorescent microscopy looking at the cell on the whole and staining the DNA, respectively. It was confirmed that cells treated with cardamonin and its complexes displayed chromatin condensation, cell shrinkage and apoptotic bodies which are all the distinct features of cells undergoing apoptosis. Although nuclear staining using Hoechst stain is used widely to determine cell death, this technique does not provide quantification nor distinguish cells in early apoptosis state from those in late apoptosis state. For better characterisation of cell death, after cell staining, cells were subjected to flow cytometry analysis using annexin V.

In order to support the hypothesis that cardamonin and its complexes-induced cell death was responsible for the induction of apoptotic cell death, Jurkat cells were stained with Annexin-V FITC and propidium iodide (PI). Annexin V is a calcium dependent phospholipid binding protein that has high binding affinity to PS. This high binding affinity of Annexin-V is utilised during translocation of PS from the inner to outer leaflet of the plasma membrane that occurs during apoptosis (Widau et al. 2014). PI on the contrary has high affinity towards nucleic acids and selectively enters late apoptotic or necrotic cells. The number of stained cells was estimated *via* flow cytometry where these results indicated that cardamonin and its complexes induced significant cell death through apoptosis. The dual staining of Annexin-V and PI made it possible to identify early apoptotic, later apoptotic, live and dead cells. In current observations, the majority of cells, ranging from 65% – 75%, exposed to cardamonin and its complexes for 24 hrs were undergoing early apoptosis with less than 25% of normal cells present. These results taken together with the microscopic findings

provided further supportive evidence that treatment with cardamonin and its two complexes induced apoptotic cell death.

As mentioned earlier, the key regulator proteases of apoptotic pathways are caspases which, when activated provides confirmatory evidence of apoptotic events. In this study, cardamonin and its complexes induced caspase-3 and -9 activation but not caspase-8 following 24 hrs treatment in Jurkat T cells. To further confirm the role of caspases, activation of PARP-1 was assessed, a well-known substrate of caspase-3. Indeed, Jurkat T cells treated with cardamonin, cardamonin-Cu(II) and cardamonin-Fe(II) complex induced cleavage of PARP-1 (116 kDa) resulting in the accumulation of the 85 kDa cleavage product. Modification of this protein occurs in response to DNA damage (Bouchard et al. 2003). Furthermore, PARP-1 has been implicated in numerous vital cellular processes such as DNA repair, DNA replication and transcription, genome stability and apoptosis (Bouchard et al. 2003). In the presence of the caspase inhibitor, Z-VAD-FMK, the processing of caspase-3, -9 and the cleavage of PARP-1 mediated by cardamonin and its complexes was completely abrogated. These results demonstrated that cardamonin, cardamonin-Cu(II) and cardamonin-Fe(II) complex-induced cell death is indeed a caspase-dependent process. These findings suggested that these compounds activated the intrinsic apoptotic pathway, also known as the mitochondrial apoptosis pathway.

It has been well documented that apoptosis is initiated by two signalling pathways, extrinsic and intrinsic pathway (Green 2000). The extrinsic pathway involves interaction of cell surface receptors like tumour necrosis factor (TNF), Fas and TNF-related apoptosis-inducing ligand (TRAIL), which in turn activates the downstream initiator caspases, caspase-8. Activation of caspase-8 can lead to direct

activation and cleavage of downstream effector caspases including caspase-3 (Parrish et al. 2013). In certain cell lines, this pathway is all that is needed to cause cell death. On the contrary, in other cell types, caspase-8 must also engage the mitochondria and enter the intrinsic pathway to undergo apoptosis (Li et al. 1998, Luo et al. 1998). Principally, the initiator caspase-8 of the extrinsic pathway is initiated at the plasma membrane. FasL receptor interacts with Fas transmembrane receptor leading to receptor oligomerisation. The Fas receptor death domain (DD) allows the recruitment of FADD adaptor protein from the cell cytoplasm *via* its DD. Interaction between the death effector domain (DED) on FADD initiate the recruitment of caspase-8 to the complex. Active initiator caspase-8 can directly activate effector caspase-3 or in some cases the initiator caspase facilitates mitochondrial cytochrome c release BID cleavage, initiating the intrinsic mitochondrial pathway. Intrinsic apoptosis depends on the factors released from mitochondria. The initiator caspase-9 directly activates the mitochondria-dependent intrinsic pathway. At the mitochondria, pro-apoptotic (BAX and BAK) and anti-apoptotic BCL-2 (BCL-2 and BCL-xL) family members facilitate and inhibit cytochrome c release from the mitochondrial intermembrane space respectively (Parrish et al. 2013). Cytochrome c interacts with apoptotic protease-activating factor-1, Apaf-1, and undergoes oligomerisation into apoptosome, a heptameric structure, once it translocates into the cytosol (Shiozaki et al. 2002). The apoptosome activates the recruited initiator caspase-9, which then directly cleaves and activates effector caspase-3.

Coupled with the results observed in **Figure 5.1** and **Figure 5.4**, the presence of the caspase inhibitor Z-VAD-FMK has alleviated cell death in a dose dependent manner and the activation of initiator caspase-9 and executioner caspase-3 were

inhibited. The pathway described above further confirms that cell death in Jurkat T cells mediated by cardamonin and its two complexes are caspase-dependent and involved the intrinsic mitochondrial pathway. Although in this study caspase-8 was not activated following 24 hrs treatment with cardamonin and its two complexes, a recent study have shown activation of this initiator caspase by cardamonin in human colon cancer cells (Yadav et al. 2012). Even though the study is in conflict with the findings in this study, an interesting observation was seen in another study measuring caspase-8 luminescent in the cell-based assay that demonstrated the caspase-8 activity in Jurkat T cells was optimum 3 hrs following drug treatment (Farfan et al. 2004). As caspase-8 has the ability to indirectly activate the intrinsic mitochondrial pathway (Li et al. 1998, Parrish et al. 2013), a quantitative western blot study at different time points before 24 hrs can be carried out to assess the possible activation of caspase-8 in this study.

Several studies have reported the loss of MMP induced by chalcone derivatives i.e. loss of MMP in (1) cervical cancer cells induced by Flavokawain B (Lin et al. 2012); (2) colon cancer cells by Ch1 and Ch2 chalcone derivatives (Kello et al. 2016); and (3) nasopharyngeal cancer cell by curcumin (Kuo et al. 2011), where caspase-3-dependent apoptotic death took place. It has been well established that the loss of MMP occurs during early stages of apoptosis where caspase activation further induces permeabilisation of the mitochondrial membrane. Depolarisation of mitochondria plays a vital role in triggering cell death and activation of apoptosis. Cell death is triggered through the release of apoptotic proteins to the cytoplasm from the disturbed and disrupted mitochondrial membrane (Ferreira et al. 2012). The MMP results obtained in this study confirmed that cardamonin, cardamonin-Cu(II) and

cardamonin-Fe(II) induced mitochondrial dysfunction and decreased in MMP. Loss of MMP is an initial requirement for cellular apoptosis. This finding further supports Annexin-V-FITC binding results and also correlates to the morphological studies which all displayed the hallmarks of apoptotic cell death in Jurkat T cells induced by cardamonin and its two complexes.

Taken together, induction of apoptotic cell death can be regarded as a therapeutic function that is aimed to eliminate damaged cells. Hence, the goal for therapy against neoplastic cells now aims to trigger apoptosis, programmed cell death. In this chapter, it was shown that cardamonin-Cu(II) and cardamonin-Fe(II) complexes have higher cytotoxic activity than cardamonin itself. Both complexes and cardamonin induced cellular morphological changes that were typical of apoptosis. The exposure of PS and decline in the MMP indicated that both these complexes are promising anti-cancer agents as inducers of apoptotic cell death. Cardamonin-Cu(II) and cardamonin-Fe(II)-induced apoptosis in Jurkat T cells are through caspase-dependent mitochondrial pathway, similar to cardamonin. Based on the data obtained in this study thus far, the hypothesis that DNA damage in cells could be highly preferentially due to oxidative species produced by transition metal ions will be further evaluated in the following chapter to better elucidate the mechanism of action of these novel compounds.

**CHAPTER 6: OXIDATIVE MECHANISMS OF
CARDAMONIN, CARDAMONIN-Cu(II) AND
CARDAMONIN-Fe(II) COMPLEXES IN JURKAT T
CELLS**

6.1 Introduction

In previous chapter, the mechanism of action of cardamonin, cardamonin-Cu(II) and cardamonin-Fe(II) complexes were investigated in Jurkat T cells. The results illustrated that both complexes and cardamonin induced cellular morphological changes that are typical of apoptosis, exposing PS and the loss of MMP. All three compounds induced apoptosis in Jurkat T cells through caspase-dependent mitochondrial pathway, activating caspase-3, caspase-9 and PARP-1. In this study, cardamonin was complexed with metal ions, and cytotoxicity of cardamonin-Cu(II) and cardamonin-Fe(II) in Jurkat T cells was examined. As previous studies have reported the ability of metals to induce cytotoxicity through oxidative stress (Aruoma et al. 1991, Shi et al. 2004, Valko et al. 2005, Fahmy and Cormier 2009), this chapter explored possibilities of cardamonin and its complexes eliciting oxidative stress or anti-oxidant pathway predisposing the Jurkat T cells to apoptosis. Metal-induced cytotoxicity has been widely recognised with its ability to generate reactive oxygen and nitrogen species as well as depleting GSH levels in cells (Ercal et al. 2001, Shi et al. 2004, Valko et al. 2005). Metal has the ability to bind directly to thiols or involve in the formation of H₂O₂. On the other hand, anti-oxidants have been shown to provide protection against metal-mediated free radical attacks (Curtin et al. 2002). Examples of commonly used anti-oxidants include NAC, Trolox, L-cysteine and GSH that have been shown to protect cells and reverse cell death (Buttke and Sandstrom 1994, Poliandri et al. 2003, Hadzic et al. 2005, Park et al. 2007, Marreilha et al. 2008, Sun 2010, Maheshwari et al. 2011, Saxena et al. 2014). Accordingly, GSH is the most abundant non-protein thiol that plays a vital role in regulating apoptosis and functioning as a ROS scavenging enzyme substrate (Circu and Aw 2008). In addition,

the amino-thiol, NAC, is a commonly used synthetic research tool to investigate the role of oxidative stress in the induction of apoptosis due to its ability to act as a precursor of GSH and intracellular cysteine (Zafarullah et al. 2003). Although NAC is widely used to demonstrate the involvement of oxidative stress in treatment-induced apoptosis, Sun (2010) suggested the use of multiple anti-oxidants including both thiols and non-thiols to confirm the implications of oxidative stress and apoptosis.

6.2 Results

6.2.1 Effects of cardamonin, cardamonin-Cu(II) and cardamonin-Fe(II) complexes on cell viability in the presence of NAC in Jurkat T cells

NAC, a thiol known to be a ROS scavenger and a precursor of GSH synthesis, was added to Jurkat T cells to determine if NAC could alleviate the cytotoxicity effects of cardamonin, cardamonin-Cu(II) and cardamonin-Fe(II)-mediated cell death. As illustrated in **Figure 6.1**, NAC was able to significantly block cardamonin and cardamonin-Fe(II)-induced Jurkat T cell death by >40% compared to treatment in the absence of NAC following 24 hrs treatment. On the contrary, NAC was not able to restore cell death mediated by cardamonin-Cu(II) complex. The presence of NAC alone at 1 mM has no effect on Jurkat T cell viability compared to the control as depicted below. Since NAC was able to block cell death mediated by cardamonin and cardamonin-Fe(II) complex in Jurkat T cells, these results suggest that oxidative stress is involved in the cytotoxic effects of these two compounds. These results and initial findings further warrant the analysis of intracellular ROS and GSH levels following cardamonin and its complexes treatment in Jurkat T cells.

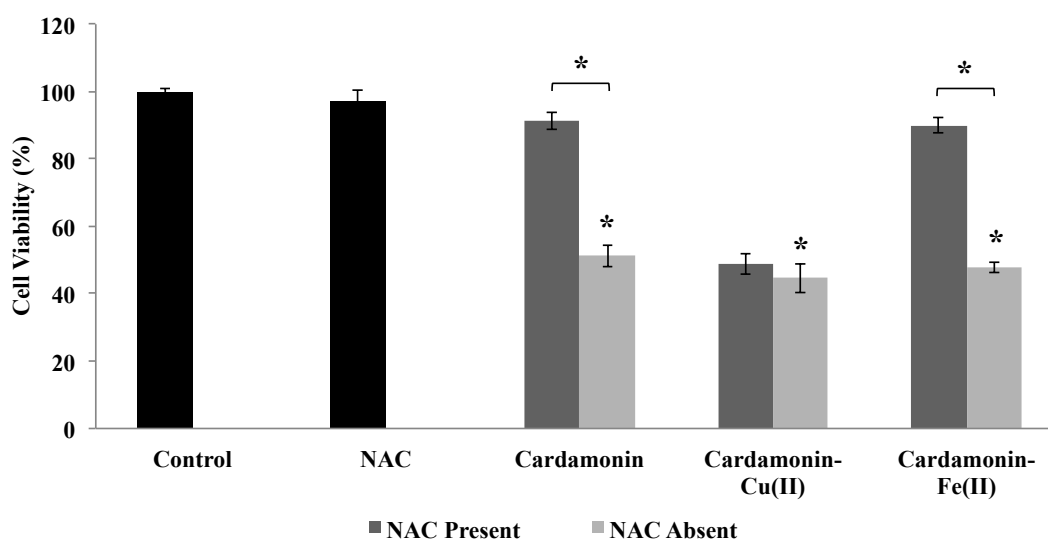


Figure 6.1 Effects of cardamonin, cardamonin-Cu(II) and cardamonin-Fe(II) complexes on cell viability in the presence or absence of NAC in Jurkat T cells.

Jurkat T cells were treated with cardamonin, cardamonin-Cu(II) or cardamonin-Fe(II) complexes in the presence or absence of NAC for 24 hrs and cell viability was assessed *via* the MTS assay as outlined in the Materials and Methods section. Results are means \pm SEM of three independent experiments. *indicates significant decrease ($p < 0.05$) from control; *above bracket indicates significant different ($p < 0.05$) from the respective compound treatment alone.

6.2.2 Effects of cardamonin, cardamonin-Cu(II) and cardamonin-Fe(II) complexes on intracellular ROS levels in Jurkat T cells

The potential of cardamonin and cardamonin-Fe(II) complex to induce oxidative stress as shown in **Figure 6.1** was further assessed by measuring the intracellular ROS levels. Results in **Figure 6.2** revealed that all three compounds, cardamonin, cardamonin-Cu(II) and cardamonin-Fe(II) complexes significantly induced the intracellular production of ROS. Cardamonin-Fe(II) and cardamonin induced intracellular ROS levels by 1.36 and 0.98-fold respectively compared to control in Jurkat T cells. Surprisingly, cardamonin-Cu(II) complex was shown to significantly increase intracellular ROS by 0.80-fold compared to control despite NAC having no effect on cell viability of cardamonin-Cu(II)-induced cell death. Since NAC also acts as a precursor of GSH synthesis besides scavenging ROS, we next examine the effects of cardamonin, cardamonin-Cu(II) and cardamonin-Fe(II) complexes on intracellular GSH levels.

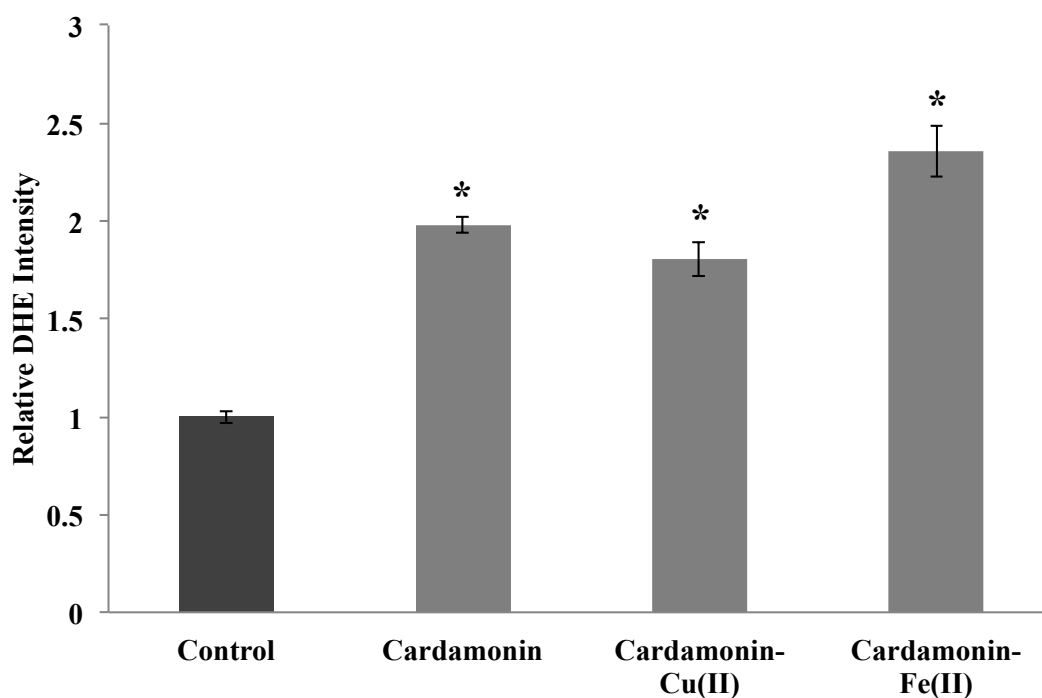


Figure 6.2 Effects of cardamonin, cardamonin-Cu(II) and cardamonin-Fe(II) complexes on intracellular ROS levels in Jurkat T cells.

Jurkat T cells were treated with cardamonin, cardamonin-Cu(II) or cardamonin-Fe(II) complexes for 24 hrs and the intracellular ROS levels were measured using the DHE probe as outlined in the Materials and Methods section. Results are means \pm SEM of three independent experiments. *indicates significant increase ($p < 0.05$) from control.

6.2.3 Effects of cardamonin, cardamonin-Cu(II) and cardamonin-Fe(II) complexes on intracellular GSH levels in Jurkat T cells

As all three compounds were shown to increase intracellular ROS levels in Jurkat T cells, the intracellular GSH levels of Jurkat T cells were further assessed following cardamonin, cardamonin-Cu(II) and cardamonin-Fe(II) complexes treatment. The GSH levels were measured based on 5×10^5 cells per treatment to ensure the GSH levels determined were representative of the intracellular GSH and not due to the decreased cell number following treatment. As illustrated in **Figure 6.3**, both cardamonin and cardamonin-Fe(II) significantly reduced intracellular GSH levels in Jurkat T cells by 43.73% and 39.21% respectively. Conversely, a slight decrease of 9.79% in intracellular GSH levels induced by cardamonin-Cu(II) was not significantly different from the control. These findings support the results observed in **Figure 6.1** suggesting that cardamonin and cardamonin-Fe(II) complex-induced cell death is dependent on the intracellular GSH levels. To confirm these findings, low molecular weight thiols were added to Jurkat T cells in the presence of cardamonin and its complexes and assessed for the effects on cell viability as shown in the following study.

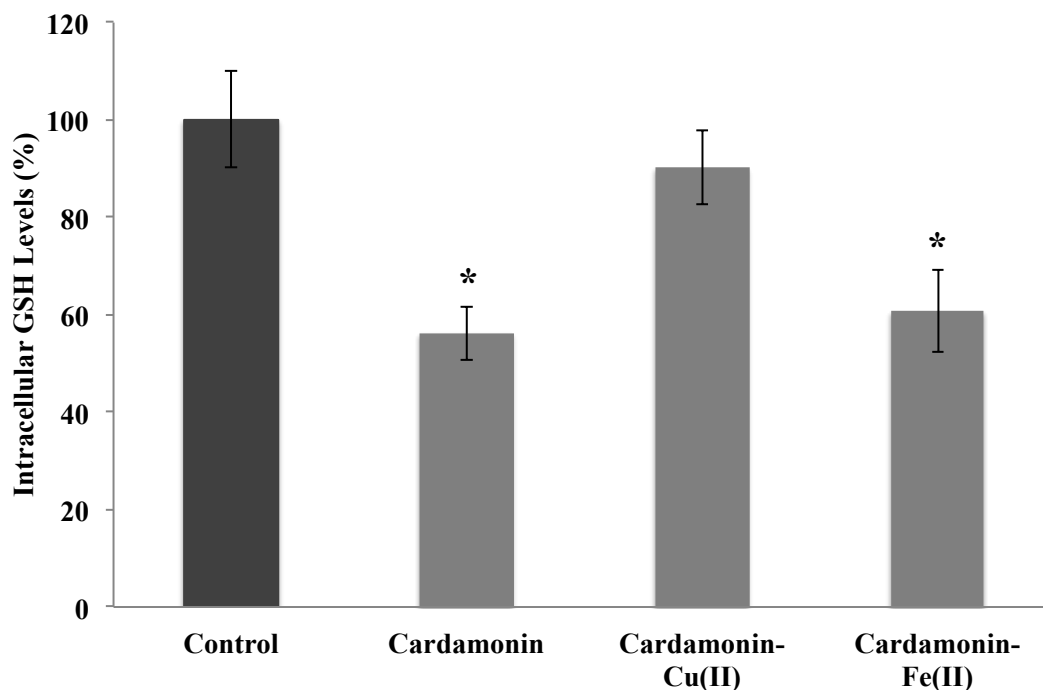


Figure 6.3 Effects of cardamonin, cardamonin-Cu(II) and cardamonin-Fe(II) complexes on intracellular GSH levels in Jurkat T cells.

Jurkat T cells were treated with cardamonin, cardamonin-Cu(II) or cardamonin-Fe(II) complexes for 24 hrs and the intracellular GSH levels were measured using the fluorescent dye MCB as outlined in the Materials and Methods section. Results are means \pm SEM of three independent experiments. *indicates significant decrease ($p < 0.05$) from control.

6.2.4 Effects of cardamonin, cardamonin-Cu(II) and cardamonin-Fe(II) complexes on cell viability in the presence of L-cysteine in Jurkat T cells

L-cysteine, a low molecular weight thiol required for GSH synthesis (Monick et al. 2003, Hadzic et al. 2005) was added to Jurkat T cells to determine if L-cysteine could alleviate the cytotoxic effects of cardamonin, cardamonin-Cu(II) and cardamonin-Fe(II)-mediated cell death. As de-acetylation of NAC is known to increase L-cysteine levels, is it possible that introduction of L-cysteine would similarly recover cell death as observed in **Figure 6.1** in the presence of NAC. As shown in **Figure 6.4**, L-cysteine was indeed able to significantly increase cell viability of cardamonin and cardamonin-Fe(II)-induced Jurkat cell death by 38.92% and 47.46% respectively compared to treatment in the absence of L-cysteine. In contrast, L-cysteine was not able to recover cell death mediated by cardamonin-Cu(II) complex suggesting that cardamonin-Cu(II)-induced cell death was not intracellular GSH levels dependent. The presence of L-cysteine alone at 5 mM was confirmed to not affect Jurkat T cell viability compared to the control as depicted below. Since L-cysteine was able to recover the cell death of Jurkat T cells mediated by cardamonin and cardamonin-Fe(II) complex, these results suggest that depletion of GSH levels are involved in the cytotoxic effects of these compounds that led to cell death. To support this theory, the following study assessed the effects of D-cysteine, a thiol that cannot be metabolised to GSH (Jones et al. 1995), on Jurkat T cells viability.

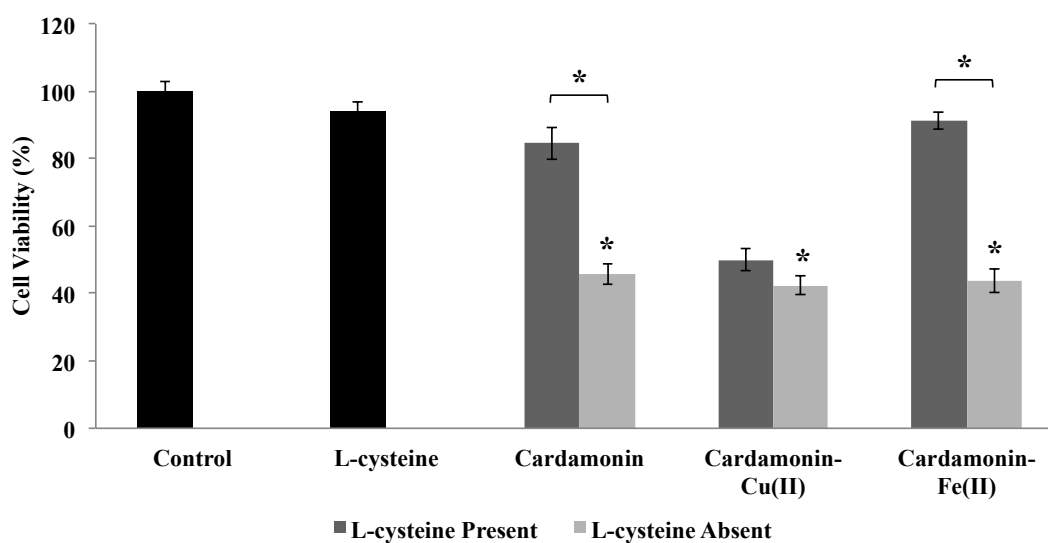


Figure 6.4 Effects of cardamonin, cardamonin-Cu(II) and cardamonin-Fe(II) complexes on cell viability in the presence or absence of L-cysteine in Jurkat T cells.

Jurkat T cells were treated with cardamonin, cardamonin-Cu(II) or cardamonin-Fe(II) complexes in the presence or absence of L-cysteine for 24 hrs and cell viability was assessed *via* the MTS assay as outlined in the Materials and Methods section. Results are means \pm SEM of three independent experiments. *indicates significant decrease ($p < 0.05$) from control; *above bracket indicates significant different ($p < 0.05$) from the respective compound treatment alone.

6.2.5 Effects of cardamonin, cardamonin-Cu(II) and cardamonin-Fe(II) complexes on cell viability in the presence of D-cysteine in Jurkat T cells

Since the cell death mediated by cardamonin and cardamonin-Fe(II) were significantly recovered by NAC (**Figure. 6.1**) and L-cysteine (**Figure. 6.4**), we examine whether another low molecular weight thiol, D-cysteine, which cannot be metabolised into GSH (Jones et al. 1995, Rajah and Chow 2014) had any effects on cell viability of treated Jurkat T cells. Results in **Figure 6.5** revealed the presence of D-cysteine had little effect on the cell viability of cardamonin, cardamonin-Cu(II) and cardamonin-Fe(II)-treated Jurkat T cells following 24 hrs treatment. The presence of D-cysteine alone at 5 mM was found to have no effect on Jurkat T cell viability compared to the control as depicted below. Taken together, these results suggest that the cytotoxic effects of cardamonin and cardamonin-Fe(II) were due to oxidative stress *via* GSH depletion.

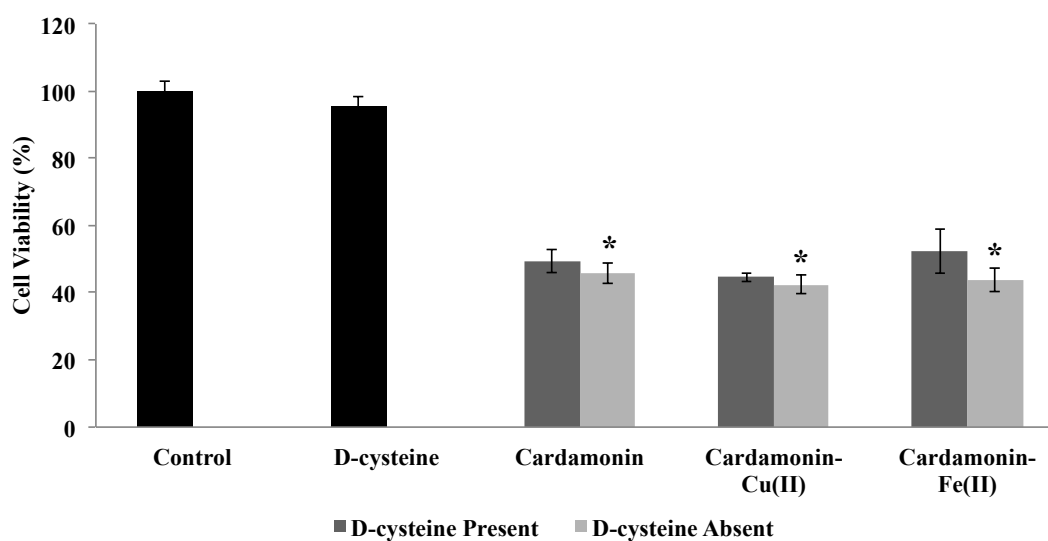


Figure 6.5 Effects of cardamonin, cardamonin-Cu(II) and cardamonin-Fe(II) complexes on cell viability in the presence or absence of D-cysteine in Jurkat T cells.

Jurkat T cells were treated with cardamonin, cardamonin-Cu(II) or cardamonin-Fe(II) complexes in the presence or absence of D-cysteine for 24 hrs and cell viability was assessed *via* the MTS assay as outlined in the Materials and Methods section. Results are means \pm SEM of three independent experiments. *indicates significant decrease ($p < 0.05$) from control.

6.2.6 Effects of cardamonin, cardamonin-Cu(II) and cardamonin-Fe(II) complexes on cell viability in the presence of GSH in Jurkat T cells

Since previous results suggested that GSH played an important role in the cardamonin and cardamonin-Fe(II)-mediated cell death, the effect of exogenously added GSH on treated Jurkat T cells were assessed next. As shown in **Figure 6.6**, in the presence of exogenous GSH, cardamonin and cardamonin-Fe(II)-treated Jurkat T cells' viability were significantly restored by 46.89% and 52.68% respectively compared to treatment alone in the absence of exogenous GSH. On the contrary, similar to NAC (**Figure. 6.1**) and L-cysteine (**Figure. 6.4**), the presence of exogenous GSH was not able to restore cell death mediated by cardamonin-Cu(II) complex. These data strongly suggest that cell death mediated by cardamonin-Cu(II) was not associated with the intracellular GSH levels of Jurkat T cells. The presence of exogenous GSH alone at 5 mM was confirmed to not affect Jurkat T cell viability compared to the control as depicted below. As cardamonin, cardamonin-Cu(II) and cardamonin-Fe(II) complexes were shown to increase intracellular ROS levels (**Figure. 6.2**), we next examine the effects of a free radical scavenger, Trolox, on the cell viability of treated Jurkat T cells.

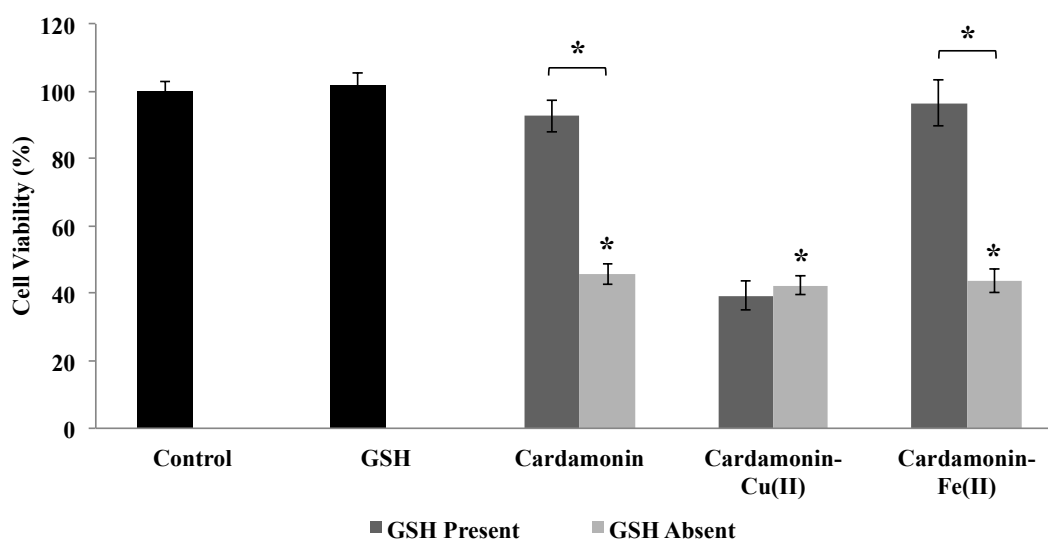


Figure 6.6 Effects of cardamonin, cardamonin-Cu(II) and cardamonin-Fe(II) complexes on cell viability in the presence or absence of GSH in Jurkat T cells.

Jurkat T cells were treated with cardamonin, cardamonin-Cu(II) or cardamonin-Fe(II) complexes in the presence or absence of GSH for 24 hrs and cell viability was assessed *via* the MTS assay as outlined in the Materials and Methods section. Results are means \pm SEM of three independent experiments. *indicates significant decrease ($p < 0.05$) from control; *above bracket indicates significant different ($p < 0.05$) from the respective compound treatment alone.

6.2.7 Effects of cardamonin, cardamonin-Cu(II) and cardamonin-Fe(II) complexes on cell viability in the presence of Trolox in Jurkat T cells

In an effort to determine if the intracellular ROS levels had an effect on the cell viability of cardamonin, cardamonin-Cu(II) and cardamonin-Fe(II) complexes-treated Jurkat T cells, Trolox, a water soluble derivative of Vitamin E, was added to remove generated intracellular ROS (Forrest et al. 1994, Castro et al. 2006). As illustrated in **Figure 6.7**, Trolox was indeed able to significantly increase cell viability of cardamonin, cardamonin-Cu(II) and cardamonin-Fe(II)-induced Jurkat cell death by 34.86%, 45.24% and 32.19% respectively compared to treatment in the absence of Trolox. The presence of Trolox alone at 1 mM was confirmed to not affect Jurkat T cell viability compared to the control as depicted below. Taken together, these results indicate that besides depleting GSH in Jurkat T cells, cardamonin and cardamonin-Fe(II) complex also induced oxidative stress through generation of ROS leading to cell death. Cardamonin-Cu(II) complex on the other hand mediated oxidative stress in Jurkat T cell death *via* the generation of ROS but did not alter the levels of GSH in the treated cells.

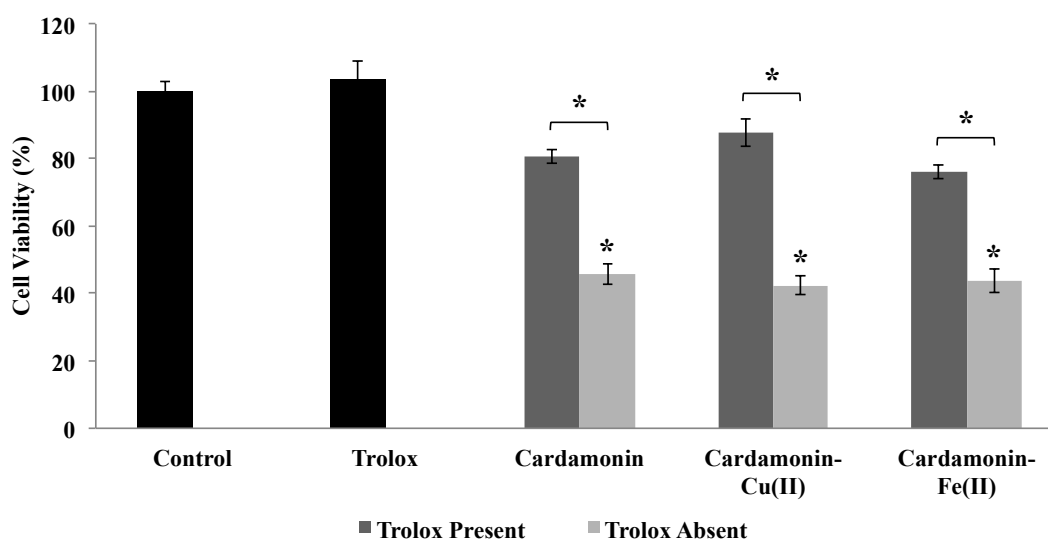


Figure 6.7 Effects of cardamonin, cardamonin-Cu(II) and cardamonin-Fe(II) complexes on cell viability in the presence or absence of Trolox in Jurkat T cells.

Jurkat T cells were treated with cardamonin, cardamonin-Cu(II) or cardamonin-Fe(II) complexes in the presence or absence of Trolox for 24 hrs and cell viability was assessed *via* the MTS assay as outlined in the Materials and Methods section. Results are means \pm SEM of three independent experiments. *indicates significant decrease ($p < 0.05$) from control; *above bracket indicates significant different ($p < 0.05$) from the respective compound treatment alone.

6.2.8 Effects of cardamonin, cardamonin-Cu(II) and cardamonin-Fe(II) complexes on intracellular ROS levels in the presence of Z-VAD-FMK in Jurkat T cells

As the caspase inhibitor, Z-VAD-FMK, has been shown in **Figure 5.1** to recover cell viability of cardamonin, cardamonin-Cu(II) and cardamonin-Fe(II)-treated Jurkat T cells, we examined whether oxidative stress is alleviated by measuring the intracellular ROS levels of cells in the presence of Z-VAD-FMK. As demonstrated in **Figure 6.8**, in the presence of the pan caspase inhibitor, the intracellular ROS levels dropped significantly compared to the respective treatment alone in Jurkat T cells. The intracellular ROS levels of cardamonin, cardamonin-Cu(II) and cardamonin-Fe(II) decreased by approximately half in the presence of Z-VAD-FMK. The presence of Z-VAD-FMK alone at 100 μ M has no effect on Jurkat T cell intracellular ROS levels compared to the control as depicted below. Taken together, these data confirmed that the caspase-dependent apoptotic cell death was mediated by oxidative stress specifically by induction of ROS by cardamonin, cardamonin-Cu(II) and cardamonin-Fe(II). We next examined whether intracellular GSH levels were altered in treated Jurkat T cells in the presence of Z-VAD-FMK under similar conditions.

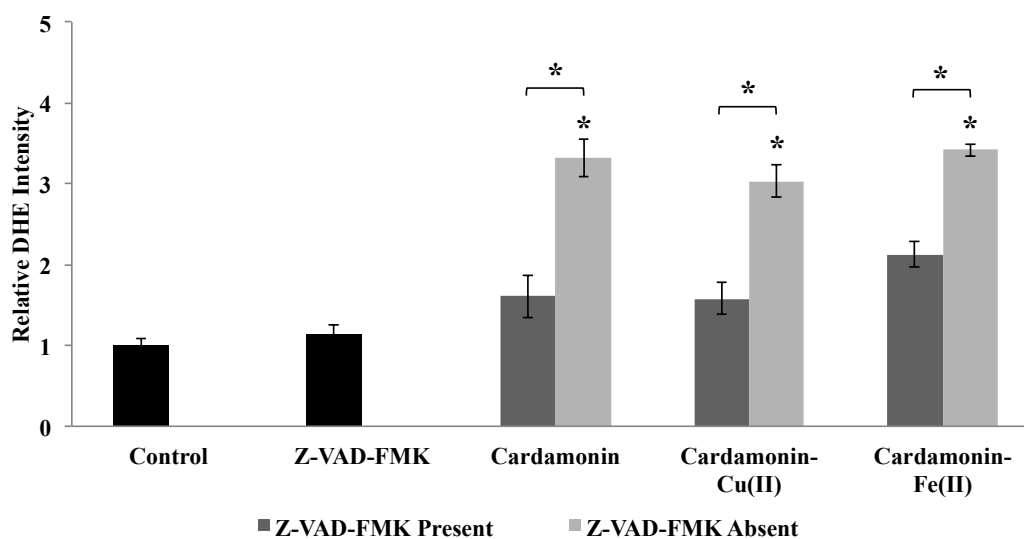


Figure 6.8 Effects of cardamonin, cardamonin-Cu(II) and cardamonin-Fe(II) complexes on intracellular ROS levels in the presence or absence of Z-VAD-FMK in Jurkat T cells.

Jurkat T cells were treated with cardamonin, cardamonin-Cu(II) or cardamonin-Fe(II) complexes in the presence or absence of Z-VAD-FMK for 24 hrs and the intracellular ROS levels were measured using the DHE probe as outlined in the Materials and Methods section. Results are means \pm SEM of three independent experiments. *indicates significant increase ($p < 0.05$) from control; *above bracket indicates significant different ($p < 0.05$) from the respective compound treatment alone.

6.2.9 Effects of cardamonin, cardamonin-Cu(II) and cardamonin-Fe(II) complexes on intracellular GSH levels in the presence of Z-VAD-FMK in Jurkat T cells

Since the depletion of GSH has been reported to be critical for apoptotic enzymes activation and an early hallmark observed in apoptosis (Franco et al. 2007, Franco and Cidlowski 2009), we examine if Z-VAD-FMK in treated Jurkat T cells were able to recover the intracellular GSH levels. As seen in **Figure 6.9**, Z-VAD-FMK had little effect on the GSH levels in cardamonin-Cu(II)-treated Jurkat T cells compared to the respective treatment alone. This finding corresponded to the results illustrated in **Figure 6.3** where cardamonin-Cu(II) had no effect on intracellular GSH levels further confirming the apoptotic cell death induced by the compound was not associated with the GSH levels. However, in the presence of Z-VAD-FMK, the cardamonin and cardamonin-Fe(II)-treated cells exhibited significant increase in intracellular GSH levels compared to cells with treatment alone. Collectively, these results confirmed that the caspase-dependent apoptotic cell death induced by cardamonin and cardamonin-Fe(II) also mediate oxidative stress *via* depletion of intracellular GSH levels.

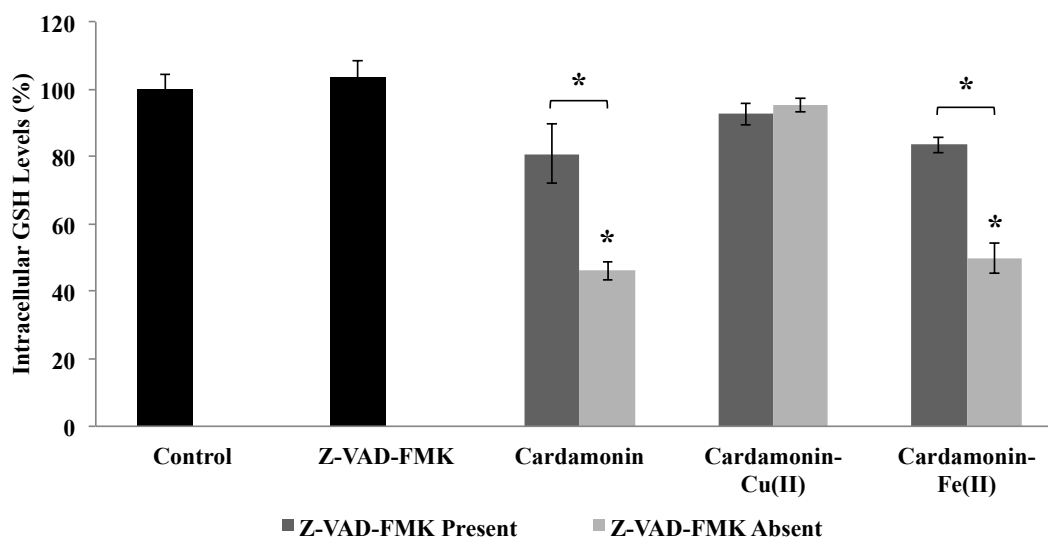


Figure 6.9 Effects of cardamonin, cardamonin-Cu(II) and cardamonin-Fe(II) complexes on intracellular GSH levels in the presence or absence of Z-VAD-FMK in Jurkat T cells.

Jurkat T cells were treated with cardamonin, cardamonin-Cu(II) or cardamonin-Fe(II) complexes in the presence or absence of Z-VAD-FMK for 24 hrs and the intracellular GSH levels were measured using the fluorescent dye MCB as outlined in the Materials and Methods section. Results are means \pm SEM of three independent experiments. *indicates significant decrease ($p < 0.05$) from control; *above bracket indicates significant different ($p < 0.05$) from the respective compound treatment alone.

6.3 Discussion

In the previous chapter, cardamonin, cardamonin-Cu(II) and cardamonin-Fe(II) have been shown to induce apoptotic cell death in Jurkat T cells. Accumulating evidences suggest that cardamonin is involved in oxidative stress (Mohamad et al. 2004, Li et al. 2008, Aderogba et al. 2012) with various studies reporting cardamonin having anti-oxidant (Ahmad et al. 2006, Simirgiotis et al. 2008) as well as a pro-oxidant (Yadav et al. 2012) properties. Our results demonstrated that cardamonin and both its complexes, cardamonin-Cu(II) and cardamonin-Fe(II), induced Jurkat T cell death that was mediated by oxidative stress. Specifically, cardamonin and cardamonin-Fe(II) treatment led to depletion of intracellular GSH levels and increase in intracellular ROS. The cytotoxic action of cardamonin and cardamonin-Fe(II) were readily abolished by low molecular weight thiols added exogenously including NAC, L-cysteine and GSH. These findings suggested GSH as the rate-limiting thiol required for Jurkat T cell viability since NAC and L-cysteine are both precursors of GSH biosynthesis. This proposed theory was further corroborated when studies revealed that D-cysteine, the low molecular weight thiol that cannot be metabolised to GSH, was unable to restore Jurkat T cell viability in the presence of cardamonin and cardamonin-Fe(II) complex. As the previous chapter has shown that 100 μ M Z-VAD-FMK was able to restore cell death of Jurkat T cells in the presence of cardamonin and cardamonin-Fe(II), the ability of Z-VAD-FMK to alter intracellular GSH and ROS levels further suggest that oxidative stress potentially mediated the apoptotic cell death of cardamonin and cardamonin-Fe(II)-treated Jurkat T cells. These findings corresponded with multiple studies reporting the importance of GSH as a regulator for T cells suggesting a direct relationship between T cells viability and intracellular GSH

availability (Zmuda and Friedenson 1983, Hamilos and Wedner 1985, Gmünder and Dröge 1991, Kohno et al. 1996, Iwata et al. 1997, Chang et al. 2002). Studies have also shown the depletion of intracellular GSH leads to accumulation of high ROS levels (Zucker et al. 1997, Armstrong et al. 2002). As previous studies have reported the ability of peptidyl methylketones to alter the intracellular GSH levels (Angliker et al. 1987, Rajah and Chow 2014), we confirmed in this study that Z-VAD-FMK did not have an effect on cell viability, intracellular GSH and ROS levels at the tested concentration of 100 μ M in Jurkat T cells.

Interestingly, in this chapter, we first observed a notable difference in the mechanism of action between the complex cardamonin-Cu(II) and the parent compound cardamonin. Studies carried out in previous chapters have demonstrated the biological activity of cardamonin-Cu(II) to be similar to the parent compound. However, in determining the oxidative stress involvement of these compounds, cardamonin-Cu(II) was found to have no effect on the intracellular GSH levels, which was different from cardamonin and cardamonin-Fe(II) where both compounds significantly depleted the intracellular GSH levels in Jurkat T cells. The findings that exogenous NAC, L-cysteine and GSH were not able to restore the cell viability as well as the unaffected intracellular GSH levels highly suggest that the cardamonin-Cu(II)-induced cytotoxicity was not GSH dependent.

On the other hand, cardamonin-Cu(II) was found to induce oxidative stress in Jurkat T cells *via* the induction of ROS as demonstrated by the significant increase of intracellular ROS levels and the ability of the ROS scavenger, Trolox, to significantly improve cell viability of cardamonin-Cu(II) treated cells. Similar to cardamonin and

cardamonin-Fe(II) complex, 100 μ M Z-VAD-FMK was able to attenuate cell death of cardamonin-Cu(II)-treated Jurkat T cells as shown in the previous chapter. Hence, the ability of Z-VAD-FMK to reduce intracellular ROS levels in the presence of cardamonin-Cu(II) further suggested that oxidative stress possibly mediated the apoptotic cell death of cardamonin-Cu(II)-treated Jurkat T cells *via* generation of ROS.

In spite of its initially recognised anti-oxidant property, cardamonin has been found to be able to work as a pro-oxidant. The ability of cardamonin to induce oxidative stress was recently reported by Yadav et al. (2012) where cardamonin was found to sensitise tumour cells to TRAIL and generate ROS in a dose dependent manner in HCT 116 human colon carcinoma cell line. Pre-treatment of HCT 116 with NAC was reported to reduce the death receptor 4 and 5 expression and reversed the effect of caspase-3, -8 and PARP cleavage by TRAIL-induced cardamonin. Contrary to the findings in this study, cardamonin has also been more often reported to act as an anti-oxidant agent with the ability to inhibit generation of intracellular ROS in RAW 264.7 macrophage cell line (Ahmad et al. 2006), display anti-radical DPPH activity and ferric reducing anti-oxidant in SW-480 human colon carcinoma cells (Simirgiotis et al. 2008). There have also been other studies carried out to determine the anti-oxidant activity of cardamonin but reported its inactivity in scavenging free radicals and $O_2^{\cdot-}$ (Mohamad et al. 2004, Li et al. 2008, Aderogba et al. 2012).

The differences in the mechanism of action suggest the presence of relationship between structure and oxidative stress activity. Previous studies have shown curcumin, another chalcone often used as cardamonin's reference compound,

mediated apoptosis through modulation of the redox status of the cells *via* pro-oxidant and anti-oxidant mechanisms (Piwocka et al. 2001, Syng-Ai et al. 2004, Yoshino et al. 2004, Chan et al. 2005, McNally et al. 2007, Sandur et al. 2007). Pathway studies performed on Jurkat T cells using curcumin showing pro-oxidant activity reported the increase of intracellular ROS production following 60 mins of treatment with 10 μ M curcumin and pre-treatment with NAC drastically lowered ROS production (Gopal et al. 2014). Similar to cardamonin, curcumin was found to deplete GSH levels, increased caspase-3 and -9 activity, and cleavage of PARP in Jurkat cells with minimal effect on normal peripheral blood mononuclear cells. In another study, low doses of curcumin were reported to protect hepatocytes by reducing cytochrome c release and lipid peroxidation while higher curcumin concentrations led to GSH depletion and caspase-3 activation (Ghoneim 2009) suggesting the different concentration of cardamonin may lead to different implications on oxidative stress. In a recent study, the researchers reported an interesting finding on curcumin's cytotoxicity and its induction of oxidative stress (Zheng et al. 2012). Contrary to the findings in the present study where the cytotoxicity of cardamonin, cardamonin-Cu(II) and cardamonin-Fe(II) were attenuated in the presence of Trolox in Jurkat T cells, Trolox was found to enhance curcumin's cytotoxicity by further increasing the generation of ROS in A2780 human ovarian carcinoma cell line (Zheng et al. 2012). Curcumin's enhanced cytotoxicity was not limited to addition of Trolox but also in the presence of vitamin E and vitamin C as well as in other cancer cell lines including MCF-7 and MDA-MB-231 human breast adenocarcinoma cell lines. These interesting findings highlight the possibility of cardamonin to induce different mechanisms of action in other cell lines.

Curcumin has also been reported to induce heme oxygenase 1 (HO-1), a stress-response protein, through generation of ROS in human hepatoma cells where pre-treatment with NAC, vitamin E and catalase attenuated HO-1 induction by curcumin (McNally et al. 2007). Accumulating evidence demonstrated that external inducers such as heavy metals could induce HO-1 suggesting cardamonin and its metal complexes could possibly induce oxidative stress in a similar pathway. Furthermore, similar to cardamonin, curcumin treatment has been extensively reported to induce apoptosis through mitochondria-dependent pathway (Bhaumik et al. 1999, Morin et al. 2001, Pan et al. 2001). Previous studies have reported the relationship of ROS and the disruption of mitochondrial potential where excessive oxidative stress and ROS reaching threshold levels triggered opening of mitochondrial channels that led to collapse of the MMP and transient increase of ROS by the electron transfer chain (Zorov et al. 2006). This finding is in good agreement with the current study where cardamonin, cardamonin-Cu(II) and cardamonin-Fe(II) significantly increased intracellular ROS levels and studies in Chapter 5 establish the significant drop in MMP of treated Jurkat T cells.

Taken together, both cardamonin metal complexes, cardamonin-Cu(II) and cardamonin-Fe(II) demonstrated greater cytotoxicity in a dose-dependent manner against Jurkat T cells as shown in Chapter 5. Although there was a difference in Jurkat T cell susceptibility threshold against these compounds, all three compounds induced similar apoptotic pathway as discussed in the previous chapter. However, the mode of action of cardamonin-Cu(II) differed from both cardamonin and cardamonin-Fe(II) complex in mediating oxidative stress where cardamonin and cardamonin-Fe(II) depleted intracellular GSH and increased ROS, while cardamonin-Cu(II)

generated ROS without affecting intracellular GSH levels of Jurkat T cells. A recent study carried out to compare the pulmonary cytotoxicity of metal oxide nanoparticles, which include silicon oxide, ferric oxide and copper oxide nanoparticles against Hep-2 human epithelial type 2 cells found copper oxide induced the greatest cytotoxicity (Fahmy and Cormier 2009). Moreover, the study found that copper oxide was even able to overwhelm anti-oxidant defences like glutathione reductase and catalase as well as increase levels of 8-isoprostane, an oxidative stress marker and lipid peroxidation (Morrow and Roberts 1997, Fahmy and Cormier 2009, Anastopoulos et al. 2016), by 1000%. This study supports the findings in the present study indicating there is a great degree of variability in cytotoxic effect depending on the type of transition metals present. Fahmy and Cormier (2009) suggested that this observed variation was not due to the transition metals solubility as previously postulated but instead was possibly due to redox cycling. Examples of redox cycling compounds include quinones and bleomycin that induce apoptosis by increasing intracellular concentration of ROS (Dypbukt et al. 1994, Hamilton et al. 1995). Stohs and Bagchi (1995) reviewed the oxidative mechanisms of transition metal ions in regards to ROS production and oxidative tissue damage. The authors highlighted the ability of metal ions including copper and iron to undergo redox cycling leading to production of ROS such as H_2O_2 , hydroxyl radical and superoxide ion as well as the participation in Fenton-type reaction. Cardamonin-Cu(II) was found most cytotoxic in this study and exhibited a different mode of action in mediating oxidative stress. As the reduction potential of copper (+0.337V, Cu^{2+}/Cu) is higher than that of iron (-0.44V, Fe^{2+}/Fe), this difference could possibly account for the greater cytotoxicity induced by cardamonin-Cu(II). In general, copper ions cytotoxic effects have been extensively studied (Zhai et al. 2000, Gaetkea and Chow 2003, Qiao et al. 2011, Sarkar et al.

2011) and previous studies proposed copper ions induce cytotoxicity *via* DNA binding resulting in DNA damage and cell death (Aruoma et al. 1991). Another study reported the ability of copper ions to cause apoptotic cell death in neuronal cells by directly altering apoptotic genes expression (Chan et al. 2008). Furthermore, in the presence of Cu(II), curcumin has been reported to cause DNA strand scission, which was mediated by ROS (Ahsan and Hadi 1998). Other anti-oxidants have also demonstrated the ability to generate ROS in the presence of transition metals like copper and iron ions, consistent with the findings in the current study. For instance, plant-derived anti-oxidants were capable of causing DNA strand breakage in the presence of transition metal ions including flavonoids (Rahman et al. 1989, Said et al. 1992) and tannic acid (Bhat and Hadi 1994). Vitamin C (ascorbic acid) and uric acid, otherwise an anti-oxidant, acted as a pro-oxidant in the presence of iron ions (Herbert 1990) and cleaved DNA in the presence of copper ions (Shamsi and Hadi 1995) respectively.

Generally, understanding the relationship between the onset of oxidative stress and the cellular response will be useful in understanding and elucidating the mode of action by which cardamonin and its metal complexes generate intracellular ROS and deplete GSH levels. The exact mechanism of how ROS was generated in cardamonin, cardamonin-Cu(II) and cardamonin-Fe(II)-treated cells but only cardamonin and cardamonin-Fe(II) treated cells depleted GSH levels, remains unclear. It is possible that different metal complexes have the ability to generate diverse radicals in Jurkat T cells leading to different oxidative potency. Overall, this study highlights the chemical composition of cardamonin and its metal complexes pose a great influence on the biological response of exposed cells and should be further investigated.

CHAPTER 7: CONCLUSION AND FUTURE WORK

7.1 General discussion and conclusion

The effectiveness of cancer treatment with chemotherapeutic agents is based primarily on their ability to induce apoptotic cell death. The large number of articles published yearly on cardamonin by various researchers reflects the growing interest towards the subject. It is well established that cardamonin possesses diverse biological activities that encompass anti-inflammatory, anti-microbial, anti-oxidant, oxidative properties, anti-neoplastic, vasorelaxant, hypoglycaemic, anti-fungal as well as anti-cancer properties (Gonçalves et al. 2014). The development of natural product derivatives remains an important goal in enhancing the bioactivity of a compound. In this study, our interest has been directed to the cytotoxicity of novel semi-synthesised cardamonin derivatives and elucidating the mode of action of the two most active compounds in comparison to the parent compound, cardamonin. From a total of 20 derivatives, the cardamonin-Cu(II) complex and cardamonin-Fe(II) complex emerged as valuable hit compounds exhibiting cytotoxicity 5-times and 2-times more cytotoxic than cardamonin in Jurkat T cells. This trend was observed across all cell lines tested including nasopharyngeal HK1 and lung A549 cancer cell lines where these two novel complexes appeared more cytotoxic than the parent compound. Since cardamonin-Cu(II) and cardamonin-Fe(II) were the two most cytotoxic in the different cell lines tested, both compounds possibly act on different targets or generate different effects upon binding to a specific background/ receptor compared to the parent compound, cardamonin. Due to scarcity of knowledge about their target(s) and interactions, a precise structure activity relationship is not deduced at this point. However, it is certain that the cytotoxicity of diverse cardamonin derivatives was affected by a range of factors, which include the modification of hydroxyl group,

presence of alkene group and addition of chemical groups, with the greatest cytotoxicity advantage being complexing with metal ions. Subsequent cytotoxicity studies found that Jurkat T cells were most susceptible towards cardamonin, cardamonin-Cu(II) and cardamonin-Fe(II), which prompted us to further investigate the possible correlation between adherent/ suspension cells and the observed differential susceptibility.

Previous studies have reported that suspension cells are slightly more susceptible to inhibition of cell growth compared to adherent cells (Kimura et al. 2004, Daigneault et al. 2010), possibly due to the increase of some survival signals in adherent cells compared to suspension cells (Kohro et al. 2004). In this study, THP-1 cell lines were used as our experimental model to assess this theory as it can be cultured in both suspension and adherent phase making the susceptibility studies more relatable and comparable considering these cells were derived from the same tissue origin. Indeed our results revealed cardamonin, cardamonin-Cu(II) and cardamonin-Fe(II) complexes became less cytotoxic following THP-1-derived macrophages *via* PMA stimulation compared to the monocytes counterpart suggesting activation of some survival signals. To further assess our hypothesis that this change in susceptibility involved activation of a survival signal, namely MAP kinase known to be activated in PMA-stimulated cells (Huang et al. 2008), the effects of interference from inhibitors of p38 α and p38 β MAP kinase (Figure of the p38 and SB202190 structure) on THP-1-derived macrophages were explored. Although results showed that the inhibition of p38 MAP kinase did not alter the cell susceptibility towards cardamonin and its complexes in THP-1-derived macrophages, the involvement of the MAP kinase pathway particularly in human acute myeloid leukaemia is definite and

activation of other MAP kinases should be explored including ERK and JNK protein kinases.

Subsequent studies were carried out to explore the cytotoxicity of cardamonin and its metal complexes and its underlying mechanism of action using Jurkat T cells as IC₅₀ values were reported lowest in this cell line. We found that even though both complexes, cardamonin-Cu(II) and cardamonin-Fe(II) were more cytotoxic compared to cardamonin, the mode of inducing apoptotic cell death were similar. Collectively, our results showed that cardamonin, cardamonin-Cu(II) and cardamonin-Fe(II) induced apoptotic cell death that was caspase-dependent and the presence of the caspase-inhibitor Z-VAD-FMK was able to inhibit caspase processing and block cell death in Jurkat T cells. Cardamonin and both its complexes induced Jurkat T cell morphological changes such as cell shrinkage, DNA/ chromatic condensation, nuclear fragmentation, plasma membrane blebbing and formation of apoptotic bodies, all of which were typical of apoptosis. There were no enlargement/ swelling of cells observed morphologically, which further confirms cell death was apoptotic rather than necrotic. Furthermore, the exposure of PS and collapse of the MMP indicate that both these compounds could be promising anti-cancer agents as inducers of apoptotic cell death. As the Z-VAD-FMK caspase inhibitor was able to block cell death induced by cardamonin and its two complexes, caspase activation was analysed in the presence or absence of Z-VAD-FMK. All three compounds activated caspase-9 and caspase-3 as well as PARP-1, a caspase-3 substrate, which was cleaved from p116 to the signature p85 fragment. Modification of this protein is known to occur in response to DNA damage. Caspase-8 however was not activated suggesting cardamonin and its two complexes induced apoptosis *via* the intrinsic mitochondrial pathway. In the

presence of Z-VAD-FMK, the processing of caspase-3, -9 and the cleavage of PARP-1 by cardamonin and its complexes was completely abrogated confirming this cell death pathway is indeed a caspase-dependent process.

As previous studies have reported the ability of metals to induce apoptosis through oxidative stress, in the final chapter of this study, we investigated the effects of cardamonin, cardamonin-Cu(II) and cardamonin-Fe(II) on Jurkat T cells' oxidative state. Results revealed oxidative stress caused by the depletion of intracellular GSH and production of ROS was involved in cardamonin and cardamonin-Fe(II)-induced Jurkat T cell death. Cardamonin-Cu(II) however did not significantly affect intracellular GSH levels but generated the production of ROS. The presence of NAC, L-cysteine and GSH was able to significantly increase cell viability of cardamonin and cardamonin-Fe(II)-induced Jurkat T cell death but had no significant effect on cardamonin-Cu(II)-treated cells. Trolox, the ROS scavenger, was the only antioxidant to significantly improve cell viability of cardamonin-Cu(II) treated cells suggesting cardamonin-Cu(II)-induced cytotoxicity *via* generation of ROS. Interestingly, in the presence of Z-VAD-FMK the intracellular GSH and ROS levels significantly increased and decreased, respectively from the cells with cardamonin- and cardamonin-Fe(II)-treatment alone. The ROS levels significantly decreased in cardamonin-Cu(II)-treated Jurkat T cells in the presence of Z-VAD-FMK. These findings further suggest that oxidative stress potentially mediated the apoptotic cell death of cardamonin, cardamonin-Cu(II) and cardamonin-Fe(II)-treated Jurkat T cells. It is important to note that this is the first notable difference observed in the mechanism of action between complex cardamonin-Cu(II) and parent compound, cardamonin. This difference in bioactivity is further substantiated as copper ions are

known to undergo redox cycling that leads to production of ROS and studies have reported the ability of copper oxide to induce great cytotoxicity and overwhelm antioxidant defences like glutathione reductase and catalase (Morrow and Roberts 1997, Fahmy and Cormier 2009, Anastopoulos et al. 2016, Deo et al. 2016). Hence, this study truly highlights the degree of variability in cytotoxicity and the extent of cytotoxicity depending on the type of transition metal that is complexed to the lead compound. It is possible that different metal complexes have the ability to generate diverse radicals in Jurkat T cells leading to the observed different oxidative potency seen in this study. Overall, oxidative stress analysis suggested that ROS played a more vital role in cardamonin-Cu(II)-induced cytotoxicity in Jurkat T cells compared to GSH. As these free radicals are known to be typically generated from the mitochondria, cardamonin and its complexes are proposed to target the mitochondria pathway mediated by oxidative stress *via* production of ROS, subsequently triggering the intrinsic mitochondrial apoptotic pathway as summarised in **Figure 7.1**. Taken together, these findings highlight the potential of cardamonin-Cu(II) and cardamonin-Fe(II) complexes as promising candidates of novel cardamonin-based derivatives for the development of anti-tumour therapies, particularly for targeting leukaemia.

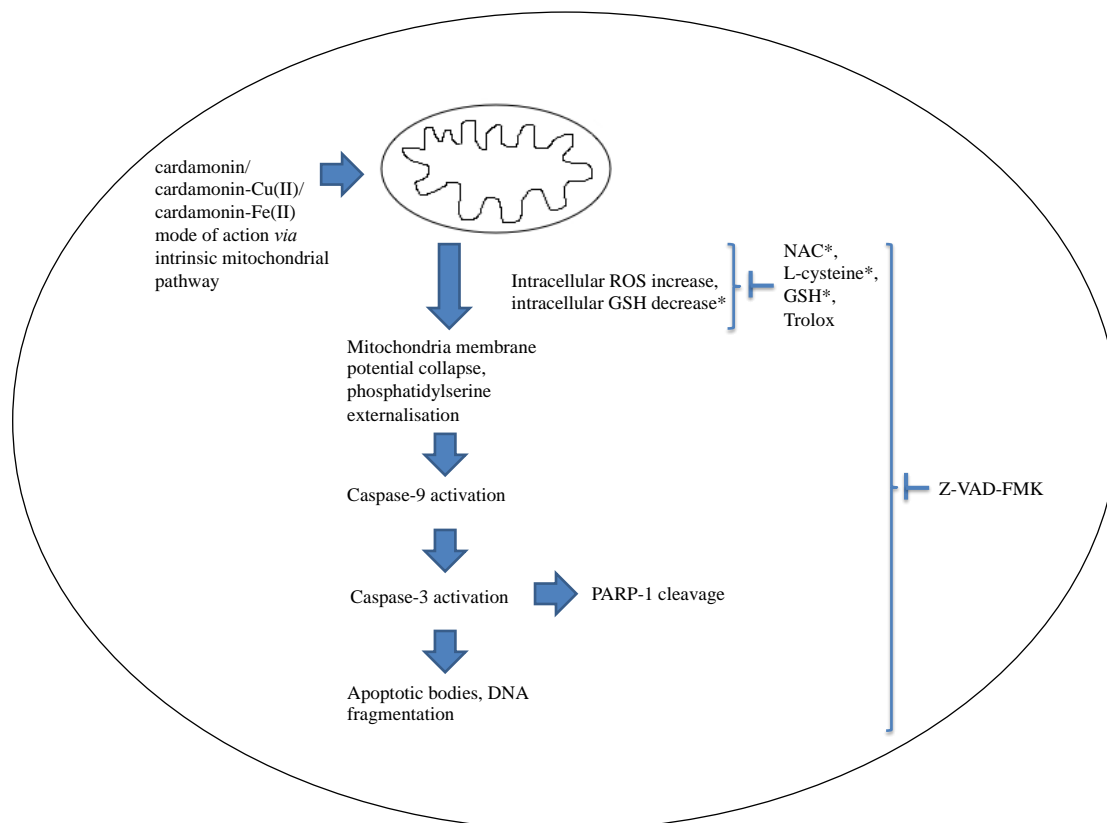


Figure 7.1 Proposed model of cardamonin-, cardamonin-Cu(II) and cardamonin-Fe(II)-induced apoptosis in Jurkat T cells.

Cardamonin, cardamonin-Cu(II) and cardamonin-Fe(II) is proposed to target the cell mitochondria leading to generation of intracellular ROS and the depletion of intracellular GSH (only observed in cardamonin and cardamonin-Fe(II)-treated Jurkat T cells). Subsequently, the mitochondria mediated intrinsic apoptotic pathway elicit the collapse of mitochondria membrane potential and externalisation of phosphatidylserine with caspase-9 activation that is followed by activation of downstream executioner caspase-3 and cleavage of PARP-1, the downstream substrate of caspase-3. DNA condensation and fragmentation into apoptotic bodies were observed morphologically. The caspase inhibitor, Z-VAD-FMK, readily blocks this caspase-dependent apoptotic pathway. Intracellular ROS and GSH levels were recovered close to levels of untreated Jurkat T cells in the presence of Z-VAD-FMK. Furthermore, anti-oxidants NAC, L-cysteine, GSH and Trolox significantly increased cell viability in cardamonin and cardamonin-Fe(II)-treated cells whereas the radical scavenger, Trolox, was the only anti-oxidant capable of increasing cell viability in cardamonin-Cu(II)-treated cells. This study demonstrates cardamonin and its metal complexes, cardamonin-Cu(II) and cardamonin-Fe(II), induced apoptotic cell death in Jurkat T cells *via* an oxidative stress mediated caspase-dependent pathway. *indicates no effect in cardamonin-Cu(II)-treated Jurkat T cells.

7.2 Future work

Data presented in this study thus far suggest that cardamonin, cardamonin-Cu(II) and cardamonin-Fe(II) induced apoptosis in Jurkat T cells by generating intracellular ROS and depleting intracellular GSH levels (only in cardamonin and cardamonin-Fe(II)-treated cells). Following on from the work presented in Chapter 3, it would be interesting to study the effect of these three compounds on normal peripheral blood mononuclear cells. Determining the cytotoxicity of these compounds against normal peripheral blood cells is important for their potential use in treating blood related disorders. Furthermore, initial screening of cardamonin and its derivatives reveals complexing cardamonin with metal ions offer the greatest cytotoxicity advantage. Hence, future studies should focus on complexing cardamonin to other metal ions particularly transition metal intercalators like platinum, ruthenium, nickel and gold, which are highly biologically active with exceptional versatility (Deo et al. 2016). Additionally, an iodine-derived-metal complex should be semi-synthesised and assessed for cytotoxicity since iodination of cardamonin has been shown to improve the cytotoxic activity. In Chapter 4, inhibition of p38 MAP kinase did not alter cell susceptibility in treated THP-1-derived macrophages suggesting p38 α and p38 β MAP kinase may not be mainly responsible for the increase in cell resistance. Subsequent studies should determine the involvement of other MAP kinase pathway such as ERK and JNK protein kinase activation. Determining the protein kinase involved is important in elucidating the mode of action observed from increased resistance in matured macrophages compared to monocytes. This chapter also highlighted the novel use of cardamonin and its complexes as potential anti-leukemia agent that was more effective against immature leukaemic cells than mature cells. Therefore, apart

from Jurkat T leukaemic lymphoblast cell, other leukaemic cell lines should be tested against cardamonin, cardamonin-Cu(II) and cardamonin-Fe(II) such as HL60 promyelocytic leukaemia and K562 chronic myelogenous leukaemia cell line. In an effort to elucidate the mechanism of cytotoxicity exerted by cardamonin and its complexes, we established that these compounds induced apoptosis in Jurkat T cells *via* the intrinsic mitochondrial pathway activating caspase-9 and -3. Additional studies into cell cycle analysis to determine the stages of cell cycle arrest (G0/G1, G1, S and G2/M) induced by these compounds are desirable. Furthermore, apoptotic mitochondrial events are known to occur through B cell lymphoma-2 (BCL-2) family of proteins, which govern mitochondrial membrane permeability (Cory and Adams 2002). Based on current findings, cardamonin and its complexes activate the mitochondria pathway to induce apoptosis, substantiating the need for further investigations on the regulation of BCL-2 proteins such as pro-apoptotic proteins (BCL-10, BAX, BAK, BID, BAD, BIM, BIK, and BLK) and anti-apoptotic proteins (BCL-2, BCL-X, BCL-XL, BCL-XS, BCL-W, BAG) (Elmore 2007, Roy et al. 2014). Since cardamonin and both its complexes were found to induce oxidative stress in Jurkat T cells, future studies can also include an investigation on detecting the different species of ROS generated including effect on the mitochondrial transport chain to further elucidate how these compounds generate ROS in these cells. Additionally, studies can be carried out in cell-free systems to detect the possible anti-oxidant/ pro-oxidant capacity of cardamonin, cardamonin-Cu(II) and cardamonin-Fe(II). Ultimately, these accompanying studies are suggested to further our understanding in the roles of oxidative stress-mediated apoptosis, which may be beneficial for future development of these compounds as potential anti-cancer agents.

REFERENCES

- Aderogba, M., Kgatle, D., McGaw, L., and Eloff, J., 2012. Isolation of antioxidant constituents from *Combretum apiculatum* subsp. *apiculatum*. *South African Journal of Botany*, 79, 125–131.
- Ahmad, S., Israf, D., Lajis, N., Shaari, K., Mohamed, H., Wahab, A., Ariffin, K., Hoo, W., Aziz, N., Kadir, A., Sulaiman, M., and Somchit, M., 2006. Cardamonin, inhibits pro-inflammatory mediators in activated RAW 264.7 cells and whole blood. *European Journal of Pharmacology*, 538 (1–3), 188–194.
- Ahsan, H. and Hadi, S., 1998. Strand scission in DNA induced by curcumin in the presence of Cu(II). *Cancer Letters*, 124 (1), 23–30.
- Anestopoulos, I., Voulgaridou, G. P., Moraitis, N., Christopoulou, M., Nikita, K., Koulouridis, S., Mpakogianni, S., Panayiotidis, M., and Pappa, A., 2016. Comparative study of oxidative stress biomarkers to evaluate cellular response of Jurkat T-cells exposed to 1966 MHz electromagnetic fields. *Journal of International Society of Antioxidants in Nutrition & Health*, 1 (1), ISSN 2495-9405.
- Angliker, H., Wikstrom, P., Rauber, P., and Shaw, E., 1987. The synthesis of lysylfluoromethanes and their properties as inhibitors of trypsin, plasmin and cathepsin B. *Biochemical Journal*, 241 (3), 871–875.
- Arana-Argáez, V., Delgado-Rizo, V., Pizano-Martínez, O., Martínez-García, E., Martín-Márquez, B., Muñoz-Gómez, A., Petri, M., Armendáriz-Borunda, J., Espinosa-Ramírez, G., Zúñiga-Tamayo, D., Herrera-Esparza, R., and Vázquez-Del Mercado, M., 2010. Inhibitors of MAPK pathway ERK1/2 or p38 prevent the IL-1{beta}-induced up-regulation of SRP72 autoantigen in Jurkat cells. *Journal of Biological Chemistry*, 285 (43), 32824–32833.
- Armstrong, J., Steinauer, K., Hornung, B., Irish, J., Lecane, P., Birrell, G., Peehl, D., and Knox, S., 2002. Role of glutathione depletion and reactive oxygen species generation in apoptotic signaling in a human B lymphoma cell line. *Cell Death and Differentiation*, 9 (3), 252–263.
- Aruoma, O. I., Halliwell, B., Gajewski, E., and Dizdaroglu, M., 1991. Copper-ion-dependent damage to the bases in DNA in the presence of hydrogen peroxide. *Biochemical Journal*, 273 (3), 601–604.
- Auwerx, J., 1991. The human leukemia cell line, THP-1: a multifaceted model for the study of monocyte-macrophage differentiation. *Experientia*, 47 (1), 22–31.
- Basu, A., Castle, V., Bouziane, M., Bhalla, K., and Haldar, S., 2006. Crosstalk between Extrinsic and Intrinsic Cell Death Pathways in Pancreatic Cancer: Synergistic Action of Estrogen Metabolite and Ligands of Death Receptor Family. *Cancer Research*, 66 (8), 4309–4318.
- Batra, P. and Sharma, A., 2013. Anti-cancer potential of flavonoids: recent trends and future perspectives. *3 Biotech*, 3 (6), 439–459.
- Beecher, G., 2003. Overview of dietary flavonoids: nomenclature, occurrence and intake. *The Journal of Nutrition*, 133 (10), 3248S–3254S.
- Ben-Ze'ev, A., Farmer, S., and Penman, S., 1980. Protein synthesis requires cell-surface contact while nuclear events respond to cell shape in anchorage-dependent fibroblasts. *Cell*, 21 (2), 365–372.

- Bevers, E. and Williamson, P., 2010. Phospholipid scramblase: an update. *FEBS Letters*, 584 (13), 2724–2730.
- Bhat, R. and Hadi, S., 1994. DNA breakage by tannic acid and Cu(II): sequence specificity of the reaction and involvement of active oxygen species. *Mutation Research*, 313 (1), 39–48.
- Bhaumik, S., Anjum, R., Rangaraj, N., Pardhasaradhi, B., and Khar, A., 1999. Curcumin mediated apoptosis in AK-5 tumor cells involves the production of reactive oxygen intermediates. *FEBS Letters*, 456 (2), 311–314.
- Bheemasankara, R., Namosiva, R., and Suryaprakasam, S., 1976. Cardamonin and alpinetin from the seeds of *Amomum subulatum*. *Planta Medica*, 29, 391–392.
- Birben, E., Sahiner, U. M., Sackesen, C., Erzurum, S., and Kalayci, O., 2012. Oxidative Stress and Antioxidant Defense. *World Allergy Organisation*, 5 (1), 9–19.
- Boatright, K. and Salvesen, G., 2003. Mechanisms of caspase activation. *Current Opinion in Cell Biology*, 15 (6), 725–731.
- Bouchard, V., Rouleau, M., and Poirier, G., 2003. PARP-1, a determinant of cell survival in response to DNA damage. *Experimental Hematology*, 31 (6), 446–454.
- Boyle, P., Diehm, C., and Robertson, C., 2003. Meta-analysis of clinical trials of Cyclo 3 Fort in the treatment of chronic venous insufficiency. *International Angiology*, 22 (3), 250–262.
- Buss, E. and Ho, A., 2011. Leukemia stem cells. *International Journal of Cancer*, 129 (10), 2328–2336.
- Buttke, T. and Sandstrom, P., 1994. Oxidative stress as a mediator of apoptosis. *Immunology Today*, 15 (1), 7–10.
- Break, MKB., Hossan, MS., Khoo, Y., Qazzaz, ME., Al-Hayali, MZK., Chow, SC., Wiart, C., Bradshaw, TD., Collins, H., and Khoo, TJ., 2018. Discovery of a highly active anticancer analogue of cardamonin that acts as an inducer of caspase-dependent apoptosis and modulator of the mTOR pathway. *Fitoterapia*, 125, 161-173.
- Cai, H., Dikalov, S., Griendling, K., and Harrison, D., 2007. Detection of reactive oxygen species and nitric oxide in vascular cells and tissues: comparison of sensitivity and specificity. *Methods in molecular medicine*, 139 (293–311).
- Cárdenas, M., Marder, M., Blank, V., and Roguin, L., 2006. Antitumor activity of some natural flavonoids and synthetic derivatives on various human and murine cancer cell lines. *Bioorganic and Medicinal Chemistry*, 14 (9), 2966–2971.
- de Castro, C., Costa, P., Laktin, G., de Carvalho, P., Geraldo, R., De Moraes, J., Pinto, P., Couri, M., Pinto, P., and Da Silva Filho, A., 2015. Cardamonin, a schistosomicidal chalcone from *Piper aduncum* L. (Piperaceae) that inhibits *Schistosoma mansoni* ATP diphosphohydrolase. *Phytomedicine*, 22 (10), 921–928.

- Castro, I., Rogero, M., Junqueira, R., and Carrapeiro, M., 2006. Free radical scavenger and antioxidant capacity correlation of alpha-tocopherol and Trolox measured by three in vitro methodologies. *International Journal of Food Sciences and Nutrition*, 57 (1–2), 75–82.
- Chan, H., Liu, T., Verdile, G., Bishop, G., Haasl, R., Smith, M., Perry, G., Martins, R., and Atwood, C., 2008. Copper Induces Apoptosis of Neuroblastoma Cells Via Post-translational Regulation of the Expression of Bcl-2-family Proteins and the tx Mouse is a Better Model of Hepatic than Brain Cu Toxicity. *International Journal of Clinical and Experimental Medicine*, 1 (1), 76–88.
- Chan, W., Wu, H., and Hsuuw, Y., 2005. Curcumin inhibits ROS formation and apoptosis in methylglyoxal-treated human hepatoma G2 cells. *Annals of the New York Academy of Sciences*, 1042 (372–378).
- Chandra, J., Samali, A., and Orrenius, S., 2000. Triggering and modulation of apoptosis by oxidative stress. *Free Radical Biology & Medicine*, 29 (3–4), 323–333.
- Chang, H., Lin, H., Yi, L., Zhu, J., Zhou, Y., Mi, M., and Zhang, Q., 2010. 3,6-Dihydroxyflavone induces apoptosis in leukemia HL-60 cell via reactive oxygen species-mediated p38 MAPK/JNK pathway. *European Journal of Pharmacology*, 648 (1–3), 31–38.
- Chang, W., Yang, K., Chuang, H., Jan, J., and Shaio, M., 2002. Glutamine Protects Activated Human T Cells from Apoptosis by Up-Regulating Glutathione and Bcl-2 Levels. *Clinical Immunology*, 104 (2), 151–160.
- Chanput, W., Mess, J., and Wichers, H., 2014. THP-1 cell line: An in vitro cell model for immune modulation approach. *International Immunopharmacology*, 23 (1), 37–45.
- Chen, J. and Stubbe, J., 2005. Bleomycins: towards bettertherapeutics. *Nature Reviews Cancer*, 5, 102–112.
- Chen, L., 1988. Mitochondrial membrane potential in living cells. *Annual Review of Cell Biology*, 4, 155–181.
- Chen, S., Lin, J., Liang, Y., Pan, M., Liu, S., and Lin-Shiau, S., 2008. Involvement of activating transcription factors JNK, NF-kappaB, and AP-1 in apoptosis induced by pyrrolidine dithiocarbamate/Cu complex. *European Journal of Pharmacology*, 594 (1–3), 9–17.
- Chow, Y., Lee, K., Vidyadaran, S., Lajis, N., Akhtar, M., Israf, D., and Syahida, A., 2012. Cardamonin from *Alpinia rafflesiana* inhibits inflammatory responses in IFN- γ /LPS-stimulated BV2 microglia via NF- κ B signalling pathway. *International immunopharmacology*, 4, 657–665.
- Circu, M. and Aw, T., 2008. Glutathione and apoptosis. *Free Radical Research*, 42 (8), 689–706.
- Clutton, S., 1997. The importance of oxidative stress in apoptosis. *British Medical Bulletin*, 53 (3), 662–668.
- Cory, A., Owen, T., Barltrop, J., and Cory, J., 1991. Use of an aqueous soluble tetrazolium/formazan assay for cell growth assays in culture. *Cancer Communications*, 3 (7), 207–212.

- Cory, S. and Adams, J., 2002. The Bcl2 family: regulators of the cellular life-or-death switch. *Nature Reviews Cancer*, 2 (9), 647–656.
- Cragg, G., Grothaus, P., and Newman, D., 2009. Impact of natural products on developing new anti-cancer agents. *Chemical Reviews*, 109 (7), 3012–3043.
- Curtin, J., Donovan, M., and Cotter, T., 2002. Regulation and measurement of oxidative stress in apoptosis. *Journal of Immunological Methods*, 265 (1–2), 49–72.
- Daigneault, M., Preston, J., Marriott, H., Whyte, M., and Dockrell, D., 2010. The Identification of Markers of Macrophage Differentiation in PMA-Stimulated THP-1 Cells and Monocyte-Derived Macrophages. *Plos One*, 5 (1), e8668.
- Davies, S., Reddy, H., Caivano, M., and Cohen, P., 2000. Specificity and mechanism of action of some commonly used protein kinase inhibitors. *Biochemical Journal*, 351 (1), 95–105.
- Deegan, C., Coyle, B., McCann, M., Devereux, M., and Egan, D., 2006. In vitro anti-tumour effect of 1,10-phenanthroline-5,6-dione (phendione), [Cu(phendione)₃](ClO₄)₂·4H₂O and [Ag(phendione)₂]ClO₄ using human epithelial cell lines. *Chemico-Biological Interactions*, 164, 115–125.
- Denicourt, C. and Dowdy, S., 2004. Targeting apoptotic pathways in cancer cells. *Science*, 305 (5689), 1411–1413.
- Deo, K., Pages, B., Ang, D., Gordon, C., and Aldrich-Wright, J., 2016. Transition Metal Intercalators as Anticancer Agents—Recent Advances. *International Journal of Molecular Sciences*, 17 (11), 1818.
- Deponte, M., 2013. Glutathione catalysis and the reaction mechanisms of glutathione-dependent enzymes. *Biochimica et Biophysica Acta (BBA) - Molecular Cell Research*, 1830 (5), 3217–3266.
- Dhillon, A., Hagan, S., Rath, O., and Kolch, W., 2007. MAP kinase signalling pathways in cancer. *Oncogene*, 26 (22), 3279–3290.
- Dimmock, J., Kandepu, N., Hetherington, M., Quail, J., Pugazhenti, U., Sudom, A., Chamankhah, M., Rose, P., Pass, E., Allen, T., Halleran, S., Szydlowski, J., Mutus, B., Tannous, M., Manavathu, E., Myers, T., De Clercq, E., and Balzarini, J., 1998. Cytotoxic activities of Mannich bases of chalcones and related compounds. *Journal of Medicinal Chemistry*, 41 (7), 1014–1026.
- Dypbukt, J., Ankarcrona, M., Burkitt, M., Sjöholm, A., Ström, K., Orrenius, S., and Nicotera, P., 1994. Different prooxidant levels stimulate growth, trigger apoptosis, or produce necrosis of insulin-secreting RINm5F cells. The role of intracellular polyamines. *The Journal of Biological Chemistry*, 269 (48), 30553–30560.
- Dzoyem, J., NKuete, A., Kuete, V., Tala, M., Wabo, H., Guru, S., Rajput, V., Sharma, A., Tane, P., Khan, I., Saxena, A., Laatsch, H., and Tan, N., 2012. Cytotoxicity and Antimicrobial Activity of the Methanol Extract and Compounds from *Polygonum limbatum*. *Planta Med.*, 78 (8), 787–792.
- Ekert, P., Silke, J., and Vaux, D., 1999. Caspase inhibitors. *Cell Death and Differentiation*, 6 (11), 1081–1086.

- Elmore, S., 2007. Apoptosis: A Review of Programmed Cell Death. *Toxicology Pathology*, 35 (4), 495–516.
- Van Engeland, M., Nieland, L., Ramaekers, F., Schutte, B., and Reutelingsperger, C., 1998. Annexin V-affinity assay: a review on an apoptosis detection system based on phosphatidylserine exposure. *Cytometry*, 31 (1), 1–9.
- Ercal, N., Gurer-Orhan, H., and Aykin-Burns, N., 2001. Toxic metals and oxidative stress part I: mechanisms involved in metal-induced oxidative damage. *Current Topics in Medicinal Chemistry*, 1 (6), 529–539.
- Fadok, V., Voelker, D., Campbell, P., Cohen, J., Bratton, D., and Henson, P., 1992. Exposure of phosphatidylserine on the surface of apoptotic lymphocytes triggers specific recognition and removal by macrophages. *Journal of Immunology*, 148 (7), 2207–2216.
- Fahmy, B. and Cormier, S., 2009. Copper oxide nanoparticles induce oxidative stress and cytotoxicity in airway epithelial cells. *Toxicology in vitro : an international journal published in association with BIBRA*, 23 (7), 1365–1371.
- Farfan, A., Yeager, T., Moravec, R., and Niles, A., 2004. Multiplexing Homogeneous Cell-Based Assays. *Cell Notes*, 10, 15–18.
- Faull, R. and Ginsberg, M., 1995. Dynamic regulation of integrins. *Stem Cells*, 13 (1), 38–46.
- Fenton H, 1984. Oxidation of tartaric acid in the presence of iron. *Journal of Chemical Society*, 65, 899–910.
- Ferreira, A., Meneguelo, R., Pereira, A., Mendonça Filho, O., Chierice, G., and Maria, D., 2012. Anticancer effects of synthetic phosphoethanolamine on Ehrlich ascites tumor: an experimental study. *Anticancer Research*, 32 (1), 95–104.
- Forrest, V., Kang, Y., McClain, D., Robinson, D., and Ramakrishnan, N., 1994. Oxidative stress-induced apoptosis prevented by Trolox. *Free Radical Biology & Medicine*, 16 (6), 675–684.
- Franceschi, N. De, Hamidi, H., Alanko, J., Sahgal, P., and Ivaska, J., 2015. Integrin traffic – the update. *Journal of Cell Science*, 128 (5), 839–852.
- Franco, R. and Cidlowski, J., 2009. Apoptosis and glutathione: beyond an antioxidant. *Cell Death and Differentiation*, 16 (10), 1303–1314.
- Franco, R. and Cidlowski, J., 2012. Glutathione efflux and cell death. *Antioxidants and Redox Signaling*, 17 (12), 1694–1713.
- Franco, R., Panayiotidis, M., and Cidlowski, J., 2007. Glutathione depletion is necessary for apoptosis in lymphoid cells independent of reactive oxygen species formation. *The Journal of Biological Chemistry*, 282 (42), 30452–30465.
- Franco, R., Sánchez-Olea, R., Reyes-Reyes, E., and Panayiotidis, M., 2009. Environmental toxicity, oxidative stress and apoptosis: ménage à trois. *Mutation Research*, 674 (1–2), 3–22.
- Frisch, S. and Ruoslahti, E., 1997. Integrins and anoikis. *Current Opinion in Cell Biology*, 9 (5), 701–706.
- Gaetkea, L. M. and Chow, C. K., 2003. Copper toxicity, oxidative stress, and antioxidant nutrients. *Toxicology*, 189 (1–2), 147–163.

- Garcia-Calvo, M., Peterson, E., Leiting, B., Ruel, R., Nicholson, D., and Thornberry, N., 1998. Inhibition of human caspases by peptide-based and macromolecular inhibitors. *Journal of Biological Chemistry*, 273 (49), 32608–32613.
- Gerhauser, C., Alt, A., Heiss, E., Gamal-Eldeen, A., Klimo, K., Knauft, J., Neumann, I., Scherf, H., Frank, N., Bartsch, H., and Becker, H., 2002. Cancer chemopreventive activity of Xanthohumol, a natural product derived from hop. *Molecular Cancer Therapeutics*, 1 (11), 959–969.
- Geske, F. and Gerschenson, L., 2001. The biology of apoptosis. *Human Pathology*, 32 (10), 1029–1038.
- Ghoneim, A., 2009. Effects of curcumin on ethanol-induced hepatocyte necrosis and apoptosis: implication of lipid peroxidation and cytochrome c. *Archives of Pharmacology*, 379 (1), 47–60.
- Giancotti, F. and Ruoslahti, E., 1999. Integrin signaling. *Science*, 285 (5430), 1028–1032.
- Gilmore, A., Metcalfe, A., Romer, L., and Streuli, C., 2000. Integrin-mediated survival signals regulate the apoptotic function of Bax through its conformation and subcellular localization. *Journal of Cell Biology*, 149 (2), 431–446.
- Gmünder, H. and Dröge, W., 1991. Differential effects of glutathione depletion on T cell subsets. *Cellular Immunology*, 138 (1), 229–237.
- Gonçalves, L., Valente, I., and Rodrigues, J., 2014. An overview on cardamonin. *Journal of Medicinal Food*, 17 (6), 633–640.
- Gonzalez-Juarrero, M., Shim, T., Kipnis, A., Junqueira-Kipnis, A., and Orme, I., 2003. Dynamics of macrophage cell populations during murine pulmonary tuberculosis. *Journal of Immunology*, 171 (6), 3128–3135.
- Gopal, P. K., Paul, M., and Paul, S., 2014. Curcumin Induces Caspase Mediated Apoptosis in JURKAT Cells by Disrupting the Redox Balance. *Asian Pacific Journal of Cancer Prevention*, 15 (1), 93–100.
- Gottlieb, R., 2000. Mitochondria: execution central. *FEBS Letters*, 482 (1–2), 6–12.
- Graf, N. and Lippard, S., 2012. Redox activation of metal-based prodrugs as a strategy for drug delivery. *Advanced Drug Delivery Reviews*, 64, 993–1004.
- Green, D., 2000. Apoptotic Pathways. *Cell*, 102, 1–4.
- Green, D. and Kroemer, G., 1998. The central executioners of apoptosis: caspases or mitochondria? *Trends Cell Biol.*, 8 (7), 267–271.
- Gumbiner, B., 1996. Cell adhesion: the molecular basis of tissue architecture and morphogenesis. *Cell*, 84 (3), 345–357.
- Haber, F. and Weiss, J., 1934. The catalytic decomposition of hydrogen peroxide by iron salts. *Proceedings of the Royal Society of London A*, 147, 332–351.
- Häcker, G., 2000. The morphology of apoptosis. *Cell and Tissue Research*, 301 (1), 5–17.
- Hadzic, T., Li, L., Cheng, N., Walsh, S., Spitz, D., and Knudson, C., 2005. The role of low molecular weight thiols in T lymphocyte proliferation and IL-2 secretion. *Journal of Immunology*, 175 (12), 7965–7972.

- Hamilos, D. and Wedner, H., 1985. The role of glutathione in lymphocyte activation. I. Comparison of inhibitory effects of buthionine sulfoximine and 2-cyclohexene-1-one by nuclear size transformation. *Journal of Immunology*, 135 (4), 2740–2747.
- Hamilton, R. J., Li, L., Felder, T., and Holian, A., 1995. Bleomycin induces apoptosis in human alveolar macrophages. *The American Journal of Physiology*, 269 (3), 318–325.
- Harborne, J. and Williams, C., 2000. Advances in flavonoid research since 1992. *Phytochemistry*, 55 (6), 481–504.
- Haupt, S., 2003. Apoptosis – the p53 network. *Journal of Cell Science*, 116, 4077–4085.
- He, W., Jiang, Y., Zhang, X., Zhang, Y., Ji, H., and Zhang, N., 2014. Anticancer cardamonin analogs suppress the activation of NF-kappaB pathway in lung cancer cells. *Molecular and Cellular Biochemistry*, 389 (1–2), 25–33.
- Hecht, S., 1986. The chemistry of activated bleomycin. *Accounts of Chemical Research*, 19, 383–391.
- Hengartner, M., 2000. The biochemistry of apoptosis. *Nature*, 407 (6805), 770–776.
- Herbert, V., 1990. Viewpoint Does Mega-C Do More Good Than Harm, or More Harm Than Good? *FASEB Journal*, 4, 28–32.
- Hipfner, D. and Cohen, S., 2004. Connecting proliferation and apoptosis in development and disease. *Nature Reviews Molecular Cell Biology*, 5, 805–815.
- Hirvonen, T., Pietinen, P., Virtanen, M., Ovaskainen, M., Häkkinen, S., Albanes, D., and Virtamo, J., 2001. Intake of flavonols and flavones and risk of coronary heart disease in male smokers. *Epidemiology*, 12 (1), 62–67.
- Hood, J. and Cheresch, D., 2002. Role of integrins in cell invasion and migration. *Nature Reviews Cancer*, 2 (2), 91–100.
- Howe, C., 2016. *Gene Cloning and Manipulation By CTI Reviews*. 2nd ed. Pennsylvania, USA: Contect Technologies, Inc.
- Hu, W. and Kavanagh, J., 2003. Anticancer therapy targeting the apoptotic pathway. *The Lancet Oncology*, 4 (12), 721–729.
- Huang, Z., Wang, C., Wei, L., Wang, J., Fan, Y., Wang, L., Wang, Y., and Chen, T., 2008. Resveratrol inhibits EMMPRIN expression via P38 and ERK1/2 pathways in PMA-induced THP-1 cells. *Biochemical and Biophysical Research Communications*, 374 (3), 517–521.
- Ingber, D., Madri, J., and Folkman, J., 1987. Endothelial growth factors and extracellular matrix regulate DNA synthesis through modulation of cell and nuclear expansion. *In Vitro Cellular & Developmental Biology*, 23 (5), 387–394.
- Israfi, D. A., Khaizurin, T. A., Syahida, A., Lajis, N. H., and Khozirah, S., 2007. Cardamonin inhibits COX and iNOS expression via inhibition of p65NF-kappaB nuclear translocation and Ikappa-B phosphorylation in RAW 264.7 macrophage cells. *Molecular Immunology*, 44 (5), 673–679.

- Iwata, S., Hori, T., Sato, N., Hirota, K., Sasada, T., Mitsui, A., Hirakawa, T., and Yodoi, J., 1997. Adult T cell leukemia (ATL)-derived factor/human thioredoxin prevents apoptosis of lymphoid cells induced by L-cystine and glutathione depletion: possible involvement of thiol-mediated redox regulation in apoptosis caused by pro-oxidant state. *Journal of Immunology*, 158 (7), 3108–3117.
- Jan, M., Chao, M., Cha, A., Alizadeh, A., Gentles, A., Weissman, I., and Majeti, R., 2011. Prospective separation of normal and leukemic stem cells based on differential expression of TIM3, a human acute myeloid leukemia stem cell marker. *Proceedings of the National Academy of Sciences*, 108 (12), 5009–1014.
- Jantan, I., Raweh, S., Sirat, H., Jamil, S., Mohd Yasin, Y., Jalil, J., and Jamal, J., 2008. Inhibitory effect of compounds from Zingiberaceae species on human platelet aggregation. *Phytomedicine*, 15 (4), 306–309.
- Jiang, Y., Chen, C., Li, Z., Guo, W., Gegner, J. A., Shengcai, L., and Han, J., 1996. Characterization of the Structure and Function of a New Mitogen-activated Protein Kinase (p38 β). *The Journal of Biological Chemistry*, 271 (30), 17920–17926.
- Jiang, Y., Gram, H., Zhao, M., New, L., Gu, J., Feng, L., Di Padova, F., Ulevitch, R. J., and Han, J., 1997. Characterization of the Structure and Function of the Fourth Member of p38 Group Mitogen-activated Protein Kinases, p38delta. *The Journal of Biological Chemistry*, 272 (48), 30122–30128.
- Jin, J., Song, M., Kim, Y., Park, J., and Kwak, J., 2010. The mechanism of fucoidan-induced apoptosis in leukemic cells: involvement of ERK1/2, JNK, glutathione, and nitric oxide. *Molecular Carcinogenesis*, 49 (8), 771–782.
- Jones, D., Maellaro, E., Jiang, S., Slater, A., and Orrenius, S., 1995. Effects of N-acetyl-L-cysteine on T-cell apoptosis are not mediated by increased cellular glutathione. *Immunology Letters*, 45 (3), 205–209.
- Julian, L. and Olson, M., 2015. Apoptotic membrane dynamics in health and disease. *Cell Health and Cytoskeleton*, 2015 (7), 133–142.
- Kagan, V., Fabisiak, J., Shvedova, A., Tyurina, Y., Tyurin, V., Schor, N., and Kawai, K., 2000. Oxidative signaling pathway for externalization of plasma membranephosphatidylserine during apoptosis. *FEBS Letters*, 477 (1–2), 1–7.
- Kannan, K. and Jain, S., 2000. Oxidative stress and apoptosis. *Pathophysiology*, 7 (3), 153–163.
- Kello, M., Drutovic, D., Pilatova, M., Tischlerova, V., Perjesi, P., and Mojzis, J., 2016. Chalcone derivatives cause accumulation of colon cancer cells in the G2/M phase and induce apoptosis. *Life Sciences*, 150, 32–38.
- Kepp, O., Galluzzi, L., Lipinski, M., Yuan, J., and Kroemer, G., 2011. Cell death assays for drug discovery. *Nature Reviews Drug Discovery*, 10 (3), 221–237.
- Kerr, J., Wyllie, A., and Currie, A., 1972. Apoptosis: A Basic Biological Phenomenon with Wide-ranging Implications in Tissue Kinetics. *British Journal of Cancer*, 26 (4), 239–257.
- Khoo, B., Chua, S., and Balaram, P., 2010. Apoptotic effects of chrysin in human cancer cell lines. *International Journal of Molecular Sciences*, 11 (5), 2188–2199.

- Kimura, E., Nishimura, K., Sakata, K., Oga, S., Kashiwagi, K., and Igarashi, K., 2004. Methotrexate differentially affects growth of suspension and adherent cells. *The International Journal of Biochemistry and Cell Biology*, 36 (5), 814–825.
- Kingston, D., 2008. A Natural Love of Natural Products. *The Journal of Organic Chemistry*, 73 (11), 3975–3984.
- Kohno, T., Yamada, Y., Hata, T., Mori, H., Yamamura, M., Tomonaga, M., Urata, Y., Goto, S., and Kondo, T., 1996. Relation of oxidative stress and glutathione synthesis to CD95(Fas/APO-1)-mediated apoptosis of adult T cell leukemia cells. *Journal of Immunology*, 156 (12), 4722–4728.
- Kohro, T., Tanaka, T., Murakami, T., Wada, Y., Aburatani, H., Hamakubo, T., and Kodama, T., 2004. A comparison of differences in the gene expression profiles of phorbol 12-myristate 13-acetate differentiated THP-1 cells and human monocyte-derived macrophage. *Journal of Atherosclerosis and Thrombosis*, 11 (2), 88–97.
- Koppenol, W. H. and Bounds, P. L., 2012. *Redox-active metals: Iron and copper*. Volume 1. Principles of Free Radical Biomedicine. New York: Nova Science Publishers, Inc.
- Krahling, S., Callahan, M., Williamson, P., and Schlegel, R., 1999. Exposure of phosphatidylserine is a general feature in the phagocytosis of apoptotic lymphocytes by macrophages. *Cell & Death Differentiation*, 6 (2), 183–189.
- Kroemer, G. and Reed, J., 2000. Mitochondrial control of cell death. *Nature Medicine*, 6 (5), 513–519.
- Kuete, V., Nkuete, A., Mbaveng, A., Wiench, B., Wabo, H., Tane, P., and Efferth, T., 2014. Cytotoxicity and modes of action of 4'-hydroxy-2',6'-dimethoxychalcone and other flavonoids toward drug-sensitive and multidrug-resistant cancer cell lines. *Phytomedicine*, 21 (12), 1651–1657.
- Kuo, C., Wu, S., Ip, S., Wu, P., Yu, C., Yang, J., Chen, P., Wu, S., and Chung, J., 2011. Apoptotic death in curcumin-treated NPC-TW 076 human nasopharyngeal carcinoma cells is mediated through the ROS, mitochondrial depolarization and caspase-3-dependent signaling responses. *International Journal of Oncology*, 39 (2), 319–328.
- Latt, S. and Stetten, G., 1976. Spectral studies on 33258 Hoechst and related bisbenzimidazole dyes useful for fluorescent detection of deoxyribonucleic acid synthesis. *The journal of histochemistry and cytochemistry*, 24 (1), 24–33.
- Leist, M. and Nicotera, P., 1997. The shape of cell death. *Biochemical and Biophysical Research Communications*, 236 (1), 1–9.
- Leventis, P. and Grinstein, S., 2010. The distribution and function of phosphatidylserine in cellular membranes. *Annual Review of Biophysics*, 39, 407–427.
- Li, H., Zhu, H., Xu, C., and Yuan, J., 1998. Cleavage of BID by caspase 8 mediates the mitochondrial damage in the Fas pathway of apoptosis. *Cell*, 94 (4), 491–501.

- Li, N., Liu, J., Zhang, J., and Yu, B., 2008. Comparative Evaluation of Cytotoxicity and Antioxidative Activity of 20 Flavonoids. *Journal of Agricultural and Food Chemistry*, 56 (10), 3876–3883.
- Li, Z., Jiang, Y., Ulevitch, R. J., and Han, J., 1996. The Primary Structure of p38 γ : A New Member of p38 Group of MAP Kinases. *Biochemical and Biophysical Research Communications*, 228 (2), 334–340.
- Lin, E., Lin, W., Wang, S., Chen, C., Liao, J., Chang, H., Chen, S., Lin, K., Wang, L., Yang, H., and Hseu, Y., 2012. Flavokawain B inhibits growth of human squamous carcinoma cells: Involvement of apoptosis and cell cycle dysregulation in vitro and in vivo. *Journal of Nutritional Biochemistry*, 23 (4), 368–378.
- Llado, V., Gutierrez, A., Martínez, J., Casas, J., Terés, S., Higuera, M., Galmés, A., Saus, C., Besalduch, J., Busquets, X., and Escribá, P., 2008. Minerval Induces Apoptosis In Jurkat And Other Cancer Cells. *Journal of Cellular and Molecular Medicine*, 14 (3), 659–670.
- Lock, R. and Debnath, J., 2008. Extracellular matrix regulation of autophagy. *Current Opinion in Cell Biology*, 20, 583–588.
- Lourenço, A., Ferreira, L., and Branco, P., 2012. Molecules of natural origin, semi-synthesis and synthesis with anti-inflammatory and anticancer utilities. *Current Pharmaceutical Design*, 18 (26), 3979–4046.
- Luo, X., Budihardjo, I., Zou, H., Slaughter, C., and Wang, X., 1998. Bid, a Bcl2 interacting protein, mediates cytochrome c release from mitochondria in response to activation of cell surface death receptors. *Cell*, 94 (4), 481–490.
- Ma, Q., 2013. Role of nrf2 in oxidative stress and toxicity. *Annual Review of Pharmacology and Toxicology*, 53, 401–426.
- Magalhães, P., Carvalho, D., Cruz, J., Guido, L., and Barros, A., 2009. Fundamentals and health benefits of xanthohumol, a natural product derived from hops and beer. *Natural Product Communications*, 4 (5), 591–610.
- Maheshwari, A., Misro, M. M., Aggarwal, A., Sharma, R. K., and Nandan, D., 2011. N-acetyl-L-cysteine counteracts oxidative stress and prevents H₂O₂ induced germ cell apoptosis through down-regulation of caspase-9 and JNK/c-Jun. *Molecular Reproduction and Development*, 78 (2), 69–79.
- Maier, M., 2015. Design and synthesis of analogues of natural products. *Organic & Biomolecular Chemistry*, 13, 5302–5343.
- Maioral, M., Gaspar, P., Rosa Souza, G., Mascarello, A., Chiaradia, L., Licínio, M., Moraes, A., Yunes, R., Nunes, R., and Santos-Silva, M., 2013. Apoptotic events induced by synthetic naphthylchalcones in human acute leukemia cell lines. *Biochimie*, 95 (4), 866–874.
- Manning, T., Leggett, T., Jenkins, D., Furtado, I., Phillips, D., Wylie, G., Bythell, B., and Zhang, F., 2013. Structural and some medicinal characteristics of the copper(II)–hydroxychloroquine complex. *Bioorganic and Medicinal Chemistry Letters*, 4453–4458.

- Manning, T., Phillips, D., Wylie, G., Bythell, B., Clark, S., Ogburn, R., Ledwitch, K., Collis, C., Patterson, S., and Lasseter, L., 2014. Copper ion as a delivery platform for taxanes and taxane complexes. *Bioorganic and Medicinal Chemistry Letters*, 24 (11), 371–377.
- Marastoni, S., Ligresti, G., Lorenzon, E., Colombatti, A., and Mongiat, M., 2008. Extracellular matrix: a matter of life and death. *Connective Tissue Research*, 49, 203–206.
- Margarona, P., Sorrentia, R., and Levy, J. G., 1997. Photodynamic therapy inhibits cell adhesion without altering integrin expression. *Biochimica et Biophysica Acta (BBA) - Molecular Cell Research*, 1359 (3), 200–210.
- Margolin, N., Raybuck, S., Wilson, K., Chen, W., Fox, T., Gu, Y., and Livingston, D., 1997. Substrate and inhibitor specificity of interleukin-1 beta-converting enzyme and related caspases. *Journal of Biological Chemistry*, 272 (11), 7223–7228.
- Marreilha, dos S. A., Santos, D., Au, C., Milatovic, D., Aschner, M., and Batoréu, M., 2008. Antioxidants prevent the cytotoxicity of manganese in RBE4 cells. *Brain Research*, 1236, 200–205.
- Masella, R., Di Benedetto, R., Varì, R., Filesi, C., and Giovannini, C., 2005. Novel mechanisms of natural antioxidant compounds in biological systems: involvement of glutathione and glutathione-related enzymes. *Journal of Nutritional Biochemistry*, 16 (10), 577–586.
- Matés, J., Segura, J., Alonso, F., and Márquez, J., 2012. Oxidative stress in apoptosis and cancer: an update. *Archives of Toxicology*, 88 (11), 1649–1665.
- Mattson, M. and Bazan, N., 2012. Apoptosis and Necrosis. In: Siegel, G., Albers, R., Brady, S., and Price, D., eds. *Basic Neurochemistry*. London, UK: Elsevier Academic Press, 663–676.
- McIlwain, D., Berger, T., and Mak, T., 2013. Caspase functions in cell death and disease. *Cold Spring Harbor Perspectives in Biology*, 5 (4), a008656.
- McNally, S., Harrison, E., Ross, J., Garden, O., and Wigmore, S., 2007. Curcumin induces heme oxygenase 1 through generation of reactive oxygen species, p38 activation and phosphatase inhibition. *International Journal of Molecular Medicine*, 19 (1), 165–172.
- Menezes, J., Orlikova, B., Morceau, F., and Diederich, M., 2016. Natural and Synthetic Flavonoids: Structure-Activity Relationship and Chemotherapeutic Potential for the Treatment of Leukemia. *Critical Reviews in Food Science and Nutrition*, 56 (1), S4–S28.
- Meredith, J., Fazeli, B., and Schwartz, M., 1993. The extracellular matrix as a cell survival factor. *Molecular Biology of the Cell*, 4 (9), 953–961.
- Meredith, J. and Schwartz, M., 1997. Integrins, adhesion and apoptosis. *Trends in Cellular Biology*, 7 (4), 146–150.
- Meyer, A., van Golen, C., Kim, B., van Golen, K., and Feldman, E., 2004. Integrin expression regulates neuroblastoma attachment and migration. *Neoplasia*, 6 (4), 332–342.

- Mi, X., Song, Z., Sun, L., Bao, Y., Yu, C., Wu, Y., and Li, Y., 2016. Cardamonin inhibited cell viability and tumorigenesis partially through blockade of testis-specific protease 50-mediated nuclear factor-kappaB signaling pathway activation. *International Journal of Biochemistry and Cell Biology*, 73, 63–71.
- Mittar, D., Paramban, R., and McIntyre, C., 2011. *Flow Cytometry and High-Content Imaging to Identify Markers of Monocyte-Macrophage Differentiation* [online]. BD Biosciences. Available from: https://www.bdbiosciences.com/documents/BD_Multicolor_MonocyteMacrophageDiff_AppNote.pdf.
- Mohamad, H., Abas, F., Permana, D., Lajis, N., Ali, A., Sukari, M., Hin, T., Kikuzaki, H., and Nakatani, N., 2004. DPPH free radical scavenger components from the fruits of *Alpinia rafflesiana* Wall. ex. Bak. (Zingiberaceae). *Journal of Biosciences*, 59 (11–12), 811–815.
- Monick, M., Samavati, L., Butler, N., Mohning, M., Powers, L., Yarovinsky, T., Spitz, D., and Hunninghake, G., 2003. Intracellular thiols contribute to Th2 function via a positive role in IL-4 production. *Journal of Immunology*, 171 (10), 5107–5115.
- Morin, D., Barthélémy, S., Zini, R., Labidalle, S., and Tillement, J., 2001. Curcumin induces the mitochondrial permeability transition pore mediated by membrane protein thiol oxidation. *FEBS Letters*, 495 (1–2), 131–136.
- Morrow, J. and Roberts, L., 1997. The isoprostanes: unique bioactive products of lipid peroxidation. *Progress in Lipid Research*, 36 (1), 1–21.
- Murakami, A., Kondo, A., Nakamura, Y., Ohigashi, H., and Koshimizu, K., 1993. Possible Anti-tumor Promoting Properties of Edible Plants from Thailand, and Identification of an Active Constituent, Cardamonin, of *Boesenbergia pandurata*. *Bioscience, Biotechnology, and Biochemistry*, 57 (11), 1971–1973.
- Murray, P. and Wynn, T., 2011. Protective and pathogenic functions of macrophage subsets. *Nature Reviews Immunology*, 11 (11), 723–737.
- Nam, N., Kim, Y., You, Y., Hong, D., Kim, H., and Ahn, B., 2003. Cytotoxic 2',5'-dihydroxychalcones with unexpected antiangiogenic activity. *European Journal of Medicinal Chemistry*, 38 (2), 179–187.
- Nemoto, S., Xiang, J., Huang, S., and Lin, A., 1998. Induction of Apoptosis by SB202190 through Inhibition of p38 β Mitogen-activated Protein Kinase. *Journal of Biological Chemistry*, 273 (26), 16415–16420.
- Neumeister, P., Pixley, F. J., Xiong, Y., Xie, H., Wu, K., Ashton, A., Cammer, M., Chan, A., Symons, M., Stanley, E. R., and Pestell, R. G., 2003. Cyclin D1 Governs Adhesion and Motility of Macrophages. *Molecular Biology of the Cell*, 14 (5), 2005–2015.
- Newman, D. and Cragg, G., 2012. Natural products as sources of new drugs over the 30 years from 1981 to 2010. *Journal of Natural Products*, 75 (3), 311–335.
- Ni, L., Meng, C., and Sikorski, J., 2004. Recent advances in therapeutic chalcones. *Expert Opinion on Therapeutic Patents*, 14 (12), 1669–1691.
- Nicholson, D. and Thornberry, N., 1997. Caspases: killer proteases. *Trends in Biochemical Sciences*, 22 (8), 299–306.

- Van Noorden, C., 2001. The history of Z-VAD-FMK, a tool for understanding the significance of caspase inhibition. *Acta Histochemica*, 103 (3), 241–251.
- Nur, E., Verwijs, M., de Waart, D., Schnog, J., Otten, H., Brandjes, D., Biemond, B., and Elferink, R., 2011. Increased efflux of oxidized glutathione (GSSG) causes glutathione depletion and potentially diminishes antioxidant defense in sickle erythrocytes. *Biochimica et Biophysica Acta (BBA) - Molecular Cell Research*, 1812 (11), 1412–1417.
- O'Neill, C., Jordan, P., and Ireland, G., 1986. Evidence for two distinct mechanisms of anchorage stimulation in freshly explanted and 3T3 Swiss mouse fibroblasts. *Cell*, 44 (3), 489–496.
- Ohtsuki, T., Kikuchi, H., Koyano, T., Kowithayakorn, T., Sakai, T., and Ishibashi, M., 2009. Death receptor 5 promoter-enhancing compounds isolated from *Catimbum speciosum* and their enhancement effect on TRAIL-induced apoptosis. *Bioorganic and Medicinal Chemistry*, 17 (18), 6748–6754.
- Orrenius, S., Nicotera, P., and Zhivotovsky, B., 2011. Cell Death Mechanisms and Their Implications in Toxicology. *Toxicological Sciences*, 119 (1), 3–19.
- Ozben, T., 2007. Oxidative stress and apoptosis: Impact on cancer therapy. *Journal of Pharmaceutical Sciences*, 96 (9), 2181–2196.
- Pan, L., Zhao, Y., Yuan, Z., and Qin, G., 2016. Research advances on structure and biological functions of integrins. *SpringerPlus*, 5 (1), 1094.
- Pan, M., Chang, W., Lin-Shiau, S., Ho, C., and Lin, J., 2001. Induction of apoptosis by garcinol and curcumin through cytochrome c release and activation of caspases in human leukemia HL-60 cells. *Journal of Agricultural and Food Chemistry*, 49 (3), 1464–1474.
- Park, E., Kim, S., Na, J., Ryu, H., Youn, S., Kim, D., Yun, H., and Park, K., 2007. Glutathione prevented dopamine-induced apoptosis of melanocytes and its signaling. *Journal of Dermatological Science*, 47 (2), 141–149.
- Park, S., Gwak, J., Han, S. J., and Sangtaek, O., 2013. *Cardamonin Suppresses the Proliferation of Colon Cancer Cells by Promoting β -Catenin Degradation* [online]. *Biol. Pharm. Bull.* Available from: https://www.jstage.jst.go.jp/article/bpb/36/6/36_b13-00158/_pdf [Accessed 12 Aug 2015].
- Parrish, A., Freel, C., and Kornbluth, S., 2013. Cellular Mechanisms Controlling Caspase Activation and Function. *Cold Spring Harbor Perspectives in Biology*, 5, a008672–a008672.
- Pascoal, A. C. R. F., Ehrenfried, C. A., Lopez, B. G.-C., de Araujo, T. M., Pascoal, V. D. B., Gilioli, R., Anhê, G. F., Ruiz, A. L. T. G., Carvalho, J. E. de, Stefanello, M. E. A., and Salvador, M. J., 2014. Antiproliferative activity and induction of apoptosis in PC-3 cells by the chalcone cardamonin from *Campomanesia adamantium* (Myrtaceae) in a bioactivity-guided study. *Molecules (Basel, Switzerland)*, 19 (2), 1843–55.
- Pasqualini, R., Bodorova, J., Ye, S., and Hemler, M., 1993. A study of the structure, function and distribution of beta 5 integrins using novel anti-beta 5 monoclonal antibodies. *Journal of Cell Science*, 105 (1), 101–111.

- Petrucci, R., Harwood, W., and Herring, F., 2002. *General Chemistry: Principles & Modern Applications*. Upper Saddle River, New Jersey: Prentice Hall.
- Pettit, G., Kamano, Y., Dufresne, C., Cerny, R., Herald, C., and Schmidt, J., 1989. Isolation and structure of the cytostatic linear depsipeptide dolastatin 15. *The Journal of Organic Chemistry*, 54 (26), 6005–6006.
- Pias, E. and Aw, T., 2002. Apoptosis in mitotic competent undifferentiated cells is induced by cellular redox imbalance independent of reactive oxygen species production. *FASEB Journal*, 16 (8), 781–790.
- Piwocka, K., Jaruga, E., Skierski, J., Gradzka, I., and Sikora, E., 2001. Effect of glutathione depletion on caspase-3 independent apoptosis pathway induced by curcumin in Jurkat cells. *Free Radical Biology & Medicine*, 31 (5), 670–678.
- Poliandri, A., Cabilla, J., Velardez, M., Bodo, C., and Duvilanski, B., 2003. Cadmium induces apoptosis in anterior pituitary cells that can be reversed by treatment with antioxidants. *Toxicology and Applied Pharmacology*, 190 (1), 17–24.
- Qiao, X., Ma, Z., Xie, C., Xue, F., Zhang, Y., Xu, J., Qiang, Z., Lou, J., Chen, G., and Yan, S., 2011. Study on potential antitumor mechanism of a novel Schiff Base copper(II) complex: Synthesis, crystal structure, DNA binding, cytotoxicity and apoptosis induction activity. *Journal of Inorganic Biochemistry*, 105 (5), 728–737.
- Qin, Y., Sun, C., Lu, F., Shu, X., Yang, D., Chen, L., She, X., Gregg, N., Guo, T., and Hu, Y., 2012. Cardamonin exerts potent activity against multiple myeloma through blockade of NF-kappaB pathway in vitro. *Leukemia Research*, 36 (4), 514–520.
- Rahman, A., Shahabuddin, Hadi, S., Parish, J., and Ainley, K., 1989. Strand scission in DNA induced by quercetin and Cu(II): role of Cu(I) and oxygen free radicals. *Carcinogenesis*, 10 (10), 1833–1839.
- Rajah, T. and Chow, S., 2014. The inhibition of human T cell proliferation by the caspase inhibitor z-VAD-FMK is mediated through oxidative stress. *Toxicology and Applied Pharmacology*, 278 (2), 100–106.
- Ren, W., Qiao, Z., Wang, H., Zhu, L., and Zhang, L., 2003. Flavonoids: promising anticancer agents. *Medicinal Research Reviews*, 23 (4), 519–534.
- Rice, G., Bump, E., Shrieve, D., Lee, W., and Kovacs, M., 1986. Quantitative analysis of cellular glutathione by flow cytometry utilizing monochlorobimane: some applications to radiation and drug resistance in vitro and in vivo. *Cancer Research*, 46, 6105–6110.
- Riss, T., Moravec, R., Niles, A., Duellman, S., Benink, H., Worzella, T., and Minor, L., 2013. Cell Viability Assays. In: Sittampalam, G., Coussens, N., and Brimacombe, K., eds. *Assay Guidance Manual*. Maryland, USA: Eli Lilly & Company and the National Center for Advancing Translational Sciences.
- Roy, M., Vom, A., Czabotar, P., and Lessene, G., 2014. Cell death and the mitochondria: therapeutic targeting of the BCL-2 family-driven pathway. *British Journal of Pharmacology*, 171 (8), 1973–1987.

- Ryter, S., Kim, H., Hoetzel, A., Park, J., Nakahira, K., Wang, X., and Choi, A., 2007. Mechanisms of Cell Death in Oxidative Stress. *Antioxidants and Redox Signaling*, 9 (1), 49–89.
- Sahu, N., Balbhadra, S., Choudhary, J., and Kohli, D., 2012. Exploring pharmacological significance of chalcone scaffold: a review. *Current Medicinal Chemistry*, 19 (2), 209–225.
- Said, A. M., Fazal, F., Rahman, A., Hadi, S., and Parish, J., 1992. Activities of flavonoids for the cleavage of DNA in the presence of Cu(II): correlation with generation of active oxygen species. *Carcinogenesis*, 13 (4), 605–608.
- Salge, U., Seitz, R., Wimmel, A., Schuermann, M., Daubner, E., and Heiden, M., 2001. Transition from suspension to adherent growth is accompanied by tissue factor expression and matrix metalloproteinase secretion in a small cell lung cancer cell line. *Journal of Cancer Research and Clinical Oncology*, 127 (2), 139–141.
- Sandur, S., Ichikawa, H., Pandey, M., Kunnumakkara, A., Sung, B., Sethi, G., and Aggarwal, B., 2007. Role of pro-oxidants and antioxidants in the anti-inflammatory and apoptotic effects of curcumin (diferuloylmethane). *Free Radical Biology & Medicine*, 43 (4), 568–580.
- Sarkar, A., Das, J., Manna, P., and Sil, P. C., 2011. Nano-copper induces oxidative stress and apoptosis in kidney via both extrinsic and intrinsic pathways. *Toxicology*, 290 (2–3), 208–217.
- Savill, J., 1997. Recognition and phagocytosis of cells undergoing apoptosis. *British Medical Bulletin*, 53 (3), 491–508.
- Savill, J., Fadok, V., Henson, P., and Haslett, C., 1993. Phagocyte recognition of cells undergoing apoptosis. *Immunology Today*, 14 (3), 131–136.
- Saxena, N., Rao, P., Bhaskar, A., and Bhutia, Y., 2014. Protective effects of certain pharmaceutical compounds against abrin induced cell death in Jurkat cell line. *International Immunopharmacology*, 21 (2), 412–425.
- Scarlett, J., Sheard, P., Hughes, G., Ledgerwood, E., Ku, H., and Murphy, M., 2000. Changes in mitochondrial membrane potential during staurosporine-induced apoptosis in Jurkat cells. *FEBS Letters*, 475 (3), 267–272.
- Schneider, U., Schwenk, H., and Bornkamm, G., 1977. Characterization of EBV-genome negative ‘null’ and ‘T’ cell lines derived from children with acute lymphoblastic leukemia and leukemic transformed non-Hodgkin lymphoma. *International Journal of Cancer*, 19 (5), 621–626.
- Schroecksnadel, S., Jenny, M., and Fuchs, D., 2011. Myelomonocytic THP-1 cells for in vitro testing of immunomodulatory properties of nanoparticles. *Journal of Biomedical Nanotechnology*, 7 (1), 209–210.
- Shamsi, F. and Hadi, S., 1995. Photoinduction of strand scission in DNA by uric acid and Cu(II). *Free Radical Biology & Medicine*, 19 (2), 189–196.
- Shi, H., Hudson, L. G., and Liu, K. J., 2004. Oxidative stress and apoptosis in metal ion-induced carcinogenesis. *Free Radical Biology & Medicine*, 37 (5), 582–593.
- Shi, Q. and Jackowski, G., 1998. *Gel electrophoresis of proteins: A practical approach*. 3rd ed. Oxford University Press.

- Shiozaki, E., Chai, J., and Shi, Y., 2002. Oligomerization and activation of caspase-9, induced by Apaf-1 CARD. *In: Proceedings of the National Academy of Sciences*, 4197–4202.
- Shukla, S. and Gupta, S., 2010. Apigenin: a promising molecule for cancer prevention. *Pharmaceutical Research*, 27 (6), 962–978.
- Sigma-Aldrich, 2017. *p38 MAP Kinase Inhibitor IV* [online]. Available from: <http://www.sigmaaldrich.com/catalog/product/sigma/sml0543?lang=en®ion=MY> [Accessed 24 Nov 2016].
- Simirgiotis, M., Adachi, S., To, S., Yang, H., Reynertson, K., Basile, M., Gil, R., Weinstein, I., and Kennelly, E., 2008. Cytotoxic chalcones and antioxidants from the fruits of *Syzygium samarangense* (Wax Jambu). *Food Chemistry*, 107 (2), 813–819.
- Slater, A., Stefan, C., Nobel, I., van den Dobbelen, D., and Orrenius, S., 1995. Signalling mechanisms and oxidative stress in apoptosis. *Toxicology Letters*, 82, 149–153.
- Sloma, I., Jiang, X., Eaves, A., and Eaves, C., 2010. Insights into the stem cells of chronic myeloid leukemia. *Leukemia*, 24 (11), 1823–1833.
- Soh, Y., Shin, M., Lee, J., Jang, J., Kim, O., Kang, H., and Surh, Y., 2003. Oxidative DNA damage and glioma cell death induced by tetrahydropapaveroline. *Mutation Research*, 544 (2–3), 129–142.
- Srinivasan, B., Johnson, T., Lad, R., and Xing, C., 2009. Structure-activity relationship studies of chalcone leading to 3-hydroxy-4,3',4',5'-tetramethoxychalcone and its analogues as potent nuclear factor kappaB inhibitors and their anticancer activities. *Journal of Medicinal Chemistry*, 52 (22), 7228–7235.
- Stohs, S. and Bagchi, D., 1995. Oxidative mechanisms in the toxicity of metal ions. *Free Radical Biology & Medicine*, 18 (2), 321–326.
- Stubbe, J. and Kozarich, J., 1987. Mechanisms of bleomycin-induced DNA degradation. *Chemical Reviews*, 87, 1107–1136.
- Sugibayashi, R., Shimizu, T., Suzuki, T., Yamamoto, N., Hamada, H., and Takeda, K., 2001. Upregulation of p21(WAF1/CIP1) leads to morphologic changes and esterase activity in TPA-mediated differentiation of human prostate cancer cell line TSU-Pr1. *Oncogene*, 20 (10), 1220–1228.
- Sugiyama, H., Kashihara, N., Maeshima, Y., Okamoto, K., Kanao, K., Sekikawa, T., and Makino, H., 1998. Regulation of survival and death of mesangial cells by extracellular matrix. *Kidney International*, 54 (4), 1188–1196.
- Sun, S., 2010. N-acetylcysteine, reactive oxygen species and beyond. *Cancer Biology & Therapy*, 9 (2), 109–110.
- Sun, Y., Huang, W., Hsiao, C., Chen, Y., Lu, P., and Guh, J., 2010. Methoxychalcone induces cell-cycle arrest and apoptosis in human hormone-resistant prostate cancer cells through PI 3-kinase-independent inhibition of mTOR pathways. *Prostate*, 70 (12), 1295–1306.

- Susin, S., Zamzami, N., Castedo, M., Daugas, E., Wang, H., Geley, S., Fassy, F., Reed, J., and Kroemer, G., 1997. The central executioner of apoptosis: Multiple connections between protease activation and mitochondria in Fas/APO-1/CD95- and ceramide-induced apoptosis. *The Journal of Experimental Medicine*, 186 (1), 25–37.
- Syng-Ai, C., Kumari, A., and Khar, A., 2004. Effect of curcumin on normal and tumor cells: role of glutathione and bcl-2. *Molecular Cancer Therapeutics*, 3 (9), 1101–1108.
- Tabata, K., Motani, K., Takayanagi, N., Nishimura, R., Asami, S., Kimura, Y., Ukiya, M., Hasegawa, D., Akihisa, T., and Suzuki, T., 2005. Xanthoangelol, a major chalcone constituent of *Angelica keiskei*, induces apoptosis in neuroblastoma and leukemia cells. *Biological and Pharmaceutical Bulletin*, 28 (8), 1404–1407.
- Tait, S. and Green, D., 2010. Mitochondria and cell death: outer membrane permeabilization and beyond. *Nature Reviews Molecular Cell Biology*, 11, 621–632.
- Tang, J., Li, N., Dai, H., and Wang, K., 2010. Chemical constituents from seeds of *Alpinia katsumadai*, inhibition on NF-kappaB activation and anti-tumor effect. *Zhongguo Zhong Yao Za Zhi*, 35 (13), 1710–1714.
- Tang, X. and Liang, X., 2013. Metal-mediated Targeting in the Body. *Chemical Biology & Drug Design*, 81, 311–322.
- Tang, Y., Fang, Q., Shi, D., Niu, P., Chen, Y., and Deng, J., 2014. mTOR inhibition of cardamonin on antiproliferation of A549 cells is involved in a FKBP12 independent fashion. *Life Sciences*, 99 (1–2), 44–51.
- Teillet, F., Boumendjel, A., Boutonnat, J., and Ronot, X., 2008. Flavonoids as RTK inhibitors and potential anticancer agents. *Medicinal Research Reviews*, 28 (5), 715–745.
- Torres, F., Quintana, J., Díaz, J., Carmona, A., and Estévez, F., 2008. Trifolin acetate-induced cell death in human leukemia cells is dependent on caspase-6 and activates the MAPK pathway. *Apoptosis*, 13 (8), 716–728.
- Traore, K., Trush, M., George, M., Spannhake, E., Anderson, W., and Asseffa, A., 2005. Signal transduction of phorbol 12-myristate 13-acetate (PMA)-induced growth inhibition of human monocytic leukemia THP-1 cells is reactive oxygen dependent. *Leukemia Research*, 29 (8), 863–879.
- Tsuchiya, S., Kobayashi, Y., Goto, Y., Okumura, H., Nakae, S., Konno, T., and Tada, K., 1982. Induction of maturation in cultured human monocytic leukemia cells by a phorbol diester. *Cancer Research*, 42 (4), 1530–1536.
- Tsuchiya, S., Yamabe, M., Yamaguchi, Y., Kobayashi, Y., Konno, T., and Tada, K., 1980. Establishment and characterization of a human acute monocytic leukemia cell line (THP-1). *International Journal of Cancer*, 26 (2), 171–176.
- Valko, M., Morris, H., and Cronin, M., 2005. Metals, Toxicity and Oxidative Stress. *Current Medicinal Chemistry*, 12 (10), 1161–1208.

- Vermes, I., Haanen, C., Steffens-Nakken, H., and Reutelingsperger, C., 1995. A novel assay for apoptosis. Flow cytometric detection of phosphatidylserine expression on early apoptotic cells using fluorescein labelled Annexin V. *Journal of Immunological Methods*, 184 (1), 39–51.
- Wall, M. and Wani, M., 1996. Camptothecin and taxol: from discovery to clinic. *Journal of Ethnopharmacology*, 51 (1–3), 239–253.
- Wani, M., Taylor, H., Wall, M., Coggon, P., and McPhail, A., 1971. Plant antitumor agents. VI. The isolation and structure of taxol, a novel antileukemic and antitumor agent from *Taxus brevifolia*. *Journal of American Chemical Society*, 93 (9), 2325–2327.
- Widau, R., Parekh, A., Ranck, M., Golden, D., Kumar, K., Sood, R., Pitroda, S., Liao, Z., Huang, X., Darga, T., Xu, D., Huang, L., Andrade, J., Roizman, B., Weichselbaum, R., and Khodarev, N., 2014. RIG-I-like receptor LGP2 protects tumor cells from ionizing radiation. *In: Proceedings of the National Academy of Sciences*. E484–E491.
- Win, N., Awale, S., Esumi, H., Tezuka, Y., and Kadota, S., 2007. Bioactive secondary metabolites from *Boesenbergia pandurata* of Myanmar and their preferential cytotoxicity against human pancreatic cancer PANC-1 cell line in nutrient-deprived medium. *Journal of Natural Products*, 70 (10), 1582–1587.
- Wu, N., Liu, J., Zhao, X., Yan, Z., Jiang, B., Wang, L., Cao, S., Shi, D., and Lin, X., 2015. Cardamonin induces apoptosis by suppressing STAT3 signaling pathway in glioblastoma stem cells. *Tumour Biology*, 36 (12), 9667–9676.
- Xiao, X., Hao, M., Yang, X., Ba, Q., Li, M., Ni, S., Wang, L., and Du, X., 2011. Licochalcone A inhibits growth of gastric cancer cells by arresting cell cycle progression and inducing apoptosis. *Cancer Letters*, 302 (1), 69–75.
- Xue, Z., Niu, P., Shi, D., Liu, Y., Deng, J., and Chen, Y., 2016. Cardamonin Inhibits Angiogenesis by mTOR Downregulation in SKOV3 Cells. *Planta Medica*, 82 (1–2), 70–75.
- Yadav, V., Prasad, S., and Aggarwal, B., 2012. Cardamonin sensitizes tumour cells to TRAIL through ROS- and CHOP-mediated up-regulation of death receptors and down-regulation of survival proteins. *British Journal of Pharmacology*, 165 (3), 741–753.
- Yadav, V., Prasad, S., Sung, B., and Aggarwal, B., 2011. The role of chalcones in suppression of NF- κ B-mediated inflammation and cancer. *International Immunopharmacology*, 11 (3), 295–309.
- Yan, N. and Shi, Y., 2005. Mechanisms of apoptosis through structural biology. *Annual Review of Cell and Developmental Biology*, 21, 35–56.
- Yang, C., Chang, C., Lee, H., Chi, C., Pan, J., and Yang, W., 2012. Curcumin induces the apoptosis of human monocytic leukemia THP-1 cells via the activation of JNK/ERK pathways. *BMC Complementary and Alternative Medicine*, 12 (22), 1–8.

- Yoshino, M., Haneda, M., Naruse, M., Htay, H., Tsubouchi, R., Qiao, S., Li, W., Murakami, K., and Yokochi, T., 2004. Prooxidant activity of curcumin: copper-dependent formation of 8-hydroxy-2'-deoxyguanosine in DNA and induction of apoptotic cell death. *Toxicology in vitro : an international journal published in association with BIBRA*, 18 (6), 783–789.
- Zafarullah, M., Li, W., Sylvester, J., and Ahmad, M., 2003. Molecular mechanisms of N-acetylcysteine actions. *Cellular and Molecular Life Sciences*, 60 (1), 6–20.
- Zarubin, T. and Han, J., 2005. Activation and signaling of the p38 MAP kinase pathway. *Cell Research*, 15 (1), 11–18.
- Zhai, Q., Ji, H., Zheng, Z., Yu, X., Sun, L., and Liu, X., 2000. Copper induces apoptosis in BA/F3beta cells: Bax, reactive oxygen species, and NFkappaB are involved. *Journal of Cellular Physiology*, 184 (2), 161–170.
- Zhang, T., Yamamoto, N., Yamashita, Y., and Ashida, H., 2014. The chalcones cardamonin and flavokawain B inhibit the differentiation of preadipocytes to adipocytes by activating ERK. *Archives of Biochemistry and Biophysics*, 554, 44–54.
- Zheng, J., Payne, K., Taggart, J. E., Jiang, H., Lind, S. E., and Ding, W. Q., 2012. Trolox Enhances Curcumin's Cytotoxicity through Induction of Oxidative Stress. *Cellular Physiology and Biochemistry*, 29 (3–4), 353–360.
- Zhou, J., Zhu, P., Jiang, J. L., Zhang, Q., Wu, Z. B., Yao, X. Y., Tang, H., Lu, N., Yang, Y., and Chen, Z. N., 2005. Involvement of CD147 in overexpression of MMP-2 and MMP-9 and enhancement of invasive potential of PMA-differentiated THP-1. *BMC Cell Biology*, 6 (1), 25.
- Zhu, Y., Huang, S., Tan, B., Sun, J., Whiteman, M., and Zhu, Y., 2004. Antioxidants in Chinese herbal medicines: a biochemical perspective. *Natural Product Reports*, 21 (4), 478–489.
- Ziegler, U. and Groscurth, P., 2004. Morphological features of cell death. *News in Physiological Science*, 19 (124–128).
- Zimmermann, K., Bonzon, C., and Green, D., 2001. The machinery of programmed cell death. *Pharmacology and Therapeutics*, 92 (1), 57–70.
- Zmuda, J. and Friedenson, B., 1983. Changes in intracellular glutathione levels in stimulated and unstimulated lymphocytes in the presence of 2-mercaptoethanol or cysteine. *Journal of Immunology*, 130 (1), 362–364.
- Zoratti, M. and Szabò, I., 1996. The mitochondrial permeability transition. *Biochimica et Biophysica Acta (BBA) - Molecular Cell Research*, 1241 (2), 139–176.
- Zorov, D., Juhaszova, M., and Sollott, S., 2006. Mitochondrial ROS-induced ROS release: an update and review. *Biochimica et Biophysica Acta (BBA) - Molecular Cell Research*, 1757 (5–6), 509–517.
- Zucker, B., Hanusch, J., and Bauer, G., 1997. Glutathione depletion in fibroblasts is the basis for apoptosis-induction by endogenous reactive oxygen species. *Cell Death and Differentiation*, 4 (5), 388–395.